Assessing Social Behaviour, Ontogenetic Change and Taxonomic status in a Juvenile *Gorgosaurus libratus (*Dinosauria; Theropoda; Tyrannosauridae)*:* A multidisciplinary analysis

By

Gavin Bradley

A thesis submitted in partial fulfilment of the requirements for the degree of

Master of Science

in

Systematics and Evolution

Department of Biological Sciences
University of Alberta

©Gavin Bradley, 2015

Abstract

The sparseness of the fossil record and the subjectivity of interpreting behaviour from morphological and taphonomic evidence have impeded studies on the behaviour of juvenile theropod dinosaurs. Most evidence for social behaviour in juvenile dinosaurs comes from multi individual bone beds or parent dinosaurs preserved while brooding on eggs or young. There is therefore a desire for alternative methods of assessing social behaviour, leading to the two key questions of this thesis: 1) can inferences about social behaviour be made using isolated specimens?, and 2) does gregariousness change with ontogeny in *Gorgosaurus*? A multidisciplinary study using isolated specimens of *Gorgosaurus libratus,* including a newly described juvenile specimen from Dinosaur Provincial Park in southern Alberta, was carried out in the hopes of answering these two questions.

A review of social behaviour in modern animals suggests that gregariousness is gradational and varies from taxon to taxon, even within closely related groups such as Felidae. Inferences of social behaviour for dinosaurs based solely on phylogenetic bracketing is therefore not recommended. However, numerous analyses can be performed on isolated specimens in order to infer social behaviours including parental care, group living, sexual display and combat. For example, palaeopathologies may indicate intraspecific combat. Ontogenetic changes, such as growth curves, allometry of horns and crests, and changes in stable isotopes because of dietary changes may also indicate changing behavioural as well as ecological roles during development.

Femoral circumferences are useful in inferring body mass of theropods, and in bone bed aggregations this can aid in studies of growth rates, which can inform social behaviour. Taphonomic damage can reduce sample sizes and make such studies problematic. Statistical analyses, however, suggest that three femoral-diameter-based estimation models may be used to predict femoral circumference measurements in tyrannosaurids.

Ontogenetic morphological changes in *Gorgosaurus* may also inform inferences about social behaviour. Positive allometric growth of the lacrimal horns may imply a display function, as seen in modern bovid and cervid mammals. Slow maximum growth rates of juvenile *Gorgosaurus*, compared to other tyrannosaurids, calculated using lines of arrested growth and body mass estimations, may indicate social aggregation during early ontogeny in order to survive alongside faster growing and

larger predators, such as *Daspletosaurus* or, alternatively, reduced growth due to nutritional stresses on juveniles.

Macrowear patterns in the teeth of UALVP 49500 and UALVP 10, an adult specimen, exhibit four major types of tooth wear: enamel spalling, longitudinal facets, tip wear, and barrel-shaped puncture marks. Adult teeth were typified by tip wear, and juvenile teeth were typified by longitudinal wear facets. This is hypothesised to reflect a change in feeding behaviour during ontogeny, from shearing and slicing of meat, with high levels of tooth occlusion in the young, to the "puncture and pull" method previously hypothesized for adults. A slicing feeding method for juveniles is further supported by thinner teeth with higher denticle densities, smaller bite forces, and a more circular orbit shape that is less resistant to the strain of high bite forces on the skull.

This multidisciplinary analysis shows that substantial ontogenetic change occurred in *Gorgosaurus,* and demonstrates that social behaviour may be inferred from isolated specimens. As well, a description of a juvenile *Gorgosaurus libratus,* UALVP 49500, presents the first examination of post cranial material in such a specimen, and supports a genus-level distinction between *Albertosaurus sarcophagus* and *Gorgosaurus libratus*.

Preface

The majority of chapter three of this thesis has been published in *Cretaceous Research*, although additional text has been added in the version seen in this thesis, to better contextualise the chapter within the overall goals of the masters research. The two co-authors of this manuscript are Michael Burns and Dr. Philip Currie. Both co-authors reviewed various stages of the manuscript and offered suggestions for improvements. The article was peer reviewed by one anonymous reviewer and by Dr. Nicolás Campione, whose suggestions were immensely helpful in the creation of the published version. The citation for the published version of the article is:

- Bradley, G. J., Burns, M. E., & Currie, P. J. (2015). Missing data estimation in tyrannosaurid dinosaurs: Can diameter take the place of circumference? *Cretaceous Research*, *55*, 200-209.

For chapter five, a manuscript has been submitted for publication to the Canadian Journal of Earth Sciences. An initial description of tooth wear in UALVP 10 was carried out over five years ago by James Glasier, but was redescribed by the author of this thesis based on both photographs of the specimen taken by Dr. Eric Snively and Dr. Ryan McKellar, my own physical examination of the teeth. James Glasier and Dr. Philip Currie will appear as co-authors on the manuscript, and both have provided initial reviews of the manuscript; some of the suggested changes have made their way into version submitted as Chapter 4 of this thesis. The article will be submitted in the following format:

- Bradley, G.J., Glasier, J. and Currie, P.J. Comparing tooth macrowear in a juvenile and adult specimen of *Gorgosaurus libratus: changes in feeding behaviour throughout ontogeny in tyrannosaurids.*

Furthermore, the circumference prediction models produced in chapter two, and body mass estimation methods used in Chapter three were utilised in a publication that I co-authored. None of this data, however, is included in this thesis. The full citation for this article is:

- Funston, G. F., Persons, W. S., Bradley, G. J., & Currie, P. J. 2015. New material of the large-bodied caenagnathid *Caenagnathus collinsi* from the Dinosaur Park Formation of Alberta, Canada. Cretaceous Research, 54, 179-187.

Dedication

This thesis is dedicated to my family: Mum, Dad, Anna, Matt, and Andy, who have supported my every move thus far, even the one across the Atlantic Ocean.

Acknowledgements

There are a great number of people who contributed in the writing of this thesis. Firstly, I would like to thank my girlfriend Kelsey Biggs, who has suffered more than anyone else at the hands of this thesis, but has shown phenomenal understanding and patience, even during late nights spent working in the lab. I would like to thank my supervisor, Dr. Philip Currie for accepting me into the lab, allowing me to work on such a remarkable specimen and for helpful reviews and comments on the various forms of this final work. Thanks also go to Dr. Eva Koppelhus for organising many of the administrative tasks associated with the thesis and for the support and understanding she has given me during my graduate studies. Immense thanks are owed to Michael Burns who not only dedicated a large portion of his time in supervising and teaching the histological portion of this thesis, but also reviewed chapters at various stages and made hugely useful comments, right down to the wire. I would also like to reserve special thanks for Dr. Nicolás Campione for sharing his expertise on MASSTIMATE, answering countless questions about statistics, and for a host of thoughtful and useful revisions on Chapter three.

I am grateful to Dr. Ryan McKellar who gave me his only copy of Lawrence Lambe's original *Gorgosaurus* manuscript to help guide my description, and who first introduced me to descriptions through the wonderful world of hymenopterans. I would like to show my appreciation for Ian MacDonald, who put in most of the hours preparing the skull material of Matilda; he did a wonderful job, and also managed to glue the bits I did back together. Thanks go to Clive Coy and Howard Gibbins for their help with all my collections queries, and for their part in the preparation of the salient specimen. I am also grateful to Dr. Michael Caldwell for the ongoing use of his camera equipment. Thanks also go to James Glasier, whose initial description of the teeth of UALVP 10 provided an excellent foundation for Chapter five, and to Dr. Eric Snively for providing pictures of tooth wear in UALVP 10. Access to UALVP 10 was provided by Andrew Locock and Lisa Budney for which I am grateful. I appreciate all the help provided over the past couple of years by Dr. Angelica Torices, who has taught me everything I know about tyrannosaurid teeth, but I suspect, not everything she knows, as it would take too long. Dr. Victoria Arbour and Scott Persons were also always there for me when I had questions, no matter how inane.

No matter what the outcome of this thesis, I have been incredibly fortunate to have had the support of a phenomenal group of friends throughout. I'd like to thank Michelle Campbell for all the happy days we spent unwinding from thesis work by cutting out footprints, Hallie Street for being the only person to get my Terry Pratchett references, Jasmine Croghan for seeing me through my first year, Betsy Kruk for also being willing to chat and for multiple rides to and from field sites, Doug Higginson for always helping me see the bigger picture; Greg Funston for incredibly helpful discussions and for co-creating the sport of 'Brush Ball', Michelle Viengkone for her positivity as we both slogged through the final months, Susan Kagan for reminding me not to forget my other interests, and Katherine Bramble for her support in the last few months of the thesis writing.

I would also like to thank all of my friends outside of palaeontology, whom I have neglected in the past few months, particularly Richard Hyndman, Dalton Schamehorn (and all the Schamehorn clan) and Jeffrey Pratt, who have been incredibly patient as I declined their offers of joviality to lock myself away for the past few months. Finally, I would like to thank Sir Terry Pratchett whose books have not only got me through the last few weeks, but the preceding 12 years since I first picked one up.

Table of Contents

Abstract II
Preface IV
Dedication V
Acknowledgements VI
List of Tables XII
List of Figures XIV
List of Abbreviations XX
Chapter 1- Introduction 1
Chapter 2 – A Review of Social Characteristics in Dinosaurs 4

2.1 Introduction 4
2.2 Gregariousness as a spectrum in modern animals 5
2.3 Social behaviour in modern animals 6
2.3.1 Early sociality: nest emergence and embryonic communication 6
2.3.2 Parental care 7
2.3.3 Juvenile play and agonism 10
2.3.4 Sexual dimorphism/Mating displays 11
2.3.5 Social groups 12
2.4 Modern social behaviour: a useful analogue for dinosaur palaeobiology? 14
2.5 Social behaviour in dinosaurs: palaeontological evidence 16
2.5.1 Social groups 16
2.5.2 Play fighting/Intraspecific competition 18
2.5.3 Parental behaviour 19
2.5.4 Sexual display 21
2.6 Is there palaeontological evidence of social behaviour in dinosaurs? 22
2.7 Final remarks 24

Chapter 3 – Missing data estimation in tyrannosaurid dinosaurs: can diameter take the place of circumference for social studies? 25
3.1 Introduction 25
3.2 Materials and methods 27
3.3 Results 28
3.4 Discussion 31
3.5 Conclusions 34
3.6 Tables 36
3.7 Figures

Chapter 4 – Gregariousness in *Gorgosaurus:* a description of UALVP 49500 with multidisciplinary analyses to assess the extent of social behaviour **42**

4.1 Introduction **42**
4.2 Materials and methods **43**
4.3 *Gorgosaurus libratus:* history and context **44**

4.4 Description of UALVP 49500 ('Matilda') **45**
4.4.1 Material **45**
4.4.2 Systematic palaeontology **46**
4.4.3 Cranium **47**
Maxilla
Maxillary teeth (Described in greater detail in Chapter 4)
Jugal
Quadrate
Quadratojugal
Lacrimal
Postorbital
Squamosal
Frontal
Ectopterygoid
Epipterygoid
Pterygoid
Palatine
Dentary
Dentary teeth (Described in greater detail in Chapter 5)
Surangular
Angular
Splenial
Supradentary/Coronoid
Prearticular and articular
4.4.4 Axial skeleton **56**
Cervical vertebrae
Dorsal vertebrae
Dorsal ribs
Caudal vertebrae
4.4.5 Appendicular skeleton **58**
Scapula-coracoid
Humerus
Manual phalanges
Ischium

Pubis
Fibula
Metatarsals
Pedal Phalanges
4.5 Social behaviour in *Gorgosaurus*? **62**
4.6 Intraspecific Agonism/Play: palaeopathologies **63**
4.7 Diet: denticle differences between juvenile and adult **64**
4.8 Sexual display: lacrimal horn allometry **64**
4.9 Ecological niche difference between juveniles and adults: Orbital aspect ratio **66**
4.10 Growth rates: Body mass vs. age **67**
4.11 Von Ebner Lines **69**
4.12 Conclusion **70**
4.13 Tables **72**
4.14 Figures **75**

Chapter 5 – Comparing tooth macrowear in a juvenile and adult specimen of *Gorgosaurus libratus*: Changes in feeding behaviour throughout ontogeny in tyrannosaurids **110**

5.1 Introduction **110**
5.2 Description of tooth wear in UALVP 10 (Adult *Gorgosaurus libratus*) **110**
5.2.1 Left maxilla **110**
5.2.2 Right maxilla **111**
5.2.3 Left dentary **112**
5.3 Description of teeth in UALVP 49500 (Juvenile *Gorgosaurus libratus*) **112**
5.3.1 Right maxilla **112**
5.3.2 Left maxilla **112**
5.3.3 Right dentary **113**
5.3.4 Left dentary **113**

5.4 Discussion **114**
5.5 Conclusions **119**
5.6 Tables **120**
5.7 Figures **121**

Chapter 6- Conclusion **135**

Bibliography **140**

Appendix 1- Prediction Data Set for Femoral Circumference Estimation **159**

Appendix 2- Regression Data for APR, MLR and ELLR **171**

Appendix 3-PPE and SEE student t-tests **189**

Appendix 4-*Albertosaurus* vs. *Gorgosaurus* Characteristics **192**

Appendix 5- UALVP 49500 Measurements **197**

List of Tables

Chapter 3-Missing data estimation in tyrannosaurid dinosaurs: can diameter take the place of circumference for social studies?

Table 3.1. Summary statistics for model predictions vs. true femoral circumferences for five tyrannosaurid genera; two sample t-test of model predicted vs. true femoral circumferences, percent prediction error (PPE) and standard error of the estimate (SEE).

Table 3.2. Comparison of body mass estimations for five tyrannosaurid genera made with true femoral circumferences, **ELLR**, **CML** and **MLR** estimated circumferences

Chapter 4 – Gregariousness in *Gorgosaurus: a description of UALVP 49500 with multidisciplinary analyses to assess the extent of social behaviour*

Table 4.1. UALVP 49500 cranial elements visible from original quarry maps of Q253

Table 4.2. Post-cranial skeletal elements visible from original quarry maps of Q253

Table 4.3. Skull length of UALVP 49500 compared to other *Gorgosaurus* specimens

Table 4.4. *Gorgosaurus* lacrimal vs. femur/skull length raw regression measurements

Table 4.5. Orbit length vs. height for six genera of tyrannosaurids

Table 4.6. Orbit length vs. height for six specimens of *Gorgosaurus* after Erickson et al., 2004

Table 4.7. Circumference estimation data for specimens of *Gorgosaurus* using **ELLR.** All estimations based on mediolateral circumference data, except NMC2120, which use anteroposterior data.

Table 4.8. Modified developmental mass extrapolation of 4 juvenile specimens of *Gorgosaurus libratus* (Modified after Erickson et al., 2000)

Table 4.9. Growth rate data for *Gorgosaurus* specimens following histological sectioning of ribs and body mass estimations*After Erickson et al., 2004 †Calculated using **ELLR**, ®Calculated using: y=1.2533x-1.1638 (Y=Log femoral circumference, x=log femoral length; Currie, Pers. Comm.)

Table 4.10. Modified body growth rate data for *Albertosaurus sarcophagus* from Erickson et al., (2004) ®Calculated using: y=1.2533x-1.1638 (y=Log femoral circumference, x=log femoral length; Currie, Pers. Com

Chapter 5- Comparing tooth macrowear in a juvenile and adult specimen of *Gorgosaurus libratus: changes in feeding behaviour throughout ontogeny in tyrannosaurids*

Table 5.1. Distribution and type of wear marks on teeth of adult: UALVP 10

Table 5.2. Distribution and type of wear marks on teeth of juvenile: UALVP 49500

Table 5.3. Percentage of teeth in UALVP 10 and UALVP 49500 displaying each type of wear mark

List of Figures

Chapter 3 – Missing data estimation in tyrannosaurid dinosaurs: can diameter take the place of circumference for social studies?

Figure 3.1. Linear regression of true anteroposterior diameters of tyrannosaurid femoral shafts and their corresponding true circumference **(APR).** All data log transformed (Log10) and weighted.

Figure3.2. Linear regression of true mediolateral diameters of tyrannosaurid femoral shafts and their corresponding true circumferences **(MLR)**. All data log transformed (Log10) and weighted.

Figure 3.3. Multiple Linear regression of true femoral diameters vs true femoral circumferences (**ELLR**-Anteroposterior). All data log transformed (Log10) and weighted.

Figure 3.4. Multiple Linear regression of true femoral diameters vs true femoral circumferences (**ELLR**-Mediolateral). All data log transformed (Log10) and weighted.

Figure 3.5. Mean PPE values for six femoral circumference estimation models' predictions using data from five tyrannosaurid genera. Bars represent upper and lower 95% confidence boundaries for each model.

Figure 3.6. Intertaxonomic mean PPE values for six femoral circumference estimation models' predictions using data from five tyrannosaurid genera. Bars represent upper and lower 95% confidence boundaries for each genus of tyrannosaurid in each particular model.

Chapter 4 – Gregariousness in *Gorgosaurus*

Figure 4.1. Recent phylogenetic tree showing *Gorgosaurus libratus* position as a basal tyrannosaurid within Tyrannosauroidea and sister taxon to *Albertosaurus sarcophagus* (Modified from Loewen et al. 2013).

Figure 4.2. Quarry map of UALVP 49500 excavation site in Dinosaur Provincial Park (Quarry 253-Photo: Philip Currie.)

Figure 4.3. Striated bone in lateral view on antorbital fossa in UALVP 49500

Figure 4.4. Right maxilla in lateral view. Arrows showing anterior rims of maxillary fenestra (anterior) and antorbital fenestra (posterior)

Figure 4.5. Ventral view of mild depressions in right maxilla palatal shelf

Figure 4.6. Ovate cross section at base of isolated maxillary tooth from UALVP 49500 scanned using a Skyscan MicroCT scanner

Figure 4.7. Left jugal of UALVP 49500 in lateral view. Arrow showing pneumatopore.

Figure 4.8. Right Quadrate of UALVP 49500 in lateral view.

Figure 4.9. Medial fossa in right quadrate of UALVP 49500, dorsomedial view

Figure 4.10. Left quadratojugal of UALVP 49500 in lateral view. Arrows showing flaring of squamosal contact

Figure 4.11. Right quadratojugal ofUALVP 49500, showing rugose medial quadrate articulation

Figure 4.12. Right lacrimal of UALVP 49500 in lateral view. Arrows showing lacrimal horn (dorsal) and pneumatic fossa (ventral).

Figure 4.13. Right postorbital of UALVP 49500 in lateral view. Arrow showing dorsolateral fenestra.

Figure 4.14. Right postorbital of UALVP 49500 in medial view. Arrow showing medial central fossa.

Figure 4.15. Left squamosal of UALVP 49500 in dorsal view

Figure 4.16. Left squamosal of UALVP 49500 in ventral view. Arrow showing the anterior pneumatic foramen.

Figure 4.17. Partial left and right frontals of UALVP 49500 in dorsal view

Figure 4.18. Partial left and right frontals of UALVP 49500 in ventral view. Arrow showing intrafrontal suture.

Figure 4.19. Left and right ectopterygoids of UALVP 49500 in dorsal view.

Figure 4.20. Left ectopterygoids from UALVP 49500 in ventral view. Arrow showing ventral pneumatopore.

Figure 4.21. Left epipterygoid of UALVP 49500 in lateral view

Figure 4.22. Left pterygoid of UALVP 49500 in ventral view

Figure 4.23. Left palatine of UALVP 49500 in lateral view. Arrows showing two pneumatopores and one possible pneumatopore (anterior) on lateral shelf

Figure 4.24. Left dentary of UALVP 49500 in lateral view.

Figure 4.25. Right surangular of UALVP 49500 in lateral view.

Figure 4.26. Articulated left angular from UALVP 49500 in lateral view.

Figure 4.27. Medial view of articulated right splenial. Arrow showing the anterior mylohyoid foramen.

Figure 4.28. Left supradentary/coronoid from UALVP 49500 in medial view

Figure 4.29. Right prearticular of UALVP 49500 in medial view

Figure 4.30. Articular/Surangular/Prearticular contact to make quadrate articulation concavity in UALVP 49500, medial view.

Figure 4.31. Anterior view of Atlas/Axis articulation in UALVP 49500

Figure 4.32. Ventral foramen on axis in UALVP 49500

Figure 4.33. Ventral view of articulated cervical vertebrae in UALVP 49500

Figure 4.34. Anterior view of dorsal vertebra B from UALVP 49500

Figure 4.35. Posterior view of largest dorsal vertebra from UALVP 49500, showing fused distal portion of left scapula

Figure 4.36. Anterior view of left dorsal rib A from UALVP 49500

Figure 4.37. Three anterior most caudal vertebrae of UALVP 49500 from lateral view: CVA, CVB and CVC

Figure 4.38. Three most posterior caudal vertebrae of UALVP 49500 from lateral view: CVD, CVE and CVF

Figure 4.39. Chevron A from UALVP 49500 in anterior view

Figure 4.40. Chevron B from UALVP 49500 in lateral view

Figure 4.41. Right scapula/coracoid of UALVP 49500 in lateral view. Arrow showing glenoid cavity.

Figure 4.42. Anterior view of right humerus of UALVP 49500.

Figure 4.43. Manual phalanges of UALVP 49500 from dorsal view

Figure 4.44. Ischia of UALVP 49500 in ventral view. Arrow showing extension of obturator process

Figure 4.45. Pubes of UALVP 49500 in left lateral view

Figure 4.46. Right fibula of UALVP 49500 in posterior view. Arrow showing contact for the soleus muscle of the calf.

Figure 4.47. Left MTI of UALVP 49500 in lateral view

Figure 4.48. Anterior view of left MTII and MTII in articulation; arctometatarsalian condition displayed

Figure 4.49. Right MTV of UALVP 49500 in lateral view

Figure 4.50. DIV and DII of left foot from UALVP 49500 in dorsal view

Figure 4.51. Elements of DII (ventral), DIII and DIV (dorsal) of the right foot from UALVP 49500; dorsal view

Figure 4.52. Potential bite/claw mark in right dentary of TMP 1994.012.0155

Figure 4.53. Ceratopsian parietal horn with tyrannosaurid bite marks, collected from Dinosaur Provincial Park

Figure 4.54. Denticle density vs. Fore-aft basal length (FABL) for right dentary teeth of 3 juvenile *Gorgosaurus* specimens and two adult specimens

Figure 4.55. Allometric relationship between height of lacrimal horn and lateral skull length in seven specimens of *Gorgosaurus libratus*

Figure 4.56. Allometric relationship between height of lacrimal horn and length of femur in seven specimens of *Gorgosaurus libratus*

Figure 4.57. Lines of arrested growth in thin section of UALVP 49500 dorsal rib

Figure 4.58. Lines of arrested growth in thin section of TMP 91.36.500 dorsal rib

Figure 4.59. Lines of arrested growth in thin section of UALVP 10 dorsal rib

Figure 4.60. Secondary bone structure in TMP 1991 163 001; lamellar bone encircles secondary osteons and there is little to no fibrolamellar bone/vascularisation

Figure 4.61. Secondary bone structure in UALVP 10; lamellar bone encircles secondary osteons and there is little fibrolamellar bone/vascularisation

Figure 4.62. Isolated maxillary tooth from UALVP 49500 embedded in epoxy resin for histological section

Figure 4.63. Incremental lines of von Ebner in frontal plane thin section of UALVP 49500

Figure 4.64. Gompertz growth curve showing mean body mass vs. age at death for six *Gorgosaurus libratus* specimens

Figure 4.65. Gompertz growth curve showing minimum body mass estimation vs. age at death for six *Gorgosaurus libratus* specimens

Figure 4.66. Gompertz growth curve showing maximum body mass estimation vs. age at death for six *Gorgosaurus libratus* specimens

Figure 4.67. Gompertz growth curve showing mean body mass estimation vs. age at death (after Erickson et al., 2004) for five *Albertosaurus sarcophagus* specimens

Figure 4.68. Gompertz growth curve showing minimum body mass estimation vs. age at death (after Erickson et al., 2004) for five *Albertosaurus sarcophagus* specimens

Figure 4.69. Gompertz growth curve showing maximum body mass estimation vs. age at death (after Erickson et al., 2004) for five *Albertosaurus sarcophagus* specimens

Figure 4.70. Incremental lines of von Ebner in tyrannosaurid tooth of unknown age (Slide by Paul Johnston)

Chapter 5 – Comparing tooth macrowear in a juvenile and adult specimen of *Gorgosaurus libratus:* changes in feeding behaviour throughout ontogeny in tyrannosaurids

Figure 5.1. Skull of UALVP 10 mounted in University of Alberta Earth Sciences Museum

Figure 5.2. George M. Sternberg c.a. 1920 with the newly excavated left dentary of UALVP 10

Figure 5.3. Left dentary and maxilla of UALVP 49500

Figure 5.4. Right dentary and maxilla of UALVP 49500

Figure 5.5. Lingual view of spalling wear on LM4, of UALVP 10

Figure 5.6. Lingual view of spalling wear on LM5, of UALVP 10

Figure 5.7. Lingual view of apical wear on LM9, UALVP 10

Figure 5.8. Lingual view of LM13, of UALVP 10 showing occlusal wear facet

Figure 5.9. Lingual view showing occlusal wear facet on RM4 and tip wear on RM5, of UALVP 10

Figure 5.10. Spalling wear on LD1 UALVP 10

Figure 5.11. Labial view of barrel shaped puncture wear (A) on LD5, and tip wear (B,C) on LD6, LD7 of UALVP 10

Figure 5.12. Labial view of tip wear in LD6 and LD7 of UALVP 10

Figure 5.13. Labial view of spalling wear on LD11 (A), tip wear on LD13 and LD15 (B, C), from UALVP 10

Figure 5.14. Lingual view of occlusal wear facet on RM8 of UALVP 49500

Figure 5.15. Lingual view of occlusal wear facet on LM4 of UALVP 49500

Figure 5.16. Lingual view of occlusal wear facet on LM6 of UALVP 49500

Figure 5.17. Lingual view showing occlusal wear facet on LM8, of UALVP 49500

Figure 5.18. Lingual view of occlusal wear on LM10 of UALVP 49500

Figure 5.19. Labial view of spalling wear on RD3, of UALVP 49500

Figure 5.20. Labial view of tip wear on RD7, of UALVP 49500

Figure 5.21. Labial view of occlusal wear facet on RD10 on UALVP 49500

Figure 5.22. Lingual view of spalling wear on LD3 of UALVP 49500

Figure 5.23. Lingual view of tip wear on LD7 of UALVP 10

Figure 5.24. Lingual view of tip wear on LD 8 of UALVP 49500

Figure 5.25. Labial view of occlusal tooth wear on LD14 of UALVP 49500

Figure 5.26. Bar chart showing percentage of teeth in UALVP 10 and UALVP 49500 displaying each type of wear mark

List of Institutional abbreviations used in this thesis

AMNH, American Museum of Natural History, New York, New York, U.S.A.

BMNH, Burpee Museum of Natural History, Rockford, Illinois, U.S.A.

CMMD, Central Museum of Mongolian Dinosaurs, Ulaanbaatar, Mongolia

CM, Children's Museum of Indianapolis, Indiana, U.S.A.

DMNH, Denver Museum of Nature and Science, Denver, Colorado, U.S.A.

FMNH, Field Museum of Natural History, Chicago, Illinois, U.S.A.

MOR, Museum of the Rockies, Bozeman, Montana, U.S.A.

MPC, Mongolian Palaeontological Centre, Ulaanbaatar, Mongolia

NMC, Canadian Museum of Nature, Ottawa, Ontario, Canada

NMMNH, New Mexico Museum of Natural History and Science, Albuquerque, U.S.A.

PIN, Museum of Palaeontology, Moscow, Central Federal District Russia

ROM, Royal Ontario Museum, Toronto, Ontario, Canada

RSM, Royal Saskatchewan Museum, Regina, Saskatchewan, Canada

TMP, Royal Tyrrell Museum of Palaeontology, Drumheller, Alberta, Canada

UALVP, University of Alberta Laboratory for Vertebrate Palaeontology, Edmonton, Alberta, Canada

USNM, National Museum of Natural History, Washington, D.C., U.S.A.

ZPAL, Institute of Palaeobiology, Polish Academy of Sciences, Warsaw, Poland.

Chapter 1

Introduction

The sparseness of the fossil record and the subjectivity of assessing behavioural evidence may impede studies on the behaviour of juvenile dinosaurs. Jepsen (1964) accounted for the lack of well preserved juveniles by proposing that they were kept in upland areas, whereas adults scoured the more dangerous, yet more taphonomically favourable riversides. A potential taphonomic bias against juveniles has also been supported by Lockley (1996), but with little elaboration, whereas Richmond (1965) suggested that juvenile dinosaurs were always scarce, by analogy with the extant desert tortoise (*Gopherus agassizi*) which boasts a minimal juvenile population percentage. More recently, reinterpretations of several dinosaur taxa as juvenile stages of others have increased the number of recognised sub-adult fossils (Horner & Goodwin, 2009; Scannella & Horner 2010; Scannella & Horner, 2011). However, with few exceptions, such as the reconsideration of *Jenghizkhan*, *Maleevosaurus*, and *Shanshanosaurus* as ontogenetic stages of *Tarbosaurus* (Currie et al., 2003), these taxonomic reinterpretations have been met with resistance and inspired phylogenetic debates (e.g. Carr, 1999; Currie, 2003b; Carr and Williamson, 2004; Larson, 2013).

The second issue inhibiting the study of juvenile theropod behaviour is the subjectivity of interpreting behavioural evidence. Behaviour is never directly observable in extinct taxa, but may be inferred. Herding behaviour has been demonstrated in hadrosaurines based on multiple trackway sites (Currie, 1983), and the idea of social groups have also been supported in some small theropods such as *Coelophysis* (Schwartz & Gilette, 1994) and *Sinornithomimus* (Varrichio et al., 2008b). Larger-bodied non-avian theropods, such as *Gorgosaurus,* have traditionally been overlooked for this characteristic due to their large body size and the scarcity of adequate material. Recently though, bone bed assemblages have aided in remedying this. At Dry Island Buffalo Jump Provincial Park, Alberta, Canada, more than 26 individuals of *Albertosaurus* have been interpreted as representing a social aggregation (Currie, 2000; Currie & Eberth, 2010). Well- preserved dinosaur brooding sites like those known for some oviraptorosaurs (Norrell et al., 1995) have also provided information on parental behaviour in dinosaurs. The examples, however, are based on rare and unpredictable assemblages. For taxa for which these are unknown, such as *Gorgosaurus*, other forms of evidence are necessary.

Objectives

Due to the paucity of the fossil record and the need for different methods of assessing social behaviour, a study combining the two factors can improve understanding of both problems. This thesis addresses two questions:

1. Can inferences about social behaviour in dinosaurs be made using isolated specimens?
2. Does gregariousness change with ontogeny in *Gorgosaurus*?

A multi disciplinary approach, using techniques from various subfields of dinosaur palaeontology, is employed in answer to these two questions.

Multidisciplinary analysis outline

1. Social behaviour in animals, the meaning of "gregarious" and evidence for social behaviour in Dinosaurs

   The second chapter of this thesis reviews social behaviour in modern and extinct taxa and discusses the suitable application of the term 'gregariousness' to extinct taxa. This provides a context for the study of social behaviour in *Gorgosaurus*.

2. Missing data and mass estimation for tyrannosaurid dinosaurs: can diameter take the place of circumference for studies of sociality?

   This chapter assesses the statistical success of six different diameter-based femoral circumference estimation models in tyrannosaurids, which may be used to increase the data available for body mass estimations, some growth dynamic curves and the population estimations from bonebeds.

3. Description of UALVP 49500 and analyses of social behaviour in *Gorgosaurus*

   Chapter four provides the description of a juvenile *Gorgosaurus* specimen, UALVP 49500, which includes articulated and associated cranial and post-cranial material, and assesses the taxonomic validity of *Gorgosaurus libratus* in relation to *Albertosaurus sarcophagus*. UALVP 49500 is then used to identify differences in gregarious behaviour between juvenile and adult *Gorgosaurus,* in the hopes that such differences might allow us to make inferences about social behaviour. These techniques include: palaeopathological observation, denticle density counts, lacrimal horn allometry, orbit aspect ratio comparisons, bone histology and body mass estimation.

4. Comparing tooth macrowear in a juvenile and adult specimen of *Gorgosaurus libratus:* Changes in feeding behaviour throughout ontogeny in tyrannosaurids

   Chapter five contrasts tooth macrowear in UALVP 49500 and an adult *Gorgosaurus* specimen, UALVP 10, to document any change in tooth pathologies during ontogeny. Contrasting patterns of tooth wear may have implications on the interpretation of feeding mechanism, diet and ecological niche of juveniles, and may be used to assess the likelihood that juveniles fed at the same kill site as adults, or hunted independently.

This thesis attempts to circumvent two salient problems in theropod palaeontology: the paucity of the juvenile fossil record and the subjectivity of social behavioural studies, by carrying out a multidisciplinary analysis to assess the prospect of social behaviour in a juvenile *Gorgosaurus*. In examining a variety of ontogenetic changes in *Gorgosaurus,* this thesis presents a novel approach

in making inferences about the social behaviour of a dinosaur taxon, and may provide a template for future studies in the field.

Chapter 2

A Review of Social Characteristics in Dinosaurs

2.1 Introduction

The traditional image of dinosaurs amongst the general public for much of previous century was one of large, sluggish, cold blooded reptiles, with little to no social complexity (Lambe, 1917; Norman 2005). This view, perpetuated by the very same depictions in the media that popularised palaeontology, dominated the literature and attached to these extinct animals the unwarranted stigma of low intelligence, inactivity and social simplicity (Buffetaut, 1997). Their anatomical similarity to reptiles, and the limited knowledge of sociality in extant reptilian populations (Burghardt, 1977), created a culture of study in which dinosaurs were assumed to be lacking the social complexities of mammals and birds.

This period of stagnation in which dinosaur palaeontologists threatened to fulfil the stereotype of the 'stamp collecting' natural scientist (Thomson, 1985; Johnson, 2007), ended with descriptions of swift, actively predatory theropods such as *Deinonychus* (Ostrom, 1969). Such finds, combined with the phylogenetic reassessment of Dinosauria to include birds (Ostrom, 1973, 1976), catalysed a paradigm shift in the study of gregarious behaviour in these extinct organisms, and the development of a better understanding of endothermy (Bakker, 1988), intelligence (Russell, 1972), and social complexity (Ostrom 1972; Burghardt, 1977), which are no longer traits exclusive to mammals and modern birds.

The renaissance of dinosaur palaeontological thought, brought about by this string of critical discoveries, has turned the study of gregariousness on its head. Coupled with the removal of themindset that led to earlier depictions of relatively sedentary and unintelligent dinosaurs, an increase in spectacular finds such as monospecific bone beds (e.g. Currie and Dodson, 1984; Colbert, 1989; Currie, 1998; Varrichio et al., 2008), non-lethal conspecific bite marks (Peterson et al. 2009) and apparent cases of brooding over nests (Norell et al., 1995; Dong and Currie, 1996; Clark et al., 1999; Fanti et al., 2012), have led to the widespread adoption of theories of gregarious behaviour for many dinosaur groups. Pack hunting, at least opportunistically, has been suggested for relatively small theropods such as *Aniksosaurus* (Ibiricu et al., 2013) and the previously mentioned *Deinonychus* (Maxwell and Ostrom, 1995), as well as large theropods such as *Allosaurus* (Bakker, 1997), *Albertosaurus* (Currie, 1998; Currie and Eberth, 2010), *Daspletosaurus* (Currie et al., 2005) and *Mapusaurus* (Coria and Currie, 2006). Similarly, herding has been proposed for sauropod dinosaurs (Salgado et al., 2013) and herbivorous ornithischians such as *Psittacosaurus* (Zhao et al., 2007), *Edmontosaurus* (Bell and Campione, 2014), and *Pachyrhinosaurus* (Ralrick and Tanke, 2008).

Despite the ubiquity of theories of gregariousness in current dinosaur palaeontology, there have been some challenges to researchers favouring socially complex behaviours. Roach and

Brinkman (2007) reinterpreted phylogenetic, pathological and trackway evidence associated with pack hunting in *Deinonychus,* as representative of opportunistic associations between conspecifics, resulting in agonistic encounters. Isles (2009) also pointed to spectacular fossil finds such as the 'fighting dinosaurs', as proof that small theropods did, at least on occasion, attempt to bring down larger prey individually. That fossil evidence may be so flexibly interpreted to construct theories of dinosaur behaviour remains the core caveat in trying to assess gregarious potential; behavioural evidence in extinct animals can never be observed directly and subjectivity will always persist (Currie and Eberth, 2010).

Whereas the inherent subjectivity in behavioural studies of extinct animals makes substantiating theories of gregariousness in dinosaurs a challenging prospect, the combination of various forms of evidence, utilising different techniques within the field, may still produce viable scientific hypotheses. The significance of persisting in the study of dinosaurian social behaviour, too, should not be overlooked. Behavioural studies, along with the introduction of newly discovered species, constitute some of the most attractive publications to the general public; they are incorporated into movies, such as the pack hunting '*Velociraptor*' in the hugely successful Jurassic Park franchise, and documentaries, such as the migrating herds of *Iguanodon* in the popular BBC documentary series 'Walking with Dinosaurs'. Not only do behavioural studies engage the imagination of the public, thus raising awareness of palaeontological research, but an understanding of dinosaur behaviour is also required of palaeontologists, to appreciate these extinct organisms as animals in themselves, rather than simply mineralised fragments of bone that require categorising.

This chapter presents a review of how sociality is expressed in modern vertebrates, with a view to juxtaposing the various levels of gregariousness seen in extant animals with those hypothesised for dinosaurs. Furthermore, the plethora of different avenues of evidence, which have been, and may be used to explore social behaviour for different dinosaur taxa are summarised, creating an investigative template for future studies. Finally, using this review of social characteristics in extinct and extant taxa, the current evidence for pack structures, incorporating juveniles, for *Gorgosaurus libratus* is examined.

2.2 Gregariousness as a spectrum in modern animals

Gregariousness, when proposed for a particular dinosaur taxon, must be defined to reflect the term's variation in the animal kingdom; social behaviour is a spectrum encompassing many different behavioural traits and morphological characteristics (Doody et al., 2013). As a foundation for any intraspecific sociality proposed for extinct taxa, such as dinosaurs, Ostrom (1972) suggested that an individual's behaviour needs to have been motivated by the group, rather than simply cohabiting with other individuals in a manner similar to frogs in a pond. Currie and Eberth (2010) supported this base definition, proposing that for behaviour to be considered truly gregarious, it must be inspired by biotic factors, rather than environmental pressures, such as the restriction of available habitat due to a natural disaster e.g. widespread flooding. These biological factors, such

as increased defence from predation and protection of territories (Packer et al., 1990), increased access to food, learned skills by young through play fighting (Tanke and Currie, 1990), and increased chances of mating (Luhrs et al., 2013), must outweigh the costs. Potential costs include increased susceptibility to disease (Ostrom, 1972), increased competition for resources and mates (Krause and Ruxton, 2002), and increased chances of injury by intraspecific agonism (Tanke and Currie, 1990; Bell and Currie, 2010; Peterson et al., 2009). Taking these factors into account, a minimum criteria based definition for the identification of social behaviour in extinct taxa can therefore be summarised as: Interaction with a group of conspecifics that is not driven soley by environtmental pressures, and which increases the Darwinian fitness of an individual.

The appearance and extent of social behaviour is hugely variable among closely related taxa. Currie and Eberth (2010) suggested that gregariousness is not always consistent within a family or genus, presenting the big cats of *Panthera* as an example of this phylogenetic inconsistency in behaviour; lions display complex social dynamics in prides, whereas cheetahs, leopards and tigers are solitary animals most of the time. Indeed gregariousness is not even always consistent within a species; facultative sociality is a phenomenon amongst some mammalian taxa, such as the Madagascan fossa, in which individuals may choose to join an associated group centred on a solitary female, or lead a solitary lifestyle (Luhrs et al., 2013). Considering the taxonomic inconsistency of sociality witnessed in modern day taxa, it is therefore prudent to be conservative with applications of social inferences to extinct groups of animals; evidence of social behaviour in one genus of tyrannosaurid does not imply ubiquity of such behaviour within all members of Tyrannosauridae.

Within particular taxa, however, many modern animals display behaviour that, expressed in various forms and through different levels of complexity, satisfy the minimum definition of sociality. Such behaviour, far from being limited to so-called higher vertebrates, such as birds and mammals, may also be identified in less derived groups of organisms. For example, socially learned hunting behaviour, famously a trait of killer whales (Pitman and Durban, 2012), has also been demonstrated in cartilaginous fishes such as lemon sharks (Guttridge et al., 2013). Some different manifestations of social behaviour in extant taxa are herein discussed, with an increase in perceived complexity of behaviour that mirrors the concept of gregariousness as a gradient rather than a catch all term. In each case, the behaviour complies with the aforementioned criteria for sociality i.e. that it must be biologically driven, group motivated and be beneficial to the physical fitness of the organism. The relevance of each example as a potential analogue for dinosaur behavioural studies, especially those concerning tyrannosaurid social behaviour, is also considered.

2.3 Social behaviour in modern animals

2.3.1 Early sociality: nest emergence and embryonic communication

Despite traditionally being considered archetypal solitary animals (Wilson, 1998), some extant reptiles display sociality to varying degrees through a range of behaviours. One of the most

rudimentary of these is nest emergence in iguanas; newly hatched iguanas often coordinate timing of head movements out of a communal tunnel, in order to avoid predators such as birds of prey before dispersing (Greene et al. 1977). Furthermore, they have been recorded emerging, migrating and often sleeping in close proximity, within small groups after this initial display of sociality (Burghardt et al., 1977). Whereas the presence of other juveniles increases the likelihood of survival for these animals, socially complexity does not extend much further than the allocation of appropriate sleeping areas and sleep mates (Burghardt, 1977). Such social behaviour, limited though it is, is extremely rare in other species of lizard; less than 1% of known species exhibit similarly gregarious actions (Davis et al., 2011; Doody et al., 2013). Even earlier in development, although such behaviour would be impossible to infer from extinct remains, Doody et al. (2012) recorded an extraordinary social hatching process in pig nose turtles; embryonic individuals emerge early from the egg in times of stress, in response to vibrations from siblings in nearby eggs. Similarly, some crocodile embryos can synchronise hatching with specific vocalisations that are understood by siblings and the mother (Burghart, 1977; Vergne et al., 2009; Doody et al., 2012). Although, evidence for social behaviour in reptiles is rare outside of crocodilians (Garrick, 1977; Brazaitas and Watanabe, 2011), these early instances of loose social organisations in modern, terrestrial reptiles makes an intriguing appeal against the exclusivity of gregariousness to higher vertebrates, and the rejection of the phenomena in non-avian theropods. However, although phylogenetically close to dinosaurs, these small reptilian examples make poor ecological comparisons for any of the larger dinosaurs, such as tyrannosaurids.

2.3.2 Parental care

Parental care is another social behaviour that is evidenced, to varying degrees, all across Vertebrata. Again, the lower vertebrates are surprisingly well represented in this aspect of sociality, a trait that has been traditionally considered typical of higher vertebrate taxa (Sargent and Gross, 1986). Part of this bias towards parental behaviour as a mammalian trait may be due to the persistent and oft criticised anthropocentric view of biological researchers (Hejnol, 2014). However, the too rigid implementation of the 'r-K species selection' paradigm introduced by McArthur and Wilson, (1967), also promotes assumptions of all or nothing based theories of parental care, based on the reproductive strategies of the taxa (Pianka, 1970). This ecological theory suggests that species may be divided into 'r' or 'K' types, depending largely on the amount of young they produce in one reproductive cycle, and the size and rate of growth of the taxon; r species are typically considered smaller, faster growing, with greater numbers of young, whereas K species are larger, display slower growth and have relatively few young per generation (Dash, 2001). Concomitantly, K selected species are usually associated with higher levels of parental care as they have altrical young that need protection and feeding for long periods of time, whereas r selected species have many precocial young that are assumed to require little parental care (Varricchio et al., 2008a). Despite the presence of this trade off between parental investment and amount of young per generation in various taxa, the identification of r and K selected species is not sufficient in itself a sufficient reflection of parental behaviour; this concept, much like generalised

social behaviour, is best considered as a spectrum with varying levels of parental interference after fertilisation (Pianka, 1970).

The extent of parental care, therefore, varies from taxon to taxon, and the number of young in a generation may not be an excellent indicator in itself. In many species of fish, for example, large deposits of eggs are often protected through the nest guarding behaviour of a parent (Andrén and Kvarnemo, 2014). In some species, such as the smallmouthed bass *(Micropterus dolomievi)*, guarding also persists once the fry are free-swimming, and continues until juvenile independence is reached (Jeffrey et al., 2014). Furthermore, male-only parental care is present in numerous fish groups and some amphibians (Sargent and Gross, 1986) and 90 species of birds (Cockburn, 2006), but is entirely absent in extant reptiles. In mammals, the behaviour has thus far only been recorded in some rodent species (De Jong et al., 2012). Although neither fish nor amphibians arephylogenetically or ecologically analogous to large dinosaurs, these examples again show the fallacy of ruling out sociality in the form of parental behaviour in dinosaurian taxa, on the grounds that they are more primitive than modern mammals and birds.

Within extant reptiles, a potentially more apt comparative group for dinosaurs than fish or amphibians, parental care is limited to around three percent of species found, however some smaller squamates such as the long-tailed-skink (*Takydromus sexlineatus*) have been recorded attending nests to deter predators (Huang, 2006). Another lizard, the great-desert-skink (*Liopholis kintorei*) displays an even more complex behaviour in cooperatively digging tunnels with other adults to protect their underdeveloped offspring (McAlpin et al. 2011). It is within crocodylia that parental behaviour in reptiles gets most complex; mothers aggressively defend the nest and, once hatched, audibly communicate with, carry and feed the young (Garrick and Lang, 1977; Whitaker, 2007; Brazaitis and Watanabe, 2011). Although parental care is universal across Crocodylia, like most social behaviour the longevity of parental care varies from taxon to taxon; alligators may stay with their hatchlings for up to two years, whereas old world crocodiles can leave their young within weeks of hatching (Garrick and Lang, 1977). The young themselves often stay together in large groups, known as crèches, during early ontogeny, which are associated with a small number of dominant or well developed adults, mostly female, although biparental care has been recorded in eight crocodylian species (Charruau and Henaut, 2012). Two examples of extreme sociality through parental care is witnessed in the gharial (*Gavialis*), which displays immense crèche sizes of between 200 and 1000+ juveniles, monitored by dominant males (Lang et al., 2013). This instance of paternal care alongside large juvenile crèches depicts a capacity within the second branch of extant archosaurians for complex social behaviour that might increase the likelihood of juvenile survival.

Although numerous crocodilian species practice complex parental behaviour, this trait is atypical for most other reptiles, for which the norm is highly precocial young that achieve independence early on (Burghardt, 1988; Doody et al. 2013). Paternal care is almost ubiquitous in birds, a group which, along with crocodylians, constitutes the extant branches of Archosauria. With

the exception of brood parasitic taxa, such as the cuckoo (Payne, 1977; Spottiswoode et al., 2012), nest guarding is the minimum level of parental care within Aves; 99% of all birds brood on their eggs, with only 1% practising brood parasitism (Cockburn 1996). The level of post-hatching care, however, varies hugely between species; many aquatic and cursorial birds do not feed their young, which tend to exhibit high levels of early growth and independence (Clutton Brock, 1991). Amongst most birds, however, parental care of juveniles is not only extensive, but necessary. Many altricial young are born with eyes closed and little to no plumage; they are completely reliant on parental care for food and the learning of basic survivial traits, such as flight, as well as more complex characteristics to increase physical fitness, such as the acquisition of songs from parents and siblings in the passerines (Starck and Ricklefs, 1998; Bertin et al., 2007; Catchpole and Slater, 2008). Commonly in monogamous birds and communal breeders, juveniles will stay close to their parents within a larger flock for at least one seasonal cycle, even after they have reached physical independence (Clutton Brock, 1991).

Most mammals, too, are considered archetypal K-strategist species with extremely high levels of maternal care, although biparental care is extremely rare (De Jong et al., 2012). The most basic and ubiquitous level of parental care in mammals is lactation by the mother; however, the parental investment after the nursing stage largely depends on the developmental rate of the young and the overall sociality of the species. With highly precocial taxa such as hares, parental behaviour does not extend beyond protection from predators, whereas within carnivora, a typically altricial group, parents may protect, provide for and teach important social skills to juveniles after weaning (Thurnston, 2002; Mandal, 2012).

Mammals that have a strong attachment between parents and offspring therefore tend to be typified by slow growth rates and long life histories, and eventually become incorporated into larger social groups. For example, in killer whales, which have extremely long life histories, parental care involves feeding, protection and skill teaching; this effort is then repaid when the juveniles become useful members of an efficient, cooperatively hunting pod (Olesiuk et al., 1990; Pitman and Durban, 2012). Similarly, altricial lion cubs are subject to high levels of communal parental care, with protection, grooming and kill sharing, and eventually grow to join a highly complex social structure known as the pride (Poole, 1985; Pusey and Packer, 1994). Exceptions to this trend do exist; for example altricial tiger and leopard cubs are completely dependent on their mothers for up to a year after birth, yet become mostly solitary predators (Mandal, 2012). In the case of tigers, however, their generally slow life history may be compensated for by the relatively faster development of the essential tools for hunting. For example, their canines grow significantly faster than those of the highly social lions (Smuts, 1978; Mazal, 1981; Feranec, 2005).

Allomaternal care is extremely common amongst many eutherian mammals and can involve communal nursing, carrying or thermoregulation of the young by other members of a social group (Isler and Schaik, 2012). This social activity not only reduces the strain on mothers, but has also been demonstrated to increase the physical fitness of female ‘helpers’ by teaching them valuable

skills for motherhood (Dugatkin, 2009). This intraspecific transfer of parental knowledge must be regarded as one of the most complex forms of parental behaviour in the animal kingdom, benefitting as it does not just the mother and offspring, but the entire genetic pool; it also lays the foundations of a sophisticated social structure evidenced in other forms such as herd, flock, or pack organisation.

2.3.3 Juvenile play and agonism

Play, defined loosely as immediately purposeless animal behaviour (Kefoff and Byers, 1981; Burghardt, 2005), is an activity that can be carried out in isolation, or between different members of a species. Isolated play is generally associated with two types of behaviours: object play and locomotor play (Paukner and Suomi, 2008). The first form, object play, refers to the interaction between an animal and an inanimate object, such as that witnessed with rock and stick manipulation in capuchin monkeys (Visalberghi, 1988), or the interaction between juvenile ravens and any novel object (Bugnyar et al., 2007). Another is locomotor play, which involves a rapid change in the direction or style of movement; for example domestic pigs will hop or turn on the spot (Donaldson et al., 2002), whereas bonobos may somersault or spin sharply (Palagi, 2008).

Intraspecific social play is perhaps more relevant to the application of sociality to unobservable, extinct groups such as dinosaurs, and again can be witnessed in various degrees across different taxa, from non-fatal agonistic interactions between two individuals of the same species to more complex, play behaviour moderated with social signals (Palagi et al., 2007; Dugatkin, 2009); both may leave physical marks that in extinct species may be interpreted as evidence of social interactions.

Agonistic or aggressive encounters may be considered as the least socially complex of the two behaviours as they do not imply restraint or an increase to the physical fitness of both parties, but rather improve the access of one individual to an important resource, while decreasing that of another (Drummond, 2006). For example, aggressive behaviour is employed to compete for mates during the breeding season, where the reproductive fitness of the winner is increased, but that of the loser is decreased (Leuthold, 1977). Whereas agonistic behaviour is often associated with times of reproductive readiness, as in the 'necking' combat between male giraffes (Brand, 2007; Mitchell et al., 2009), it can also be witnessed earlier in ontogeny in some animals, and may be important in establishing early social hierarchies, as it discourages challenges when the animals are more developed and might incur or inflict serious injuries (Brien et al., 2013a). For example, juvenile saltwater crocodiles enact agonistic displays of head pushing, biting and tail wagging with conspecifics as early as 2 weeks after hatching (Brien et al., 2013b; 2013c). Similarly, (Mott and Maret, 2011) recorded heightened levels of aggressive behaviour towards conspecifics in the larvae of three species of Ambystomatidae.

In spotted hyenas, highly social animals with pack cooperation and extended parental care, there is a marked transition between intense agonistic interactions to demarcate dominance

between pups in their natal den, and less aggressive, reciprocal play behaviour, which occurs after their first introduction to the communal den (Drea et al., 1996). Even if prefaced by the sort of unrefined aggression displayed by newborn spotted hyenas, true play behaviour is almost always found in juveniles, as they tend to have more time than adults, who are temporally constrained by the energetic pressures of hunting or mating (Burghardt, 1988).

The benefits of social play behaviour during early ontogeny extend beyond those of agonistic interactions. Head butting play action in juvenile big horned sheep, for example, may represent a method of improving a technique that will affect their reproductive fitness at sexual maturity (Berger, 1980). Similarly, away from mammals, juvenile American pond turtles have also been recorded engaging in play behaviour with their foreclaws, in a display extremely similar to that used during sexual display later on in life (Graham and Burghardt, 2010; Burghardt, 2015). Alternatively, Thompson (1996) suggested that play behaviour between partners of juvenile ungulates represents a method of assessing their relative strength and physical improvement between sessions. The prevalence of social play in juvenile ground squirrels has been linked to the faster development of coordination and fine motor skills (Nunes et al., 2004), whereas in the young of extant large predators, such as lions (which may be seen as modern ecological equivalents of large tyrannosaurids), play mimics the skills that they will require later on to successfully hunt, such as stalking, leaping and grappling (Ncube and Ndagurwa, 2010). Play can therefore become an important foundation of complex social activities in many animal groups.

2.3.4 Sexual dimorphism/Mating displays

Sexually dimorphic displays or structures are often important factors in the reproductive fitness of individual organisms, particularly in highly competitive social groups. Strictly behavioural sexually dimorphic factors are herein considered those that are not dependent on the attraction of the opposite sex to some unusual physical structure, or the use of said structure in physical confrontation with a rival. For example, songs in birds are primarily used by males to attract females; the latter are generally attracted to longer, more complex songs, which may be learned by males from their kin group or copied from rival males (Genter and Hulse, 2000; Sockman et al., 2009). Similarly mating behaviour in some lekking birds such as the lance-tailed manakin involves ritual dances accompanying songs, and includes numerous males (Duval, 2013). Such behaviour is relatively easy to observe in modern ecosystems, but would be extremely difficult to infer from fossils, save for the case of exceptional preservation of a syrinx, for example, or some other complex auditory structure.

Combat between males either prior to or after the arrival of a female is also common in extant animals, especially those living in groups. Fights between males over the right to mate with a female are well known in large carnivorous mammals such as lions and wolves (Pusey and Packer, 1982; Derix et al., 1993), whereas fights may occur between male or female crocodylians during the courtship season (Brazaitis and Watanabe, 2011). Aggressive sexual behaviour may lead to more serious injuries in adults than would be incurred during juvenile play fighting, when social signals

are used to moderate physical encounters (Bekoff, 1995; Brien et al., 2013a), and such injuries could reasonably be interpreted as evidence of this particular social behaviour in the fossil record.

Perhaps more useful to the morphological based evidence available to dinosaur palaeontologists are physical structures similar to those used in modern intraspecific sexual competition, which may survive in the fossil record. Extant examples of sexual display structures include the horns of big horned sheep, used in headbutting encounters between males during the rutting season (Geist, 1971), the casques of cassowaries, used for vocalisations in females and head bobbing display in males (Richardson, 1991), and the frills of agamid lizards, which are also used in head bobbing displays (Shine, 1990). Such structures, energetically expensive as they are, are often explicitly associated with sexual display and may present strong evidence of sexual display when found on dinosaurian specimens; especially if associated with pathological features associated with their use in intraspecific sexual combat.

2.3.5 Social groups

Groups of individuals of the same species in the same area might appear to be the clearest evidence of gregariousness in a taxon; however, in modern ecosystems, which assumedly mirror those of the past, there are a number of reasons why animals might congregate. Concomitantly, and typical of previously discussed gregarious behaviours, there is also a gradient of the complexity and longevity of these aggregations.

The first major reason for the congregation of extant animals discussed here is reproduction. Communal spawning in fish such as salmon (Salmonidae) and bass (Centrarchidae) (Neilsen and Geen, 1981; Ingram et al., 2013) is a well known phenomenon, thought to increase the chances of successful fertilisation and reduce the amount of energy that might be wasted in predator avoidance per individual (Jungwirth et al., 2015). Communal egg-laying, the deposition of eggs with those of numerous conspecifics is also an incredibly common occurrence within reptiles and amphibians, with at least 481 modern species taking part in such aggregations (Doody et al., 2009). For example, some ambystomatid salamanders (Harris and Lucas, 2002) and neotropical tree frogs (Roberts. 1994) have been found in vast numbers within these breeding groups, and the practice is also famously well recognised in sea turtles (Doody, 2003).

Communal nesting is the allocation of responsibilities such as protection, feeding and brooding (Brown, 2014) and often occurs in birds, such as geese and sandpipers, both of which also aggregate prior to hatching for reproduction (Melhum, 1998; Johnson and Walters, 2011). It may also occur in larger flightless birds, more potentially analogous to larger non-avian theropod dinosaurs, such as ostriches (Betram, 2014). It may also be found in many small mammals, such as marmots, rats and squirrels ; milk may even be occasionally passed from mother to the offspring of another adult (Koprowski, 1996; Blumstein and Armitage, 1999; Hayes, 2000). Extensive juvenile crèches in crocodylians have already been discussed, but represent another excellent example of sociality within the extant archosaurians.

Animals may also congregate for reasons of thermoregulation. This is particularly apparent in ectothermic animals, such as reptiles and amphibians, which must adapt to the extreme temperatures of high altitudes and latitudes. Toads living at high altitudes in the Argentinean Andes, for example, have been found in aggregations that maintain individuals' body temperature (Espinoza and Quinteros, 2008). Huddling groups, aggregations formed to reduce the surface area exposed to the cold or to absorb the body heat of conspecifics are present in many species of mammals and birds (Doody et al., 2009). However, many of these endothermic taxa, such as king penguins or rats, display other highly social behaviours such as communal nesting, and hence, these aggregations may be simply one aspect of a larger, more complex social structure (Gilbert et al., 2009).

Perhaps more surprisingly for animals typically considered asocial, snakes living at extreme latitudes escape below-freezing temperatures by congregating in underground hibernacula; although the temperatures may remain low here, the overall loss of body temperature per snake is less than that experienced outside of the group (Reiserer et al., 2008). Although there may be concomitant benefits to staying together in aggregations, such as the decreased likelihood of attack or facilitate fertilisation, the primary goal of these groupings is thermoregulation, and cannot be considered gregarious in the same sense as herds or cooperative packs (Aubret and Shine, 2009).

Temporary opportunistic aggregations may also occur, that are not necessarily followed or prompted by more complex social behaviour. Currie and Eberth (2010), for example, suggested that the opportunistic gathering of predators or scavengers around an atypically bountiful food source, such as bears congregating around salmon crowded rivers during the spawning season, should not be considered true gregarious behaviour; it does not extend beyond this meeting and is not reliant on the behaviour of conspecifics. Similarly, temporary aggregation may be induced between individuals under the common threat of predation; in birds, prey species may sometimes group together to reduce the risk of predation (Fernandez-Juricic et al., 2004), whereas others, such as chickadees, will respond to the distress call of intraspecifics or interspecifics, to mob an attacking predator (Hurd, 1996). Over a more extended period of time, it has already been discussed how generations of iguanas may stay together after hatching for protection (Burghardt, 1977). Small coalitions may be formed between two to three males of typically solitary predators such as cheetahs and fossas, to more easily procure food (Estes, 1991; Luhrs et al., 2013). Such facultative social coalitions are uncommon, however, and are usually limited to male siblings (Estes, 1991).

Fully gregarious animals are well represented in both ectothermic and endothermic taxa, and present many of the social behaviours thus far discussed, while also maintaining complex and permanent social structures consisting of various ages and genders. For prey species, grouping behaviour, such as shoals in fishes or herds in herbivorous mammals, may primarily be seen as anti-predation techniques (Stier et al., 2013), but bring a plethora of concomitant benefits. For instance, increased group size may also increase the success of foraging for food, as in the case of

bluegill sunfish (Centrarchidae) (Mittlebach, 1984), whereas some cryptic colouration, such as the stripes on zebras or zebrafish, only decreases the threat of predation when living in a group (Godfrey et al., 1987). Additional benefits from social behaviours that naturally incur within a group environment may include protection from the elements (Gilbert et al., 2009), an increase in the chances of mating (Ingram et al., 2013), less energy required for fast, early growth (Poole, 1985), and communal nesting or protection of young (Brown, 2014).

For predatory taxa, the salient evolutionary prompt for this behaviour appears to be to improve the chances of successful hunting; however, many of the benefits are also inherent in pack, pride or clan living (Gittleman, 1989). Coordinated hunting has evolved across many different groups of vertebrates and, in this review, constitutes the most sophisticated form of social complexity in that it requires cooperation, communication and often, social learning by juveniles (Pitman and Durban, 2012). Far from its early scholarly limitations to mammalian taxa socially learned cooperative hunting has recently been demonstrated in lemon sharks (Guttridge et al., 2013), scrub jay birds (Bowman, 2003), sea snakes and crocodilians. Some species of crocodylians even display role partitioning (Doody et al., 2013). In large carnivorous mammals, cooperative hunting is rare (Gittleman, 1989), but spectacularly intricate when it does occur. Killer whales for example, employ a cooperative wave-washing technique in which currents created by the pod sweep seals off the safety of ice floats and into the water; calves are often included in these hunts and learn through demonstration by adults (Pitman and Durban, 2012). In coordinated hunters such as spotted hyenas, lions or killer whales, it is interesting to note that social play in juveniles is evident; this suggests that early play behaviour may be important in refining complex physical and communication skills that will be required to join the pack/pod in coordinated hunts later in life (Martin and Caro, 1985; Guinet et al., 1991). In the case of spotted hyena, coordination has become so well refined between siblings, that kin pairs show significant coordinated problem solving abilities (Drea and Carter, 2009). As well as assisting in the procurement of food through pack hunting, a benefit of large carnivore group living is in the defence of territory against contemporary predators (Packer, Sheek and Pusey, 1990). For example, spotted hyena clans can support up to 55 individuals, giving them adequate numbers to protect their territory from larger predators, such as lions (Gittlleman, 1989).

2.4 Modern social behaviour: a useful analogue for dinosaur palaeobiology?

Although this brief examination of social behaviour in modern animals is by no means extensive, it does give an impression of the breadth of different activities that may be considered under the umbrella term of social behaviour. Therefore, it is suggested that gregariousness be considered as a spectrum rather than a singular condition, which is present or not present in a taxon. This is particularly important when attaching such a term to extinct animals, like dinosaurs, as social inferences are often based off of evidence for only one aspect of gregarious behaviour e.g. sexual display or play fighting.

The flexibility of social behaviour in certain taxa has also been demonstrated; some social aggregations are temporary or opportunistic in some species, whereas they may form part a longer socially oriented life history in others. Further to this temporal variability in sociality within individuals, the extent of social behaviour is also not necessarily consistent between phylogenetically close taxa; lions exhibit numerous types of social behaviour, in contrast to other felids, which show only facultative sociality at times. Given then that gregariousness is a phylogenetically flexible concept that may be reasonably viewed as a gradient measured by looking at numerous social behaviours of an organism extended periods of time, allocations of social/non-social dinosaurs may be considered as too simplistic.

However, from this review of sociality in modern animals, there are some features and trends that we may associate with particular types of social behaviour that may also be present in the fossils of dinosaurs. For example, intraspecific combat, through play fighting in juveniles (e.g. lion cubs (Ncube and Ndagurwa, 2010)) or agonistic sexual/dominance competitions (e.g. big horned sheep (Geist, 1971)) cause injuries of varying degrees; similar pathologies, and therefore similar behaviour may be witnessed in dinosaur bones. Structures associated with sexual displays or parental care such as casques in cassowaries (Richardson, 1991), or integumentary sense organs (ISOs) in crocodylians (Soares, 2002; Brazaitas and Watanabe, 2011), may also have been present on some species of dinosaur. Bone beds may also be interpreted as juvenile crèches by analogy to gharials (Lang et al., 2013)), temporary aggregations primarily due to environmental factors (e.g. snake hibernacula (Reiserer et al., 2008)), or complex social structures (e.g. spotted hyenas (Drea et al., 1996)) depending largely on the demographic of the preserved population. Slow early growth rates and long life histories in different animals seem to reflect the necessity of extensive parental care early in life, which may lay down the foundations of a more complex social system (e.g. altricial lion cubs (Pusey and Packer, 1994)). Conversely, rapid early growth, especially of important 'survival tools' (e.g. canines or claws in tigers (Feranec, 2005)), would seem conducive to a mostly solitary lifestyle after a short period of parental care. The type and extent of parental care (from egg guarding in some fish (Jeffery et al., 2014) to nursing, feeding, protection and teaching within Carnivora (Mandal, 2012)) may be also be inferred by comparing clutch sizes, with other factors such as the growth rates of young to speculate as to the animals reproductive strategy.

These avenues of evidence for specific social behaviours in extant animals provide a context for studies into gregarious characteristics in dinosaurs. Although Currie and Eberth's (2010) idiom that all dinosaur behaviour is by definition inferred by palaeontologists still holds true, the sheer scope and variety of social encounters in modern ecosystems suggests that some of these behaviours were likely witnessed in ancient ecosystems as well. Although phylogenetic inferences on sociality should be kept to a minimum, it is also worth noting that all of the social behaviours included in this review, from parental care to group living, are displayed at some level in the closest extant relatives of dinosaurs: birds and crocodylians. Some examples of previously described

fossil evidence for social behaviour are briefly addressed in the next section of this chapter, and should be viewed in reference to this modern review.

2.5 Social behaviour in dinosaurs: palaeontological evidence

The understanding of dinosaur behaviour has progressed significantly from the early, outspoken research of Ostrom (1969) and the broader, more dramatic inferences of Bakker (1988), such that social behaviour has been suggested for many groups of dinosaurs, herbivorous and carnivorous. As there are already rather extensive recent summaries of the palaeontological evidence for social behaviour in dinosaurs (see Isles, 2009; Currie and Eberth, 2010 for comprehensive reviews on the subject), another effort to collate all the existing evidence would be perfunctory. Instead, this section merely provides examples of the different types of palaeontological evidence for sociality that have been proposed, with a view to how they might be combined with knowledge of gregarious behaviour from modern ecosystems, to better understand dinosaur sociality. Suggestions are made for further methods of elucidating social behaviours from dinosaur material, and an initial analysis of the current evidence for any gregarious behaviour in *Gorgosaurus libratus*, the focus of this thesis, is made.

The different types of evidence for social behaviour in dinosaurs herein discussed are broadly grouped into four of the main types of gregariousness reviewed for modern taxa: social groups, play fighting/agonism, parental care and sexual display. Although each example of a palaeontological 'social characteristic' is presented as evidence of one particular type of behaviour, these are not necessarily mutually exclusive. For example, pathologies can be used to support inferences of both play fighting as well as sexual competition between males.

2.5.1 Social groups

Undoubtedly the most spectacular form of evidence for social grouping in dinosaurs is the discovery of monospecific bone beds; areas which contain numerous bones of multiple individuals of a single taxon that all died at the same place and time. One of the most famous examples is at Ghost Ranch in New Mexico, where over 1000 individuals of the Triassic theropod *Coelophysis*, have been recovered from about 30 cubic metres of rock since its discovery in 1947 (Schwartz & Gilette, 1994). Here, the mixture of juvenile bones amongst adults (Bhullar et al., 2012) suggests at least some degree of parental care in allowing the young to stay near the adults, and the identification of male and female 'morphs' (Rhinehart et al., 2009) provides further support to the idea that this might represent a truly social group, such as a pack. Whereas the presence of juveniles and the absence of clutches most likely rules out the possibility of a mating assemblage akin to the breeding beach phenomena of sea turtles (Katselidis et al., 2013), it may yet represent a temporary feeding aggregation at a pond or river, rather than a true social group; this is compounded by taphonomic evidence suggesting catastrophic death by the flooding of a nearby water source (Rhinehart et al., 2009).

Similarly, a *Sinornithomimus* bonebed at the Sohongtu site in China, contains the remains of at least 20 individuals that all perished at the same time in a debris flow; interestingly, lines of arrested growth in histological sections estimated that all the individuals were between one and seven years olds at the time of death (Varricchio et al., 2008a). Juvenile only aggregations have been described for numerous other dinosaur genera, such as the ceratopsians *Protoceratops* (Weishampel et al., 2000) and *Psittacosaurus* (Zhao et al., 2014), and may suggest no parental care early in juvenile development, prompting juveniles to band together for safety (e.g. nest emergence in iguanas (Burghardt, 1977); alternatively, they may be representative of juvenile crèches, such as is witnessed in modern crocodylians (e.g. gharials (Lang et al., 2013)); in this scenario, the difference in density between adult and juvenile bones may have caused them to be deposited in different areas, making it appear as a juvenile only aggregation (Jepsen, 1964).

A bone bed at Dry Island Buffalo Jump, in the Horseshoe Canyon formation of Alberta, contains the partial skeletons of at least 26 individuals of *Albertosaurus sarcophagus* (Erickson et al., 2010), sister taxon to *Gorgosaurus* (Holtz Jr., 2001; Currie, 2003) most likely killed during a storm-driven flash flood (Eberth and Currie, 2010). Currie and Eberth (2010) proposed that this assemblage to some extent represented gregariousness in *Albertosaurus*; this is certainly supported by the mixed age demographic of the assemblage. However, the remains of other potential prey taxa such as *Albertonykus* and *Hypacrosaurus* , suggest that it might yet represent an opportunistic aggregation over food sources (Eberth and Currie, 2010). Multiple individual bone beds are fairly common, even in large tyrannosaurids, and may be indicative of at least facultative gregariousness in these large non-avian theropods (Currie and Eberth, 2010).

Multiple trackway sites have been cited as evidence of herding or flocking behaviour in dinosaurs, originating in the early Jurassic period; the early evolution of such behaviour may have provided a platform for more complex social interactions later in the evolutionary development of dinosaur lineages (Coombs, 1990). Although monospecific bonebeds can provide accurate life history data for a local population that died contemporaneously, trackways may capture dynamic social interactions in a manner that bones cannot (Lockley, 1991).

Lockley (1999) supported the idea that multiple footprints at one site might reflect herding and pack movement in dinosaurs, but proposed strict criteria for the allocation of trackways to one gregarious group of dinosaurs. He suggested that herd/pack motion is supported only if multiple parallel trackways of the same type are present on the same surface, have similar spacing between them, and have a common preferred direction (Lockley and Matsukawa, 1999). Using these criteria, potential herd/pack trackways have been linked with most major dinosaur groups including sauropods (Bird, 1939; Barnes and Lockley, 1994; Lockley et al., 2002; Lockley et al., 2012), theropods (Barco et al., 2006), thyreophorans (Petti et al., 2010; Lockley et al., 2006), ceratopsids (Lockley and Hunt, 1995) and ornithopods (Matsukawa et al., 1997; Rodríguez-de la Rosa, 2007). However, restrictions to the interpretation of trackways include the inability to link a trace fossil to

a particular taxon and the danger that trackways have been overprinted and then time averaged by taphonomic pressures (Myers and Fiorillo, 2009).

An example of trackways appearing to reflect herd dynamics, the Peace River Canyon in British Columbia boasts more than 100 trackways in a 500 metre area of the Lower Cretaceous Gething Formation (Currie, 1983) is dominated by ornithopod tracks known as *Amblydactylus*. At some points in the trackways, most likely created by hadrosaurs, there are nine to ten parallel pairs of tracks, which not only follow the same general direction, but also curve out and in at the same time. Similar to previously discussed bone bed evidence, juvenile aggregation is supported by pairs of smaller tracks, equally spaced and leading in the same direction (Currie, 1983). Again, the trend of juvenile aggregation in dinosaurs seems to reflect what we see in some modern taxa such as crocodylians and iguanas.

Small juvenile social grouping in sauropod dinosaurs such as *Alamosaurus,* has received strong substantiation from both bone bed and trackway evidence. There have been five juvenile specific sauropod trackways found that complement juvenile crèche bone bed sites such as Mother's day quarry in Montana's Jurassic Morrison Formation and Big Bend National park from the Upper Cretaceous of Texas (Myers and Fiorillo, 2009). In modern animals too, such as ungulates, niche partitioning between adult and juvenile groups occurs in species with huge variations in body mass over ontogeny; the gulf in body size translates into an incompatible difference in energy requirements, and so it may be preferable to form social groups conspecifics of the same age, with similar lifestyles (Polis, 1983; Myers and Fiorillo, 2009). Because of the influence of intraspecific body size disparities on social grouping, comprehensive body mass estimations, especially of isolated specimens, may be beneficial in predicting whether or not a particular dinosaur was likely to form social groups while young, or inhabit the same ecological niche as their parents.

2.5.2 Play Fighting/Intraspecific competition

The most direct example for intraspecific physical encounters is in the study of palaeopathologies; particularly bite and claw marks in carnivorous dinosaurs. There certainly appears to be substantial palaeopathological evidence for intraspecific combat in tyrannosaurids; conspecific bite marks have been described on specimens of six genera, including *Albertosaurus* and *Tyrannosaurus* (Rothschild and Molnar, 2008). Face biting (e.g. Hone and Tanke, 2015) seems to be a particularly common phenomenon amongst this group of dinosaurs, concurring with the most prominent area for biting during play and sexual combat in modern animals, such as lions or crocodylians (Ncube and Ndagurwa, 2010; Brien et al., 2013a). To restrict the interpretation to a specific social behaviour, the bite or claw marks must be examined in the context of the specimen age and severity of the injuries. As play fighting mostly occurs in juvenile individuals of extant animals (Burghardt, 1988), one would expect less severe bite marks if received during play, whereas territorial or sexual competition in adults may have resulted in more severe, potentially fatal wounds.

This dichotomy appears to be reflected in the palaeontological evidence. For example, a large tyrannosaurid tooth embedded in the dentary of another adult tyrannosaurid from Dinosaur Provincial Park most likely represents fatal ante-mortem intraspecific agonism associated with mating, dominance, or territoriality (Bell and Currie, 2010). Contrastingly, Peterson et al., (2009) described juvenile tyrannosaurid skull material from the Hell Creek Formation, Montana that shows partially healed bite marks. The age and size of the individual most likely discounts an agonistic interaction associated with mating or territory, and may be indicative of early juvenile agonism to assert dominance over siblings, as witnessed in crocodylians (Brien et al., 2013a; 2013b) or spotted hyenas (Drea et al., 1996). Similarly, Tanke and Currie (1998) described multiple healed bite marks in *Gorgosaurus* and *Sinraptor*; both individuals were at least sub adult in age, implying that play behaviour was an unlikely cause. Interestingly, Rothschild (2013) proposed that many of the facial pathologies associated with bite marks were actually inflicted by manual and pedal claws, although in this example the body form of tyrannosaurids and the fact that bone is much harder than the keratin covered claws may make this unlikely. There are, however, modern animals that utilise claws in intraspecific fighting have already been alluded to in this review (e.g. lions (Ncube and Ndagurwa, 2010) and pond turtles (Graham and Burghardt, 2010)). Whichever 'weapon' was responsible for the scarring blows in such encounters between conspecifics, the social interpretation remains the same. The extent of the injury incurred by each of these animals (all of the previously listed examples involved the actual puncturing of bone), is in all probability too great to associate with play behaviour, which seldom results in such substantial damage to either playmate (Tanke and Currie, 1998). One intriguing social postulation based on a high number of tyrannosaurid bite marks on the occipital condyles of ceratopsians is that large theropod dinosaurs may have engaged in object play behaviour with the bones of kills; occipital condyles have little to no nutritional benefit for carnivores and could only be accessed in a decapitated carcass (Rothschild, 2014). As was alluded to in the modern sociality section of this review, object play behaviour is common in a variety of extant taxa, including the two surviving branches of Archosauria: crocodylians (Fagan, 1981) and birds (Bugnyar et al., 2007).

2.5.3 Parental behaviour

Spectacular finds that have apparent implications for parental behaviour in dinosaurs have been exceptional in their frequency in recent years, to the point that bird-like brooding behaviour is extremely well represented in some non-avian theropod genera. Norell et al. (1995) described an exceptionally well preserved oviraptorid that died in a brooding posture atop a clutch of eggs in the Gobi desert, Dong and Currie (1995) discovered another, more fragmentary oviraptorid skeleton in association with a clutch of six eggs, and Clark et al. (1999) later re-estimated the number of eggs to be at least 15. More recently, Fanti et al. (2012) also described a specimen of *Nemegtomaia*, in a brooding position of a nest in southern Mongolia. Within Theropoda, brooding sites have been postulated for *Deinonychus* (Makovicky & Grellet-Tinner, 2000; Grellet-Tinner, & Makovicky, 2006) and *Troodon* (Varricchio et al., 1999; 2002); the close phylogenetic relationship between these dinosaur taxa and extant birds lends substantial weight to the idea that Aves-like

nest brooding occurred within certain dinosaur species. Although brooding, the minimum parental behaviour exhibited ubiquitously by modern birds (with the exception of those that practice brood parasitism), is well evidenced among certain dinosaur groups, they likely exhibited a wide range of post-hatching parental care depending on ecological and physiological factors.

Varricchio et al. (2008) attempted to use the correlation between egg clutch size and female body mass in modern birds to predict parental care behaviour for dinosaurs (oviraptorids and troodontids) for which brooding behaviour had been attributed. For these two groups, correlations predicted high levels of paternal investment, similar to those witnessed in modern ostriches (Davies, 2002). However, the analysis may have been biased by incorporating together bird taxa with different developmental rates of young. Certainly, the technique of Varrichio et al. (2008) should only be used when discussing brooding or egg protecting behaviour. Growth rates of young are important in determining the levels of post hatching parental investment and should be considered before making inferences about the ability of dinosaur young to live independent of their parents, or the requirement for some sort of social care early in ontogeny. This considered, relying strictly on overall growth rates may also produce misleading evidence. Although modern day crocodylians exhibit an r-strategy in regards to the high number of eggs laid at once, they still invest heavily in parental care (Charruau and Henaut, 2012; Lang et al., 2013). Similarly, although tigers exhibit altricial growth, they do not receive the same extent of parental care as do lions, which grow to somatic maturity within the pride. In carnivorous dinosaurs at least, it may be worthwhile contrasting overall growth rates with the developmental rates of 'weapons' such as teeth or claws that are key to their survival, independent from conspecifics.

Bone bed evidence has already been discussed at length, and a number of monospecific, juvenile dominant sites have been described for a variety of different dinosaur taxa such as *Protoceratops* (Weishampel et al., 2000; Hone et al., 2014), *Psittacosaurus* (Zhao et al., 2014), and *Sinornithomimus* (Varricchio et al., 2008b). Trackway evidence has also substantiated the possibility of juvenile only groups in sauropods (Myers and Fiorillo, 2009) and hadrosaurs (Currie, 1983). Whereas strictly juvenile fossil or trace fossil assemblages may be indicative of kin groups or small juvenile groups, evidence for true juvenile crèches, as seen in modern crocodylians, may be present at a site in Liaoning, China, where one adult specimen of *Psittacosaurus* was discovered with 34 juveniles (Meng et al., 2004). Burns et al. (2011) also described an aggregation of four juvenile *Pinacosaurus specimens* from a site close to the Chinese/Mongolian border. In juvenile aggregations, dinosaurs may have found an excellent way to reduce energetic costs associated with parental care and produce high clutch numbers, whilst still maintaining high survival rate of young. Juvenile crèches or groups may have also led to other social behaviours, such as play fighting, which may have benefitted them later on.

Another method of examining potential independence in dinosaurian young may be to contrast their diets with those of adult specimens; any significant differences between the diets of juvenile as opposed to adults may also reflect ecological and behavioural changes that these

animals experienced during growth. For example, modern lion cubs are allowed to feed at the kills of adults (Pusey and Packer, 1994) whereas young, independent tigers have to restrict themselves to smaller prey until they are of adult size (Mandal, 2012). Few attempts have been made to explore parental care through comparing ontogenetic change in diet in dinosaurs; however, Wilkinson and Ruxton (2012) suggested that high C:N element ratios in sauropods may have implied higher activity levels in juveniles, provided for by an omnivorous diet, in contrast to the low energy levels and herbivorous diet of adults. Bakker and Bir (2004) also proposed that *Allosaurus* parents dragged kills to a lair and allowed young to feed off them, based on a mixed assemblage of juvenile and adult shed teeth associated with a kill site at Como Bluff, Wyoming.

Rather than simply excavate in the hope of finding specimens with stomach contents, two methods exist to contrast diet in adults and juveniles. First, stable ^{13}C and ^{15}N isotopes from tooth enamel can be used, and the examination of tooth wear patterns on articulated juvenile and adult specimens of a species. Carbon and nitrogen isotopic ratios (e.g. $\delta^{13}C$ & $\delta^{15}N$) have been used widely on extinct and recent mammals for determination of diet and ecology (Coltrain et al., 2004, Feranec, 2005, Codron et al., 2007), and may theoretically be applied to individuals of the same species, but of different biological ages to illustrate any change in the trophic level at which they feed throughout ontogeny. Similarly, contrasting tooth wear between juveniles and adults may reflect dietary and potentially, ecological changes throughout growth.

2.5.4 Sexual display

As previously discussed, some bite or claw marks on the bones of dinosaurs may have been incurred through agonistic interactions over mating rights. However, there are also physical structures evident in the fossil record that may have been utilised in sexual displays. The review of modern sociality reveals examples of sexual display structures in the horns of big horned sheep (Geist, 1971), the casques of cassowaries (Richardson, 1991), and the frills of agamid lizards (Shine, 1990), and similar features have been shown for certain dinosaur species. Cranial ornamentation is the most commonly found potential sexual structure in dinosaurs. Well known examples in herbivorous dinosaurs include the hollow crest of *Parasaurolophus*, which has been hypothesised as acting as a resonating chamber during sexual displays (Weishampel, 1981; 1997), and the frills and horns of ceratopsians have been considered structures useful in the attraction of mates or intraspecific combat (Farke, 2004, 2009). Similarly, the dome of *Pachycephalosaurus* has long been claimed to have been used in agonistic combat over mating rights, similar to those witnessed in big horned sheep (Maryanska et al., 2004); this oft-cited theory has been critiqued by Sues (1978) and Goodwin and Horner (2004) as the bone structure of the skulls may have directed shock towards the brain case and facilitated concussions. However, wear marks recently discovered on the domes of *Pachycephalosaurus*, mirrored those found on modern head-butting structures and seemingly substantiate the intraspecific combat hypothesis (Peterson et al., 2012); this is an excellent example of two forms of evidence complementing each other to increase confidence in a social behaviour hypothesis. Incredibly well preserved soft tissue crests, such as that recently found on

Edmontosaurus, would seem inappropriate for most mechanical roles, such as defence or combat, and likely constitute further evidence of a structure developed for sexual display or species recognition (Bell et al., 2014).

Molnar (2005) and Currie and Eberth (2010) present excellent reviews of cranial ornamentation in theropod dinosaurs, which may be incorporated into some sorts of sexual display or physical sexual competition. The prominent crests on *Cryolophosaurus* (Smith et al., 2007) and *Monolophosaurus* (Zhao and Currie, 1993) may not possess the intuitive weapon-like structure of, for example, the lance-like horns on ceratopsians, and would appear to be better utilised as sexual fitness indicators or even gender identifiers. However, some theropod cranial ornamentation, such as the supraorbital horns of *Carnotaurus,* have been hypothesised as reducing the damage incurred during head-butting displays of dominance or sexual competition (Paul, 1988), although this has not yet been associated with any corroborating cranial pathologies.

Allometric studies may play an important role in determining whether or not a structure such as a crest or horn is important in sexual display; features that experience extremely positive allometric growth to produce obvious visual cues by the time of sexual maturity would seem to fit this model. Dodson (1975), for example carried out an allometric study on the crests of the then 12 species of lambeosaurines. By measuring how the crest grew in relation to the rest of the body, he found that there was mixture of negative and positive allometry, which correlated with the size of the animal at the time. After synonymising many of the species, it was clear that crest growth was slower in smaller animals and faster in larger animals; this size difference may have correlated with sexually dimorphic forms or individuals of different biological ages (Dodson, 1975). The growth patterns of lambeosaurine crests is echoed in the aforementioned casques of cassowaries, which are relatively small until about the animal is about 80% of full size, when they become large and conspicuous, and play a key role in the mating displays of both males and females (Dodson, 1975; Richardson, 1991). Similar allometric studies could be used to illuminate positive allometry of crests or supraorbital horns in dinosaurs, given an acceptable range of samples.

Feathers have been well established as a common feature of the coelurosaurian dinosaurs (Chatterjee and Templin, 2004). Although some feather types may have been utilised in early flight or gliding (Xu et al., 2003; Longrich 2006), others could have been incorporated into sexual displays in similar manners to some modern birds such as the lance-tailed manakin (Duval, 2013) or the peacock (Loyau et al., 2005). The tails of some oviraptorosaurs, for example, seem to have incorporated pygostyles with feather fans, which in conjunction with relatively large tail muscles, could have been used in sexual displays (Barsbold et al., 2000; Li et al., 2012; Persons et al., 2013).

2.6 Is there palaeontological evidence of social behaviour in dinosaurs?

As has been demonstrated in this section, there is a wide pool of palaeontological evidence for various social behaviours in dinosaurs, all of which may be anologised to the main social behaviours evident in extant ecosystems. Social grouping in dinosaurs may be inferred from bone

beds, and can be related to different group types seen in modern animals, such as juvenile crèches or mixed herds, by examining the age demographic of the population through histological techniques. Trackways also provide evidence of the dynamic actions of social groups and comparisons of spacing, sizes, depths and directions of footprints can also illuminate details as to the nature of the aggregation. Reviewing some of the bone bed and trackway evidence for gregarious behaviour depicts a high level of juvenile-only aggregations amongst dinosaurs.

Play-fighting, such as can be seen in the juveniles of modern animals, is underrepresented in the dinosaurian fossil record. However, a high proportion of facial pathologies does indicate some degree of agonism throughout ontogeny in some carnivorous groups. These agonistic encounters may have occurred due to disputes about territory, mating or other resources. However, the severity of the injuries in the examples given, probably rules out play fighting as a viable cause. Brooding over nests, as seen in all species of modern bird except brood parasites, is well represented in some dinosaur species due to spectacular adult-egg association finds. The extent of post-hatching parental care, however, involves greater levels of inference, but has been hypothesised for some dinosaurs based on bone beds that resemble modern juvenile crèches, and allometric studies based on the clutch size of dinosaur nests.

Additional analyses for inferring post-hatching parental care in carnivorous dinosaurs are herein suggested. One method is to compare the overall growth rates of species for which ontogenetically variable samples are available. Another is to look at the the growth rates of 'defensive tools' such as claws or teeth, to determine if certain dinosaurs were more suited to hunt and live independently of parents. Another novel method of examining the potential independence of young predaceous dinosaurs, such as tyrannosaurids, may be to contrast diet through ontogenetic stages by examining tooth wear or even stable isotopes of carbon and nitrogen. Significant dietary changes throughout ontogeny may also reflect ecological and behavioural changes that these animals experienced during growth.

Sexual display, witnessed in modern animals through intraspecific combat or rituals involving specific skills and features, may be hypothesised for dinosaur taxa based on the presence and allometric growth of cranial ornamentation, pathologies incurred during intraspecific combat for mating rights or the presence of tail feathers associated similar to those used for display in modern animals.

Although there is inevitably a large degree of inference associated with hypothesising social behaviours for any extinct taxa, there exists a wide variety of evidence with which to examine the problem. Focusing only on one line of investigation, however, such as cranial ornamentation, often results in a number of unnecessarily ambiguous competing hypotheses. Multidisciplinary analyses, which examine numerous forms of evidence, are therefore proposed as the most suitable methods to investigate social behaviour in dinosaurs. Such styles of investigation have achieved some success in the past. For example, juvenile only sauropod trackways were complemented by a number of strictly juvenile sauropod bone beds, and a significant contrast in C: N elemental ratios between

juveniles and adults (Wilkinson and Ruxton, 2012), to support the theory of ontogenetic segregation in some long necked dinosaurs (Myers and Fiorillo, 2009). Similarly, the theory that *Pachycephalosaurus* head-butted to compete for mates was first proposed due to the resemblance of the characteristic thickened dome of that taxa to structures in extant taxa such as big horned sheep (Maryanska et al., 2004). This comparison to extant taxa was then corroborated by wear marks in the areas of the skull where such pathologies would be expected if the animal was indulging in headbutting (Peterson et al., 2012). A multidisciplinary approach was also used to evaluate the motivation behind aggregation behaviour in of the multiple individuals found in the *Albertosaurus* bone bed at Dry Island, Alberta. In a prime example of how numerous forms of palaeontological analyses may be used to assess social behaviour in dinosaurs, this aggregated tyrannosaurid population was examined for pathologies (Bell, 2010), growth rates and life histories (Erickson et al., 2010), and studied in the context of extant ecological correlates and phylogenetically close taxa (Currie and Eberth, 2010).

2.7 Final remarks

From a review of the immense variety of social behaviours witnessed in extant taxa, gregariousness should be considered as a spectrum, with various grades that are not necessarily consistent within phylogenetic groups. The extreme deviation amongst modern animals in the extent, investment, motivation and longevity of different social behaviours, and copious evidence for convergence between disparate groups, suggests that studies into the social behaviour of extinct taxa, such as non-avian dinosaurs, should be narrowed down to specific behaviours such as sexual display or parental care rather than broadly grouped as social or non-social animals. Saying this, modern analogues should be used to contextualise hypothesised social behaviours in dinosaurs, and examining gregarious behaviour in ecologically comparable animals may be more appropriate than that exhibited by phylogenetically close taxa.

A summary of the palaeontological evidence for social behaviour has produced numerous potential avenues of research involving bone beds, multiple trackway sites, body mass estimation, palaeopathologies, egg clutches, and the developmental rates of overall body size, and particular features such as teeth or horns. The adoption of a multidisciplinary approach by researchers was also recommended as a means to better restrict theories of sociality. This literature- based summary will form the foundation for the following chapters of this thesis, in which the potential for social behaviour for a large tyrannosaurid: *Gorgosaurus libratus* will be evaluated based on a host of different techniques such as palaeopathology, allometric growth, skull changes throughout ontogeny and growth rates.

Chapter 3

Missing data and mass estimation for tyrannosaurid dinosaurs: can diameter take the place of circumference for studies of sociality?

3.1 Introduction

Missing data is a major limitation in palaeontological studies, decreasing confidence in analyses and drastically reducing sample sizes (Kearney & Clark, 2003). The problem of missing data is far reaching within many subsets of the discipline, and affects a host of palaeontological methodologies. In fossil reconstructions, missing data can limit the accuracy and extent to which an extinct organism can be recreated (Grillo and Azevedo, 2011). It can also impact the rate at, and specificity with which new specimens may be described and assigned a phylogenetic position; missing data has prevented more exclusive phylogenetic resolution for the potential Chinese tyrannosauroid *Chingkangosaurus fragilis*, known only from fragmentary scapula remains (Brussate et al. 2013), and delayed a comprehensive phylogenetic analysis of *Deinochyrus mirificus* for fifty years (Lee et al., 2014).

The potential impact of missing data in morphometric analyses is well known, and alternative missing data estimation techniques, such as 'Bayesian Principal Component Analysis' and 'mean substitution' have been proposed and compared (Campione and Evans, 2011; Brown et al.,2012). Phylogenetic analyses are also complicated by the effect of missing data (Wilkinson, 2003; Wiens, 2003a; Wiens, 2006; Wiens and Morrill, 2011; Lemmon et al., 2009), and in this subfield of palaeontology, missing data estimation models have also been devised to reduce the effect of spaces in the sample (Norell & Wheeler, 2003).

The most common cause of missing data in a palaeontological sample is taphonomic deformation (Chapman, 1990; Dilkes, 2001; Miyashita et al., 2011; Arbour & Currie 2012; Tschopp et al., 2013; Hedrick & Dodson, 2013). The geological pressures that distort and destroy fossils as they form are beyond the control of palaeontologists, however, paucity in sample size can also be compounded by anthropological factors. Human error might lead to the destruction of fossils due to accidental damage or vandalism (Lipps, 2009), the misplacement of specimens or accompanying information between excavation and preparation, or even inappropriate measurement of specimens. Missing data can also be generated by lack of access to the complete specimen due to backlogs in fossil preparation laboratories, its inclusion in a mounted museum or university display, or even poor relations between palaeontological institutions.

This chapter looks at femoral circumference in tyrannosaurid dinosaurs as a case study in the examination of missing data sets within palaeontology, with a view to bolstering the sample sizes that may be important in elucidating social behaviour amongst dinosaurs. Load-bearing bones like femora form an important component of the mammalian-like erect posture that allowed

dinosaurs to attain great speeds and vast body sizes, and are therefore important components in the investigation of dinosaur behaviour (Persons & Currie, 2011a; Persons & Currie, 2011b, Benton et al., 2011; Seymour et al., 2011; O'Gornan & Hone, 2012). Their proportions compared to other limb bones have been used in descriptive studies, such as that of *Gigantoraptor erlianensis* (Xu et al., 2007).

More specific to the goals of this thesis, femoral circumferences are important in several subfields of palaeontology, which may be used to infer social behaviour in dinosaurs. For example allometric scaling studies widely utilise femoral dimensions, using them primarily as bones with predictable growth rates to which the relative rate of growth of other parts of the body may be compared to (Christiansen, 1998; 1999; Currie et al., 2003; Christiansen and Fariña, 2004; Carrano, 2001; Bypee et al., 2006; Kilbourne & Makovicky, 2010; Funston et al., 2015). In chapter one, the importance of positively allometric growth in the formation of sexual display structures and 'predatory tools' important for an individual's independent survival was discussed (Dodson, 1975; Feranec, 2005). If such allometric relationships are to be employed to a similar effect to explore the possibility of sexual display structures in *Gorgosaurus* (See Chapter 3), femoral dimensions are integral comparative bones (Currie et al., 2003). In bone beds, one of the prime repositories of evidence for gregariousness in dinosaurs, femoral counts are often used to estimate the minimum number of individuals present (Erickson, 2010), and Lee et al., (2008) also used femoral circumferences along with histological growth lines to create a life history model for a bone-bed population of *Hypacrosaurus*. Modern body mass estimation techniques for dinosaurian taxa rely heavily on femoral circumference data (Campione et al., 2012; 2014) and have in turn become integral parts of studies with implications on dinosaur social behaviour, such as the construction of growth curves in tyrannosaurids (Erickson et al., 2004) and the assessment of parental behaviour in oviraptorids (Varrichio et al., (2008). Extensive differences in body mass between juveniles and adults have also been cited as evidence of changing ontogenetic niches (Polis, 1983; Myers and Fiorillo, 2009).

Missing femoral data is a problem with tyrannosaurids particularly, as they are bipedal and thus have a reduced number of bones which can be used for bone loading (e.g. Farlow et al., 1995), locomotion (e.g. Heinrich et al., 1993; Persons & Currie, 2011a; Persons & Currie, 2011b) and body mass studies (e.g. Erickson et al. 2004, Campione & Evans, 2012; Campione et al., 2014; Benson et al., 2014). Tyrannosaurids face an additional problem in that they are also popular mounted exhibits in museums, and thus access to measure femoral circumference is often impossible.

Herein, we used anteroposterior and mediolateral diameter measurements to predict femoral circumference in tyrannosaurids through six different missing data estimation models, which may be divided crudely into two main groups: generalised geometric equation models and regression based equation models. By comparing the predictive success of the model generated circumferences to a set of true circumferences, and the relative performance of each model by juxtaposing error values, it was hoped to assess whether or not tyrannosaurid femoral diameters

may be used to predict circumferences in data sets with missing measurements. If so, this could increase the sample sizes for studies involving femoral circumference in tyrannosaurids and minimise the effects of missing data.

3.2 Materials and methods

Six models were tested in this study: (1) **CAP,** the circumference of a circle using the diameter of the anteroposterior shaft width (*x*); (2) **CML,** circumference of a circle using the diameter of the mediolateral shaft width (*y*); (3) **ELL,** circumference of an ellipse using both anteroposterior and mediolateral diameters; (4) **APR,** linear regression equation for the anteroposterior diameter of the shaft and true circumference; (5) **MLR**, linear regression equation for the mediolateral diameter of the shaft and true circumference; (6) **ELLR**, multiple linear regression equations for both the true anteroposterior and mediolateral diameter of the shaft and true circumference. The equation for the circular models, **CAP and CML** was:

$$C = \pi D$$

Estimating the femoral circumference using **ELL**, the anteroposterior and mediolateral diameters (*x* and *y*) were expressed as a radical fraction in the standard equation:

$$C \approx 2\pi \frac{\sqrt{x^2 + y^2}}{2}$$

Where C= circumference, D= Diameter, *x*= anteroposterior shaft width (mm), *y*= mediolateral shaft width (mm).To create predictive equations for **APR** and **MLR**, true diameters (x axis) were plotted against corresponding true circumferences (y axis) in bivariate linear regression graphs using Microsoft Excel 2007. The linear relationship between the true circumferences and their corresponding diameters was expressed in the standard regression format: $y=mx + b$, where b is the 'y axis' intercept, m is the slope of the line, and 'y' and 'x' represent the circumference and diameter values respectively (mm). These equations may be used by substituting a known diameter in place of 'x' and calculating a predicted circumference at 'y'. As regressions of raw data introduced violations of normality for the distribution of predicted circumference (Seber and Lee, 2003), all data was log-transformed before regression. Log-transformation of data has been demonstrated to reduce the influence of outliers in previous palaeontological morphometric regression analyses (Cawley and Janacek, 2010; Campione and Evans, 2012). As the experimental design was unbalanced, due to the range in sample sizes of each genus (McDonald, 2014), each raw, true diameter and circumference was appropriately weighted using the following formula in order to fulfil the statistical assumption of independence (Appendix 2):

$$WD = R \cdot \frac{1}{n}$$

Where: *WD*= Weighted Datum, *R*=Raw Datum and *n*= sample size of genus.

Paired two-tailed Student t-tests were carried out between each model's set of predicted and true circumferences using Microsoft Excel 2007 and repeated using Graph Pad 'Quick Calcs'. Prior to carrying out these t-tests, data from the regression based formulae were required to be back-transformed and weighted back to the scale of the original raw values (Appendix 2). The latter was performed using the inverse of the previous equation:

$$R = \frac{WD}{(\frac{1}{n})}$$

Percent Prediction Error (PPE) and Standard Error of the Estimate (SEE) values were calculated for each set of predictions using the 'ppe' and 'see' functions in 'MASSTIMATE' (Campione, 2013; Campione et al., 2014): a package within 'R' (R Development Core Team, 2014). Unpaired two-tailed t-tests were carried out between the PPE values of all models, as well as between SEE values. For the latter set of t-tests, five SEE values, one from each genus of tyrannosaurid, were used for each model.

Due to the high number of t-tests carried out on PPE and SEE values, it was necessary to take into account the increased potential for false discoveries, or, the 'False Discovery Rate' (Benjamini and Hochberg, 1995). For this, adjusted p-values, or 'q-values' were returned using the 'p.adjust' function within the 'stats' package in 'R' (R Development Core Team, 2014). These values were then compared to a statistical significance cut-off value (*c*), calculated at $\alpha = 0.05$, using the formula suggested by Benjamini and Hochberg, (1995), to identify false positives from the multiple t-tests.

Measurements were taken with a tape measure or digital callipers. The anteroposterior and mediolateral diameters were measured at the minimum shaft width of the femur, which in tyrannosaurids is distal to the mid-length of the femur. The original sample set consisted of 71 tyrannosaurid femora; however, only 51 had measured circumferences and therefore could be used as comparisons for predictive models (Appendix 1). The taphonomic alteration of each specimen dictated which diameters could be measured and hence, which models could be tested for which specimen. Thus, 45 anteroposterior diameters were available to test the **CAP** and **APR** models, 41 could be tested using **CML** and **MLR**, and only 35 were complete enough to be tested using **ELL** and **ELLR**. The femora represent five tyrannosaurid genera: *Gorgosaurus, Albertosaurus, Daspletosaurus, Tarbosaurus,* and *Tyrannosaurus*. One specimen, BMNH 2002.004.001, previously designated to *Nanoytrannus* was incorporated into the *Tyrannosaurus* data set on the grounds that an extra sample for this genus would be of greater statistical use than an extra sample set, with only one specimen. Carr (1999) has suggested that *Nanotyrannus* specimens represent juvenile forms of *Tyrannosaurus*.

3.3 Results

The linear regression formula produced for **APR** was:

$$y=0.89x + 0.66 \text{ (Figure 3.1)}$$

The linear regression formula generated for the **MLR** model was:

$$y=0.96x + 0.54 \text{ (Figure 3.2)}$$

The multiple regressions performed for **ELLR** produced two equations, for use with anteroposterior diameters and mediolateral diameters respectively:

$$y= 0.93x + 0.63 \text{ (Figure 3.3)}$$

$$y=0.96x +0.54 \text{ (Figure 3.4)}$$

A two tailed student t-test was conducted on each set of results to assess any significant differences between each model's predictions and their corresponding known femoral circumferences (See Appendix 1 for full data). Four of the six models predicted values that were not significantly different from the true circumferences: the three regression models, along with **CML** (p=0.20, t stat= -1.29), which had the lowest t-stat value. **ELLR** (p=0.79, t stat=-0.26) had the highest p-value, with **MLR** (p=0.43, t stat=-0.80) and **APR** (p=0.53, t stat=0.63) also showing no significant difference between predicted and true data. **CAP** and **ELL,** were the only models that produced predicted circumferences that were significantly different from the actual values (**CAP**: p < 0.01, t stat=5.13; **ELL**: p=0.0002, t stat=-4.2556). These results are summarised in Table 3.1.

Percent prediction error (PPE) was calculated for each model as a method of comparing the predictive strength of each set of results. Upper and lower confidence intervals of 95% were also produced, along with the standard deviation and range of PPE shown by a given model (Table 3.1). The models that incorporated the mediolateral diameter had the lowest mean PPE and the narrowest range of 95% confidence intervals. As seen in Figure 3.5, **CML** displayed a mean PPE of 6.55% and 95% confidence intervals of 4.60%-8.51%**,** whereas the mean PPE of **ELL** was 7.37 % with 95% confidence intervals of 5.59%- 9.14%. These error values were bettered only by the two mediolateral diameter based regression formulae. **MLR** had a mean PPE of 6.32% and a range of 95% confident intervals: 4.73%-7.88%, whereas **ELLR** had the lowest error rates of all**,** with a mean PPE of 4.16% and 95% confidence intervals of 2.65-5.67%**.** The two models, **APR** and **CAP**, which were fully reliant on anteroposterior diameter data, displayed the highest mean PPE and the widest range of 95% confidence intervals. **APR** produced a mean PPE of 11.63%, between 95% confidence intervals of 9.63% and 15.42%, whereas **CAP** performed as poorly as it did with the two tailed t-tests, with a mean PPE of 17.39% and 95% confidence intervals of 12.80%- 21.98%. Although confidence intervals are heavily influenced by sample size, the models with the broadest range, **CAP** and **APR,** were also the two models with the largest sample sizes; therefore it is likely that these broader ranges reflect a greater variability of data.

Further to the Percent Prediction Error (PPE), the Standard Error of the Estimate (SEE) was calculated for each model (Table 3.1). The highest estimate of standard error, and therefore

lowest assumed level of accuracy was produced by **CAP** (SEE= 68.13), and the other anteroposterior diameter based model, **APR,** displayed a similarly high value (SEE=50.59). Again, **ELLR** displayed the least amount of error in its predictions (SEE=26.52)), however, in this test **ELL** had marginally lower levels of standard error (SEE=33.09) than did **MLR** (SEE=33.39) and **CML** (SEE=35.32).

In order to assess the statistical significance of the variation in error across the five predictive models, two-tailed student t-tests were performed, which compared the results of PPE (Table A.1, Appendix 3) and SEE (Table A.2, Appendix 3) between the different models. In conjunction with these tests, false positives in the results were identified by using the False Discovery Rate method (Benjamini and Hochberg, 1995). For the t-tests of PPE values, the cut-off (c) at α=0.05 was calculated as: 0.0238; any test which returned a q-value ≤ c was considered likely to represent a truly significant result.

ELLR again outperformed all the other models, as the only estimation method to have significantly smaller PPE values than three others: **CAP** (p=0.0001, t stat= 4.9607, q=0.0004), **APR** (p=0.0001, t=4.1336, q=0.0004), and **ELL** (p=0.0068, t=2.7918, q=0.0126). **MLR and CML** each had PPE values significantly smaller than two others: **APR (**p=0.0042, t=2.9407, q= 0.011; p=0.0062, t-stat=2.8090, q=0.013respectively) and **CAP (**p=0.0001, t-stat=4.3287, q=0.0004**;** p=<0.0001, t-stat=4.2358, q=0.0004 respectively). **CAP** showed significantly higher levels of percent prediction error than all other models, except **APR** (p= 0.037, t-stat=2.1185, q=0.0555). Whereas **ELL** initially seemed to have significantly lower PPE levels than **APR**, this was rejected due to its high q-value (0.04)**,** which suggested that the result of the t-test had been a false positive.

The student t-tests of SEE values between predictive models were less divisive, and only one model, when analysed using FDR (α=0.05, *c*=0), displayed any sort of significant difference (Table A.2, Appendix 3). **ELLR,** the strongest model thus far, had significantly lower SEE values than **CAP** (p=0.0393, t-stat=2.4601, q=0.3702), but no other combinations could be statistically separated by their SEE values.

Between taxon comparisons were made within each model by calculating the mean PPE and 95% confidence intervals for each genus; these results are summarised in Figure 3.6 (for full results see Appendix 1). The models incorporating only anteroposterior diameter data, **CAP** and **APR,** not only displayed higher mean error levels (PPE and SEE), but also a greater variability of error values between the different taxa that made up the sample, despite having a greater overall sample size than the other models. The intertaxonomic mean values for **CAP** ranged from 30.13% in *Albertosaurus* to 5.09% in *Daspletosaurus*, and the 95% confidence intervals for *Albertosaurus* in this model do not overlap with the means of *Daspletosaurus* or *Gorgosaurus,* although its sample size was the same as the latter (n=8) (Figure 3.6). This high taxonomic variability in PPE is also witnessed in **APR,** which had a similarly wide range of mean PPE values compared to the mediolateral based models**:** 21.38% in *Albertosaurus* to 3.50% in *Daspletosaurus*. In this model, the 95% confidence intervals of *Tarbosaurus* do not overlap with the mean PPE of *Albertosaurus*, *Gorgosaurus* or *Daspletosaurus*. Its sample size is relatively similar to the first two genera (n=10,

n=8, n=8), but twice that of the latter (n=5); its relationship with the albertosaurines is therefore more likely to represent true intertaxonomic error variability. The intervals of the two albertosaurines do not overlap with the mean PPE of *Daspletosaurus* or *Tarbosaurus;* those of *Albertosaurus,* in fact, do not overlap with the means of any other taxon (Figure 3.6). Although intertaxonomic variation was strong, no individual genus had a lower mean PPE when using **CAP** or **APR**, as when using the four prediction models that incorporated mediolateral diameters, with the exception of *Daspletosaurus,* which in the mediolateral models had a negligible sample size (n=2) . In both anteroposterior diameter models, *Albertosaurus* had the highest mean PPE and widest range of 95% confidence intervals.

Daspletosaurus expanded the 95% confidence interval range for PPE in **ELLR, CML**, **ELL** and **MLR,** due to its small sample size (n=2). Whereas these two data points were correctly included in the original prediction equations, in which each raw value was considered to be independent of all others, statistical results based on two values are representative only of the uncertainty caused by the impoverished sample. Removing *Daspletosaurus* from the sample for mediolateral diameter based models, the upper and lower 95% confidence intervals for **ELL** are restricted by 27.87% each, for **CML** by 60.48% (upper) and 45.45% (lower), for **MLR** by 148.28% (upper) and 88.29% (lower), and for **ELLR** by 38.2% each (Figure 3.6). With these models**,** the ranges of mean PPE values between taxa were smaller than those produced by **CAP** and **APR**; **CML** (Range: 8.07% in *Tarbosaurus* to 5.12% in *Gorgosaurus*); **ELL** (Range: 8.92% in *Tyrannosaurus* to 3.98% in *Gorgosaurus*); **MLR** (Range: 7.52% in *Tarbosaurus* to 3.65% in *Gorgosaurus*); **ELLR** (Range: 5.01% in *Tyrannosaurus* to 2.14 in *Gorgosaurus*)**.** No one genus dominated the highest mean error values across the four mediolateral diameter inclusive models, as *Albertosaurus* did with **CAP** and **APR**, however *Gorgosaurus* produced the lowest mean PPE values in each of these four models.

3.4 Discussion

There have been a number of different techniques employed within palaeontology to reduce the effect of missing data on analyses and bolster sample sizes; each time in a manner appropriate and specific to the type of investigation being carried out. Grillo and Avezdo (2011), used regression equations to estimate the position of missing tail vertebrae in a specimen of *Staurikiosaurus* on the basis of measurements from the most anterior and posterior caudal vertebrae. Similarly, Funston et al. (2015) estimated the femoral dimensions of a large Caenagnathid specimen from a single caudal vertebra, based on allometric equations between caudal vertebrae and femora for this group of theropods. On a histological scale, Cooper et al. (2008), used an elliptical equation (Ramunjan, 1912) with minor and major radii, to find missing circumferences of concentric lines of arrested growth within femora of *Hypacrosaurus.* Through a novel study in missing data prevention, Arbour and Currie (2012) attempted to better understand the effects of taphonomic deformation in the skulls of *Euoplochephalus* and *Minotaurasaurus,* using 3D retrodeformation techniques on C-T scan images, therefore minimising the confusion of morphological features for missing data points created by geological pressures.

Missing data estimation models have also been proposed for dealing with unrecordable values in larger, multivariate data sets. Norell and Wheeler (2003) dealt with the problem of missing data in phylogenetic analyses of fossils by introducing missing entry replacement data analysis (MERDA), in which they generate a host of possible phylogenetic outcomes and identify those which rely most heavily on missing data points. Brown et al. (2012) dealt with similarly large data sets as they tested the relative success of numerous missing data estimation techniques in large, multivariate, morphometric analyses. Measurements from the skull of an extant crocodilian were taken and analysed with PCA, before missing data values were introduced to the data set. Various missing data estimation models were employed and compared, with the complex Bayesian Principle Component Analysis missing value estimator (Strauss et al., 2003; Oba et al., 2003) producing the lowest error values in its estimations.

From the results of our study, there appear to be a number of viable models through which femoral diameter may be used to estimate missing femoral circumference values in tyrannosaurids, and that may be considered alongside previously proposed missing data estimation models. The two models based solely on the anteroposterior diameter of the femur, **CAP** and **APR**, consistently performed the poorest in the statistical analyses. This suggests that the relationship between anteroposterior diameter and circumference alone in tyrannosaurid femora is not strong enough to support missing data estimation models, and we advise against the use of **CAP** and **APR** for these taxa.

The models that incorporated mediolateral diameter data: **CML**, **ELL, ELLR** and **MLR**, performed better in the statistical analyses than **CAP** and **APR.** Of these four methods, estimations using **ELLR**, performed marginally better than the rest. However, it could not be statistically separated on the basis of PPE and SEE from **MLR** or **CML.** Whereas **ELL** had fairly low PPE values, which were significantly better than **CAP,** it produced predictions that were significantly different to the true values. This may suggest that it had a relatively higher variance of predictions than other mediolateral models, or possibly that its statistical confidence was undermined by a lower sample size than was available for **CML** and **MLR**.

From these statistical analyses, it can be inferred that femoral circumference in tyrannosaurids is more closely related to its mediolateral rather than anteroposterior diameter, and **ELLR, CML**, and **MLR,** may be recommended as three acceptable missing data estimation methods for femoral circumferences across these taxa. **ELLR**, as the strongest statistical performer emerged as the best predictor of femoral circumference and should be favoured over the other five, although **MLR** and **CML** will also give low error predictive values, and are based off of larger data sets. Although **ELL** also displayed significantly lower error values than **CAP** in its predictions, this model requires two femoral measurements, anteroposterior and mediolateral diameter, rather than one, and therefore its effectiveness in increasing data sets will be diminished in comparison to **ELLR, MLR** and **CML.**

In order to demonstrate the utility of these models, two data sets were examined to see how much missing data the models could potentially recover: our own tyrannosaurid data set (Appendix 1) and Benson et al.'s (2014, Dataset S.1) data set for body mass estimations. Out of 71 tyrannosaurid specimens available in our original data set, confident femoral circumference measurements against which to test the five predictive models were only possible for 51, most likely due to taphonomic distortion. Using **ELLR, MLR** and **CML,** the most statistically successful models, the available sample size could be boosted by 35% (17 specimens) to 68 specimens.

There are only 11 specimens of the five tyrannosaurid genera in Benson et al.'s (2014, Dataset S.1) set, however **ELLR**, **MLR** and **CML** would still boost the sample by 9%. If the models, after additional testing, were extended to all theropod taxa within the same dataset, the available sample size would be increased by 62% (70 specimens). This result, although purely hypothetical, as **ELLR, MLR** and **CML** are thus far restricted to use on tyrannosaurid femoral data sets, highlights the utility of these types of missing data estimation models if they continue to be studied.

If adopted, the **ELLR**, **CML** and **MLR** models will increase the sample size for body mass estimation of tyrannosaurids, which is one of the most common applications for femoral circumferences in palaeontology (Anderson et al., 1985; Christianson & Farina, 2004; Campione & Evans, 2012; Campione, 2013; Campione et al. 2014). In order to illustrate one potential application of the **ELLR, CML** and **MLR** models, body mass estimations using the true femoral circumference of the largest adult specimen from each of the five genera were made using Campione et al.'s (2014) bipedal correction of the quadrupedal equation presented in Campione and Evans (2012) (Table 3.2). These were then compared to body mass estimates for the same specimens based on circumferences predicted using **ELLR**, **CML** and **MLR**, and also calculated with Campione et al.'s (2014) equation.

For each tyrannosaurid genus, the body mass values returned using **ELLR**, **CML** and **MLR** circumference estimations fell within the upper and lower boundaries of body mass values produced using true circumferences. In one example, *Tyrannosaurus*, the difference between the true circumference upper and lower body mass limit and the corresponding **ELLR** circumference body mass limits was only 32 and 19.6 kilograms respectively (True body mass:10592.9- 6351.6; **ELLR** body mass:10560.2-6332.1kg).

Aside from their utility in body mass estimations, which can give us insight into physiological, ecological and evolutionary questions (Farlow et al., 1995; Gillooley et al., 2001; Gillooley et al., 2009; Benson et al., 2014) femoral circumferences in tyrannosaurids have a wide range of applications; from life history studies (Cooper et al., 2008; Woodward et al. 2011), to allometric scaling studies (Carrano, 2001; Bypee et al., 2006; Kilbourne & Makovicky, 2010); both of these are important considerations in the study of dinosaurian social behaviour in general. Some of these studies have even proven useful in examples of taxonomic disputes concerning tyrannosaurids such as *Nanotyrannus* and *Gorgosaurus* (Carr, 1999; Currie 2003).

Despite the variety of their potential applications and predictive success in this set of statistical analyses, **ELLR, CML** and **MLR**, should be viewed as alternatives, rather than replacements for any of the missing data estimates that currently exist. Due to the restriction of the regression models within tyrannosaurid femora, they cannot be seen as comparable to large data set missing data recovery models such as BCPA (Brown et al., 2012) or MERDA (Norell et al., 2003), which are designed for use with multivariate morphometric and phylogenetic analyses respectively. A benefit of the currently narrow scope of predictions for which **ELLR, MLR** and **CML** are appropriate is that they lack the digital complexity of models such as BCPA and MERDA, and can be calculated by simply substituting values into one of 4 simple equations. Another benefit is the minimal size and number of measurements required to produce a predicted value; a mediolateral radius from the minimum shaft width would suffice. Radii and diameters are often measurable even in taphonomically damaged fossils, and are usually available to access even on mounted specimens where full circumferences are not.

The predictive power of the regression based formulae, particularly **MLR** and **ELLR** is unsurprising given that they are based off true tyrannosaurid femoral data. However, that simple geometric models such as **CML** and **ELL** performed well under statistical examination bodes well for future projects. Unlike the regression models, these simple equations are not necessarily limited to tyrannosaurid femoral circumferences, and may hypothetically be used with any taxa. Although regression techniques may also be used with other animals, they would need to be created anew using data sets from each new taxa, as was done in this study, whereas the simple equations are theoretically universal, and may be expanded with increased statistical testing across various taxa and limb bones.

3.5 Conclusions

The six predictive formulae, with varying levels of statistical success, display how diameter might be used in place of circumference in tyrannosaurid research, to fill voids left by missing data. Statistical testing suggests that three predictive models that incorporated mediolateral diameter measurements: **CML**, **MLR** and **ELLR** are appropriate methods of estimating femoral circumference, in five tyrannosaurid genera. Methods based exclusively on anteroposterior diameters, such as **CAP** and **APR**, showed significant levels of prediction error and should not be used for these taxa. **ELLR** performed best under statistical examination and can used with both anteroposterior and mediolateral diameter, however, its predictions were not significantly more accurate than those of **CML** or **MLR.** Although **ELLR** and **MLR** provided the most accurate predictions in this study**,** they are restricted to the taxa off which their equations are based are; **CML**, **CAP** and **ELL**, as general geometric equations may theoretically be used with other taxa, although their predictive power for each new taxon should be tested using methodology similar to that of this study. In chapter three, these successful estimation methods for femoral circumference in tyrannosaurids are employed in the ascertaining of body mass estimates and, eventually, growth rate data, as part of this thesis'

broader goal of examining different lines of evidence for gregarious behaviour in *Gorgosaurus libratus*.

3.6 Chapter 3- Tables

Model	CAP	CML	ELL	APR	MLR	ELLR
p- value (Predicted vs. True)	<0.01	0.20	<0.01	0.53	0.43	0.79
t-stat (Predicted vs. True)	5.13	-1.29	4.26	0.63	-0.80	-0.26
Mean PPE (%)	17.39	6.55	7.37	11.63	6.32	4.16
Standard Deviation of Mean PPE (%)	15.27	6.2	5.16	9.64	4.98	4.40
PPE Range (%)	2.23- 53.85	0.32- 28.10	0.19- 21.14	0.08- 37.18	0.05- 23.85	0.03-18.21
Confidence Intervals of PPE (%)	Lower95: 12.80 Upper95: 21.98	Lower95: 4.6 Upper95: 8.51	Lower95: 5.59 Upper95: 9.14	Lower95: 9.63 Upper95: 15.42	Lower95: 4.73 Upper95: 7.88	Lower95: 2.65 Upper95 5.67
Sample Size	45	41	35	45	41	35
SEE (%)	68.13	35.32	33.09	50.59	33.39	26.52

Table 3.1. Summary statistics for model predictions vs. true femoral circumferences for five tyrannosaurid genera; two sample t-test of model predicted vs. true femoral circumferences, percent prediction error (PPE) and standard error of the estimate (SEE).

Genus and Specimen	*Gorgosaurus* NMC 350	*Albertosaurus* TMP 1982.13.30	*Tarbosaurus* MPC-D107/02	*Daspletosaurus* AMNH 5434	*Tyrannosaurus* MOR 1128 "G-rex"
True Cf. (mm)	385	380	480	370	580
CML Cf. (mm)	415	388	518	377	584
MLR Cf. (mm)	400	383	510	352	583
ELLR Cf. (mm) (ML Diam.)	399	375	507	350	579
Body Mass (Kg)	3426.8-2054.8	3305.6-1982.1	6290.3-3771.8	3071.6-1841.8	10592.9-6351.6
Body Mass (Kg) **CML**	4204.8-2521.3	3508.3-2103.6	7773.7-4661.2	3234 -1939.2	10812.6-6483.4

Body Mass (Kg) **MLR**	3809.8-2284.4	3377.3-2025.1	7428.9-4454.5	2761.1-1601.6	10749-6445.3
Body Mass (Kg) **ELLR**	3787.3-2270.9	3184.4-1909.4	7317.9-4387.9	2644.2-1585.5	10560.2-6332.1

Table 3.2. Comparison of body mass estimations for five tyrannosaurid genera made with true femoral circumferences, **ELLR**, **CML** and **MLR** estimated circumferences

3.7 Chapter 3- Figures

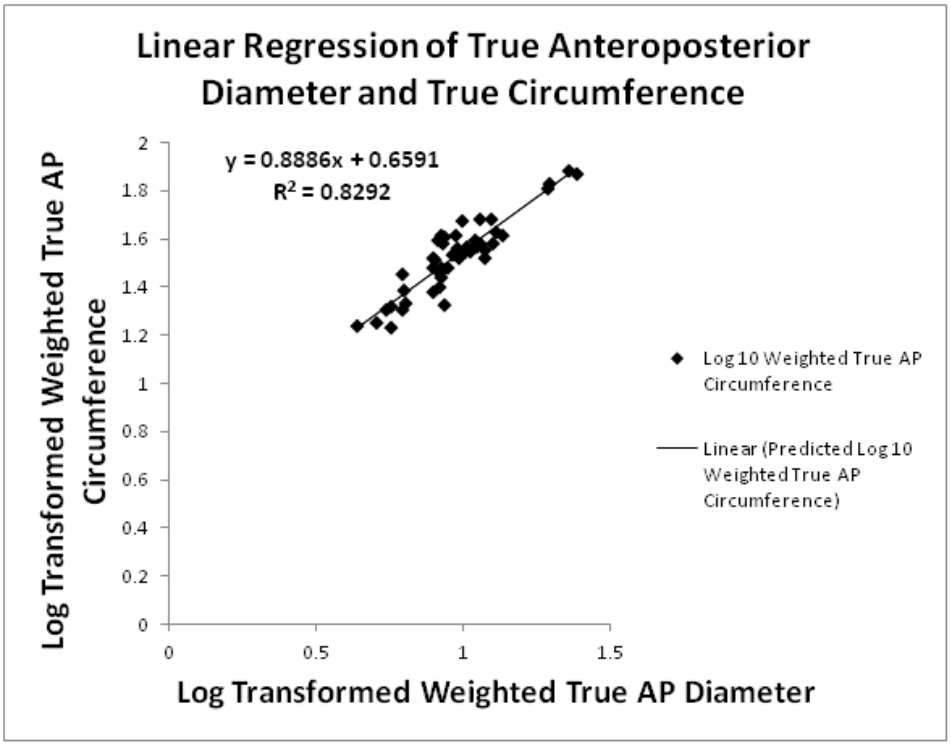

Figure 1. Linear regression of true anteroposterior diameters of tyrannosaurid femoral shafts and their corresponding true circumference **(APR).** All data log transformed (Log10) and weighted

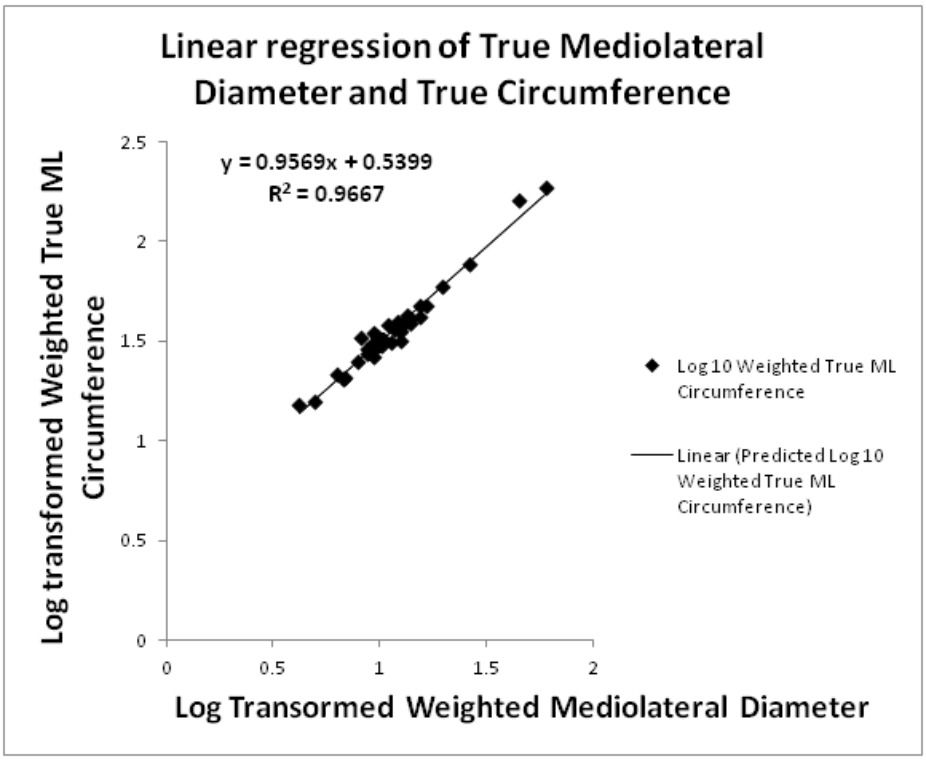

Figure 3.2. Linear regression of true mediolateral diameters of tyrannosaurid femoral shafts and their corresponding true circumferences **(MLR)**. All data log transformed (Log10) and weighted.

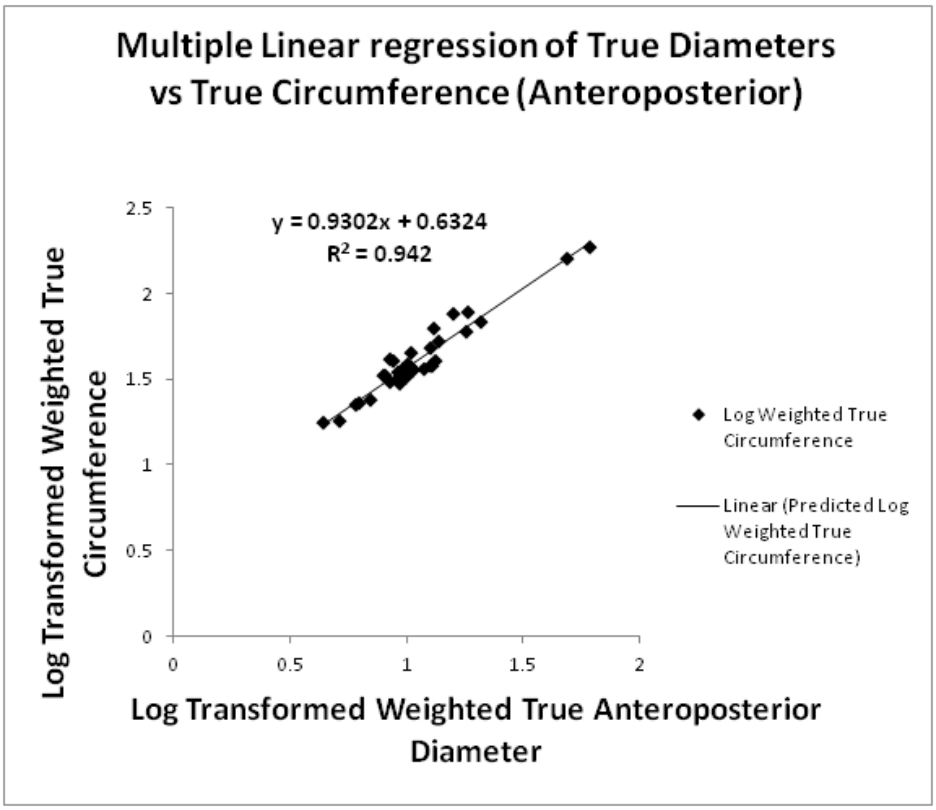

Figure 3.3. Multiple Linear regression of true femoral diameters vs true femoral circumferences (**ELLR**-Anteroposterior). All data log transformed (Log10) and weighted.

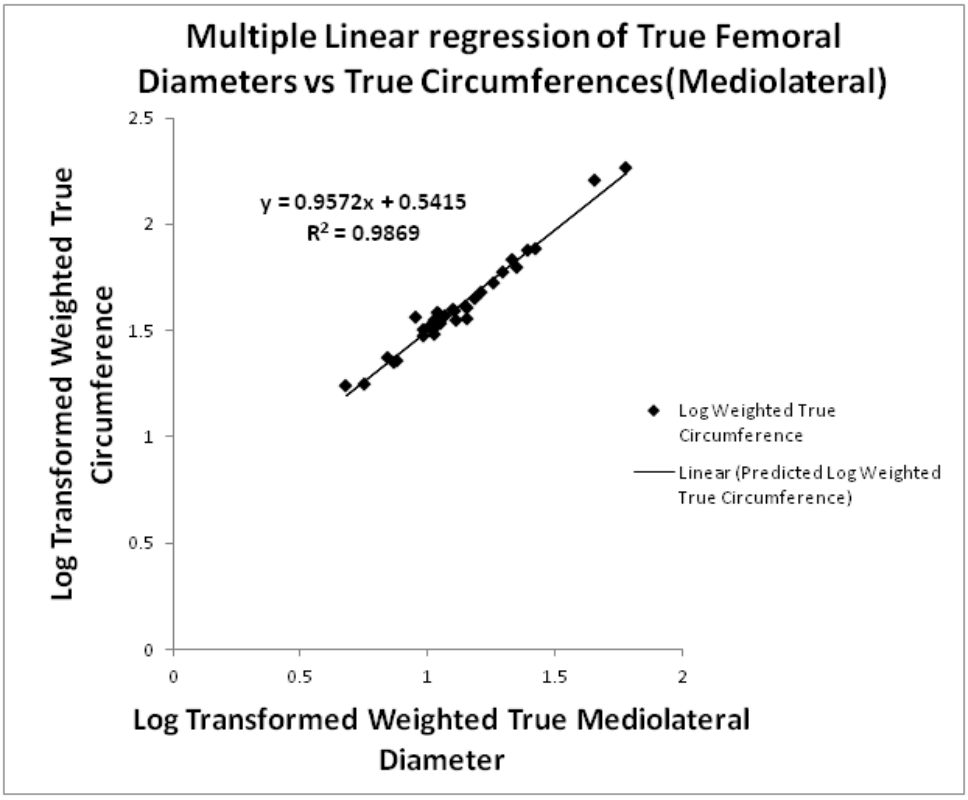

Figure 3.4. Multiple Linear regression of true femoral diameters vs true femoral circumferences (**ELLR**-Mediolateral). All data log transformed (Log10) and weighted.

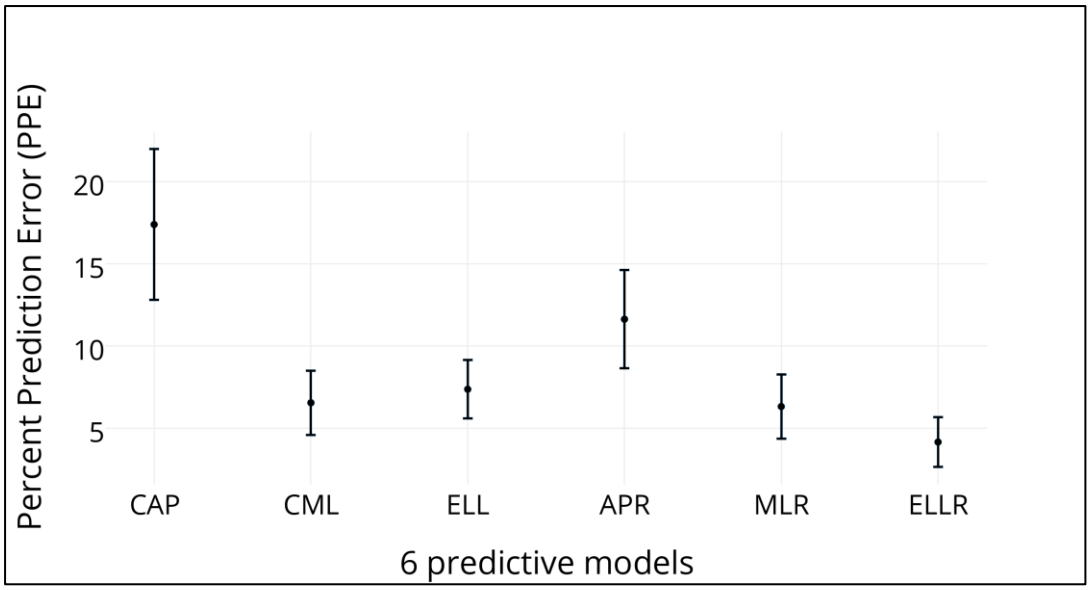

Figure 3.5. Mean PPE values for six femoral circumference estimation models' predictions using data from five tyrannosaurid genera. Bars represent upper and lower 95% confidence boundaries for each model.

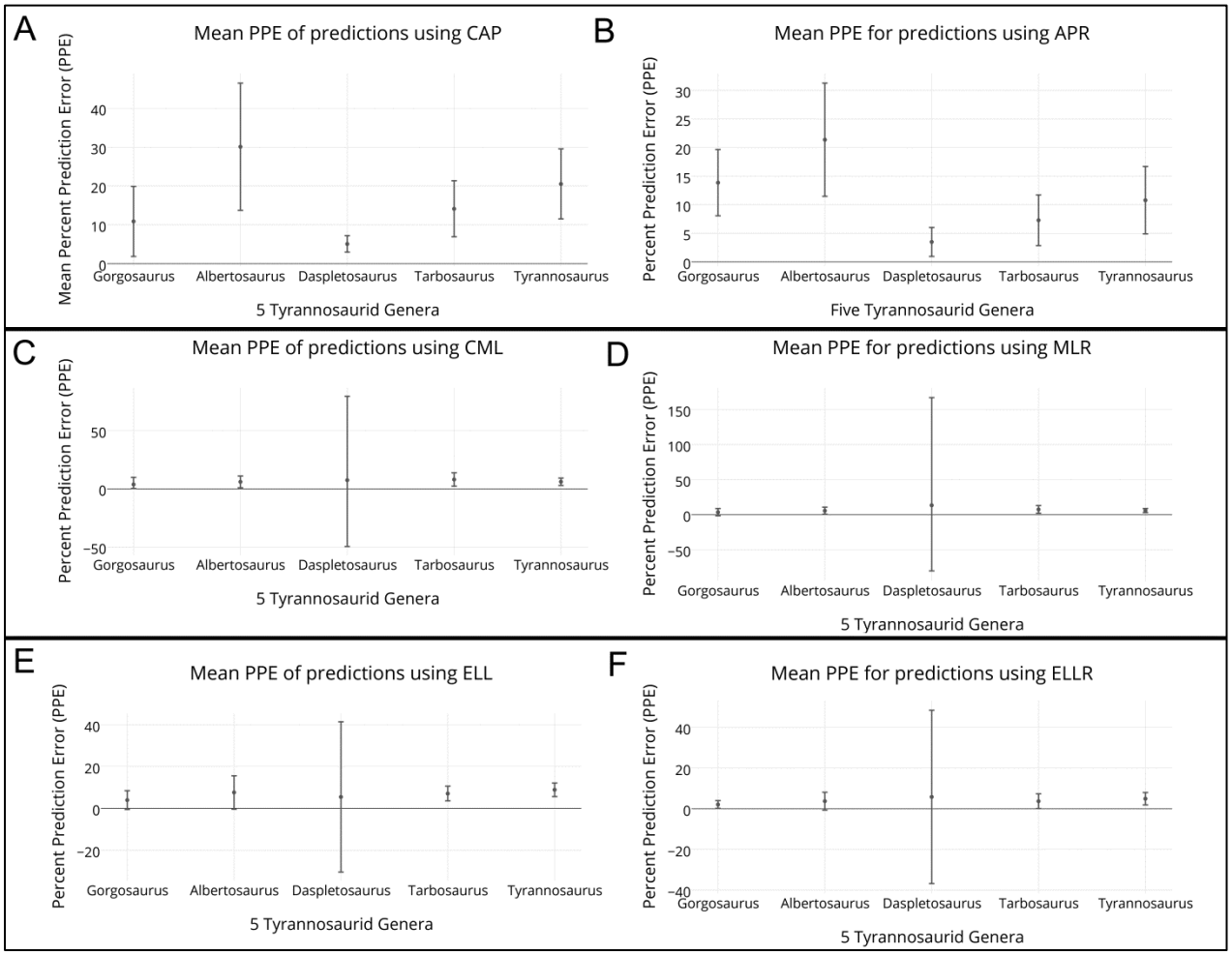

Figure 3.6. Intertaxonomic mean PPE values for six femoral circumference estimation models' predictions using data from five tyrannosaurid genera. Bars represent upper and lower 95% confidence boundaries for each genus of tyrannosaurid in each particular model.

Chapter 4

Description of UALVP 49500 and analyses of social behaviour in *Gorgosaurus*

4.1 Introduction

From the reviews of social behaviour in extant and extinct taxa carried out in Chapter 1, a multidisciplinary strategy was recommended for evaluating different social behaviours in dinosaurs. In using various forms of palaeontological evidence it is hoped to restrict inferences on social behaviour further by presenting complementary or contradictory evidence drawn from different subsets of the field such as palaeopathology and histology. This chapter will provide an introduction to *Gorgosaurus libratus*, the focal taxon of this thesis, as well as an initial description of a recently discovered juvenile specimen, UALVP 49500. By examining this specimen, other comparative specimens and previous literature on the subject, this chapter explores the different methodologies that may be used to assess gregariousness in *Gorgosaurus libratus*. In particular, any significant changes, morphological or other, between juveniles and adults of the taxon, which may correspond with ecological changes are identified and assessed in order to see if they might represent any social behaviours of *Gorgosaurus libratus*.

The potential role of body mass estimates and growth rates in the assessment of social behaviour in dinosaurs has previously been stressed (Chapter 1). Extreme differences in the body sizes of juveniles and adults in a predatory species, for example, may create a separation in ecological niches throughout ontogeny, and therefore has implications for the interpretation of social grouping in tyrannosaurids (Polis, 1983; Werner and Gilliam, 1984; De Roos et al., 2003; Myers and Fiorillo, 2009). Conversely, the presence of another apex predator with larger maximum body sizes may prompt ganging behaviour such as that witnessed in spotted hyenas in Africa living in close proximity to lions, or it may beget the exploitation of a solitary hunting lifestyle to reduce the expected amount of direct competition as witnessed in the cheetah (Hayward and Kerley, 2008).

Body mass estimates may also be used to calculate the overall developmental rate of a taxon throughout ontogeny (e.g. Erickson et al., 2004; Erickson et al., 2010). Building on this contextual knowledge, this chapter makes use of contemporary histological and allometric techniques to provide a growth curve of *Gorgosaurus libratus*. Prior to this, however, it also examines existing bone bed and trackway evidence, palaeopathological and denticle density evidence from UALVP 49500 and comparative specimens, allometric growth of the lacrimal horns, and the ontogenetic growth pattern of orbit circularity. From this multidisciplinary analysis of UALVP 49500 and other specimens, the hypotehsised reliance of the animal on a social group is discussed.

In keeping with the goal of this thesis to enable inferences about dinosaur social behaviour from a small number of isolated specimens, rather than rely on the discovery of spectacular bone bed or clutch sites (e.g. Varrichio et al., 2008b; Currie and Eberth, 2010), the maximisation of data

from minimal material is emphasised in the methodology, especially for destructive techniques such as histological sectioning.

4.2 *Gorgosaurus libratus:* history and context

Gorgosaurus libratus Lambe, 1914, is a tyrannosaurid dinosaur known from the Upper Campanian Dinosaur Park Formation of southern Alberta. The Dinosaur Park Formation comprises the sandy to muddy upper most beds of the Belly River group: the outcrop and subsurface of Dinosaur Provincial Park (Eberth, 2005), and has most recently been dated at 77.0-75.5 mya (Roberts et al., 2013). *Gorgosaurus* would have co-existed with at least one other larger tyrannosaurid in southern Alberta, referred to as '*Daspletosaurus* sp.' or 'Dinosaur Park Tyrannosaurid' in the most recent literature (Currie 2003b; Loewen et al., 2013), but may have exploited a separate habitat than its larger competitor (Farlow and Pianka, 2002). *Gorgosaurus* is the most commonly found Albertan tyrannosaurid, and is one of the best represented of any of the western North American tyrannosaurids; at least 16 specimens including articulated elements of the skull and post cranial skeleton have been collected from Dinosaur Provincial Park and surrounding localities since the discovery of the holotype in 1914 (Currie, 2003b). These remains vary in size (skull length of smallest: 364 mm;skull length of largest: 1000 mm) and, most likely, biological age, meaning that *Gorgosaurus* also remains one of the few tyrannosaurid genera appropriate for use in studies concerning ontogenetic development (Carr, 1999) and rate of growth (Erickson et al., 2004).

The genus *Gorgosaurus* was first named by Lawrence Lambe (1914) based on the skull, hind limbs, most vertebrae, and one forelimb of the holotype specimen CMN 2120, which was found about three and a half miles south of Berry Creek in Dinosaur Provincial Park (Quarry 36, Currie, 2003b) by Charles Sternberg and his team the previous year. This initial description was followed in 1917 by one of the most extensive, substantial and well written tyrannosaurid descriptions to this day, which also supported the separation of the new genus from Leidy's (1856) *Deinodon horridus* based on the incisiform nature of the 1st maxillary tooth (Lambe, 1914; 1917). *Gorgosaurus* was considered a junior synonym of the earlier established genus *Albertosaurus* (Osborn, 1905) by Russell (1970) in his expansive reassessment of the western Canadian tyrannosaurids, due to the similarities in the cranial material of *Albertosaurus sarcophagus and Gorgosaurus libratus*. However, Bakker et al. (1988), in their description of the holotype of *Nanotyrannus lancensis*, favoured the generic split on the basis of differences in braincase characteristics between *Albertosaurus sarcophagus* and *Gorgosaurus libratus*. Russell's synonymy was supported by Thomas Carr (1999) who categorised the ontogenetic development of *Gorgosaurus* specimens, dividing them into crude relative grades or stages, based primarily on size.

Holtz (2001) distinguished the two genera based on twelve characteristics (Appendix 4, Table 1); his phylogenetic analyses confirmed the sister grouping of the two taxa, at the base of the tyrannosauridae. Currie et al. (2003) formally named this two-genus subfamily Albertosaurinae, united by six synapomorphies that place its taxa closer to *Albertosaurus* than to *Tyrannosaurus*.

Following Holtz (2001), the generic separation of the two taxa was supported by Currie et al. (2003) and Currie (2003a; 2003b), to based on greater morphological difference between *Albertosaurus* and *Gorgosaurus* than between *Daspletosaurus, Tarbosaurus* and *Tyrannosaurus* (Appendix 4, Tables 2 and 3). In the most recent phylogenetic analysis of the Tyrannosauridae, including the newly described North American genera *Lythronax* (Loewen et al., 2013), *Nanuqsaurus* (Fiorillo, & Tykoski, 2014) and *Teratophoneus* (Carr et al., 2011), *Albertosaurus* and *Gorgosaurus* are again retained as separate genera within the tyrannosaurid subfamily Albertosaurinae (Fig. 4.1; Loewen et al., 2013; Appendix 4, Table 4). Similarly, Larson (2013) listed ten morphological differences between the two albertosaurine genera in his defence of the validity of *Nanotyrannus* (Appendix 4, Table 5). Although autapomorphic characteristics have been proposed for *Gorgosaurus libratus* (Appendix 4, Table 1), these have failed to be substantiated in later phylogenetic analyses (Currie et al., 2003; Currie, 2003b; Loewen et al., 2013). It is therefore best diagnosed by its identification as an albertosaurine, and then distinguished from *Albertosaurus* through unique combinations of plesiomorphic characters (Currie, 2003b). *Albertosaurus* and *Gorgosaurus* have never been found in the same formation; *Albertosaurus* is known only from the Maastrichtian aged Horseshoe Canyon Formation of Alberta, whereas *Gorgosaurus* finds have been limited to the Late Campanian Dinosaur Park Formation of southern Alberta, putting the two genera approximately three and a half million years apart (Currie, 2003b).

4.3 Materials and methods

All measurements above 40mm for UALVP 49500 were taken with a flexible tape measure, and smaller measurements were taken with electronic callipers. The specimens of *Gorgosaurus* examined for denticle density, lacrimal horn growth, palaeopathologies and comparative morphology were as follows: UALVP 10, UALVP 49500, TMP 1983.036.0100, TMP 1992.36.749, TMP 91.36.500, TMP 1994.012.0155 and TMP 99.33.1. Destructive sampling was performed with the permission of both the Royal Tyrell Museum and the University of Alberta. The specimens from which ribs were thin sectioned were UALVP 10, UALVP 49500, TMP 91.36.500 (one dorsal rib and one cervical rib) and 91.163.001. Ribs were cut at the neutral point of growth, at the proximal end of the main rib shaft, which has been reported as maintaining a constant relative position between the two ends of the rib during growth (Horner et al., 2000; Currie, Pers. Comm.). Age at death estimations were made using the 'back calculation' of LAGs to the centre of the medullary cavity, which takes into account the number of LAGs that have potentially been erased in the remodelling of the bone throughout ontogeny (Chinsamy, 1993). For those sections which did not produce a useable amount of LAGs, or for which samples were unavailable, previously published tyrannosaurid age at death estimates, attained from similar histological techniques was used (after Erickson et al., 2004).

Thin sectioned ribs and teeth were first embedded in a mixture of Buehler EpoThin low viscosity resin and hardener in order to stabilise the specimens. They were cut, and initially ground using a Hillquist thin section machine before being hand-ground on a glass plate with silicon carbide powders and glued to plastic slides. The slides were then prepared to a thickness of between 60-80

μm for microscopic observation and polished with a CeO_2 powder. Photomicrographs were taken using a Nikon DXM 1200F digital camera attached to a Nikon Eclipse E600POl trinocular polarizing microscope. All microscopic measurements or measurements of previously published material were taken using ImageJ, and lacrimal horn least square regressions, denticle density graphs and orbit ratio calculations were carried out using Microsoft Excel 2007. Body mass estimation for adult specimens was carried out using MASSTIMATE (Campione, 2013) a package in R. Gompertz growth curves were created using PAST Vol. 3.

4.4 Description of UALVP 49500 ('Matilda')

4.4.1 Material

UALVP 49500 is a juvenile specimen of *Gorgosaurus libratus* that was discovered by Dr. Philip Bell in Dinosaur Provincial Park, southern Alberta, in June 2008, within the Dinosaur Park Formation, the sandy to muddy uppermost bed in the Belly River group that constitutes the Dinosaur Park outcrop and subsurface, most likely Late Campanian in age (77-75.5 Mya; Roberts et al., 2013). It was excavated over two summers by a team from the University of Alberta, and the excavation site assigned the Quarry number Q253 (Fig. 4.2). Quarry 253 consisted solely of material from UALVP 49500, with the exception of four isolated ceratopsian teeth showing partial roots (UALVP 54838) and a partial hadrosaur limb bone and caudal vertebra with a degree of weathering inconsistent with material from UALVP 49500. The extent of weathering of this hadrosaur limb bone does correspond, however, with that of an exposed and badly weathered partially articulated hadrosaur skeleton on a surface about five meters above Quarry 253, suggesting that this bone likely fell down into the quarry after being eroded out from this higher surface.

Immature status is suggested by the small size of the specimen, the high denticle densities of its maxillary and dentary teeth, and by the presence of juvenile striated bone texture (Carr, 1999; Currie, 2003b; Longrich and Field, 2012) in various skeletal areas, such as the antorbital fossa (Figure 4.3).

UALVP 49500 is almost entirely disarticulated, but constitutes one of the most complete juvenile *Gorgosaurus* specimens ever collected. However, not all of the elements have been prepared (Tables 4.1 and 4.2). Prepared cranial material is represented by: right and left (partial) maxillae, right and left dentaries, 13 fully descended in situ maxillary teeth (two right, 11 left), 24 fully descended dentary teeth (12 right, 12 left), three partially erupted in situ dentary replacement teeth (two right, one left), one partially erupted maxillary replacement tooth, nine isolated teeth maxillary or dentary teeth, three isolated premaxillary teeth (one left, one right, one central), right lacrimal, left jugal, right quadrate (partial left), partial right and left quadratojugals, right postorbital, left squamosal (partial right), left and right ectopterygoids, left epipterygoid, partial left pterygoid, partial palatine, partial right and left frontals, left and right splenials, left supradentary/coronoid and partial right supradentary, left surangular and partial

right surangular, left and right angulars, left and right articulars, and the left and right prearticulars.

The prepared axial skeleton (discounting cranium) of UALVP 49500 is represented by eight articulated cervical vertebrae with attached cervical ribs, two isolated cervical ribs, two dorsal vertebrae, three isolated dorsal ribs, two complete gastralia, numerous fragments of gastralia, six isolated caudal vertebrae and one isolated chevron.

The prepared appendicular skeleton is represented by right scapula-coracoid and partial left scapula-coracoid, right humerus, two Ischia, left and right pubes/partial pubic boot, left fibula, two isolated manual phalanges, ten isolated pedal phalanges, five pedal unguals, articulated right foot including metatarsals I, II, III, IV, V and digit IV with the first and second phalanges.

4.4.2 Systematic Palaeontology

DINOSAURIA Owen, 1842

THEROPODA Marsh, 1881

TYRANNOSAURIDAE Osborn, 1905

ALBERTOSAURINAE Currie, Hurum and Sabath, 2003

Revised diagnosis: antorbital fenestra separated from ventral rim of antorbital fossa by 10 mm or more (Currie, 2003b); anterior margin of maxillary fenestra terminates posterior to anterior margin of antorbital fossa (Holtz Jr., 2001; Currie et al., 2003); distinct lacrimal horn (Currie, 2003b); jugal-quadratojugal suture tapers anteriorly rather than buttressing as it does in tyrannosaurines (Currie, 2003b); angle of axis of jugal pneumatopore to ventral skull margin approximately 45°, not horizontal (Currie et al., 2003); lacrimal pneumatic openings set in single fossa (Currie et al., 2003); extensive dorsal flaring of quadratojugal towards contact with squamosal (Currie et al., 2003); position of lacrimal fossa posterior, much closer to ventral process than to anterior end of anterior process (Brusatte et al., 2009; Loewen et al., 2013).

GORGOSAURUS LIBRATUS Lambe, 1914

Revised diagnosis: Differs from other tyrannosaurids based on the following combination of characters: depressions in maxilla palatal shelf minimal or absent, in contrast to *Albertosaurus sarcophagus* (Currie, 2003b), maxillary fenestra does not reach ventral margin of antorbital fossa (Carr et al. 2005), clear division between the two pneumatic openings in the lacrimal pneumatic (antorbital) fossa by a small vertical bar of bone (Currie, 2003b); postorbital central fossa (not seen in *Daspletosaurus*) (Larson, 2013); postorbital horn does not extend posteriorly to squamosal (as is the case for *Albertosaurus*) (Currie, 2003b); oval fossa on medial surface of pterygoid wing of quadrate absent (Loewen et al., 2013); surface posterior to ectopterygoid pneumatopore appears as smooth sheet, rather than the raised lip of *Albertosaurus* (Loewen et al, 2013); cross section of

maxillary tooth at base of crown ovate (Larson, 2013); anterior squamosal pneumatic foramen present (Larson, 2013); distal blade of the scapula only slightly expanded, unlike the dorsolateral expansion seen in *Albertosaurus* (Holtz Jr., 2001); lateral component of glenoid absent on juvenile scapula (Larson, 2013); foramen rather than ventral ridge on the axial centra (Loewen et al., 2013).

4.4.3 Cranium

The cranium is well represented and, as is the case with most vertebrates, provides most of the diagnostic characters for the genus. Taphonomic damage is most apparent anteroposteriorly along the dorsum of the skull; the premaxillae, nasals and braincase are missing, or are represented only by negligible fragments of material. The skull is approximately 685 mm in length (measured from the most posterior point of the articular to the anterior end of the left dentary, due to the lack of complete premaxillae and wear at the anterior end of both maxillae), making it the fifth smallest specimen of *Gorgosaurus* currently prepared (Table 4.3).

Maxilla

Erosion has destroyed much of the superior and anterior portions of the left maxilla; however, the right maxilla of UALVP 49500 is preserved almost in its entirety, with only a portion of the snout, approximately 20 mm in length, absent (Figure 4.4). It is tallest at its posterior end, where the dorsal and ventral margins of the antorbital fossa meet the right lacrimal and jugal bones respectively, and narrows towards the snout. The antorbital fenestra in UALVP 49500 is separated from the ventral rim of the antorbital fossa by 10 mm; this has been proposed as a synapomorphy of albertosaurine dinosaurs (Currie, 2003b). The maxillary fenestra is unsurprisingly smaller than in adult specimens, such as UALVP 10 (Fig 5.1.), and is situated in line with tooth positions seven and eight, at the midpoint of the anterior portion of the antorbital fossa. Whereas Carr (1999) suggests this positioning of the maxillary fenestra is a stage one juvenile characteristic, UALVP 10, an adult, and TMP 91.36.500, a young adult specimen also display this midway positioning (Currie, 2003b). The termination of the maxillary fenestra anterior margin posterior to that of the antorbital fossa may therefore be viewed as another albertosaurine synapomorphy (Holtz Jr., 2001; Currie et al., 2003).

The maxillary fenestra in UALVP 49500 does not reach the ventral margin of the antorbital fossa; this distinguishes specimens of *Albertosaurus* from those belonging to *Gorgosaurus* (Figure 4.4) (Carr et al. 2005). The shape of the maxillary fenestra is not the smooth ellipse of the adult specimens described by Lambe (1917) or Currie (2003b, Fig. 3.B), nor is it the 'strawberry' shape of Currie's (2003b Fig 3.A.) subadult specimen. The posterior rim of the maxillary fenestra is formed of two straight anterorodorsal and anteroventral lineslines in lateral view that are separated by an obtuse, rather than acute angle, whereas the ventral rim consists of a gradually upwards sloping straight portion that curves at the anterior end to form a semi-circle that meets the longer of the posterior rims at a dorsal point at the approximate mid-length of the fenestra. From Currie's (2003b) description, it most closely resembles the maxillary fenestra of a young *Tarbosaurus*

bataar, rather than *Gorgosaurus*' sister taxon *Albertosaurus*, or any adult specimens of these three taxa. This variation in shape may therefore be the result of ontogenetic change or, as it would have accommodated a portion of the maxillary antral sinus, physiological responses to climatic variations such as temperature (Witmer & Ridgely, 2008; Fastovsky & Weishampel, 2012).

The premaxillary suture of the maxilla is slightly medial to the dorsal margin of the maxilla and does not reach the nasal suture, which extends posteriorly; it does not infringe on the antorbital fossa in UALVP 49500, contrary to the sub adult specimen described by Currie (2003b) due to the presence of a dorsal ridge. The nasal and lacrimal sutures are visible only on the right maxilla due to taphonomic damage to the left. The nasal suture ends posteriorly at the anterior point of lacrimal contact with the maxilla; although the posterior end of the dorsal maxillary margin is broken off, the anterior lacrimal contact suture is represented by a short anteroposterior stretch of mediolaterally compressed bone.

Currie (2003b) noted depressions on the underside of the palatal shelf of the maxilla, to accomodate the teeth of the dentary. UALVP 49500 bears only slight depressions attributable in apposition to dentary teeth in the right maxilla (taphonomic wear of the palatal shelf in the left maxilla makes it difficult to discern), nothing akin to the dramatic concavities displayed in *Albertosaurus* (Currie, 2003b, Fig. 6). However, the corresponding teeth have made a noticeable impact above tooth positions seven and eight of the right maxilla, suggesting that at one stage, the largest teeth occupied these positions in the lower jaw (Figure 4.5).

The intermaxillary suture extends anteroposteriorly on the medial edge of the palatal shelf, dorsal to the second and third tooth formations, but only continues partially over the fourth. In both maxillae, the bone surrounding the first maxillary alveolus is entirely taphonomically degraded, but the intermaxillary suture appears to have continued above this tooth position in the right maxilla. Currie (2003b) describes the same suture running parallel to all four first maxillary tooth positions. As UALVP 49500 is not fully grown, however, it is possible that the intermaxillary suture may have expanded later in ontogeny to encompass the fourth tooth position entirely.

Jugal

The left jugal is almost complete in UALVP 49500, and was in contact with the left maxilla prior to being prepared for an exhibit (Figure 4.7). Already, despite its juvenility, there is a rugose cornual process on the ventral margin of the jugal, anterior to the lower prong of the quadratojugal contact; it may have had some sort of integuementary attachment in life. The suture with the ventral, posterior prong of the maxilla is visible and fused even in this young specimen; fusion of some skull elements has been associated with juvenility in dinosaurs (Longrich and Field, 2012) whereas patent skull sutures in *Tyrannosaurus* have been hypothesised as functioning in the reduction of stresses on the skull during feeding (Rayfield, 2005). The dorsal margin of the jugal above the anteroposterior centre of the bone forms the smooth rounded ventral margin of the orbit. Enough of the ascending jugal process that contacts the postorbital is present that an

accurate anteroposterior length of the orbit may be ascertained, despite the absence of both the left lacrimal and postorbital (Appendix 5; Table 1). Also evident on the anterior edge of the postorbital process is the thin anteroposterior ridge of bone in which the ventral portion of postorbital contacts; Currie, (2003b) has suggested that this expands during ontogeny in *Gorgosaurus*. The quadratojugal suture is formed by two posterior prongs in the jugal, and in UALVP 49500, as in other albertosaurine specimens, this suture tapers anteriorly, and displays the anterior buttressing described in tyrannosaurine specimens (Currie, 2003b). The jugal pneumatopore (Figure 4.7) opens anterolaterally just posterior to the antorbital fenestra and displays the typical orientation of albertosaurines in that its axis is approximately 45° to the ventral skull margin, rather than horizontal as is seen in tyrannosaurines (Currie et al., 2003).

Lacrimal

The right lacrimal is present from UALVP 49500, but is taphonomically damaged at its main contacts with the jugal, maxilla, nasal and, posteriorly, frontal. Despite being broken off at these points, there are a number of important features for the identification of UALVP 49500 as an albertosaurine. The formation of a distinct lacrimal horn (Currie, 2003b) had begun prior to death, expressed through an anterodorsally orientated rugosity above the pneumatic fossa; this position (Figure 4.12) is also typical of juvenile *Gorgosaurus* specimens (Currie, 2003b). The horn has not reached the prominence witnessed in subadult *Gorgosaurus* or the expansiveness recorded in adults, but a small anterodorsal protuberance, of the type described in other *Gorgosaurus* juveniles (Carr, 1999; Currie, 2003b) is present. Another albertosaurine trait, the pneumatic fossa ('banana shaped' from lateral view) is situated posterodorsally to the lacrimal margin of the antorbital fenestra and houses both posterior and anterior lacrimal pneumatic openings (Currie et al., 2003; Larson, 2013). Although matrix has obscured the dorsal interior of the pneumatic fossa, a clear division between the two pneumatic openings can be seen in the form of a small dorsally tapering strip of bone; again this division is characteristic of *Gorgosaurus*¸ although its size and shape may vary (Currie, 2003b). The depth of the lacrimal horn is less than that of the pneumatic fossa; Carr (1999) considers this a characteristic of small juvenile *Gorgosaurus* specimens (Appendix 5; Table 1). The medial pneumatopore on the ventral bar of the lacrimal, said to distinguish *Albertosaurus* and *Gorgosaurus* specimens further (Larson, 2013), is not visible because it is covered by matrix.

Postorbital

The right postorbital of UALVP 49500 is almost complete, except for the most posterior end of the squamosal contact, the ventral portion of the jugal process and a small area anteromedially, where the postorbital meets the frontal. The postorbital 'horn' is present as a rugosity posterior and dorsal to the orbital margin, but is underdeveloped and does not extend posteriorly to meet the squamosal as has been described in specimens of *Albertosaurus*. There is also a distinct foramen lateral to the dorsal ridge of the jugal ramus, and anterior to the squamosal contact that may be an important juvenile characteristic for *Gorgosaurus*; it is absent from larger specimens (Currie, 2003b) (Figure 4.13). The jugal process in UALVP 49500 tapers ventrally, and although its

most ventral portion has broken off, there is no indication of the suborbital prong recorded in larger *Gorgosaurus* specimens (Appendix 5; Table 1) (Currie, 2003b). Medially, there is a deep central fossa, similar to that described in TMP 2001.89.1, which is also found in *Nanotyrannus*, but is significantly shallower in specimens of *Albertosaurus* (Larson, 2013) (Figure 4.14). Due to taphonomic damage it is difficult to tell whether or not the postorbital contacts the lacrimal directly, as in larger specimens of the genus, or is separated from it by a thin separation where the frontal forms part of the orbital margin as has been recorded in smaller and younger individuals (Currie, 2003b). However, so small is the space occupied by the frontal in these specimens, that the upper orbital dimensions may still be measured with confidence (Appendix 5; Table 1).

Squamosal

The left squamosal is well preserved in UALVP 49500, with the majority of each of its four prongs still present (Figure 4.15). The largest of these is the process for contact with the quadratojugal; it is sharply curved anteroventrally, as has been previously described in specimens of *Gorgosaurus* and is longer than the entire squamosal is dorsoventrally tall, as in other tyrannosaurids (Currie, 2003b) (Appendix 5; Table 1). At its posterior end there is a ventral concavity for reception of the quadrate cotylus; however, erosive wear makes it difficult to discern whether or not it is modified for the double headed quadrate cotylus claimed to be a differentiating characteristic of *Gorgosaurus* (Larson, 2013). Significantly, the left squamosal of UALVP 49500 displays a deep anterior pneumatic foramen with well defined margins (Figure 4.16), which is typical for specimens of *Gorgosaurus* but not *Albertosaurus*. It has been speculated that this anterior squamosal concavity housed an air sac in life (Currie, 2003b). The postorbital processes have broken off at their anterior ends in the squamosal of UALVP 49500, as has the anterior portion of the parietal process.

Frontal

The skull roof of UALVP 49500 is preserved in the fused frontals, which are partially complete. Best preserved on the left side, the interfrontal suture, part of the postorbital contact, parietal sutures and part of the sagittal crest may be viewed in the contacting frontals of UALVP 49500 (Figure 4.17). The anterior contacts with the lacrimals, prefrontals and nasals are not visible due to postmortem damage, nor is it possible to record the width to length ratio of the frontals, which is thought to change dramatically throughout ontogeny in tyrannosaurids (Currie, 2003b). The sagittal crest is apparent, arising where the backs of the frontals are separated by the parietals, although it is extremely underdeveloped in comparison to tyrannosaurines or even adult specimens of *Gorgosaurus* such as UALVP 10 (See Fig. 5.1). The parietals posterior to the crest have been broken off (Appendix 5; Table 1). The left postorbital contact is a concavity on the dorsal surface of the frontal. Ventrally, the frontal can be seen to form part of the orbital roof. The interfrontal suture is visible in UALVP 49500, as it is in all tyrannosaurid specimens (Holtz Jr. 2004), and the tightly integrated parietal sutures are also visible at the posterior portion of the foramen housed by the sagittal crest (Figure 4.18); a condition typical in albertosaurines (Currie, 2003b).

Quadrate

A nearly complete right quadrate and partial left are present from UALVP 49500. The left is survived only by the mandibular condyle and a small portion of the pterygoid wing blade, whereas the right quadrate is missing only a small portion of the quadrate cotylus (Figure 4.8). The right quadrate is of typical tyrannosaurid form, in that it is relatively shorter to those of other theropods and retains a pneumatopore on the ventral side of the pterygoid ala (Appendix 5; Table 1) (Currie, 2003b; Holtz Jr., 2004). It also displays an important potential distinguishing characteristic between *Albertosaurus* and *Gorgosaurus* in that the deep oval fossa on the medial surface of the pterygoid wing is not present, as it is in the former genera (Loewen et al., 2013); instead, UALVP 49500 displays a mild triangular depression in this area (Figure 4.9). Although a distinct medial ridge exists on the right quadrate cotylus of UALVP 49500, due to taphonomic breakage of the lateral portion, the double headed cotylus that has been recorded as being indicative of *Gorgosaurus* rather than *Albertosaurus* cannot be confirmed, although does appear probable (Larson, 2013).

Quadratojugal

The quadratojugal is represented by partial right and left fragments of bone in UALVP 49500, between which two important features for the identification of albertosaurines may be witnessed. The first is the expansive anteroposterior flaring of the squamosal contact (Appendix 5; Table 1), which can be seen in the left quadratojugal of UALVP 49500 (Figure 4.10), even though the posterior margin has been lost dorsally; the same expansion of the squamosal contacting surface can be seen in other specimens of both *Albertosaurus* and *Gorgosaurus*, but not in tyrannosaurines (Currie et al., 2003; Currie, 2003b). Similarly, both albertosaurine genera display a concave and rugose medial quadrate suture; this feature is witnessed clearly on the quadrate contact surface of the right quadratojugal in UALVP 49500 (Figure 4.11).

Ectopterygoid

The left and right ectopterygoids in UALVP 49500 are present, although the right exhibits postmortem damage to its medial and posterior margins (Figure 4.19). They follow the same general shape displayed by all tyrannosaurid ectopterygoids, with a strongly curved process for jugal articulation tapering mediolaterally at its distal end. Interestingly, there is a noticeable size difference between the right and left ectopterygoids in UALVP 49500. The latter is much more robust than the former (Appendix 5; Table 1), suggesting that there may have been asymmetric growth in different sides of the cranium; however postmortem constriction of the right side cannot be discounted as a contributing factor. There is a large pneumatopore noticeable at the medial base of the left jugal process, on the ventral surface, and the surface posterior to this appears to form a smooth sheet, as recorded in other specimens of *Gorgosaurus,* rather than the raised lip apparent in *Albertosaurus* (Figure 4.20) (Loewen et al, 2013).

Epipterygoid

Epipterygoids are rarely preserved in tyrannosaurids (Holtz Jr., 2004). However, an almost complete left epipterygoid is present from UALVP 49500 (Figure 4.21). It is similar to those described previously for *Gorgosaurus*, in that it tapers dorsally, has a lateral concavity and splits into two separate processes ventrally for articulation with the quadrate process of the pterygoid (Currie, 2003b), although neither has been preserved fully.

Pterygoid

A partial left pterygoid has survived from UALVP 49500, although it has been heavily damaged (Figure 4.22). The quadrate process is visible; it is anteroposteriorly thin and extends anteroventrally, but has been eroded at its extremities. Similarly, the posterior component of the anterodorsal process is preserved and had begun to expand dorsoventrally, but anterior to this, the specimen has endured significant post-mortem damage.

Palatine

The left palatine from UALVP 49500 has been preserved with only minor breakage at the ends of the maxillary, jugal and pterygoid contacts (Figure 4.23). There are two visible pneumatopores on the lateral surface above the maxillary shelf and anterior to the branching of the jugal and pterygoid processes (Appendix 5; Table 1) as is the norm for tyrannosaurids (Currie, 2003b). Anterior to these foraminae is a mild depression that may reflect an incipient third pneumatopore.

Dentary

The right and left dentaries of UALVP 49500 are present, with the latter still in position within the mandible (Figure 4.24). Only five other specimens of *Gorgosaurus* have recorded smaller dentary tooth row lengths (Currie, 2003b). The dentary minimum height, taken underneath the 7th dentary tooth position, is even smaller in comparison to other *Gorgosaurus* specimens; it is larger than only three other measured specimens (Appendix 5; Table 1) (Currie, 2003b). The minimum dorsoventral height is approximately 20% of the dentary tooth row length; a similar relationship is seen in other sub adult *Gorgosaurus* and *Nanotyrannus* specimens (Currie, 2003). However, the dentary depth is also 34% greater than the tallest dentary tooth, a much greater difference than has been recorded for other juvenile and subadult *Gorgosaurus* specimens. This might suggest that UALVP 49500 is already in a positively allometric stage of jaw growth that will eventually produce the deep jaws and large bite force of adult tyrannosaurids (Hurum and Currie, 2000; Reichel, 2010) or that it exhibited slower tooth replacement rates than other juveniles due to physiological stress, trauma or individual variation. Tooth and skeletal growth rates are examined in greater detail later in this chapter.

The anterior portion of the right dentary is complete to the point that the area of mandibular symphysis is apparent in a rugose attachment anteromedially. This medial rugose attachment of the two dentaries at their anterior portion is characteristic of tyrannosaurids (Figure D1; Weishampel et al. 2004).

The level of rugosity of bone is an oft cited indicator of ontogenetic age, with more rugosity indicating an older ontogenetic age, whereas smoother, more striated bone is representative of a biologically younger specimen (Carr, 1999; Longrich & Field, 2012). Age certainly seems to be a contributing factor to the relative roughness of this attachment site; similar levels of mandibular symphysial rugosity are evident in the similarly sized right dentary of TMP 1992.36.749, whereas the smaller dentary of TMP 1994.12.0155 displays almost no visible rugosity. Currie (2003b) suggested that various levels of rugosity at this point of attachment between the two mandibles might give rise to different levels of intermandibular kinesis; more rugosity would suggest stronger attachment, a more integrated suture and less potential for movement. As more rugosity appears concomitant with greater ontogenetic age, it would be tempting to relate this to a difference in feeding mechanics between juvenile and adult individuals of *Gorgosaurus*. However, the increasing rigidity of the anterior connection of the mandibles is more likely a reflection of the gradually increasing depth of the jaws, size of the jaw adductor muscles and pressure of bite force as the animal grows.

On the lateral surface there are approximately 40 foramina, representing the cavities of blood vessels required to supplement the teeth, lips and surrounding muscles of the lower jaws (Figure 4.24). The greatest concentration is towards the acute anterior portion of the jaw, where the largest foramina serviced the skin and gums in front of the attachment site of the two mandibles. Here, the foramina appear to form three lines parallel to the ascending and most anterior portion of the dentary. Aside from this anterior cluster, the most visible pattern of foramina is a single line ventral to the tooth row; a row of grooves perpendicular to these foramina correlate with the expected attachment site of lips and vessels supplying blood to the alveoli.

Splenial

The right and left splenials of UALVP 49500 are complete. The right one is still in position on the medial side of the mandible with the dentary and supradentary (Figure 4.27). There are two notable foraminae created by the splenial in tyrannosaurids, both of which are visible in this juvenile *Gorgosaurus*. The anterior mylohyoid foramen is seen in medial view (Figure 4.27), just above the ventral margin of the mandible and is in line with the last two dentary tooth positions. Its anteroposterior length is more than three times its dorsoventral height; these proportions are again, typical of tyrannosaurids (Currie, 2003b). The splenial also forms the anterior and ventral borders of the internal mandibular fenestra, which in UALVP 49500 is similar in size to the anterior mylohyoid fenestra. The splenial in UALVP 49500 is tallest posterior to the end of the dentary tooth row and tapers posteroventrally to its thinnest point where it contacts the angular. It sits on top of the ventral angular suture, but does not extend posteriorly beyond the left prearticular. Anterior to

the foremost medial overlap of the dentary and splenial is the Meckelian canal: a dorsoventrally short groove that visibly extends anteroposteriorly until it forms the medial margin of a foramen and groove posterior to the intramandibular suture. This is a remnant of the Meckelian cartilage, which in lower vertebrates forms the first branchial arch, but which ossifies almost entirely during the formation of the dentary in tyrannosaurids (Currie, 2003b; Gray, 2009).

Surangular

Both surangulars are present in UALVP 49500; the right is disarticulated and is damaged along its ventral and anterior margins, whereas the left surangular remains articulated in the left mandible, although its posterior surangular fenestra has been covered laterally by the ventrally directed crushing of the dorsal margin of the bone (Figure 4.25). The large posterior surangular fenestra is synapomorphic for tyrannosaurids, and in UALVP 49500 it is a large and oval to circular opening underneath the lateral ridge (Currie et al., 2003; Currie, 2003b; Holtz Jr., 2004) (Appendix 5; Table 1). This ridge or surangular shelf extends anteroposteriorly from the surangular contribution to the dorsal glenoid articulation with the quadrate for about three times the length of the posterior surangular fenestra, and does not infringe beyond the dorsal margin of the posterior surangular fenestra, as is the case in *Teratophoneus* (Loewen et al., 2013). The anterior surangular fenestra, in contrast, is a narrow anteroposterior slit in the dorsal part of the lateral surface of the surangular in UALVP 49500 that opens posterior to the intramandibular joint, which is also apparent in UALVP 49500. There is a ventrally situated striated portion of the lateral surface where the surangular would have been overlapped by the angular; the external mandibular fenestra is bounded by the ventrally concave lower margin of the surangular and the dorsally concave dorsal margin of the angular.

Angular

The left angular of UALVP 49500 is articulated in the left mandible, whereas the right is disarticulated and damaged at the anterior section of its ventral process and along its posterior margin and (Figure 4.26). Medially it is almost entirely obscured from view by the surangular and prearticular, whereas laterally it forms the posteroventral portion of the lateral surface of the mandible. It is mediolaterally thin posteriorly, but thickens substantially as it curves anteroventrally to form the posterior and ventral rim of the external mandibular fenestra. Medially there is a small shelf of bone representing the dentary articulation and above this the external mandibular fenestra, which is large in relation to the posterior surangular fenestra in UALVP 49500, in contrast to previously examined small tyrannosaurid specimens (Holtz Jr., 2004) (Appendix 5; Table 1).

Supradentary/Coronoid

The supradentary/coronoid is still in articulation with the rest of the left mandible of UALVP 49500, but is not present on the right side. From medial view, the supradentary extends anteroposteriorly, dorsal to the medial alveolar margin (Figure 4.28). Beginning at the second

dentary tooth position, the supradentary is fused to the coronoid posterior to the tooth row, and twists ventrally into a slot medial to the dentary and lateral to the splenial. In UALVP 49500, as in other tyrannosaurids, but unlike some other theropods, the bones are entirely fused together (Holtz Jr., 2004). The interdental plates of the left dentary are obscured by the supradentary. The supradentary is dorsoventrally tallest at a point below the seventh dentary tooth position and shortest anterior to its first overlap with the splenial (Appendix 5; Table 1).

Prearticular and Articular

The isolated right prearticular in UALVP 49500 is damaged at its anterior end. The left prearticular is still associated with the rest of the mandible but was pushed out of position so that it is visible below the ventral margin of the angular (Figure 4.29). It expands anteriorly and posteriorly, becoming ventromedially thicker and dorsoventrally smaller in the middle of the elongate bar that forms most of its corpus. It is tallest at the point where it overlaps the splenial, before tapering anterodorsally towards the apex of the supradentary that effectively signals the posterior extent of the dentary tooth row (Appendix 5; Table 1). It extends almost half the entire length of the mandible.

The articular is well represented on the right and left sides of the skull of UALVP 49500. The left articular is tightly integrated where it contacts the prearticular and surangular to create the large concavities for articulation with the mandibular condyles of the quadrate (Figure 4.30). The right articular is still articulated with the right prearticular, and both can be manually placed in their correct positions within the sheath like concavity of the posterior surangular. The right articular of UALVP 49500 also has a small medial foramen posterior to its prearticular contact, which most likely housed the chorda tympani (Molnar, 1991; Currie, 2003b).

Maxillary teeth

The left and right maxillary tooth rows are present; however, the front two alveoli in each have been almost entirely lost due to taphonomic stresses. The incisiform tooth that has been previously been defined as characteristic for *Gorgosaurus* (Lambe, 1917; Holtz, 2001; Larson, 2013), is not present, but was most likely lost with the anterior portions of the maxillae and posterior portions of the premaxillae. Significantly for the allocation of this specimen to *Gorgosaurus*, rather than *Albertosaurus*, the maxillary teeth are ovate in cross section at the base of the crown (Figure 4.6), rather than compressed as in the latter genus (Larson, 2013). The anterior carinae twist more lingually at the base of the tooth in progressively more anterior teeth, and become more centred in the posterior teeth. This is accompanied by a labial migration of the posterior carinae in more anterior positions compared to posterior teeth; this general anteroposterior trend creates a substantial difference between the the D shaped premaxillary teeth, of which only three isolated examples are present from UALVP 49500, and those posterior to them. Teeth from the anterior or mid-portion of the maxillae are significantly larger than the posterior maxillary teeth (Appendix 5; Tables 2 and 5). Lambe (1917) noted that the teeth of the

maxilla of *Gorgosaurus* reach greater sizes than those in the dentary. This is the typical trend for tyrannosaurids and also the case in UALVP 49500, with tooth positions four, six and eight in the left maxilla larger than any teeth protruding from the dentaries. There are three denticles per mm in the anterior and posterior carinae, which may be a significant ontogenetic indicator for *Gorgosaurus*. The fore-aft basal length (FABL), crown height and base crown width for all maxillary teeth were measured, along with the density of anterior and posterior denticles per mm (Appendix 5; Tables 2-9).

Dentary teeth

Although the teeth are generally laterally compressed, in the manner expected of tyrannosaurid teeth, the mediolateral width of the base of the tooth crown gradually decreases from the front to the back of the mouth, whereas the crown height, taken as the dorsoventral length of the posterior carina, is greatest from tooth positions 6-9, again in the mid section of the jaw (Appendix 5; Tables 10-15) (Figure 4.24). The posterior carinae remain straight along their longitudinal axes. However, the anterior carinae gradually twist and migrate laterally between the front of the mouth and the 13th tooth as expected in tyrannosaurid teeth.The denticles are rectangular, as is typical of albertosaurine dinosaurs (Abler, 2013).The denticle density of the anterior and posterior carinae of the teeth of the dentary is the same as that recorded for the maxillary teeth: three per mm. This reinforces the argument that denticle density is consistent for all teeth within an individual, and is not subject to the individual variation expected of tooth count and size (Carr, 1999; Miyashita et al. 2010).

4.4.4 Axial Skeleton

Cervical vertebrae

The articulated series of cervical vertebrae is one of the most remarkable features preserved in UALVP 49500. Uncommonly in tyrannosaurids, the atlas-axis articulation is preserved almost in its entirety (Figure 4.31). Although the neural spine is broken off near the apex, itstill demonstrates the lateral flaring typical of the tyrannosaurid axis, and is substantially larger than the axial intercentrum; which is is approximately 2/3 the height of the former (Appendix 5; Table 16) (Samman, 2013). The atlas intercentrum makes a lateral crescent shape from anterior view, due to the dorsal protrusion of the odontoid, the upper surface of which also forms the ventral margin of the neural canal. The posterior face of the axial intercentrum is lower ventrally than the anterior face; a similar subparallel organisation to the rest of the cervical centra help create the classic 'S' shape known of tyrannosaurids (Madsen, 1976; Holtz Jr., 2004). There is one large lateral pneumatopore on the left side of the axial intercentrum, and there may be another on the right side, however, this area exhibits substantial taphonomic damage. In contrast to specimens of *Albertosaurus*, UALVP 49500 does not exhibit a ridge on the ventral surface of the axial intercentrum, (Loewen, 2013) however, it does present a small central foramen, which has been thus far undescribed in either taxa (Figure 4.32).

The series of cervical vertebrae in UALVP 49500 is only missing the tenth vertebra and the corpus of the centrum from the ninth cervical vertebra. Otherwise the neck is exquisitely well preserved; the pre and post-zygapophyses of the cervical vertebrae are all present and articulated with the corresponding surface, except for those of C4-C5 and C6-C7, where they are present but not articulated due to taphonomic pressure on the lateral regions of the neck (Figure 4.33). The cervical centra dimensions are typical for juvenile tyrannosaurids, in that they are substantially longer than tall (Holtz, Jr. 2004), and there is a general increase in size posterior to the axis. There are seven pairs of articulated cervical ribs from C-3 to C-9, with double headed attachment at two points lateral to the cervical centra; the tuburculum articulates with the more dorsal diapophysis and the capitulum with the more ventral parapophysis. The heads of the cervical ribs also appear to increase in size posterior to the axis, and by the eighth cervical vertebra, the ribs display the greatly expanded distal surfaces described by Lambe (1917). The anteroposterior width of the cervical neural spines, contrary to the character suggested for *Gorgosaurus* (Loewen et al., 2013), was not consistently half or more than half the length of the centra, however, this may again be a result of the juvenile age of the specimen.

Dorsal Vertebrae

Three of the thirteen dorsal vertebrae are present in UALVP 49500, preserved in a much worse condition than the cervical vertebrae. The transverse processes are larger and more laterally orientated than those of the cervical vertebrae; the spinous processes and centra are also substantially dorsoventrally taller (Figure 4.34) (Appendix 5; Table 16). The three vertebrae can be ordered relative to each other, due to the general increase in size of the centra and neural spines caudally in the back, but cannot be given specific numbers in the vertebral column. The largest, and therefore most posterior of the three dorsal vertebrae is fused to a broad, flat sheet of bone, which may represent the distal end of the left scapula (Figure 4.35) (Lambe, 1917).

Dorsal ribs

There are four isolated dorsal rib fragments present from UALVP 49500, two from the left side (Dorsal ribs A and B) and two from the right (Dorsal ribs C and D). Only one left sided rib however, dorsal rib A (Figure 4.36), is mostly complete and retains the proximal head and tubercle, as well as most of the medially concave shaft. The other left-sided thoracic rib, dorsal rib B, also retains the tubercle, but is broken off at the ventral portion of the head. Dorsal ribs C and D, from the right side of the body, are represented only by a shaft with a slight dorsoventral expansion and curve indicating its proximal end, and a partial head respectively. As tyrannosaurid dorsal ribs increase and then decrease in size caudally, it is difficult to specifically place these fragments. However, dorsal rib A's long length would suggest that it is from the centre of the thoracic ribcage; the similarity in the height and width of the proximal head of dorsal rib D implies that they may articulate with similar size vertebrae. The greater minimum shaft dorsoventral thickness of dorsal rib C, suggests that it was probably the largest of the surviving ribs, and therefore, most likely to be part of the largest series of dorsal ribs, in positions 4-8 (Lambe, 1917). Dorsal rib B, with the

smallest dimensions, probably articulated more anteriorly or posteriorly than the other three (Appendix 5; Table 16).

Caudal vertebrae

There are the remains of six disarticulated caudal vertebrae (CVA-CVF) from UALVP 49500, along with two isolated chevrons. One vertebra, CVA, is substantially larger than the others, and its large dorsoventral height in relation to its length, the steep anterodorsal incline of its prezygapophyses and its large centrum relative to the other five, suggests that it originates more anteriorly in the tail; the posterior location of its neural spine implies a mid-tail placement (Figure 4.37) (Lambe, 1917). These general dimension trends can be applied to the other five vertebrae, which exhibit less steep prezygapophyses, longer bodies relative to neural spine dorsoventral height, longer prezygapophyses, and slighter centra moving more posteriorly in the body; vertebrae C VA-CVF are therefore from increasingly posterior positions in the tail. The low neural spine and extremely long prezygapophyses of CVF, the best preserved vertebra in the tail, confirms it as originating from the final 10 caudal vertebrae (Lambe, 1917) (Appendix 5; Table 16). In general, preservation is worst at the anteroposterior and lateral extremities of the caudal vertebrae; there is significant lateral skewing or excavation of CVA, CVB, CVC and CVE and breakage of the ends of both pairs of zygapophyses in all caudal vertebrae, with the exception of CVD (Figure 4.38).

Both chevrons are well preserved at their ventral ends, and come from different localities along the tail. Chevron A, the larger of the two displays the classic ventrally elongated triangular shape characteristic of the chevrons of the first seven caudal vertebrae (Figure 4.39) (Lambe, 1917). The rounded haemal spine on the smaller of the two chevrons is well preserved and its increased posterior portion is indicative of a more posterior position in the tail, most likely attaching at some point between the seventh to fifteenth vertebrae (Lambe, 1917) (Figure 4.40).

4.4.5 Appendicular Skeleton

Scapula-coracoid

The right scapula-coracoid of UALVP 49500 is almost complete, but is missing both the posterior margin of the caudal blade of the scapula and the anterior margin of the coracoid (Figure 4.41). The left scapulocoracoid is represented only by the anterior most part of the shaft of the scapula, and the ventral portion of the anterior scapular blade/coracoid, although the anterior margin of the coracoids is present. The shaft of the scapula is highly curved, with the medial side concave to fit over the ribs. The coracoid is expanded dorsoventrally to more than five times the minimum shaft width of the scapula, and the caudal blade of the scapula is only slightly expanded, unlike the vast dorsolateral expansion seen in specimens of *Albertosaurus* and *Tyrannosaurus*. This relatively minor expansion of the caudal blade of the scapula is another differentiating characteristic between the two albertosaurine taxa (Figure 4.35) (Holtz Jr., 2001). The coracoid foramen is not present in either side, most likely due to taphonomic damage, although it is possible

that this feature may be absent in juvenile specimens of *Gorgosaurus*. The glenoid cavity is relatively shallow and does not present the lateral protrusion present in *Nanotyrannus* and juvenile specimens of *Albertosaurus* (Figure 4.41) (Larson, 2013). As is typical in tyrannosaurids, the scapula makes up most of the glenoid cavity, however, the sigmoidal suture (Lambe, 2013) between the scapula and coracoid is not visible on either side. Both have been fractured, post mortem along this point, suggesting that perhaps fusion of the scapula-coracoid suture was not yet complete, contributing to taphonomic breakage at this particular point in both sides of the body.

Humerus

The right humerus of UALVP 49500 is only missing a small portion of the posterior surface around the midshaft of the limb bone (Figure 4.42). As is typical for tyrannosaurid forelimb elements, the humerus in UALVP 49500 is underdeveloped, although less so than other tyrannosaurids; the ratio of humerus to scapula length is 1:1.6 in this specimen (Appendix 5; Table 17), compared to 2.2 in *Daspletosaurus* (Holtz., Jr. 2004). This unusual relative length for a tyrannosaurid may again be a feature of the early ontogenetic state of the specimen as the ratio of humerus to scapula length in the adult holotype NCM 2120 is much greater at 1:2.7. Although the humeral shaft tends to be straighter in tyrannosaurids than other large tetanurans (Holtz Jr. 2004), the humeral shaft of UALVP 49500 is distinctly concave in its posterior surface, and slightly convex in the distal portion of its anterior face, in accordance with the curvature described in the holotype (Lambe, 1917). The deltopectoral crest is poorly developed and extends only 10 mm out from the main shaft of the humerus.

Manual Phalanges

There are two isolated phalanges present from UALVP 49500, one much larger than the other (Figure 4.43). The largest, most likely represents the first phalanx of digit one, due to its large size and unequal symmetry of its proximal articulation surface (Lambe, 1917). The other phalanx is much smaller than the first and most likely constitutes the second phalanx of digit II due to its narrow, form and the presence of deep pits on the sides of its distal end (Lambe, 1917).

Ischium

The distal majority of the left and right ischia are present from UALVP 49500, with taphonomic damage at the proximal end preventing the description of its articulation with the rest of the pelvis (Figure 4.44); unusual for tyrannosaurids, the fusion of intra-pelvic elements has been described in a specimen of *Nanotyrannus* (Larson, 2013). The ischia are connected mediolaterally by an extension of the obturator process, which continues until about 115 mm from the distal articulation point of the Ischia. This extended obturator process is a synapomorphy of tyrannosaurids, and another is witnessed in UALVP 49500 as the shaft of the ischium is substantially thinner than that of the pubis (Holtz, Jr. 2004) (Appendix 5; Table 17). The Ischia come together

medially at their narrow distal ends, although taphonomic pressures have produced a curvature in the bone here, making it difficult to confirm the fusion of the intra-ischial suture.

Pubis

The left and right pubes are partially complete from UALVP 49500 below the point of the proximal pubic tubercle, which is not present on the specimen (Figure 4.45). The right pubis displays the expected slight anterior curvature, but the left has been badly warped by erosional pressures, and presents a posterior curve. As mentioned, the pubes are broken off at their proximal ends, but are joined together for almost all of the available surfaces from UALVP 49500. Proximally, they are connected by a mediolaterally short rugosity that extends in a sheet like fashion between the two bones. Distally, the pubes taper inwards and finally fuse together directly in the anteroposterior orientated pubic boot; the dorsal margin of which is well preserved relative to the ventral margin, which has been almost entirely lost.

Fibula

The right fibula is present from UALVP 49500, with only minor damage to its distal end (Figure 4.46). It tapers down from its laterally expanded proximal articulation with the tibia, becoming extremely narrow in the midshaft and distal to the midshaft. There is a well developed fibular process on the posterior surface, which provides a contact for the soleus muscle of the calf (Figure 4.46) (Gray, 2009). The fibula is proximodistally elongate, but as with adult specimens of *Gorgosaurus*, is smaller than the femur. The right femur of UALVP 49500 is yet to be prepared, but length and diameter measurements were taken in the field (Appendix 5; Table 17).

Metatarsals

All five right metatarsals are present in some form, either as part of the articulated right foot, as is the case for MTII, MTIII and MTIV, or isolated like MTI and MTV. MTI is significantly smaller than the others and because of this, is rarely found in tyrannosaurids; in UALVP 49500 it an arrow head shaped medial articulation point with MTII, which extends for more than half of its dorsoventral length (Figure 4.47) (Appendix 5; Table 17). There is also a rugose area on the anterior margin just underneath the proximal articulation. MTII has been heavily warped due to taphonomic pressures, such that the articulated first and second phalanges of the second digit are protruding posteriorly rather than anteriorly, however it is still possible to ascertain that it is widest at its proximal end, slightly narrower at its distal, and is dorsoventrally elongated, although not to the extent of the fibula in UALVP 49500 (Appendix 5; Table 17). MTII is in articulation with MTIII which displays the distinctive dorsal tapering arctometatarsalian condition known from the arctometatarsalian theropods, and present in all other tyrannosaurids (Figure 4.48) (Holtz, 1996). MTIV has been heavily damaged in preparation of the right foot, and it is only possible to view a portion of its anteromedial midlength. The presence or absence of the scar for the insertion of M. gastrocnemius lateralis on the posterior surface of MTIV, another possible trait distinguishing the

two albertosaurine genera is not possible to record in its current state of preparation. MTV was found isolated, but is in excellent condition; it is significantly thinner than the middle three metatarsals, but more elongate than the first (Appendix 5; Table 17). It is damaged proximally on its lateral surface; however, below this is an anteriorly orientated rugose tuberosity (Figure 4.49) (Brochu, 2002).

Pedal Phalanges

There are 15 pedal phalanges present from UALVP 49500, including five pedal unguals out of a possible 28 (tyrannosaurid pedal phalangeal formula: I-2, II-3, III-4, IV-5, V-0 (Holtz Jr. 2004). All pedal phalanges are longer than they are wide (with the exception of the fourth digit on the left foot, which has proximal and distal widths greater than its length), and in each digit, size decreases between the most proximal and distal phalanx, discounting unguals (Appendix 5; Table 18). Digit II of the left foot is represented by phalanges 1 and 2, and possibly an associated ungual. The left distal lateral recesses on phalanges 1 and 2 are deeper than those on the right, helping to side the elements (Lambe, 1917). Of the left foot, digit IV is complete, but disarticulated, and is the only toe for which the correct ungual could be assuredly assigned; this ungual is much longer than the penultimate pedal phalanx on digit IV (Figure 4.50). In the right foot, digit II is represented by the first phalanx, which is similar in size to the same on the corresponding foot. Digit III of the right foot is represented by all but the fourth phalanx; phalanx 1 on digit III is the largest of all the pedal phalangeal elements and displays bilateral symmetry reflective of its central position in the foot. Phalanges one and two of digit II from the right foot, are articulated with each other and the distal surface of MT II (Figure 4.51). The same anterior decrease in phalanx size is witnessed in the digits of the right foot as in the left, and the lateral recesses of digits II and IV also tend to be deeper on the size directly opposing digit III.

Of the five isolated pedal unguals found, only the left fifth phalanx of digit IV could be confidently placed with the corresponding toe bones. Unguals A-D are ordered by increasing size (Appendix 5; Table 18), and are difficult to place due to taphonomic damage to the penultimate phalanx of left digit II, the proximal articulation surface of ungual D, and missing distal phalanges in the other digits. Ungual A, however, is similar in shape and size to the fifth phalanx in the left digit IV, and may be from the corresponding right digit. Unguals B and C are also similar in shape and size and may articulate with digit II on the left and right foot respectively. Ungual D is damaged at its proximal articulation surface, but displays a broad shape atypical of other unguals, that Lambe (1917) accredited to the fourth phalanx of digit III (Figure 4.51).

4.5 Social behaviour in *Gorgosaurus*?

Gregarious behaviours in *Gorgosaurus libratus*, unlike some other well known tyrannosaurid taxa, such as *Albertosaurus* (Currie, 1998; Currie and Eberth, 2010; Eberth and Currie, 2010) and *Tyrannosaurus (*Rothschild and Molnar, 2008; Peterson et al., 2009) have remained relatively unexplored. The dense bone bed containing >26 individuals of *Albertosaurus,* sister taxon to

Gorgosaurus at Dry Island Buffalo Jump (Currie and Eberth, 2010; Eberth and Currie, 2010; Erickson, 2010), provides strong evidence of gregariousness within the albertosaurine clade, however, the variability of social behaviour between closely related taxa has been stressed numerous times in this work (See Chapter 1). Furthermore, the description of UALVP 49500 supports the taxonomic separation of the two taxa at the generic level. The stratigraphic difference and number of morphological distinctions warrants a generic separation, which will also be of greater use if more albertosaurine taxa are discovered in the future (Currie, 2003b). Therefore, any phylogenetic argument for gregariousness in *Gorgosaurus* would be weakened further.

In fact, although it is one of the best represented tyrannosaurid genera, in terms of the number of articulated or disarticulated skeletons, the taxonomic instability that the genus has been subject to over the past 40 years, has perhaps dissuaded behavioural research, with few exceptions. Intriguingly, *Gorgosaurus* is also one of the few well represented tyrannosaurids never to have been found in aggregation with conspecifics, in contrast to *Tarbosaurus*, *Albertosaurus*, and its contemporary in Dinosaur Provincial Park: *Daspletosaurus* (Currie and Eberth, 2010). Multiple individual finds have also been discovered of the basal tetanuran *Allosaurus fragilis* (Hunt et al., 2006), however, not for the large Cretaceous tyrannosaurine *Tyrannosaurus;* an animal for which separate ontogenetic niches have been proposed due to drastic body mass changes and a perceived proclivity towards scavenging towards adulthood (Holtz Jr., 2008; Horner et al., 2011). Although the absence of multiple individual sites of *Gorgosaurus* may certainly not be considered evidence of a solitary lifestyle in itself, it provides an interesting context for the re-examination of social behaviours through different techniques.

Multiple trackway finds have also been scarce for this genus. The best evidence for this indicator of moving social aggregations comes from a recent find in the Late Campanian-Maastrichtian Wapiti Formation of British Columbia, where multiple parallel trackways of footprints attributable to tyrannosauridae were recently discovered (McCrea et al., 2014). As previously mentioned, however, trackways can rarely be linked with a particular taxon (See Chapter 1), and this inherent trace fossil problem was compounded with these particular trackways, in that *Albertosaurus, Daspletosaurus* and *Gorgosaurus,* were all potentially present at different points in this formation (McCrea et al., 2014). Similarly, feathers and feather supporting structure, which have been cited as evidence of sexual display in some dinosaurs (Persons et al., 2013; See Chapter 1), have not yet been found on tyrannosaurids, although it has been suggested that the structures were most likely present in all coelurosaurs (Currie, 2005).

Due to the paucity of evidence which may contribute to our understanding of the social dynamics of this genus therefore, a number of the 'gregarious analyses' discussed in chapter one were performed on the skeleton of the juvenile specimen UALVP 49500 and comparative *Gorgosaurus* material. In so doing, it was hoped to highlight any changes throughout ontogeny, which may influence the behaviour, ecological requirements and, hence, requirement for asociality in this animal.

4.6 Intraspecific agonism/Play: palaeopathologies

Chapter 1 addressed the investigation of palaeopathologies with a view to inferring gregarious behaviours in dinosaurs such as play fighting or intraspecific combat. Palaeopathologies of the bones and teeth are well represented in all tyrannosaurid dinosaurs, including *Gorgosaurus*. Fractures, especially of the fibula, have been frequently found in *Gorgosaurus* specimens, suggesting a highly active lifestyle (Lambe, 1917; Russell, 1970; Rothschild and Molnar, 2008). Interestingly, although Tanke and Currie (1998) and Keiran (1999) described supposed intraspecific bite marks on the same sub-adult specimen of *Gorgosaurus*, (TMP 91.36.500), post-cranial pathologies described for the genus outnumber facial scars reported, in contrast to pathologies described for specimens of *Albertosaurus*, *Daspletosaurus* and *Tyrannosaurus* (Rothschild, 2013). As discussed in Chapter 1, facial bite marks are more prevalent in instances of intraspecific aggression and play behaviour in modern animals, and therefore, would be expected to be the dominant pathology in specimens with regular intraspecific play or agonistic interactions. In order to further explore if this asymmetric distribution of pathologies is characteristic of *Gorgosaurus* or simply a result of underdescription of skull material, all described elements of UALVP 49500 and skull elements of comparative specimens (See Material and Methods, this chapter), were examined for facial bite or claw marks, indicative of intraspecific interactions.

No facial or post cranial pathologies are evident on any bone material from UALVP 49500. However, there is extensive wear and fracturing of the teeth of both the maxillae and the dentaries in the specimen. These wear marks and fractures are discussed in great detail in chapter 4, in which they are contrasted with dental wear found in an adult *Gorgosaurus* specimen, UALVP 10, in order to evaluate the possibility of changing feeding mechanism, diet and behaviour throughout ontogeny. Only one skull element from the comparative material presented a potential pathology: a possible small tooth mark, with an orientation different to that of the neurovascular grooves, in the lateral side of the right dentary from TMP 1994.012.0155: a small, likely juvenile *Gorgosaurus* specimen known only from skull material (Figure 4.52). The potential bite mark is extremely shallow, and might reflect a minor example of the Type 2 bite mark morphology employed by Tanke and Currie, (1998), in that it is isolated and mildly curved. If it were confirmed as being inflicted by another *Gorgosaurus* specimen, it may be tempting to assign to the less extensive form of bite marks attributable to play behaviour amongst juveniles. However, as with most trace fossils from areas with more than one contemporaneous similarly sized animals, it is impossible to tell which tyrannosaurid genera created the mark, nor indeed if it had a tyrannosaurid origin, as the great depth of bite marks in bone are often the best indicator that they were inflicted by members of this the family (Jacobsen 1998; Rothschild, 2014). During field work in Dinosaur Provincial Park in May 2014, a partial ceratopsian parietal horn with apparent multiple tyrannosaurid bite marks in different orientations was collected by the author (Figure 4.53: Field Number DPP.2014.112). Similar to the tyrannosaurid bite marks reported on numerous ceratopsian occipital condyles by Rothschild (2014) (See Chapter 1), there would be little to no nutritional gain in feeding on the parietal horn of ceratopsians. However, the accidental contact between tyrannosaurid teeth and

these structures during attempts to bite the neck or back of the skull seems a far more likely explanation than the inference of object play behaviour in *Daspletosaurus* or *Gorgosaurus,* as was suggested by Rothschild (2014).

4.7 Diet: denticle differences between juvenile and adult

A key component of the success of the tyrannosaurid tooth wwas the serrated anterior and posterior carinae, and the relationship between the size of the denticles that make up these carinae and the overall size of the tooth (denticle density) density of theropod teeth can also be extremely useful in identifying isolated teeth to genus level in formations and geographical areas which hosted more than one large theropod contemporaneously (Currie, 1990). The variation in denticle density of tyrannosaurid teeth may also have concomitant functional implications for the mechanisms of food processing (Farlow et al., 1991; Abler, 2013). Considering this, the denticle density per mm of UALVP 49500 and comparative juvenile specimens was measured and compared to previously measured adult teeth (Adult specimens measured by Dr. Angelica Torices).

The denticle density of UALVP 49500 and three other specimens considered to be juvenile due to their small size and in some cases age estimation from lines of arrested growth (See Materials and Methods, this chapter), was consistently three per mm, whereas that of the two adult specimens was 2 per mm (Figure 4.54), although the overall size of teeth overlapped substantially. This greater serration density in juvenile *Gorgosaurus* teeth than in adults may reflect differences in feeding techniques; juveniles could conceivably be more adapted for the slicing and shearing of tissue of carcasses, than adults. Differences in the feeding mechanisms of juvenile and adult *Gorgosaurus* may reflect dietary and ecological changes throughout ontogeny; this concept is considered in greater detail alongside the results of tooth wear comparisons between UALVP 49500 and UALVP 10 (and adult specimen), in Chapter 5.

4.8 Sexual display: lacrimal horn allometry

Chapter 2 discussed at length the potential function of structures such as horns, crests and rugosities in sexual display or intraspecific sexual combat between males, and suggested that allometric studies may help in confirming the utility, or at least importance of such structures. Of these structures typically spectacular examples include the elongated cranial crests of the lambeosaurines (Dodson, 1975) and the wide skull crests of *Cryolophosaurus* (Smith et al., 2007), however, more understated cranial elaborations were also present in some tyrannosaurids (Molnar, 2005).

Gorgosaurus has been recorded as supporting three 'cornual processes', or facial rugosities: the ventrolateral projection of the jugal, the postorbital horn and the lacrimal horn (Carr, 1999; Currie, 2003b). In UALVP 49500, the lacrimal horn is the most prominent of these three processes, with the postorbital horn and jugal cornual process relatively undeveloped compared to the former in this juvenile specimen (See section 3.4). The lacrimal horn of UALVP 49500 or any other *Gorgosaurus* specimen is not comparable in its prominence to, for example, the supraorbital horns

of *Carnotaurus*, which were so well developed as to make Paul (1988) suggest that they were used in a head butting mating display in a manner similar to big-horned sheep. This said, they have been recorded as undergoing significant change throughout ontogeny (Carr, 1999), suggesting that they may play some significant role later on in an individual's life history, such as utilisation in sexual display. If this were the case, however, they might be expected to grow at a faster relative rate than other parts of the body which show little variation in their rate of growth throughout life.

In order to test these predictions, the height of the lacrimal horn in UALVP 49500 and six other specimens from juvenile to adult stages (See Materials and Methods), either directly measured or measured from scaled published illustrations (Table 4..4), were plotted against their respective skull lengths and femoral lengths, which were either personally measured or attained from a pre-existing tyrannosaurid measurement data set. Femoral and skull lengths were chosen as suitable bones for comparison as the latter has been show to vary relatively little throughout growth in many animals, including tyrannosaurids, and the latter displays isometric growth with the femur in the tyrannosauridae (Currie, 2003a). The measurements were logarithmically transformed in order to reduce the effect of outliers (Cawley and Janacek, 2010; Campione and Evans, 2012) and then plotted against each other in least-squares linear regressions, and used to solve, the basic allometric equation: $y=bx^{a}$ (Naroll and Von Bertalanffy, 1956). Here, α represents the allometric coefficient, and in tyrannosauridae an α value of >1 represents positive allometric growth, whereas an α value of <1 represents negative allometric growth (Currie, 2003a).

The results of the allometric study showed that lacrimal height in the specimens of *Gorgosaurus* is positively allometric in comparison to the length of both the femur and the skull throughout ontogeny. The allometric coefficient in this comparison between lacrimal height and femoral length (Figure 4.55) was high (α=1.54; R^2=0.86; p=<0.01) even in relation to other cranial components of tyrannosaurids (Currie, 2003a), and a similarly high allometric coefficient (α=1.46; R^2=0.89; p=<0.01), also suggested positively allometric growth in comparison to the length of the skull in *Gorgosaurus* (Figure 4.56).

This faster relative growth of the lacrimal horn compared to the femoral and skull length provide support for the idea that these lacrimal horns may be related to some function related to the maturity of the animal, such as sexual display. Currie (2003a) showed that the height of the orbit in tyrannosaurid grows with positive allometry during ontogeny, and that this is concomitant with the growth in height of the skull, however, the lacrimal rugosity/horn is above the level of all lacrimal sutures and is not necessarily influenced by the growth of the lacrimal and postorbital bars below. Furthermore, the anteroposterior thickness of the lacrimal and postorbital ventral processes have been demonstrated as the important dimensions of the orbit in maintaining the strength of the skull during the increase in volume of the jaw adductor muscles (Henderson, 2007), thus it is unlikely that a dorsally situated lacrimal rugosity has any major influence in the resistance of the skull to the strain created by larger bite forces. Although the study has a relatively low sample size (n=7), it provides some initial corroboration for the theory that these structures in *Gorgosaurus*

may be important in a potentially social context. A greater sample size with a large number of juveniles and adults is desirable to explore the possibility that the lacrimal horn in *Gorgosaurus* might grow with negative allometry during its early years, and positive allometry closer to the age of sexual maturity, in a manner similar to sexual display structure in modern animals, such as the casque in Cassowaries (Dodson, 1975; Richardson, 1991).

4.9 Ecological niche difference between juveniles and adults: orbital aspect ratio

The orbits of theropods have been recognised as an extremely important component of behavioural studies and their dimensions have influenced theories on predation ability (Paul, 1988) and probable time of activity; that is whether or not the animal was nocturnal, diurnal or crepuscular, as has been suggested for *Troodon* (Russell and Seguin, 1982). Currie (2003a) reported that the orbit in tyrannosaurids grew in size with more positive allometry in earlier in ontogeny, with the result that the eye would have been relatively larger in juvenile than adult individuals of the same taxon. Substantial differences during tyrannosaurid ontogeny in the shape and size of the orbit, may reflect behavioural differences in the juvenile and adult form of the taxon, and thus have implications for the extent of gregarious interactions.

In order to examine any trends which may have implications for the potential partitioning of ontogenetic stages in *Gorgosaurus*, and hence the extent of gregarious behaviour expected of the animal, the aspect ratio (anteroposterior length: dorsoventral height) of the orbits of UALVP 49500 and comparable specimens were examined and analysed. First, the aspect ratio of 34 specimens (most dimensions obtained from Dr. Philip Currie's previously measured data set) of tyrannosaurids from six genera including *Gorgosaurus* were compared (Table 4.5). This supported previous reports that *Gorgosaurus* had the most circular orbits of the tyrannosauridae, a condition considered to be primitive, and closer in shape to the orbits of basal theropods such as *Coelophysis* and *Herrerasaurus*, than *Tyrannosaurus* (Chure, 1998). The ontogenetic stages of the six specimens of *Gorgosaurus* were then ascertained either through histology (see Growth Rates section), or inference from body size, in order to make intraspecific comparisons (Table 4.6). From these results, there was a large difference between the four smallest juvenile specimens, which had an average aspect ratio of 0.9:1, and the two largest specimens (a probable sub-adult and confirmed adult) which showed a much lower average aspect ratio of 0.72:1.

This trend suggests that, concomitant with the relative decrease in the size of the orbit over ontogeny in *Gorgosaurus*, there is also a decrease in the circularity of the orbit. The function of this change may be important in contrasting the behaviour of juvenile and adult individuals of *Gorgosaurus*. A larger and more circular orbit for example, may allow the reception of greater levels of light, and juveniles may be better suited to a crepuscular lifestyle than the adults, as has been suggested for *Troodon* (Russell and Seguin, 1982), thus reflecting an ontogenetic niche separation in *Gorgosaurus*. Alternatively, Henderson (2003) has demonstrated the potential utility of reducing the circularity of the orbits in strengthening the skull for the increased bite forces that come with larger skulls, jaws, and jaw adductor muscles. A high level of contrast in the strength of

the jaw between juveniles and adults however, may still indicate a difference in feeding mechanisms, diet, and again, ecological niches in *Gorgosaurus*, as has been suggested for *Tyrannosaurus* (Horner et al., 2011). The possibility of an ontogenetic shift in feeding behaviour, diet and ecological niches are dealt with in greater detail in Chapter 4.

4.10 Growth Rates: body mass vs. age

The importance of understanding growth rates in the assessment of parental or group association early in life for a dinosaur taxon was first discussed in Chapter 1. Whether an animal exhibits rapid or slow growth during early ontogeny will reflect its ability to live independent of their parents and a group, or infer their requirement for some form of sociality, at least during juvenility. Towards the goal of assessing the likely dependence on a social environment of a juvenile *Gorgosaurus* therefore, growth curves for the genus were created with a view to updating the current growth rate information for this albertosaurid that was last updated over a decade ago (Erickson et al., 2004) using some now outdated methods. Herein, body mass estimates were compared to lines of arrested growth in histological sections of *Gorgosaurus* dorsal ribs. Body mass estimates have been used to infer growth dynamics and palaeobiology for dinosaurs (Curry, 1999; Erickson & Tumanova, 2000; Erickson et al. 2001; Erickson et al. 2004; Lehman & Woodward, 2009). The appeal of body mass predictions in palaeontology is in their relationship with metabolism, and dietary requirements of dinosaurs; their use can give insight into physiological, ecological and evolutionary questions (Farlow et al., 1995; Gillooley, 2001; Benson, 2014). The scaling relationship among the dimensions of the femora, humeri, and the body mass of an animal was first introduced by Anderson et al. (1985), based on extant quadrupedal mammals. The resulting regression equation based on femoral circumference has been heavily used by palaeontologists (Currie & Carpenter, 2000; Smith et al. 2007; Benson et al. 2009). Whereas volumetric alternatives have emerged utilising modern computational methods (Henderson, 1999; Seebacher, 2001; Hutchinson et al., 2007; Bates et al., 2009; Brassey et al., 2015), well supported allometric equations remain useful; they are both accessible without sophisticated computer programs and do not require complete or nearly complete specimens.

Recently, Campione & Evans (2012) proposed bivariate and multivariate equations for estimating the body mass of quadrupedal vertebrates based on femoral and humeral circumferences, and the scaling work previously done by Anderson et al., (1985). This formula was then mathematically corrected to scale for bipedal vertebrates (Campione et al., 2014). Both the quadrupedal (QE) and bipedal (cQE) equations showed less statistical error than existing equations involving the stylopodial skeleton (Anderson et al. 1985; Christiansen, 1999). This most successful body mass estimation technique based on femoral circumference (Campione et al., 2014) was used to estimate the mass of adult specimens of *Gorgosaurus*. The majority of the sample set, however, consisted of juvenile specimens; Erickson and Tumanova, (2000), Erickson et al., (2002; 2004) and Campione et al., (2012; 2014) mentioned the unsuitability of using scaling relationship methods of body mass estimation for juvenile dinosaur specimens due to unknown rates of allometric growth in

juvenile dinosaurs versus extant mammalian analogues. Erickson and Tumanova (2000) suggested a proportional technique called Developmental Mass Extrapolation Femoral Scaling Principle in which femoral lengths of juveniles were compared relatively to the largest known adult specimen. As Campione et al. (2012) showed, femoral circumference outperforms femoral length in the estimation of body mass, a modified version using femoral circumference of Erickson's (2000) method was developed and used for the juvenile specimens of *Gorgosaurus* (Table 4.8). In order to boost the data set of available specimens, the best performing of the femoral circumference prediction techniques discussed in Chapter 2, **ELLR,** was used to predict femoral circumference in three specimens (Table 4.8), and one specimen was calculated using the simple regression equation for femoral circumference and length in tyrannosaurids: y=1.2533x-1.1638 (Y=Log femoral circumference, x=log femoral length; Currie, Pers. Comm.) (Table 4.9).

Lines of arrested growth (LAGs) in histological sections of dinosaurs are thought to reflect periods of reduced or halted growth (Reid, 2012); the periodicity of these lines has been supported by the presence of such histological cycles in some extant archosaurs (Castanet, 1994) and through studies of stable oxygen isotopic ratios (Tütken et al., 2004). In order to attain age at death estimates for the *Gorgosaurus* specimens, LAGs were identified in histological thin sections of dorsal ribs from four specimens (see Materials and Methods). Dorsal ribs were chosen as they are more common than long bones, and as non-weight bearing bones, have been postulated as exhibiting minimal secondary remodelling of the medullary cavity (O'Connor, 1982; Erickson et al., 2004). Lines were considered to represent true LAGs if they depicted uninterrupted mineralisation in concentric rings and the continuation of these rings could be traced around a large proportion of the rib. Other lines were inferred as being intra-annual seasonally affected variations in growth, as they were not completely mineralised and did not continue round the ribs.

Rib sections from only two specimens: UALVP 49500 and TMP 91.36.500 displayed enough LAGs to predict the age of death of the animal (Figure 4.57; Figure 4.58), which were calculated as being between 7-14 years and 4-7 years respectively (Table 4.9). Although LAGs were present in the dorsal rib thin section of UALVP 10 (Figure 4.59), back calculation resulted in an unrealistically high age at death estimate (>40 years), most likely due to the slowing of growth towards the end of life, shortening the distance between the few growth lines visible, therefore it was not included in the growth curve. Another specimen sampled, TMP 1991.163.001, did not display any growth lines and both this specimen and UALVP 10 exhibited bone texture associated with adult specimen; secondary remodelling was apparent in the production of numerous haversian canals, encircled by slowly deposited lamellar bone, the lack of extensive vascularisation and presence of almost no fibrolamellar bone or primary osteons (Chinsamy-Turan, 2005; Padian and Lamm, 2013) (Figure 4.60; Figure 4.61).

Three Gompertz growth rate curves were returned for *Gorgosaurus* results, created using minimum (Figure 4.62), maximum (Figure 4.63) and mean body mass estimates (Figure 4.64). The growth curves are more conservative in their estimation of the maximum rate of growth (Kg/year)

previously published for *Gorgosaurus*. This analysis suggests a maximum growth rate using the mean body mass estimations of 95 kg/year (in TMP 94.12.602), compared to 114 kg/year suggested by Erickson et al., (2004); only using the maximum body mass estimations are these levels of growth rates reached (119.39 kg/year in TMP 94.12.602). Significantly, for the goals of this thesis, the growth rate for the youngest specimens RTMP 86.144.1 (29.79 kg/year) and FMNH PR: 2211 (26 kg/year), calculated using mean body mass are much lower than those of the two oldest specimens RTMP 94.12.602 (95 kg/year) and RTMP 99.33.1 (88.68 kg/year).

Using the same methodology for body mass estimation, alongside previously published age at death estimates (Table 4.10) (After Erickson et al., 2004), three Gompertz growth rate curves of *Albertosaurus,* the tyrannosaurid with perhaps the best evidence of extensive social aggregations (Currie and Eberth, 2010), were created in order to compare the results to those for *Gorgosaurus* (Figure 4.65; Figure 4.66; Figure 4.67). Overall, the growth rate of *Albertosaurus* is greater than that of *Gorgosaurus,* with the former showing mean growth rates for minimum, maximum and mean body estimates of 53.53 kg/year, 89.28 kg/year and 71.4 kg respectively. In comparison, *Gorgosaurus* specimens show mean growth rates of 44.05 kg/year, 73.71 kg/year and 58.85 kg/year, when using minimum, maximum and mean body mass estimates (Table 4.10). The rate of growth for the one juvenile specimen of *Albertosaurus* at mean body mass (TMP 2002.45.46, 19.73 kg/year) is similarly low to that of the youngest *Gorgosaurus,* suggesting slow rates of juvenile body size growth in both albertosaurine genera.

As discussed in Chapter 1 the slow growth rates of juvenile dinosaurs may imply the necessity for high degrees of parental or other social care whereas relatively faster growth rates may imply independence from an early age. The growth rate of overall body size in *Gorgosaurus* juveniles has here been shown to be slower than previously thought (Erickson et al., 2004), and the genus grows slower at all sizes than its sister taxon *Albertosaurus*, which has been found in a dense multi aged individual bone bed (Currie and Eberth, 2010). This may then suggest that juvenile *Gorgosaurus* individuals were dependent on social care for the early years of its life, when growth was slowest, in the form of parental care, pack care or in juvenile only aggregations such as those known from other dinosaurian groups (e.g. Sauropods; Myers and Fiorillo, 2009). The social aggregation of young or old *Gorgosaurus* individuals might represent one possible method of survival and protection of hunting territories, when cohabiting with an even larger apex predator, *Daspletosaurus*.

Alternatively, the slow juvenile growth rate of *Gorgosaurus* could represent nutritional detriment caused by a shortage of food in a separate ecological niche than adults, created by the large disparity in body mass sizes and slow growth (Table 4.9). Some instances of nutritional deprivation in solitary juveniles are known from modern taxa; Siberian tiger cubs, which are largely solitary animals after brief initial levels of parental care, have displayed malnutrition conditions such as nutritional secondary hyperparathyroidism (Won et al., 2004).

4.11 Von Ebner lines

Growth rates of dinosaurian taxa may potentially reveal r or k parental strategies, however, as was discussed in Chapter 1, the comparison of overall growth rates to those of 'hunting tools', such as teeth in juvenile tyrannosaurids may help confirm the level of social or parental care that would have been required for survival (Feranec, 2005). To this end, an isolated maxillary tooth from UALVP 49500 was histologically sectioned (Figure 4.68), in the hopes of identifying lines of Von Ebner, which are thought to represent daily depositions of dentine, in a manner similar to modern crocodylians (Erickson, 1996). Once a substantial number of von Ebner lines had been identified and the distance measured between them, in keeping with the philosophy of this thesis to limit the destruction of samples from the juvenile *Gorgosaurus*, the left maxilla and dentary of UALVP 49500 were C-T scanned. It was hoped that if the daily dentine deposition lines in the isolated tooth exhibited regular spacing, then, using the calculated lateral areas of a descended and replacement tooth at one tooth position in the C-T scan, the number of von Ebner lines in each may be extrapolated, and the tooth replacement rate calculated (See Michael et al. 2013, for similar method).

Although some von Ebner lines were identified in one frontal section of the isolated maxillary tooth (Figure 4.69), with the aid of comparative slides made by Paul Johnston in the 1970's (Figure 4.70; See Johnson, 1979), they were not in abundance, nor did many of them extend for more than a short distance. Further lateral thin sections of the same tooth were even less successful and no incremental lines could be identified. Given the extremely low number of von Ebner lines witnessed in the tooth, due to poor preservation, an extrapolation to two separate teeth could not be justified; the destruction of further teeth from UALVP 49500 was subsequently decided against. For this project to be continued, numerous isolated juvenile teeth should be histologically sectioned in different planes to observe if the distance between incremental lines of von Ebner is constant for different teeth of different individuals.

4.12 Conclusion

This chapter is comprised of numerous sections that better the current understanding of *Gorgosaurus libratus*. The description of UALVP 49500 presents multiple characteristics that support the generic distinction of *Albertosaurus* and *Gorgosaurus*, and is the first comprehensive description of a juvenile *Gorgosaurus* that includes post-cranial material. The specimen was then included in a range of different analyses inspired by the review of social behaviour in extant and extinct taxa found in Chapter 1. This was carried out in order to assess the theory that *Gorgosaurus* may have participated in some gregarious interactions throughout its lifetime, and particularly may have required a social environment during juvenility.

Observation of skull elements in UALVP 49500 and other *Gorgosaurus* specimens failed to identify substantial bite marks that could be attributed to play or intraspecific combat behaviour; consistent with the absence of any definitive *Gorgosaurus* bone beds or multiple trackway sites. There were, however, vast ontogenetic changes evident between juvenile and adult *Gorgosaurus* specimens, which may hold some inferential merit concerning social behaviours. Positively

allometric growth of the lacrimal horn may imply use as a sexual display structure later in ontogeny, whereas the higher denticle density of juveniles than adults may have implications for feeding mechanisms and diet. The reduction of the circular shape of the orbit in juveniles into the more irregular one of adults may also signal a change in the feeding mechanics of *Gorgosaurus* throughout ontogeny, or even a difference in the time of highest activity levels between the two forms. The growth curves produced for *Gorgosaurus* was created using the most up to date body mass estimations, including an original modification of a previous femoral scaling method for juveniles, and the data set was increased using the most successful femoral circumference estimation method from Chapter 2. They depicted generally lower growth rates for *Gorgosaurus* than previously published, lower growth rates in comparison to its sister taxon *Albertosaurus*, and similarly slow rates of growth during early ontogeny. These slow juvenile growth rates may be indicative of young that require parental care, or a social group for survival, or may represent nutritional deficiency accrued during an isolated lifestyle. The ontogenetic changes between juvenile and adult *Gorgosaurus*, and their relationship with the requirement for social behaviour during early growth, are explored further in Chapter 4, in which the tooth wear of two differently aged *Gorgosaurus* specimens is compared.

4.13 Chapter 4- Tables

UALVP 49500 Cranial Elements	Number Present
Left Maxilla Partial	1
Right Maxilla Partial	1
Left Dentary	1
Right Dentary	1
Partial Left Jugal	1
Lacrimal	2
Splenial	1
Frontal	1
Parietal	1
Quadratojugal	1
Large skull block	1

Table 4.1. UALVP 49500 cranial elements visible from original quarry maps of Q253

UALVP 49500 Post Cranial Skeletal Element	Number Present on Quarry Maps
Vertebrae	17 (Not including Head block) 11 caudal, approximately 10 dorsal
Gastralia	17 (Maximum)
Rib	11-13
Chevron	6
Phalanges	12
Tarsals	1
Metatarsals	4
Scapula	2 (1 Scapula-Coracoid)
Femur	1
Humerus	1
Tibia	2
Fibula	2 (Possible)
Pelvis- Ischium, Pelvis, Pubis	1
Ungual	5
Ulna	1
Radius	1

Table 4.2. Post-cranial skeletal elements visible from original quarry maps of Q253

Gorgosaurus libratus Specimen	Skull Length (mm)
UALVP 49500	**685**
AMNH 5336	962
AMNH 5458	990
CMN 2120	1000
TMP 86.144.1	500
TMP 91.36.500	670
TMP 94.12.155	364
TMP 94.12.602	870
TMP 99.33.1	700
UALVP 10	870
USNM 12814 (AMNH 5428)	820
AMNH 5664	670

Table 4.3. Skull length of UALVP 49500 compared to other *Gorgosaurus* specimens

Gorgosaurus libratus specimen	Femur length (mm)	Log Femur Length	Lacrimal horn height (mm)	Log Lacrimal Horn Height	Skull length (mm)	Log Skull Length
AMNH 5336	958	2.981366	38.27	1.582858	962	2.983175
NMC 2120	1030	3.012837	41.33	1.616265	1000	3
ROM 1247	765	2.883661	20.917	1.320499	782	2.893207
TMP 86.144.1	545	2.736397	14.3	1.155336	500	2.69897
TMP 91.36.500	645	2.80956	25.16	1.400711	670	2.826075
UALVP 10	901	2.954725	32.1	1.506505	870	2.939519
UALVP 49500	730	2.863323	21.57	1.33385	685	2.835691

Table 4.4. *Gorgosaurus* lacrimal horn vs. femur/skull length raw regression measurements

	Orbit Anteroposterior length (mm)	Orbit Dorsoventral Height (mm)	Sample Size	% Difference between length and height	Aspect Ratio (Length: Height)
Gorgosaurus	92.5	111.3	6	17%	0.83:1
Nanotyrannus	87	113	2	23%	0.75:1
Albertosaurus	102.5	175	2	41%	0.6:1
Tarbosaurus	108.9	194.6	12	44%	0.55:1
Daspletosaurus	112.5	206.5	5	45%	0.55:1
Tyrannosaurus	130.3	312.3	7	58%	0.4:1

Table 4.5. Orbit length vs. height for six genera of tyrannosaurids

Gorgosaurus specimen	Orbit Anteroposterior Length (mm)	Orbit Dorsoventral Height (mm)	Ontogenetic Stage	Method of Aging
UALVP 49500	94	98	Juvenile: 7-14	L.A.G.
TMP 86.144.1	90	100	Juvenile: 7*	L.A.G.
TMP 91.36.500	93.5	105	Juvenile: 4-7	L.A.G.
TMP 2009.12.14a	81.2	90.3	Juvenile	Body size
UALVP 10	115	160	Adult	Secondary Remodelling Extensive
AMNH 5664	81	112	Sub-adult	Body size

Table 4.6. Orbit length vs. height for six specimens of *Gorgosaurus* *After Erickson et al., 2004

	Mediolateral Diameter (ML) (mm)	Weighted ML (mm)	Log ML	Log/Weighted Circumference (mm)	Back Transformed Circumference (mm)	Back Transformed and Re-Weighted Circumference (mm)
UALVP 49500	65	13	1.1	1.66	45.23	226
91.163.001	98	19.6	1.3	1.83	68.20	341
99.33.1	83	16.6	1.2	1.76	57.76	289

Table 4.7. Circumference estimation data for specimens of *Gorgosaurus* using **ELLR.** All estimations based on mediolateral circumference data, except NMC2120, which use anteroposterior data.

Specimen	Femoral Circumference (mm)	Femoral Circumference^3 (mm)	Relative percentage of biggest adult
NMC 2120	378	54010152	100

UALVP 49500	226.16	11567709.8	21
TMP 91.36.500	191	6967871	13
TMP 86.144.1	162	4251528	8
FMNH PR: 2211	136	2515456	5

Table 4.8. Modified developmental mass extrapolation of 4 juvenile specimens of *Gorgosaurus libratus* (Modified after Erickson et al., 2000)

Specimen	Age	Femoral Circumference (mm)	Mean Body Mass Estimation (Campione et al. 2014; modified from Erickson et al., 2000)	Upper Boundary	Lower Boundary
NMC 2120 (Holotype)	Adult	378	2605.7	3258	1953.5
UALVP 49500	7-14	226.16†	547.197	684.18	410.2
TMP 91.163.001	Adult	341†	1962.1	2453.2	1471.9
TMP 91.36.500	4-7	191	338.65	423.54	254
RTMP 94.12.602	18*	330	1710.7	2149.1	1272.2
RTMP 99.33.1	14*	288.79†	1241.5	1552.3	930.8
RTMP 86.144.1	7*	162	208.5	260.64	156.3
FMNH PR: 2211	5*	136	130.3	162.9	97.7
UALVP 10	Adult	346.22^{+}	2046	2558	1533.9
Mean Gorgosaurus growth rate (Kg/Year)	-	-	58.85	73.71	44.05

Table 4.9. Growth rate data for *Gorgosaurus* specimens following histological sectioning of ribs and body mass estimations*After Erickson et al., 2004 †Calculated using **ELLR**, $^{+}$Calculated using: y=1.2533x-1.1638 (Y=Log femoral circumference, x=log femoral length; Currie, Pers. Comm.)

Albertosaurus sarcophagus Specimen	Age (Erickson et al., 2004)	Femoral Circumference (mm)	Mean Body Mass Estimation (Kg) (Campione et al. 2014; modified from Erickson et al., 2000)	Upper Boundary (Kg)	Lower Boundary (Kg)
TMP 81.10.1	24	305	1443.1	1804.2	1081.9
AMNH 5432	22	391.1^{+}	2861.9	3578.2	2145.5
USNM 12814	18	326.6^{+}	1742.1	2178.2	1306.1
TMP 86.64.01	15	241	754.4	943.2	565.6
TMP 2002.45.46	2	93.1^{+}	39.46	49.3	29.7
Mean Albertosaurus Growth Rate (Kg/Year)	-	-	71.4	89.4	53.5

Table 4.10. Modified body growth rate data for *Albertosaurus sarcophagus* from Erickson et al., (2004) $^{+}$Calculated using: y=1.25x-1.16 (Y=Log femoral circumference, x=log femoral length; Currie, Pers. Comm.)

4.14 Chapter 4-Figures

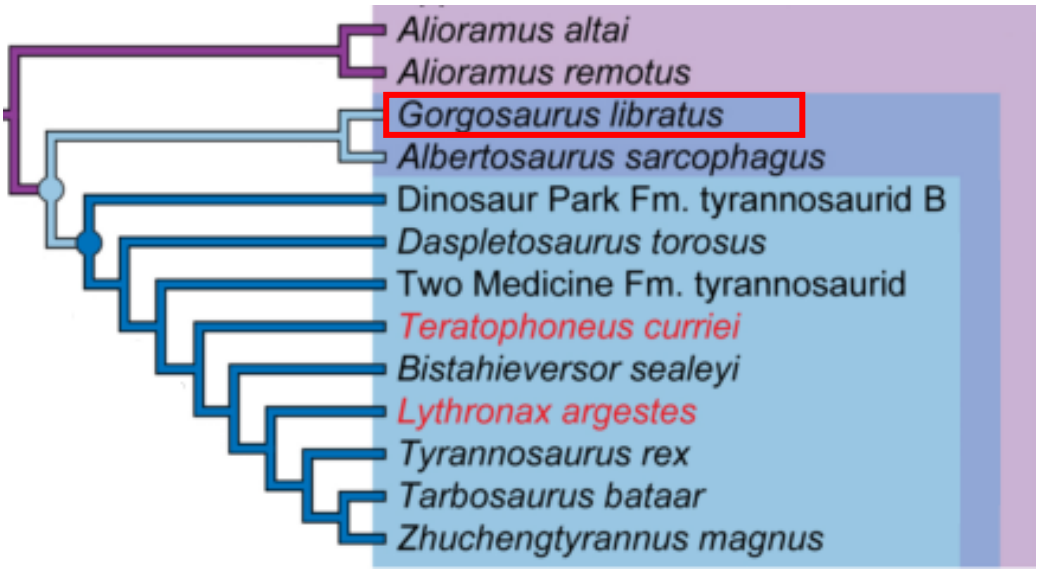

Figure 4.1. Recent phylogenetic tree showing *Gorgosaurus libratus* position as a basal tyrannosaurid within Tyrannosauroidea and sister taxon to *Albertosaurus sarcophagus* (Modified from Loewen et al. 2013).

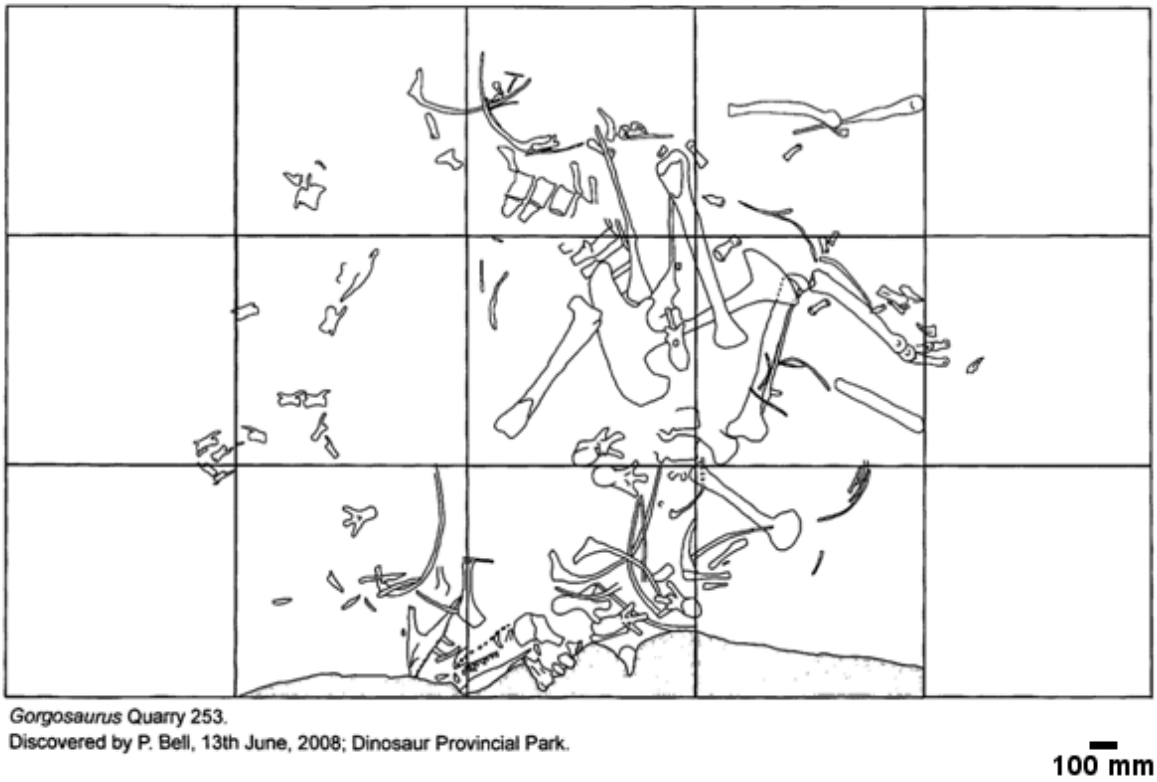

Figure 4.2. Quarry map of UALVP 49500 excavation site in Dinosaur Provincial Park (Quarry 253-Photo: Philip Currie.)

Figure 4.3. Striations in lateral view on antorbital fossa in UALVP 49500

Figure 4.4. Right maxilla in lateral view UALVP 49500. Arrows showing anterior rims of maxillary fenestra (anterior) and antorbital fenestra (posterior)

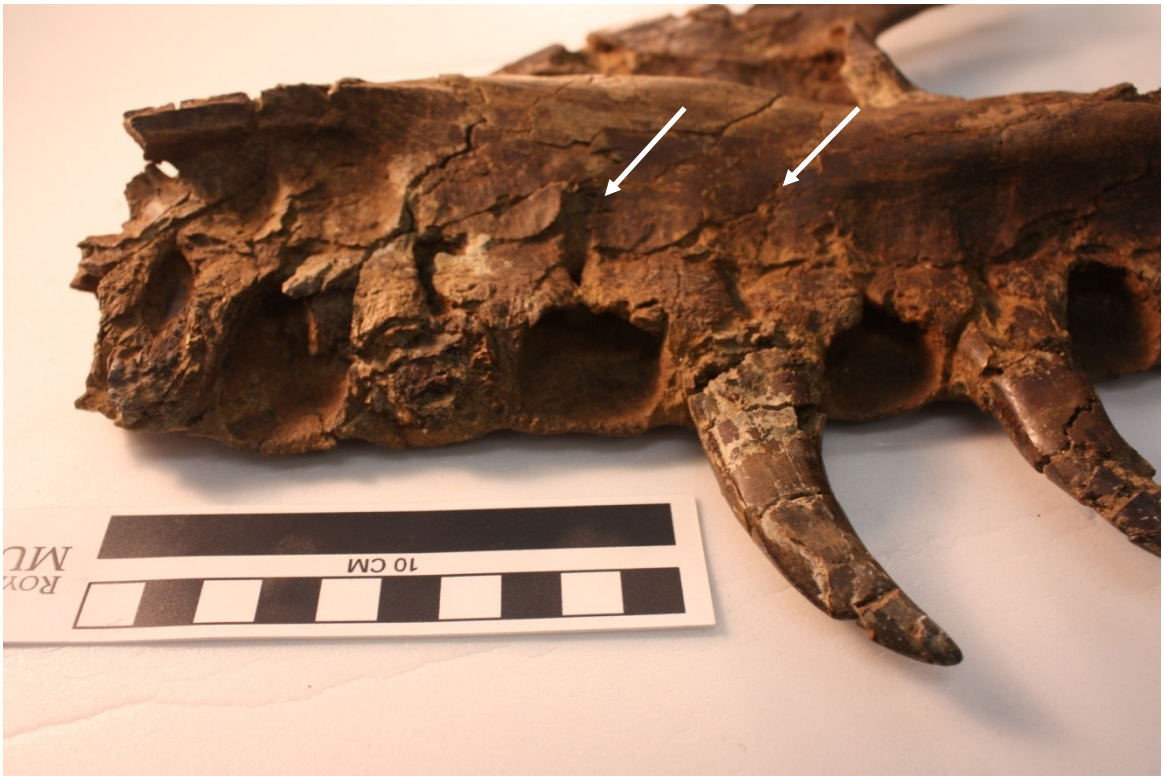

Figure 4.5. Ventral view of mild depressions in right maxilla (arrows) palatal shelf of UALVP49500

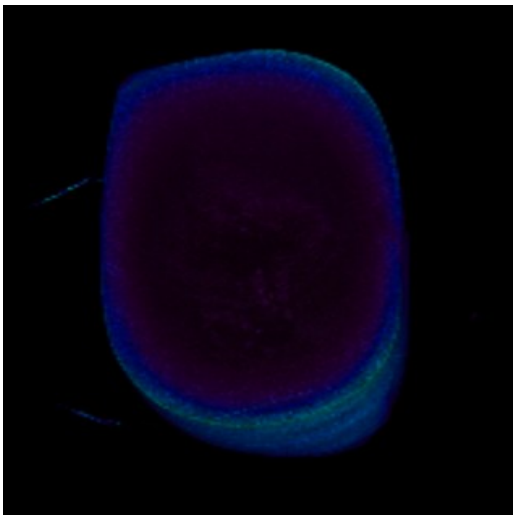

Figure 4.6. Ovate cross section at base of isolated maxillary tooth from UALVP 49500 scanned using a Skyscan MicroCT scanner

Figure 4.7. Left jugal of UALVP 49500 in lateral view Arrow showing pneumatopore.

Figure 4.8. Right Quadrate of UALVP 49500 in lateral view.

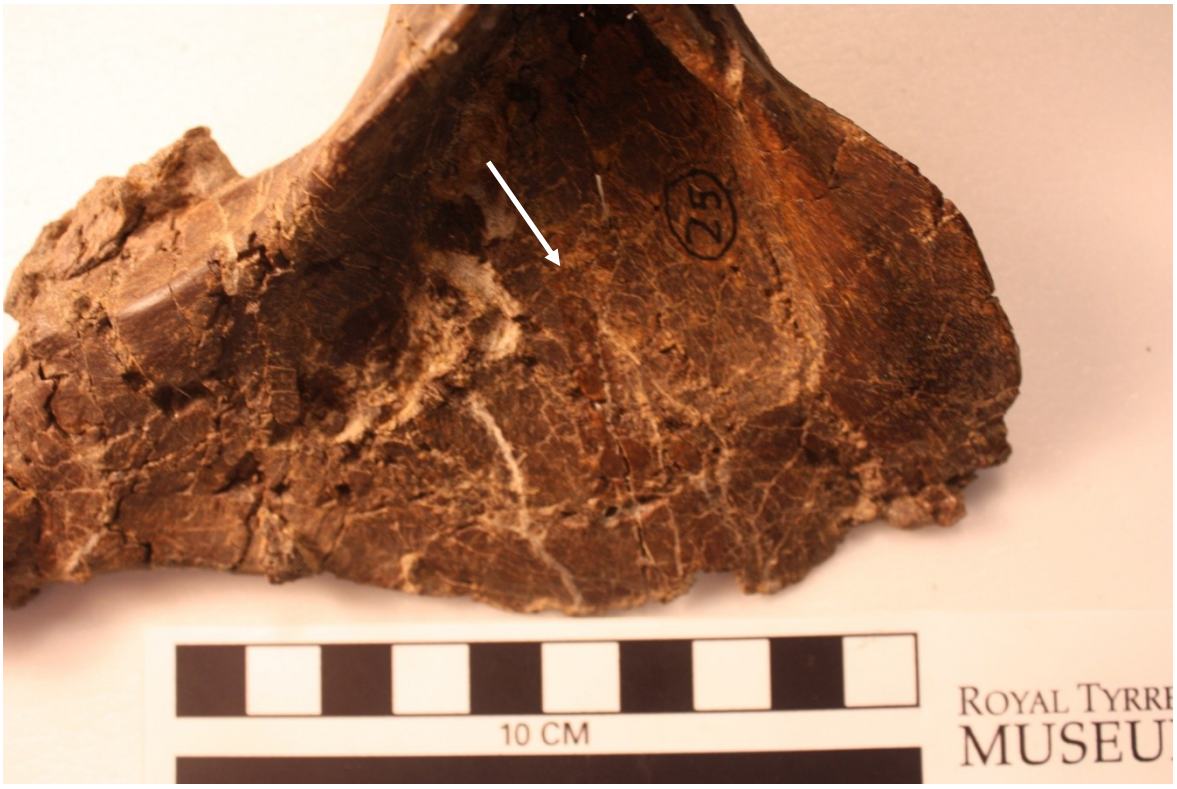

Figure 4.9. Medial fossa (arrow) in right quadrate of UALVP 49500, dorsomedial view

Figure 4.10. Left quadratojugal of UALVP 49500 in lateral view. Arrows showing flaring of squamosal contact

Figure 4.11. Right quadratojugal ofUALVP 49500, showing rugose medial quadrate articulation

Figure 4.12. Right lacrimal of UALVP 49500 in lateral view. Arrows show lacrimal horn (dorsal) and pneumatic fossa (ventral).

Figure 4.13. Right postorbital of UALVP 49500 in lateral view. Arrow showing dorsolateral fenestra.

Figure 4.14. Right postorbital of UALVP 49500 in medial view. Arrow showing medial central fossa.

Figure 4.15. Left squamosal of UALVP 49500 in dorsal view

Figure 4.16. Left squamosal of UALVP 49500 in ventral view. Arrow showing the anterior pneumatic foramen.

Figure 4.17. Partial left and right frontals of UALVP 49500 in dorsal view

Figure 4.18. Partial left and right frontals of UALVP 49500 in ventral view. Arrow showing intrafrontal suture.

Figure 4.19. Left and right ectopterygoids of UALVP 49500 in dorsal view.

Figure 4.20. Left ectopterygoid from UALVP 49500 in ventral view. Arrow showing ventral pneumatopore.

Figure 4.21. Left epipterygoid of UALVP 49500 in lateral view

Figure 4.22. Left pterygoid of UALVP 49500 in ventral view

Figure 4.23. Left palatine of UALVP 49500 in lateral view. Arrows showing two pneumatopores and one possible pneumatopore (anterior) on lateral shelf

Figure 4.24. Left dentary of UALVP 49500 in lateral view.

Figure 4.25. Right surangular of UALVP 49500 in lateral view.

Figure 4.26. Articulated left angular (arrow) from UALVP 49500 in lateral view.

Figure 4.27. Medial view of articulated right splenial. Arrow shows the anterior mylohyoid foramen.

Figure 4.28. Left supradentary/coronoid (arrow) from UALVP 49500 in medial view.

Figure 4.29. Right prearticular of UALVP 49500 in medial view

Figure 4.30. Articular/Surangular/Prearticular contact to make quadrate articulation concavity in UALVP 49500, medial view.

Figure 4.31. Anterior view of Atlas/Axis articulation in UALVP 49500

Figure 4.32. Ventral foramen (arrow) on axis in UALVP 49500

Figure 4.33. Ventral view of articulated cervical vertebrae in UALVP 49500

Figure 4.34. Anterior view of dorsal vertebra B from UALVP 49500

Figure 4.35. Posterior view of dorsal vertebra C from UALVP 49500, showing fused distal portion of left scapula

Figure 4.36. Anterior view of left dorsal rib A from UALVP 49500

Figure 4.37. Three anterior most caudal vertebrae of UALVP 49500 from lateral view: CVA, CVB and CVC

Figure 4.38. Three most posterior caudal vertebrae of UALVP 49500 from lateral view: CVD, CVE and CVF

Figure 4.39. Chevron A from UALVP 49500 in anterior view

Figure 4.40. Chevron B from UALVP 49500 in lateral view

Figure 4.41. Right scapula/coracoid of UALVP 49500 in lateral view. Arrow showing glenoid cavity.

Figure 4.42. Anterior view of right humerus of UALVP 49500.

Figure 4.43. Manual phalanges of UALVP 49500 from dorsal view

Figure 4.44. Ischia of UALVP 49500 in ventral view. Arrow showing extension of obturator process

Figure 4.45. Pubes of UALVP 49500 in left lateral view

Figure 4.46. Right fibula of UALVP 49500 in posterior view. Arrow showing contact for the soleus muscle of the calf.

Figure 4.47. Right MTI of UALVP 49500 in lateral view

Figure 4.48. Anterior view of right MTII and MTII in articulation; arctometatarsalian condition displayed

Figure 4.49. Right MTV of UALVP 49500 in lateral view

Figure 4.50. DIV and DII of left foot from UALVP 49500 in dorsal view

Figure 4.51. Elements of DII (ventral), DIII and DIV (dorsal) of the right foot from UALVP 49500; dorsal view

Figure 4.52. Potential bite/claw mark in right dentary of TMP 1994.012.0155

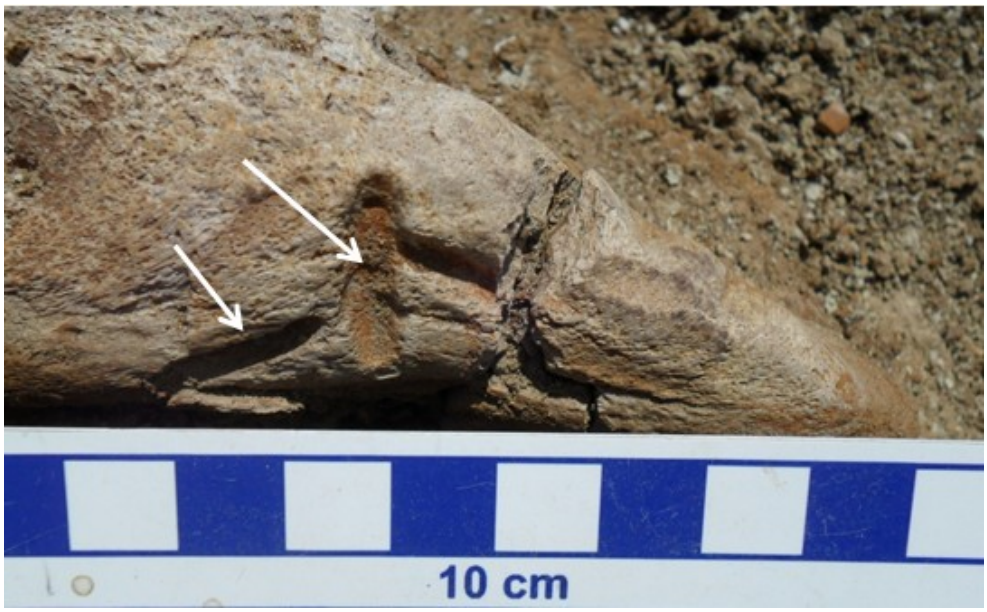

Figure 4.53. Ceratopsian parietal horn with tyrannosaurid bite marks, collected from Dinosaur Provincial Park

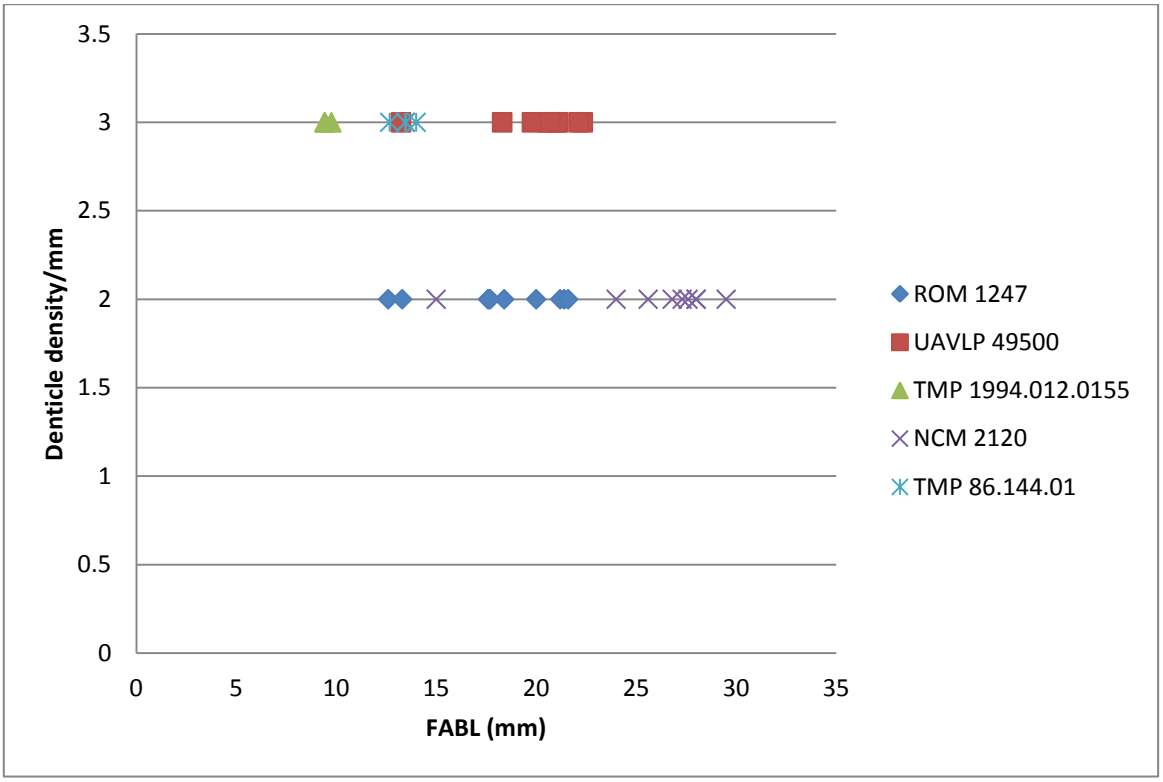

Figure 4.54. Denticle density vs. Fore-aft basal length (FABL) for right dentary teeth of 3 juvenile *Gorgosaurus* specimens and two adult specimens

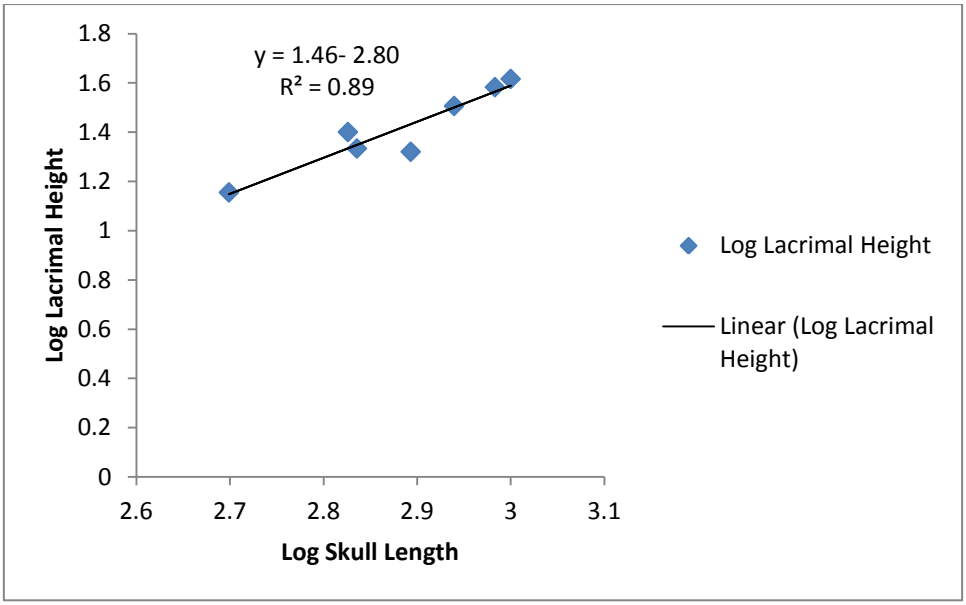

Figure 4.55. Allometric relationship between height of lacrimal horn and lateral skull length in seven specimens of *Gorgosaurus libratus*

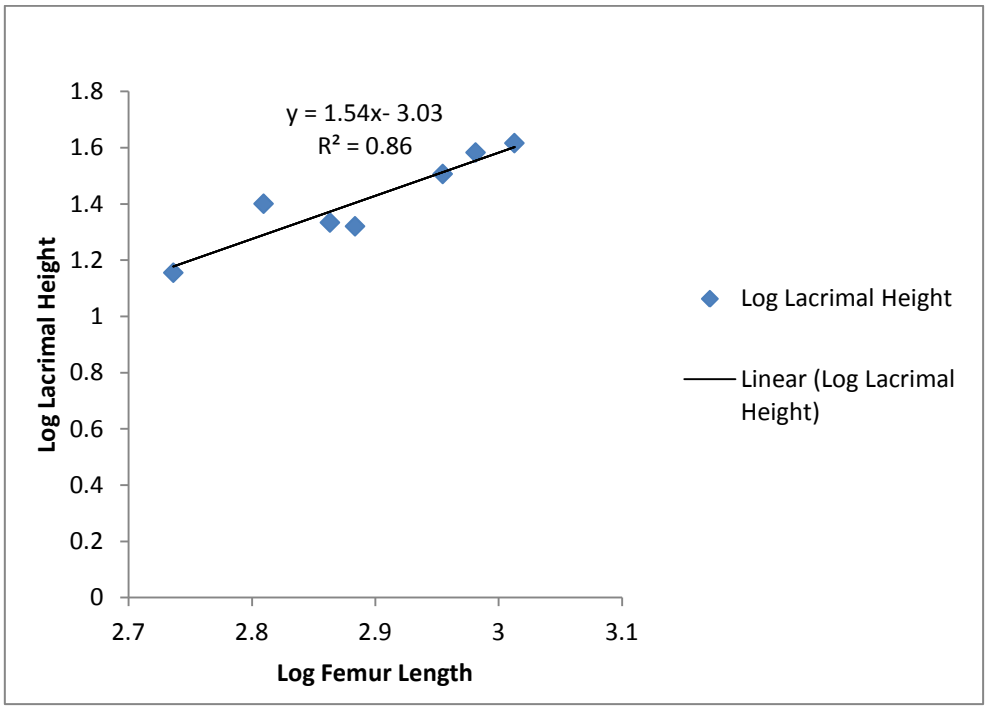

Figure 4.56. Allometric relationship between height of lacrimal horn and length of femur in seven specimens of *Gorgosaurus libratus*

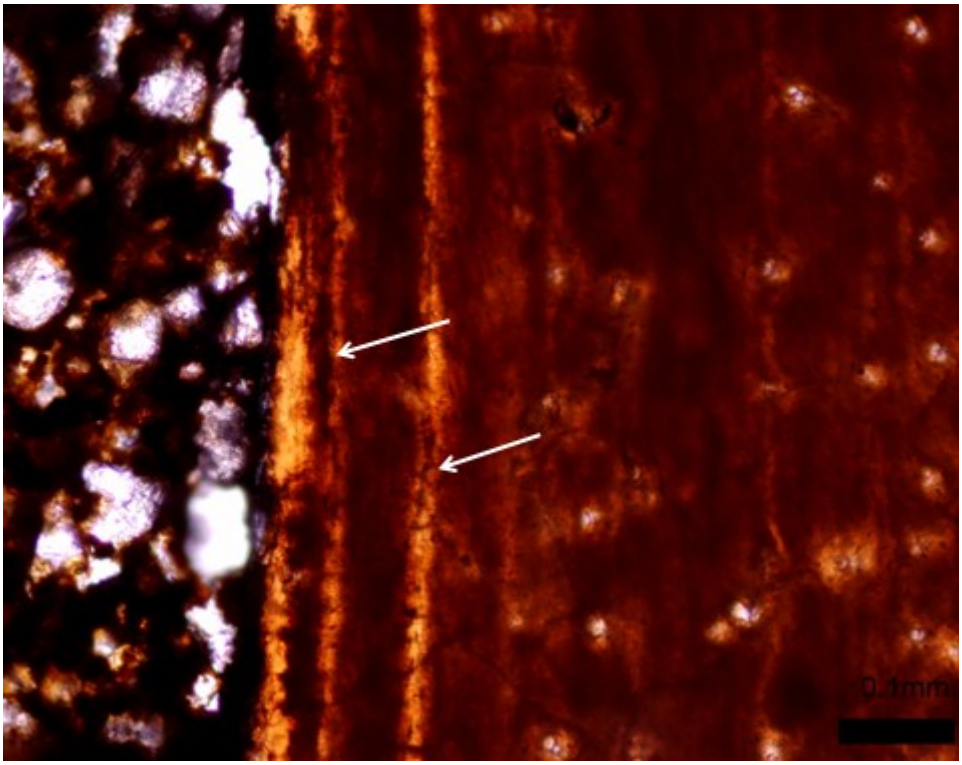

Figure 4.57. Lines of arrested growth (arrows) in thin section of UALVP 49500 dorsal rib

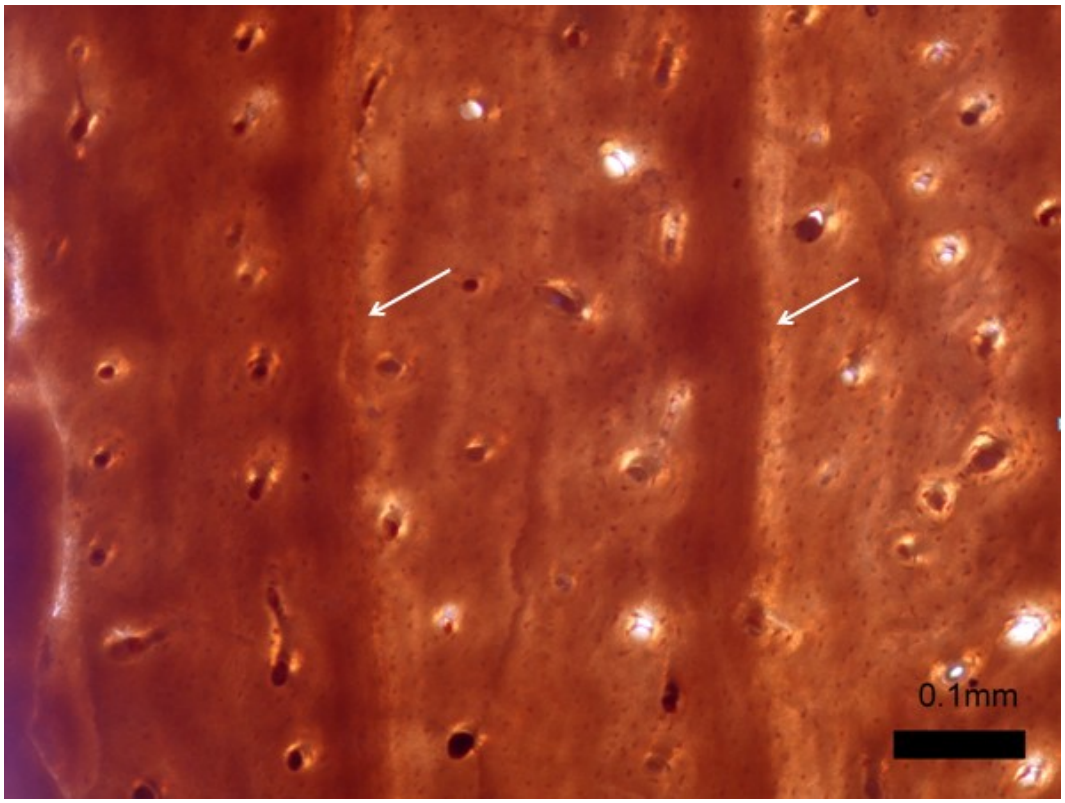

Figure 4.58. Lines of arrested growth (arrows) in thin section of TMP 91.36.500 dorsal rib

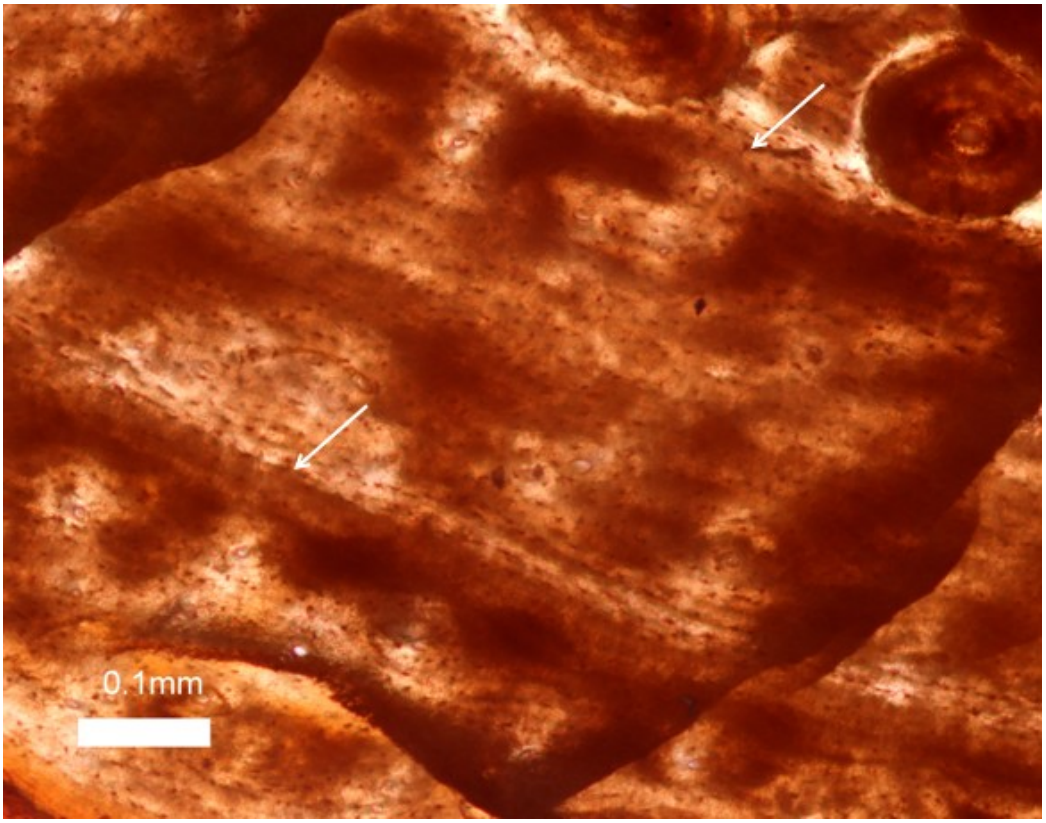

Figure 4.59. Lines of arrested growth in thin section of UALVP 10 dorsal rib

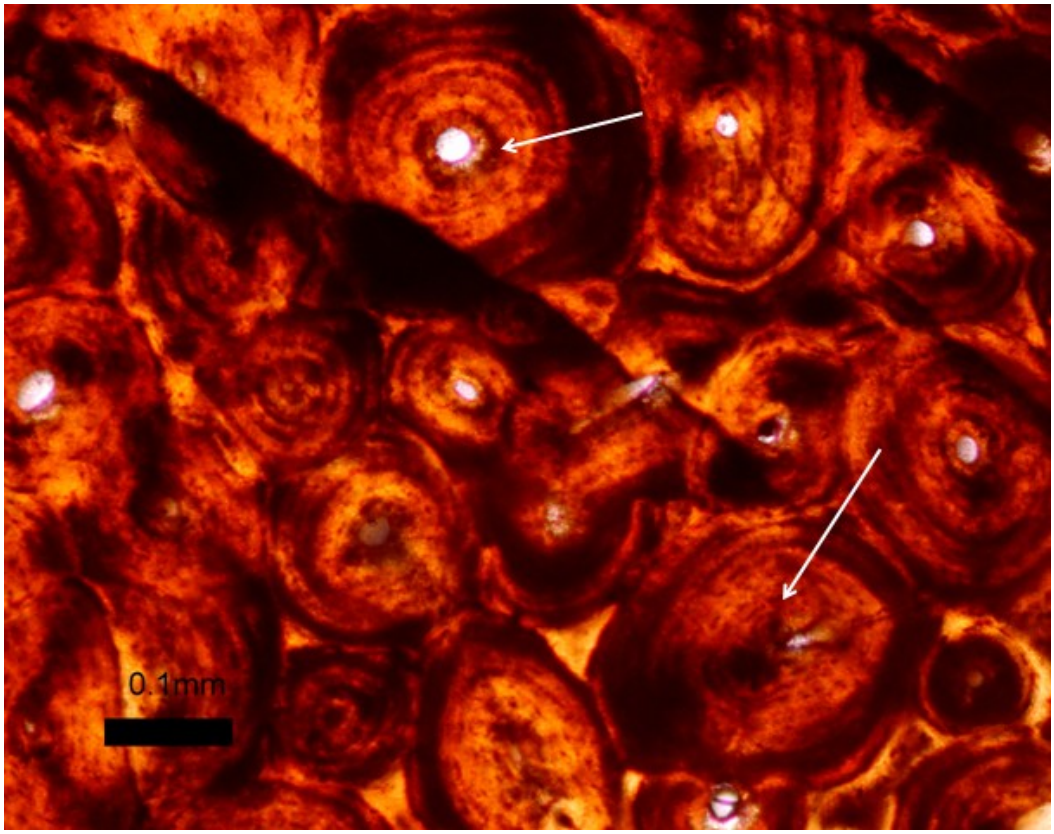

Figure 4.60. Secondary bone structure in TMP 1991 163 001 dorsal rib; lamellar bone encircles secondary osteons and there is little to no fibrolamellar bone/vascularisation

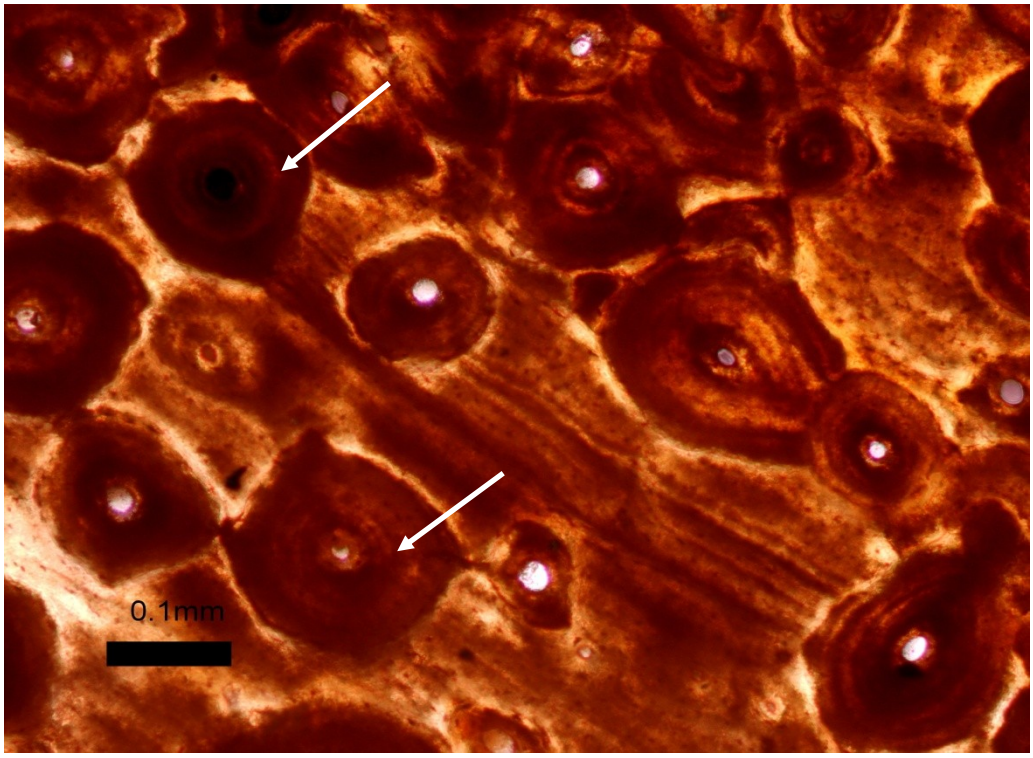

Figure 4.61. Secondary bone structure in UALVP 10; lamellar bone encircles secondary osteons and there is little fibrolamellar bone/vascularisation

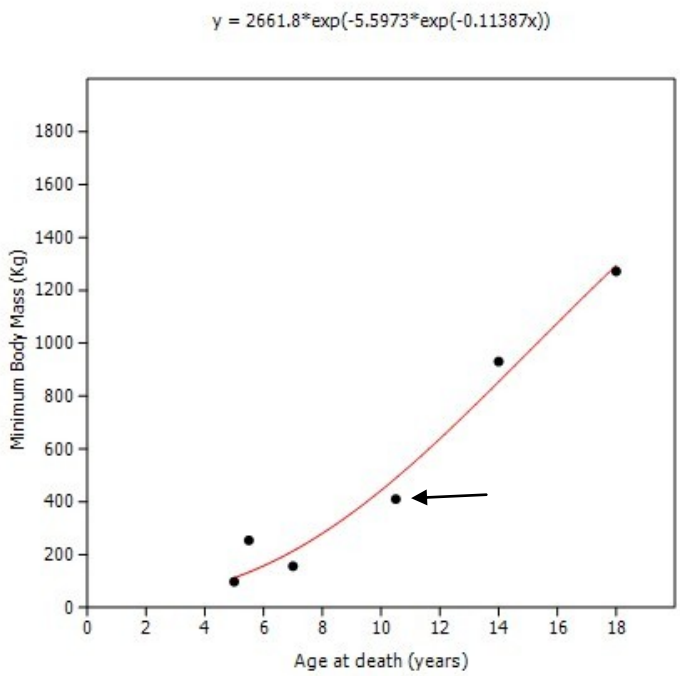

Figure 4.62. Gompertz growth curve showing minimum body mass estimation vs. age at death for six *Gorgosaurus libratus* specimens

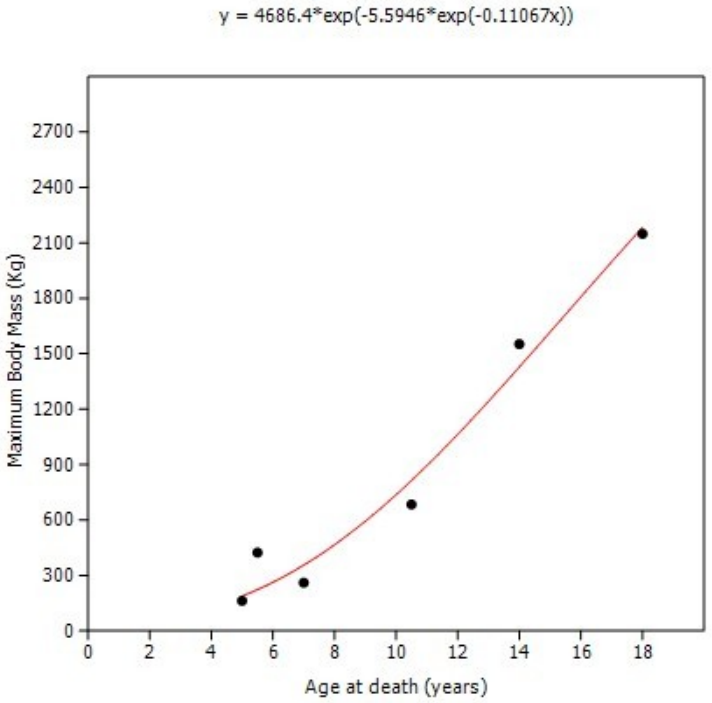

Figure 4.63. Gompertz growth curve showing maximum body mass estimation vs. age at death for six *Gorgosaurus libratus* specimens

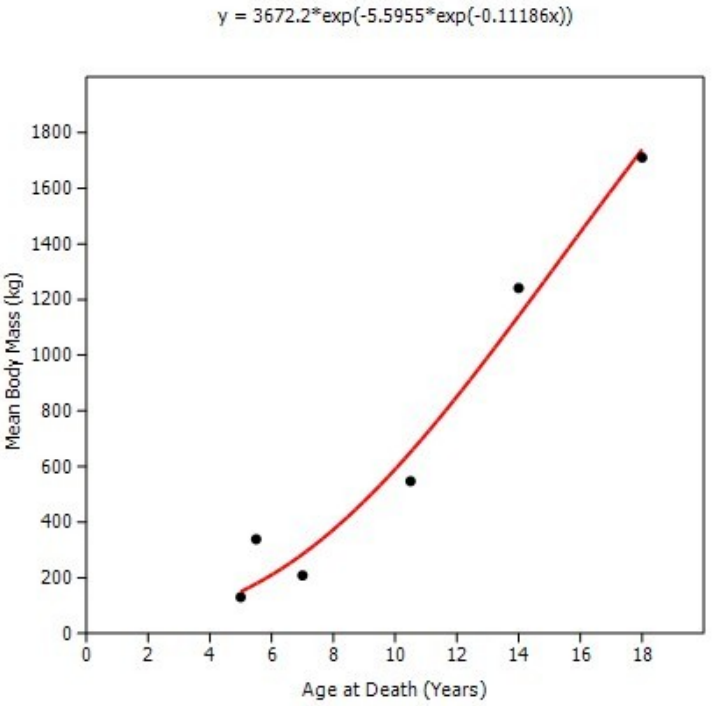

Figure 4.64. Gompertz growth curve showing mean body mass vs. age at death for six *Gorgosaurus libratus* specimens

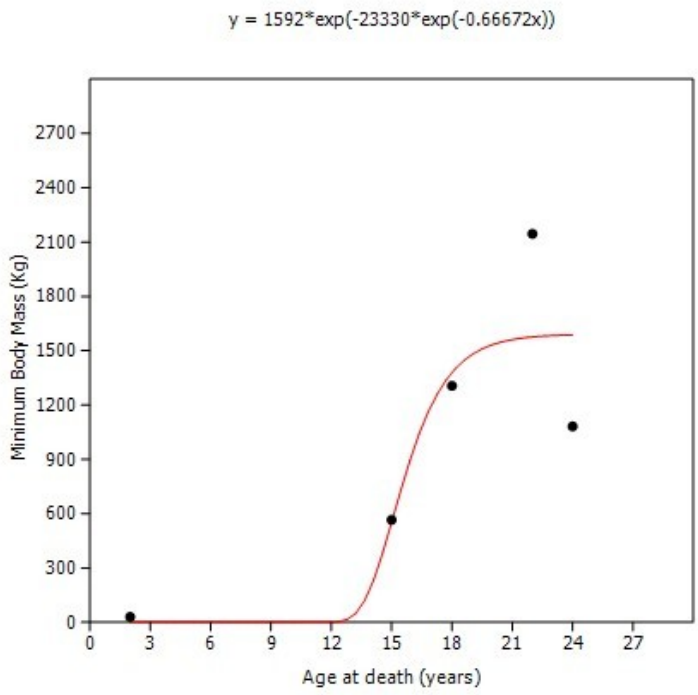

Figure 4.65. Gompertz growth curve showing minimum body mass estimation vs. age at death (after Erickson et al., 2004) for five *Albertosaurus sarcophagus* specimens

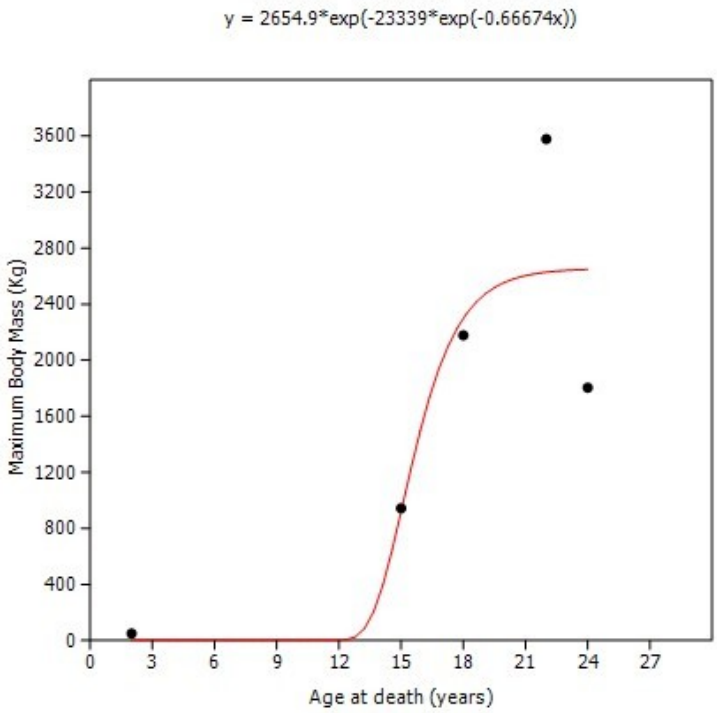

Figure 4.66. Gompertz growth curve showing maximum body mass estimation vs. age at death (after Erickson et al., 2004) for five *Albertosaurus sarcophagus* specimens

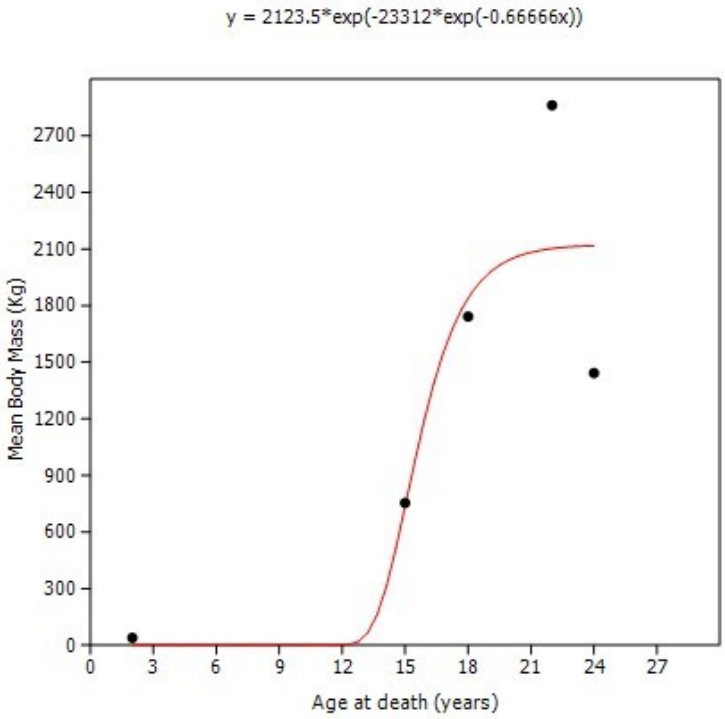

Figure 4.67. Gompertz growth curve showing mean body mass estimation vs. age at death (after Erickson et al., 2004) for five *Albertosaurus sarcophagus* specimens

Figure 4.68. Isolated maxillary tooth from UALVP 49500 embedded in epoxy resin for histological section

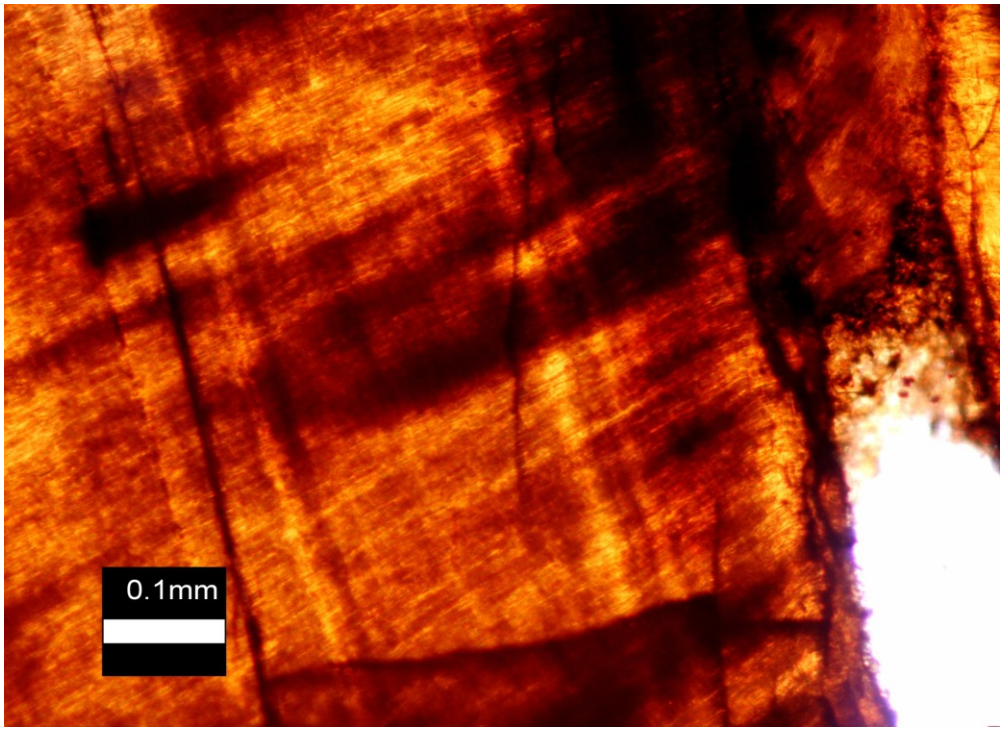

Figure 4.69. Incremental lines of von Ebner in frontal plane thin section of UALVP 49500

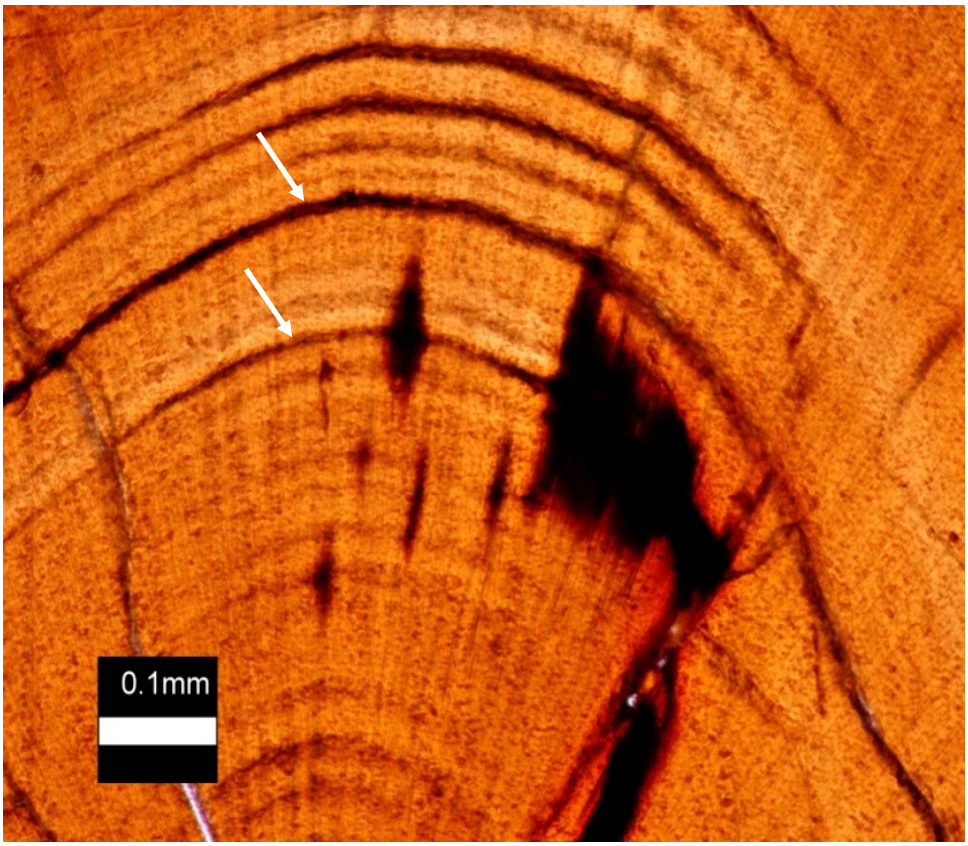

Figure 4.70. Incremental lines of von Ebner in tyrannosaurid tooth of unknown age (Slide by Paul Johnston)

Chapter 5

Comparing tooth macrowear in a juvenile and adult specimen of *Gorgosaurus libratus*: changes in feeding behaviour throughout ontogeny

5.1 Introduction

Pathological features found on fossil bones and teeth may provide us with unique insight into the behaviour of dinosaurs and the physical stresses that they faced. Palaeopathologies are particularly prevalent in tyrannosaurid dinosaurs, most likely due to their highly active lifestyles (Molnar and Rothschild, 2008; Rothschild, 2013). Healed fractures, and claw and/or bite marks have been cited as evidence of intraspecific combat (Tanke and Currie, 1998; Peterson et al., 2009; Bell and Currie, 2010; Rothschild, 2013) whereas stress fractures have been linked to highly active, predatory lifestyles (Rothschild and Martin, 2006).

Bite marks on the bones of prey species from tyrannosaurid teeth have been used as evidence for predation and feeding methods in recent years (Fiorillo, 1995; 1998; 2008; 2011; Goswami et al., 2005; Williams et al., 2009; Whitlock, 2011; Diez Diaz et al. 2012), however, the teeth of theropod dinosaurs are the subject of only a handful of these studies (Fiorillo, 1997; 2008; Schubert and Ungar, 2005; Osi et al., 2010). Furthermore, microwear provides a glimpse of feeding behaviour and tooth use over a more limited period of time than macrowear, which constitutes larger wear facets and documents the impact of dental interactions with the environment from the moment of eruption to replacement (Mallon and Anderson, 2014).

Two articulated specimens of *Gorgosaurus libratus*, UALVP 10 (Figures 5.1 and 5.2) and UALVP 49500 (Figures 5.3 and 5.4; See chapter 3 for full description), representing an adult and juvenile of the species. They were collected almost 100 years apart, and provide a unique opportunity to compare the changes in macrowear of tyrannosaurids throughout ontogeny. Tooth wear is a direct result of feeding behaviour of these dinosaurs, and any significant differences between juvenile and adult tyrannosaurids may lend some insight as to the dietary, ecological and behavioural changes that these animals experienced during growth. These ontogenetic changes may be used to make inferences about the extent of some gregarious interactions during life (See chapter 1). Tooth wear is described first in the adult *Gorgosaurus,* as it is expected to most closely reflect typical tyrannosaurid feeding.

5.2 Description of tooth wear in UALVP 10 (Adult *Gorgosaurus libratus*)

5.2.1 Left maxilla

The left maxilla of UALVP 10 has 14 visible tooth sockets and is only missing the first tooth, LM1 (left maxillary 1), described as incisiform (close to the D shape of tyrannosaurid premaxillary teeth) in shape by Lambe (1917). Whether this tooth was lost pre/post-mortem is difficult to discern, as

the anterior portion of the left maxilla is obscured by matrix in the original excavation photographs. Whereas ontogenetic and individual variation in tooth count is well recognized in tyrannosaurids (Currie, 2003b), this number falls within the tooth count range previously recorded for maxillae of the species: 13 in CMN 2120 (Lambe, 1917), 14 in TMP 91.36.500, and 15 in ROM 1247 (Larson, 2013; Torices et al., 2013). Whereas plaster around the bases of Lm4 and Lm9 suggest extensive preparation to keep them in place, the carinae positions, height, mediolateral width and fore-aft basal length of the teeth seem consistent for their locations in the mouth. Such is the consistency with the rest of the teeth in UALVP 10, therefore, that LM4 and LM9 are best considered as part of the original specimen and in their original locations.

The most obvious pre-mortem maxillary tooth alteration is the enamel spalling present in LM4 and LM5. LM4 (Fig. 5.5) has slight conchoidal fracturing to the apex of the tooth, which is worn and rounded. The wear on LM5 (Fig. 5.6) is more extensive, the tooth is shorter, and has irregular conchoidal breaks extending towards the base of the tooth on all sides. The edges of these breaks have been worn smooth, suggesting that these spalled teeth were still in regular use before the animal died (Shubert and Ungar, 2005).

Furthermore, LM8 has an elongate, narrow wear surface that extends almost to the base of the tooth on its anterior side. Less conspicuous wear marks are also present on the apices of LM9 (Fig. 5.7) and LM11. The wear on LM11 is more extensive than on LM9, and there is a seemingly attritional concavity, one potentially caused by mild, regular wear due to contact with other teeth or food during processing, on the apex of the tooth that is not present on the latter. The wear apparent on the tip of LM9 exposes the dentine layer, but the facet is not concave (Fig. 5.7). LM13 has a similar wear facet on its apex that extends dorsoventrally along the anterior side of the tooth (Fig. 5.8). Additionally, this tooth has a longitudinal wear facet that measures approximately two thirds of the dorsoventral height, and is located lingually, midway between the two carinae (Fig. 5.8).

5.2.2 Right maxilla

The right maxilla has been repaired and its sockets have been obscured by plaster, which makes it difficult to determine the origins of the teeth. However, similar to LM4 and LM9, the continuity of the dimensions and carinae positions between teeth suggests that the majority are indeed in their original locations. Those that appear anomalous to the trend of carinae twisting, or that seem improperly and artificially mounted in the maxilla, such as RM13, were not considered for analysis. Wear facets are less frequently found in the right maxilla of UALVP 10, although at least a portion of this paucity may be attributed to restoration, which has obscured the presence of *in vivo* damage. Two exceptions, however, are RM4 and RM5 (Fig. 5.9). RM4 is kept in place with a plaster base, however the orientation of the tooth and direction of its carinae suggest that it may be in its correct position. As with LM8 and LM13, RM4 has an elongate, narrow wear facet that extends almost to its base. However, this heavily worn surface is unusual in its location on the posterior

face of the tooth. RM5 also appears to be in situ, and has a typical apical wear facet similar to that described in LM9 (Fig. 5.7), and is not as extensively worn as RM4 (Fig. 5.9).

5.2.3 Left dentary

The left dentary has little damage to it, and seems to have all original 15 teeth. This tooth count falls within the norm of 15-17 for other specimens of the genus, including TMP 1994.012.0001, and TMP 86.144.0001, both of which have 16 (Larson, 2013; Torices et al., 2013). LD3 and LD4 have been broken at their bases, and are represented only by their roots; it is difficult to determine if this damage occurred during life, post-mortem, or during collection and preparation. Spalling is present on LD1, which displays conchoidal fractures on both the labial and lingual sides of the tooth, reducing the apex to a flattened, chisel-like termination, that is smoothly worn, presumably because of continued use post-fracture (Fig. 5.10). LD5 also has what appears to be a puncture-drag mark on the posterior-labial base of the tooth; this short, barrel-shaped depression in the enamel is distinct from other examples of wear found in any of the other teeth of UALVP 10 (Fig. 5.11). Wear facets on the apices of the left dentary teeth exist on LD6 and LD7 (Figs. 5.11 and 5.12); both display the characteristic form of other examples of apical wear in that rounded wear marks expose the dentine around the tip of the tooth. LD11 has one conchoidal fracture on the labial side of its apex that also exhibits the typical post-traumatic smooth wear texture associated with spall marks (Fig. 5.13). LD13 and LD15 (Fig. 5.13) present two more typical examples of tip wear, similar in form and extent to those described in LD6 and LD7 (Figs. 5.11 and 5.12).

5.3 Description of teeth in UALVP 49500 (Juvenile *Gorgosaurus libratus*)

5.3.1 Right maxilla

There are 12 visible alveoli in each maxilla, although, as the most anterior portion of each is weathered away, the true tooth count was more likely 13-14. The right maxilla contains two *in situ* teeth, RM6 and RM8, out of the twelve visible alveoli. There are two replacement teeth, one in alveoli eleven and another in alveoli two, as well as broken roots in spaces four and two. There is a dramatic difference in the fore-aft basal length between the alveoli of the penultimate posterior tooth of the right maxilla and the most posterior; the former is substantially greater. Anterior to this, however, there is comparably little variation of this measurement (Appendix 5; Tables 2-9). An elongate, longitudinal wear facet is visible on the lingual side of RM8 (Fig. 5.14). This is consistant with the expected position of wear marks caused by the occlusion of teeth as the medial side of the upper maxillary tooth row comes in contact with the lateral side of the opposing dentary tooth (Lambe 1917; Schubert and Ungar, 2005).

5.3.2 Left maxilla

The front two alveoli of the left maxilla have been almost entirely lost due to taphonomic distortion. The left maxilla, in contrast to the right, has nine original teeth in place, from positions

four to twelve. Subsequently, the greater prevalence of wear marks on this side compared to the right is more than likely due to preservational bias, rather than any behavioural factors, such as a preference for this side of the mouth while processing food. Located lingually and posterior to the midline of the tooth, there is a longitudinal wear facet extending dorsoventrally on the crown of LM4 (Fig. 5.15). Again on the lingual side, there are extensive longitudinal wear facets extending dorsoventrally between the apex and the mid-height of the crown on LM6 (Fig. 5.16) and LM8 (Fig. 5.17). Both wear marks are similar in dorsoventral height; however, LM6 also contains a shallow, elliptical concavity within the borders of the wear mark, suggesting extensive use after the initial wear mark was formed or that greater force was applied in its creation (Fig. 5.16). Further to this possible occlusion mark, LM6 also displays minor levels of wear on the tip, although not to the degree described in LM11 in UALVP 10, in which the apex was worn to a noticeable concavity. There is a minor longitudinal wear facet on the lingual side of LM10 (Fig. 5.18), similar to those seen on various teeth belonging to UALVP 10 and the corresponding maxilla of UALVP 49500. Like many wear facets of this style, it extends dorsoventrally, and is located slightly posterior to the midline of the tooth face.

5.3.3 Right dentary

Although there are 15 visible alveoli, only twelve *in situ* teeth are present in the right dentary of UALVP 49500; two recently erupted ante-mortem replacement teeth are visible in tooth positions RD4 and RD9, and only the fourteenth position has no tooth in place at all. Despite the majority of teeth still being present in this portion of the jaws, there is little recordable wear, in comparison to maxillae of the same specimen. On RD3 (Fig. 5.19), however, there is a large conchoidal fracture, the entire width of the labial face of the tooth. This spall mark is accompanied by another, smaller irregular fracture situated on the labial side of the same tooth, closer to the apex. On RD7 (Fig. 5.20), there is a small section of wear on the apex, of the less extreme, non-concave type described from teeth in the jaws of UALVP 10 and UALVP 49500. There is also what appears to be a slight longitudinal wear facet present on the labial side of RD10 (Fig. 5.21). However, as it is cut off by the fracturing of the apex, it is difficult to tell whether this was created ante-mortem, or post-mortem, due to the chipping off of the enamel near the tip after fracturing. The paucity of wear marks on the teeth relative to the other jaws of the specimen may be influenced by the taphonomic fractures below the apices of RD2, RD3, RD5, RD10, RD12 and RD13. This preservational bias could potentially be responsible for the underrepresentation of wear features, particularly tip wear and longitudinal wear; the former is by definition located on the apex of the tooth, and the latter typically extends dorsoventrally to the tip. As the apices of these six teeth have all been broken off above transverse fractures, most likely post mortem due to the absence of wear marks on the fracture surfaces, there may have been tip wear and longitudinal wear that were present, but cannot be recorded.

5.3.4 Left dentary

Similar to the right dentary, there are 15 tooth sockets in the left dentary of UALVP 49500; only 12 of these are fully crowned teeth, and there is one replacement tooth in position LD11, and potentially two teeth missing from the most anterior positions in the jaw. As with the teeth of the right dentary, there are fractured tips in LD4, LD5, LD10, LD12, LD14, and any apical and longitudinal wear facets that were present at points above the fractures in these teeth could not be described. Nonetheless, LD3 shows an extreme example of spall wear; at least four irregular conchoidal fractures are visible in anterior, posterior, lingual and labial views (Fig. 5.22). Many of the edges of these fractures have also been worn smooth in the manner already described for LD1, LM5 and LD11 in the adult specimen, UALVP 10. LD7 (Fig. 5.23) and LD8 (Fig. 5.24) display typical examples of tip wear; the latter is more extensive, and the dentine layer is exposed in a ring surrounding the apex of the tooth. There is also a small longitudinal wear facet present on the labial face of LD14, which, atypically for this style, does not extend dosoventrally all the way to the tip of the tooth (Fig. 5.25).

5.4 Discussion

These two well preserved specimens provide a rare opportunity to compare the tooth wear in an adult tyrannosaurid with a juvenile of the same species. It is clear that the presence of *in situ* tooth wear is prevalent throughout the ontogeny of *Gorgosaurus,* with significant changes in the frequency and extent of different styles of tooth wear, most likely due to differences in the feeding behaviour of juveniles and adults. There were 30 wear marks evident between the two specimens: 17 in the adult and 13 in the juvenile. Whereas the adult specimen shows a slightly greater number of examples, the extent of wear relative to the number of teeth in both ontogenetic states was similar; 15 of the 42 adult teeth examined (36%) displayed wear, whereas 12 of the 37 juvenile teeth examined (32%) displayed some features of wear.

The tooth wear of UALVP 10 and UALVP 49500 can be divided into four distinct types: spalling/conchoidal fractures, longitudinal wear facets, tip wear, and puncture drag wear. As tooth wear constitutes a physical impression created by a range of behavioural actions and feeding types, the frequency, extent and position of different wear types in UALVP 10 compared to UALVP 49500, may be interpreted to chronicle behavioural change throughout ontogeny in *Gorgosaurus*.

The most common type of wear facet in the adult specimen was tip wear; 9/17, or 53% of all examples of tooth wear on UALVP 10 were apical wear facets (Table 5.1; Table 5.3; Fig. 5.26). In contrast, longitudinal wear facets were the most frequently recorded in the juvenile specimen, with this style making up 7/13, or 54% of the wear marks seen in UALVP 49500 (Table 5.2; Table 5.3). This clear dichotomy in the dominant style of wear on the teeth of a juvenile vs. adult *Gorgosaurus* may reflect significant changes in both diet and mechanics of feeding throughout ontogeny in this tyrannosaurid.

The high amount of apical wear witnessed in UALVP 10 is unsurprising given hypothesised bite forces and feeding strategies of adult tyrannosaurids. There have been numerous studies

contributing to the currently accepted 'puncture and pull' theory of how large tyrannosaurids processed their prey; this supposes that the serrated teeth drove through muscle, tendon and bone before ripping out large chunks of the carcass (Abler, 1999; Abler 2001; Barrett and Rayfield, 2006). The capacity of adult tyrannosaurids to perforate and crush bone during feeding has also been well substantiated by the study of bones displaying bite marks, and efforts to estimate the bite forces of these large theropods. There is ample evidence for tyrannosaurid tooth contact with bones of various typical prey species such as hadrosaurids or ceratopsians (Erickson et al., 1996; Jacobsen, 1998; Fowler and Sullivan, 2006; Fowler et al., 2012; Murphy et al., 2013), as well as with those of other theropods and even conspecifics (Peterson et al. 2009; Bell and Currie, 2010; Bell et al., 2012; Rothschild, 2013). Further evidence for this proposed method of feeding comes in the form of tyrannosaurid coprolite and stomach contents (Chin et al., 1998a; Chin et al., 1998b; Varrichio, 2001), which include partially digested bones.

In order to accommodate this crushing and tearing feeding technique, tyrannosaurids required extremely powerful jaws. The potential bite forces of adult tyrannosaurid jaws have received much attention within palaeontological literature; relatively low bite force estimates of between 6,410-13,400 Newtons based on simulations using modern fauna (Erickson et al. 1996), have gradually increased to as high as 183,000- 235,000 Newtons by scaling up values witnessed in extant predators (Meers, 2002). More conservative estimates between 35,000 and 57,000 Newtons were proposed for a single tooth using computer model techniques such as Multi Body Dynamic Analysis (Bates and Falkingham, 2012). Such immense bite forces would have placed great amounts of strain on the skull (Rayfield, 2005), but also on the tips of the teeth as they came into contact with bone. The prevalence of apical wear on the teeth of UALVP 10 may therefore represent compelling evidence of the puncturing manner of feeding employed by adult tyrannosaurids.

The dominance of longitudinal wear facets on the teeth of the juvenile specimen of *Gorgosaurus*, and scarcity of tip wear relative to the adult, may suggest a different cause: contact of teeth during food processing. Wear marks caused by tooth to tooth contact have been documented in extant mammals such as toothed whales (Schubert and Ungar, 2005; Werth, 2007) and although rare in reptiles, have also been noted in the marine, Mesozoic crocodylomorph *Dakosaurus* (Young et al. 2012). This occlusal explanation was first proposed for lateral wear recorded in isolated tyrannosaurid teeth found by the Red Deer River in Alberta by Lawrence Lambe in his comprehensive description of the holotype specimen of *Gorgosaurus libratus* (1917). The dentition of the type specimen (CMN 350) itself, however, lacks any trace of these 'occlusal' wear facets, leading Lambe to suggest that the maxillary and dentary teeth pass clear of each other during feeding (Lambe, 1917).

Despite the proposal of the tooth occlusion hypothesis almost a century ago, it has remained unsubstantiated in tyrannosaurids due to inconsistencies in the location of these longitudinal wear marks and the difficulty of identifying the *in vivo* placement of isolated teeth sporting these features (Farlow and Brinkman, 1994; Shubert and Ungar, 2005). If contact of the

teeth of the upper and lower jaws took place during biting in tyrannosaurids, the expected location of longitudinal wear facets would be on the lingual side of maxillary teeth, and the labial side of mandibular teeth. In this, UALVP 49500 represents the best evidence for the occlusion hypothesis to date; all five longitudinal wear facets on maxillary teeth are located on the lingual side of the teeth, and both examples of this feature on dentary teeth are situated on the labial side (Table 5.2).

The prevalence of possible tooth occlusion marks in juveniles, but not adults, seems logical; there is little variation in tooth counts in *Gorgosaurus* throughout ontogeny (Currie 2003a), and FABL (Fore Aft Basal Length) values overlap significantly between juvenile and adult teeth, (7-24 mm in juveniles, 6-43 mm in adults, n=175) (Torices et al., 2013). Considering the significant growth of the skull during ontogeny (UALVP 49500: 685 mm in length; UALVP 10: 870 mm in length), one might theorise that a juvenile *Gorgosaurus* may have had relatively more tooth crowding in the jaw, which in turn was conducive to higher levels of tooth occlusion. However, the teeth in juveniles are also relatively smaller than the adults (Samman et el., 2005), which would suggest that there is a negligible difference in the amount of space between teeth as a result of a smaller jaw.

This contrast in tooth wear between the adult and juvenile specimens might also reflect a change in the feeding behaviour and diet of *Gorgosaurus* throughout ontogeny. The relatively small amount of tip wear found in the juvenile specimen, for example, suggests that it may not have regularly perforated bone during hunting or while processing kills; the 'puncture' component of the 'puncture and pull' method, evidenced in the adult specimen through heavy apical wear, may not have been the most efficient feeding technique for tyrannosaurid young. Again this hypothesis finds support in bite force evidence. Molnar (2013) suggested that *Nanotyrannus lancencis* may have had a less powerful bite than other adult tyrannosaurids. Regardless of whether or not this species actually represents a juvenile *Tyrannosaurus*, as has been proposed (Carr, 1999; 2005), it does, at least in stature, resemble a juvenile form of a large tyrannosaurid such as *Gorgosaurus*, and may be a useful and appropriate analogue for lower bite forces in juveniles. Indeed a similar trend is witnessed in *Gorgosaurus;* the increased depth of the jaws between juvenility and adulthood is significant, (UALVP 49500 minimum dentary height: 58mm; UALVP 10 minimum dentary height: 77mm) and reflects the changing biting capabilities of the animal throughout ontogeny.

Substantially less powerful jaws, coupled with little to no tooth wear on the apices of their teeth, compared to the adult specimens, may reflect a different feeding strategy injuveniles. Similar to modern day Nile crocodiles (Hutton, 1987), young *Gorgosaurus* may have been required to prey on smaller taxa, until they had the capacity to hunt larger animals. Alternatively, if juveniles fed at larger kills made by adults in a pack or 'grex' environment in a manner similar extant lion cubs (Pusey & Packer (1994), their small size and narrow snout would allow them to be more particular about which parts of the carcasses they ate, and avoid the bones and tougher tendons encountered by adults. This theory, however, presumes a level of social complexity not

previously evidenced for *Gorgosaurus,* although similar levels of gregariousness have been proposed for its sister taxon *Albertosaurus* (Currie and Eberth, 2010). They may also have practiced more slicing and tearing of tissue than fracturing of bones and tendons with their relatively thinner and less powerful teeth. This technique would have made use of the higher density of serrations recorded in juvenile specimens (3 per mm) of *Gorgosaurus*, in comparison to adults (2 per mm), to better shear off tissue (Torices et al., 2013; See Chapter 3). Corroborating this theory is the high amount of apparent occlusional wear facets on the teeth of UALVP 49500, reflecting a substantial amount of close contact between the maxillary and dentary teeth; similar to, but not reaching the complexity of, carnassials in mammalian carnivores (Greaves, 1983). Such wear facets have previously been attributed to both food processing and tooth on tooth wear (Shubert and Ungar, 2005), and change in the utilisation of teeth over ontogeny is not uncommon in extant carnivores; it has been recorded in cougars and spotted hyenas (Biknevicius, 1996; Binder and van Valkenburgh, 2000).

Although the contrast between the tooth wear of these two specimens is stark, it is also possible that such pathologies might vary from specimen to specimen; the individual variation of tyrannosaurid teeth is well documented (Miyashita et al., 2010), and a similar trend is seen in human dentistry, in which over-bites, under-bites and even tooth grinding are individually determined (Varma and Singh, 2008).

The most damaging wear type, enamel spalling, was found in both animals, and was always present on more than one side of a tooth as one continuous, or numerous conchoidal fractures. The smoothed edges of these fractures in the enamel suggest that the tooth was still regularly used after the initial break; this is substantiated by the presence of microwear striations recorded in isolated tyrannosaurid teeth presenting spalling (Schubert and Ungar, 2005), and other vertebrates e.g. the teeth of early hominids (Ungar and Grine, 1991; Ungar et al., 2012). The adult specimen displayed spalled enamel or broken tips in four teeth (Table 5.1), and the juvenile in two (Table 5.2); all but one (LD 11, UALVP 10) of these six instances of enamel spalling were situated at the front of the mouth, or the more anterior teeth of the mid-jaw. Tyrannosaurid teeth drastically increase in crown height, basal width, and F.A.B.L between the most posterior teeth and the mid-anterior section of the maxilla and dentary; the largest teeth tend to be located from the fourth to the sixth tooth positions in the upper and lower jaws (Lambe, 1917; Russell, 1970; Currie, 2003a) (Appendix 5; Tables 2-15). The concentration of spalling wear towards the anterior of the mouth, is most likely, therefore, a result of more frequent use of the the generally larger teeth in this region of the mouth. Alternatively, the greater distance between the jaw musculature situated posteriorly in the skulls of tyrannosaurids (Molnar, 2013), and the teeth at the anterior end of the snout, may have affected a greater force upon the anterior teeth, when the jaws snapped down upon prey.

The severity and irregularity of enamel spalling fractures suggest a traumatic, rather than attritional cause, such as high impact contact with bones of prey, or opposing teeth during hunting (Schubert and Ugar, 2005). Analogously, van Valkenburgh (1988) attributed modern day carnivore

tooth breakage to hunting, where unpredictable actions of the prey cause damage to the teeth. Abler, (2013) suggests that the labiolingually broad, typically rectangular denticles of tyrannosaurids, serve as small segments that the animal can afford to fracture, as a mechanism to cope with the high bite forces whilst preserving the majority of the tooth. Spalling, might therefore represent an area of the tooth where too many denticles have been removed, decreasing the structural integrity of the enamel, and eventually producing the large, irregular fractures indicative of this dental pathology as chipped teeth were continuously used. This theory, based on the structural change in the typically smooth surface of the enamel that denticles present, is difficult to substantiate; if spalling is created by the continuous loss of denticles, the original wear will be obligatorily masked by the large resultant spall mark. This hypothesis is not mutually exclusive with those of traumatic impact on bone or unpredictable actions of prey during hunting but may have been a precursor to both. Either way, the regularity with which such large enamel fractures occur in only these two specimens, gives some insight into why tooth replacement in tyrannosaurs was needed every two years (Erickson, 1996b).

The fourth type of wear facet was recorded on a single tooth, LM4, from the adult *Gorgosaurus* specimen UALVP 10, and depicts a noticeably different style of tooth wear from the three previously discussed. The 'puncture-drag' wear facet, a short barrel shaped depression on the postero-labial base of the tooth, does not match tip wear, occlusional wear or enamel spalling. Whereas a study comparing microwear patterns of tooth wear created either taphonomically or during preparation would be required to rule out such causes, if this wear facet was sustained *ante mortem*, it may constitute evidence of face biting in tyrannosaurids. This behaviour has been proposed for tyrannosaurids based on embedded teeth and apparently conspecific bite marks on specimens (Tanke and Currie, 1998; Peterson et al., 2009; Bell and Currie, 2010), and if such aggressive interspecific or intraspecific behaviour occurred, due to competition for resources, territory or mates, tooth on tooth contact might be an expected result.

Although each particular style of wear facet has been linked to its own unique, corresponding cause, the overall prevalence of tooth wear in *Gorgosaurus* may have been a result of a need to feed rapidly in an extremely competitive environment. A similar trend has been witnessed in large African carnivores that often suffer tooth breakage as they feed rapidly at a carcass, due to the threat of larger carnivores stealing their kill or find (van Valkenburgh, 1996). A higher incidence of tooth damage has also been linked to carnivores with greater levels ofaggression in modern ecosystems, such as lions and spotted hyenas (van Valkenburgh, 2009), and even species with high levels of sociality, who would have faced competition over carcasses (Binder and van Valkenburgh, 2010). Gregariousness has previously been proposed for large tyrannosaurids, such as *Albertosaurus* (Currie and Eberth, 2010) the sister taxon of *Gorgosaurus*, and the high levels of tooth wear in UALVP 10 and UALVP 49500, could potentially be indicative of the hypercompetitive environment within a pack, of tyrannosaurids. However, in the case of *Gorgosaurus,* an animal sharing its habitat with an even larger top predator, *Daspletosaurus,* as

well as various other smaller carnivores, the competitive pressures leading to tooth breakage may not have necessarily been intraspecific.

5.5 Conclusions

To understand the major ecological pressures contributing to the ubiquity of tooth wear in tyrannosaurids would require a comprehensive study inclusive of more genera than simply *Gorgosaurus*. However, in comparing the wear types exhibited by UALVP 10 and UALVP 49500, a picture of significant physical and perhaps behavioural change throughout the ontogeny of this large theropod has emerged. A shift in dominant types of wear facets, from longitudinal to apical, suggests that juveniles were subject to levels of occlusion between the teeth of the upper and lower jaws that adults were not. The extent of damage sustained to the teeth from occlusion may have been exacerbated by a slicing and tearing feeding technique employed by juveniles, which compensated for underdeveloped jaw strength. A greater number per mm of finer denticles in juvenile specimens of *Gorgosaurus*, compared to a smaller number of broader denticles in adults may have also assisted in a slicing and tearing dominant feeding method. Apical wear in the adult specimen, in contrast, implies that frequent contact was made with the bones of prey. This supports previous claims of a puncturing aspect to the feeding method for large tyrannosaurids that relied on colossal bite forces of fully developed jaws. Such dramatic changes in feeding behaviour, from immature to adult stage in *Gorgosaurus,* may also reflect differences in the way they ate prey, and/or diet and/or ecological niche between tyrannosaurids of different biological ages. Instances of enamel spalling potentially constitute evidence of traumatic incidents during hunting or feeding, which caused large portions of the tooth to shatter, or areas where too many denticles had broken off, decreasing the structural integrity of the enamel.

Tempting as it might be to categorise the puncture and drag mark on a tooth of the adult specimen as an artefact of tooth to tooth contact during an intraspecific display of aggression, it is insufficient evidence in itself to substantiate such a complex behavioural hypothesis. It is, however, an intriguing theory, and a testament to the behavioural implications that can be drawn from studying dental pathologies in large theropods, and the potential of larger, more comprehensive future analyses of tooth wear in tyrannosaurids.

5.6 Tables

Specimen	Occlusion	Tip Wear	Spalling	Barrel-Puncture	No wear
UALVP 10	20%	53%	27%	7%	64%
UALVP 49500	54%	33%	17%	0%	68%

Table 5.1 Percentage of teeth in UALVP 10 and UALVP 49500 displaying each type of wear mark

Tooth Position	Position	Type of Wear
LM4	Apex	Spalling
LM5	All sides	Spalling
LM8	Anterior	Occlusal
LM9	Apex	Tip wear
LM11	Apex	Tip Wear/Concavity
LM13	Apex/Anterior and Lingual	Tip wear and occlusal
LD1	Labial, Lingual, Apex	Spalling
LD4	Labial/Posterior	Barrel/Puncture
LD6	Apex	Tip wear
LD7	Apex	Tip wear
LD11	Apex, Labial	Spalling
LD13	Apex	Tip wear
LD15	Apex	Tip wear
RM4	Apex, Posterior	Tip wear and occlusal
RM5	Apex	Tip wear

Table 5.2. Distribution and type of wear marks on teeth of adult: UALVP 10

Tooth Position	Position	Type of Wear
LM4	Lingual	Occlusal
LM6	Lingual and Apex	Occlusal and Tip Wear
LM8	Lingual	Occlusal
LM10	Lingual	Occlusal
LD3	All sides	Spalling
LD7	Apex	Tip Wear
LD8	Apex	Tip Wear
LD14	Labial	Occlusal
RM6	Lingual	Occlusal
RD3	Labial and Lingual	Spalling
RD7	Apex	Tip Wear
RD10	Labial	Occlusal

Table 5.3. Distribution and type of wear marks on teeth of juvenile: UALVP 49500

Percentage of teeth in UALVP 10 and UALVP 49500 displaying each type of wear mark

5.7 Figures (Figures 5.5-5.13 Modified from originals by Dr Eric Snively)

Figure 5.1. Skull of UALVP 10 mounted in University of Alberta Earth Sciences Museum

Figure 5.2. Charles H. Sternberg c.a. 1920 with the newly excavated left dentary of UALVP 10 (Courtesy of Clive Coy, University of Alberta)

Figure 5.3. Left dentary and maxilla of UALVP 49500

Figure 5.4. Right dentary and maxilla of UALVP 49500

Figure 5.5. Lingual view of spalling wear on LM4, of UALVP 10

Figure 5.6. Lingual view of spalling wear on LM5, of UALVP 10

Figure 5.7. Lingual view of apical wear on LM9, UALVP 10

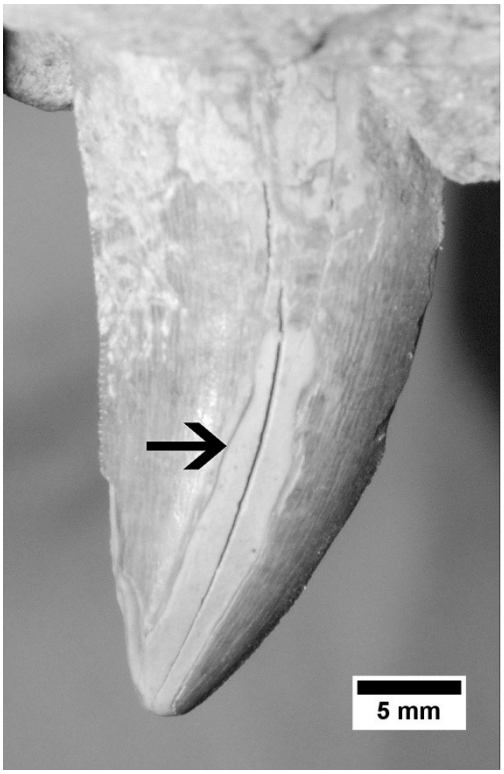

Figure 5.8. Lingual view of LM13, of UALVP 10 showing occlusal wear facet

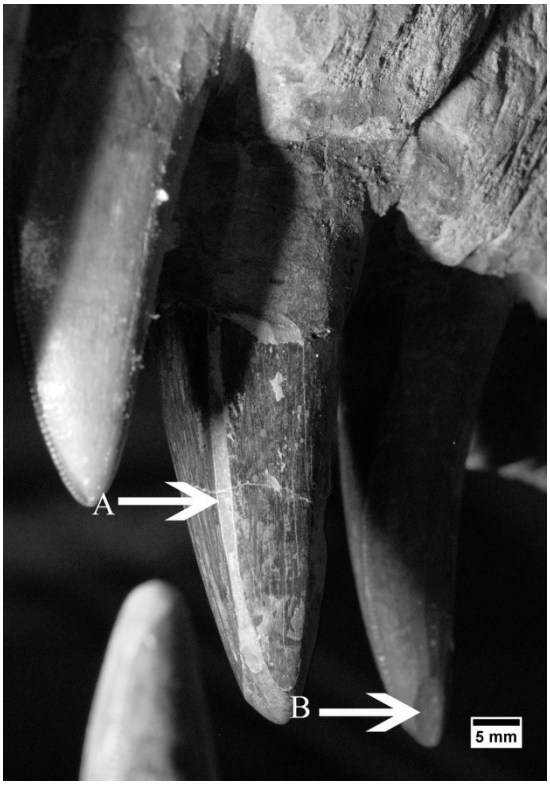

Figure 5.9. Lingual view showing occlusal wear facet on RM4 and tip wear on RM5, of UALVP 10

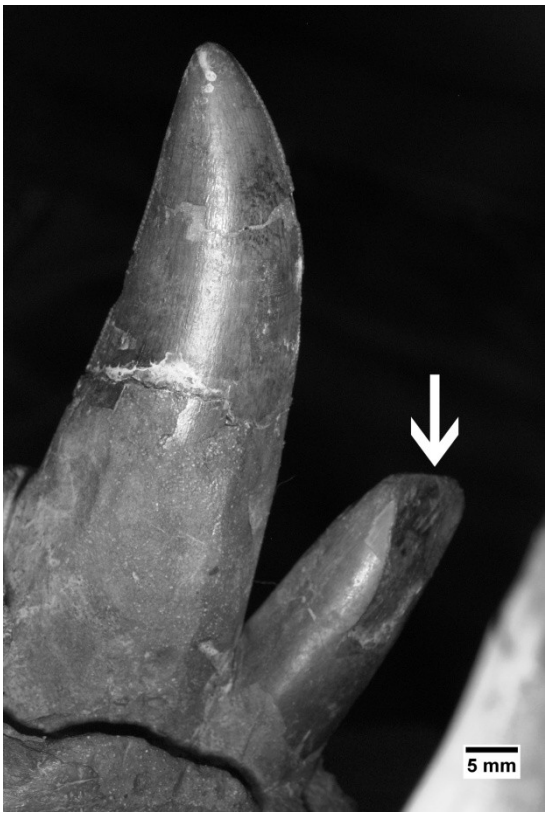

Figure 5.10. Spalling wear on LD1 UALVP 10

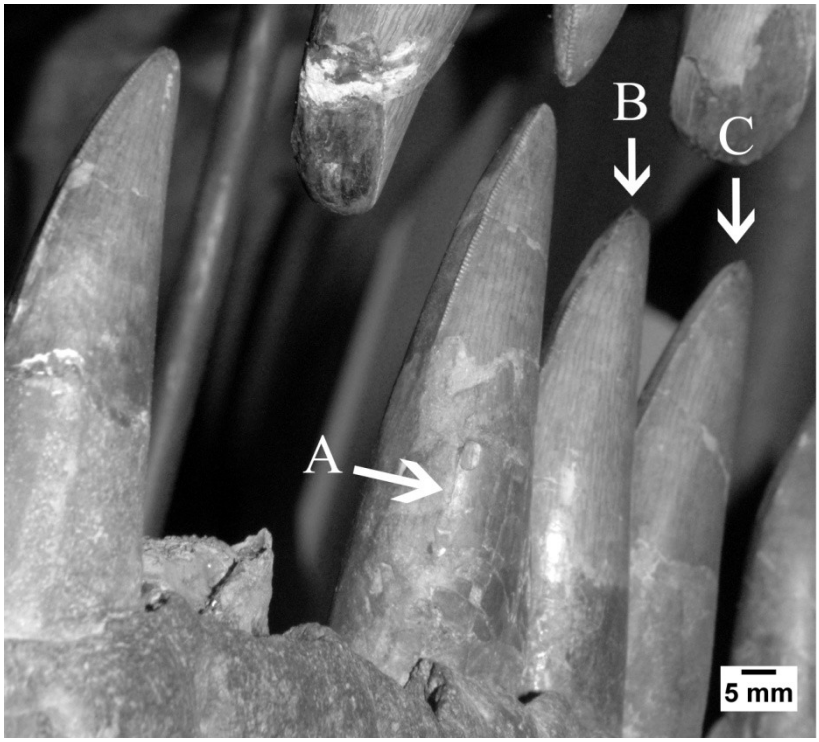

Figure 5.11. Labial view of barrel shaped puncture wear (A) on LD5, and tip wear (B,C) on LD6, LD7 of UALVP 10

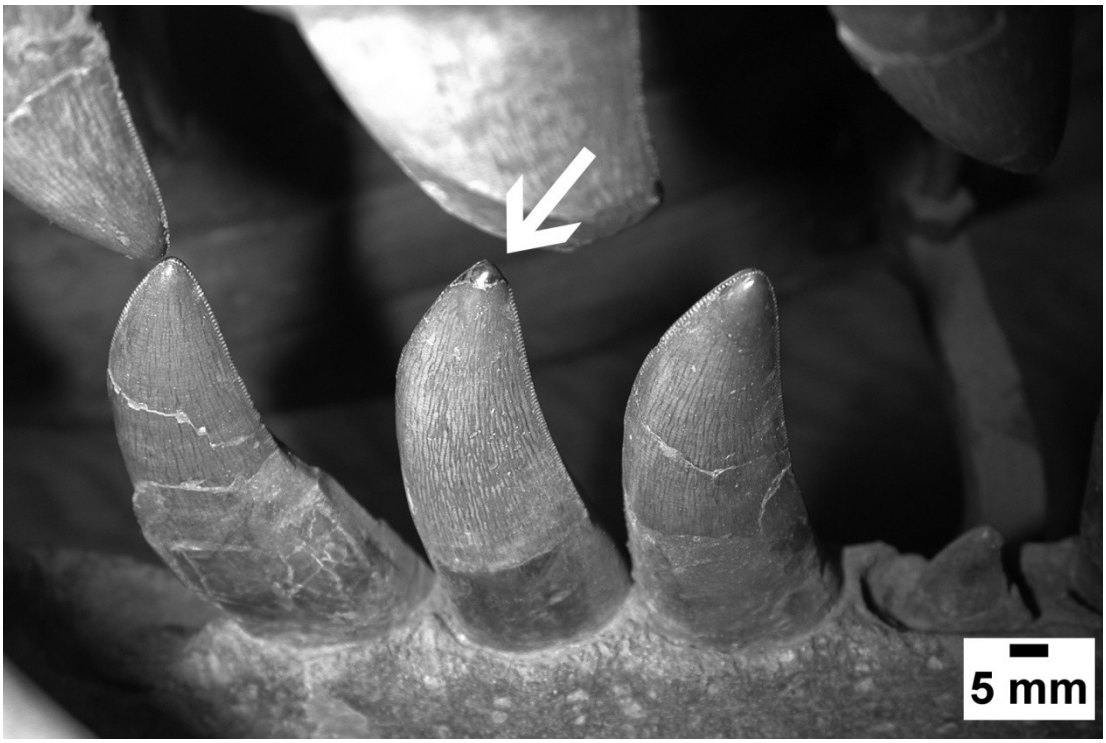

Figure 5.12. Labial view of tip wear in LD6 and LD7 of UALVP 10

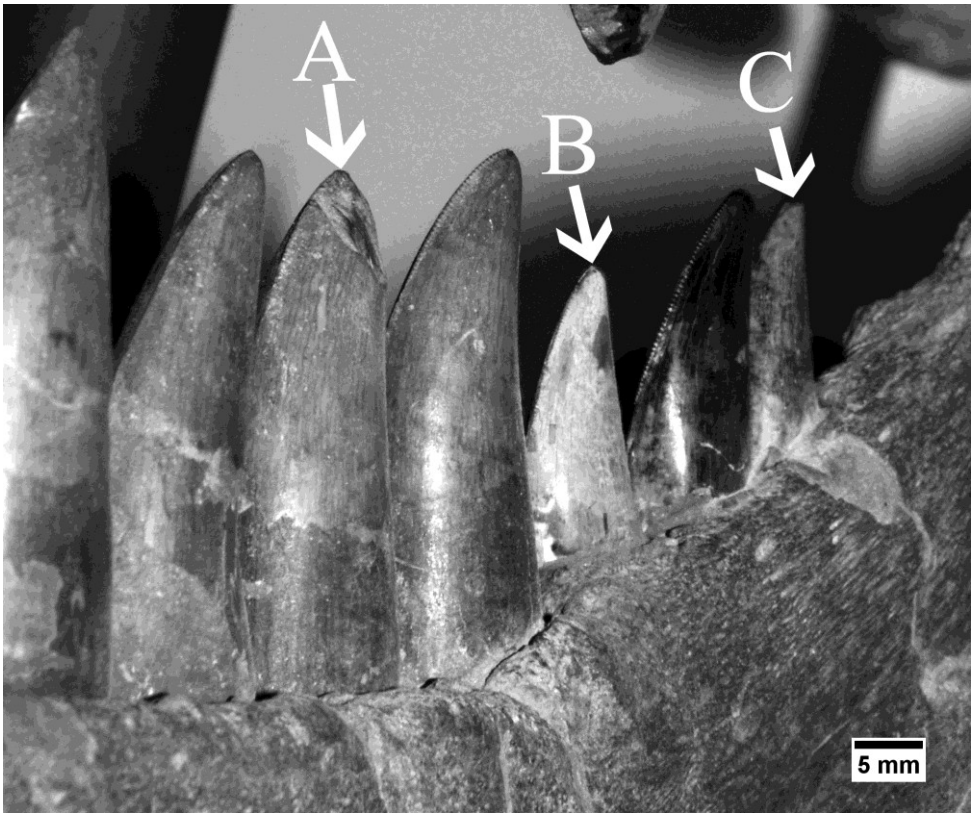

Figure 5.13. Labial view of spalling wear on LD11 (A), tip wear on LD13 and LD15 (B, C), from UALVP 10

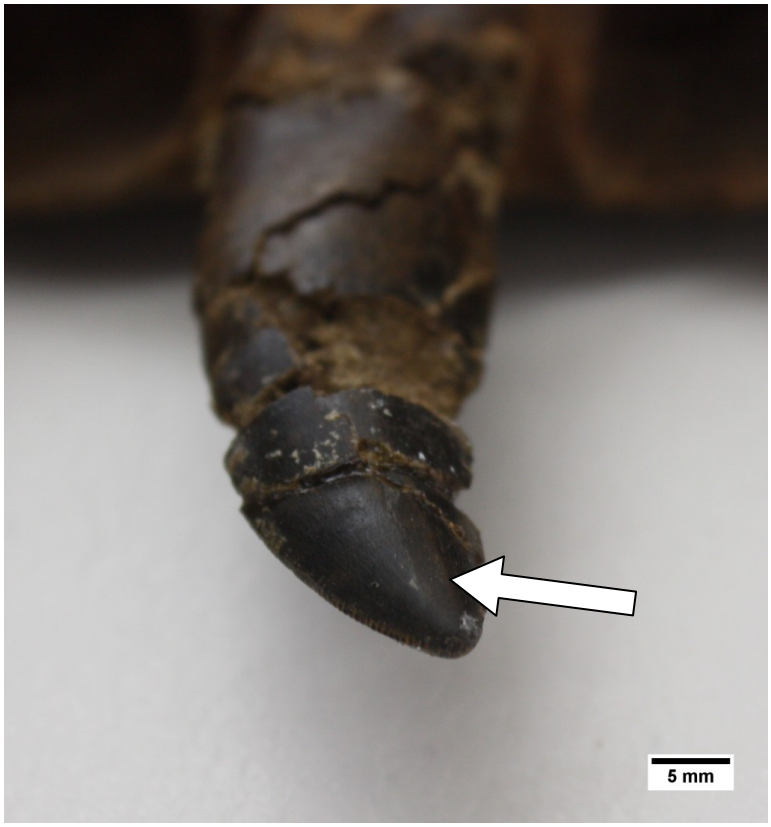

Figure 5.14. Lingual view of occlusal wear facet on RM8 of UALVP 49500

Figure 5.15. Lingual view of occlusal wear facet on LM4 of UALVP 49500

Figure 5.16. Lingual view of occlusal wear facet on LM6 of UALVP 49500

Figure 5.17. Lingual view showing occlusal wear facet on LM8, of UALVP 49500

Figure 5.18. Lingual view of occlusal wear on LM10 of UALVP 49500

Figure 5.19. Labial view of spalling wear on RD3, of UALVP 49500

Figure 5.20. Labial view of tip wear on RD7, of UALVP 49500

Figure 5.21. Labial view of occlusal wear facet on RD10 on UALVP 49500

Figure 5.22. Lingual view of spalling wear on LD3 of UALVP 49500

Figure 5.23. Lingual view of tip wear on LD7 of UALVP 10

Figure 5.24. Lingual view of tip wear on LD 8 of UALVP 49500

Figure 5.25. Labial view of occlusal tooth wear on LD14 of UALVP 49500

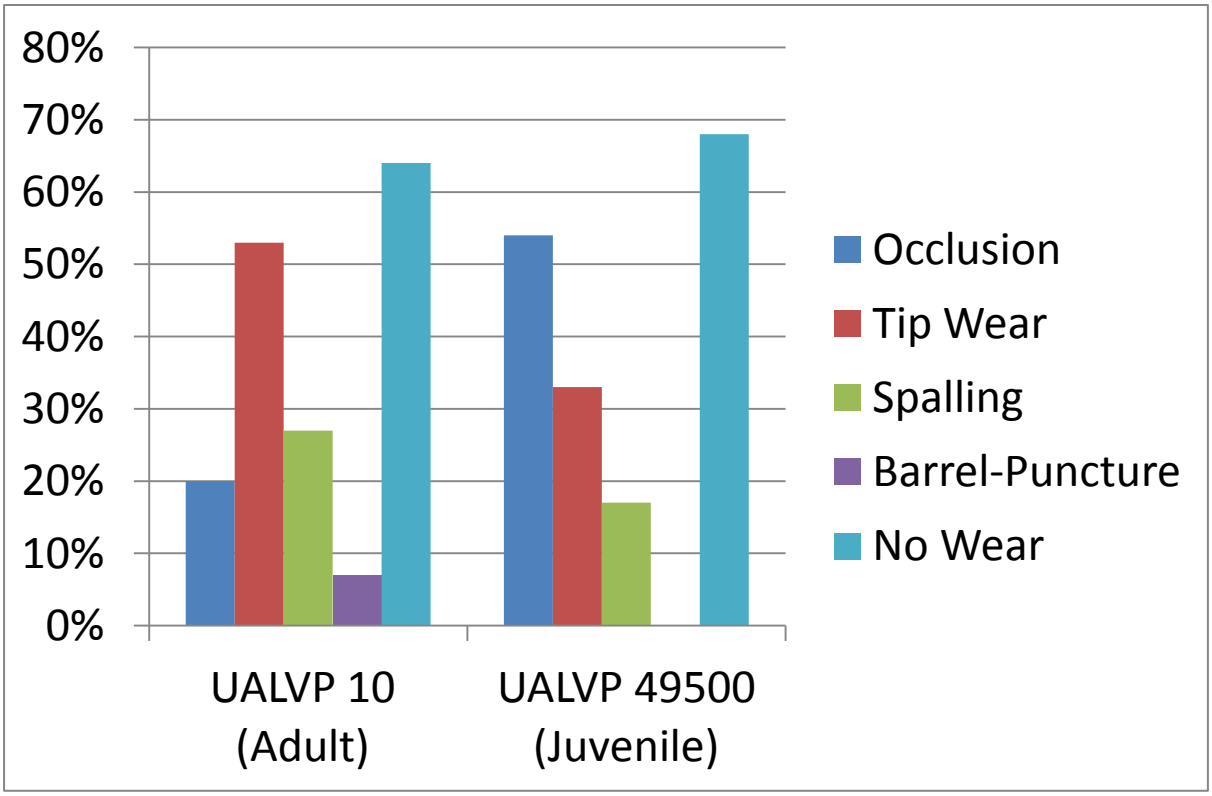

Figure 5.26. Bar chart showing percentage of teeth in UALVP 10 (n=42) and UALVP 49500 (n=37) displaying each type of wear mark

Chapter 6: Conclusions

A review of social behaviour in modern vertebrates produces two main conclusions: (1) that gregariousness should be viewed as a highly variable suite of behaviours that vary in their extent from taxon to taxon and (2) extrapolation of behaviours in extant taxa to dinosaurs should be exercised with caution because variation in extant animals, even among closely-related taxa is enormous. Social behaviour in modern animals can range from brief, tenuous coalitions such as the coordinated juvenile nest emergence displayed in iguanas (Burghardt et al., 1977), to complex gregarious societies that inspire learned cooperative behaviour as in killer whales (Pitman and Durban, 2012). Inferences of social behaviour solely due to its appearance in a phylogenetically close taxon should be avoided; Felidae provides an example of one taxon, lions, exhibiting complex pack behaviour in contrast to the other members of this family. Reviews of social behaviour in dinosaurs are dominated by spectacular evidence such as bone beds (Currie and Eberth, 2010) or brooding sites (Fanti et al., 2012), but suggestions for alternative techniques are suggested such as: palaeopathological observation, interpretation of growth rates and the assessment of stable isotope data to infer diet.

Missing values within a data set can undermine confidence in analyses, skew results in promoting analyses of small portions of a population, not necessarily representative of the entire data set, and drastically decrease sample sizes. Statistical analyses for the prediction of femoral circumferences in tyrannosaurids suggest that estimation models based on anteroposterior diameter values are poor predictors of circumference, whereas those based on mediolateral diameters are more successful. Three models, **ELLR**, **MLR** and **CML,** are proposed as viable alternatives to missing circumferences. **MLR** and **ELLR** are derived from linear regressions between measured femoral circumferences and diameters of tyrannosaurids, and may be used by inserting diameter values into the following formulae: $y=0.959x + 0.5399$ (**MLR**), $y= 0.9302x + 0.6324$ (**ELLR** using anteroposterior diameter) and $y=0.9572x +0.5415$ (**ELLR** using mediolateral diameter). **CML** is the universal equation for the circumference of a circle, and again uses mediolateral diameter data. These three models may be used to boost tyrannosaurid samples in studies of social behaviour. Femoral circumferences are useful in inferring body mass, growth rates and life history of a population, all of which, in turn, can inform social behaviour.

UALVP 49500 represents a juvenile specimen of *Gorgosaurus libratus* and includes the following elements: maxilla, maxillary teeth, premaxillary teeth, jugal, lacrimal, postorbital, quadratojugal, quadrate, squamosal, frontal, ectopterygoid, epipterygoid, pterygoid, palatine, dentary, dentary teeth, splenial, supradentary/coronoid, surangular, angular, prearticular, articular, cervical vertebra, cervical rib, dorsal vertebra, dorsal rib, gastralia, caudal vertebra, chevron, scapula-coracoid, humerus, manual phalanx, ischium, pubis, fibula, metatarsal I, II, III, IV, V, pedal phalanx, pedal ungual. It can be identified as an albertosaurine based on: the distance bewteen the antorbital fenestra and the ventral rim of the antorbital fossa (Currie, 2003b); the position of the maxillary fenestra (Holtz Jr., 2001; Currie et al., 2003); the presence of a distinct

lacrimal horn (Currie, 2003b); the tapering of the jugal-quadratojugal suture (Currie, 2003b); the diagonal axis of the jugal pneumatopore (Currie et al., 2003); the position of the lacrimal pneumatopores (Currie et al., 2003); the dorsal flaring of the quadratojugal (Currie et al., 2003); and the position of lacrimal fossa (Brusatte et al., 2009; Loewen et al., 2013).

Gorgosaurus is supported here as a taxon distinct from *Albertosaurus*. This is based on: the size of maxilla palatal shelf depressions (Currie, 2003b), the ventral extent of the maxillary fenestra (Carr et al. 2005), the division of the lacrimal pneumatic openings (Currie, 2003b); the limited posterior extension of the jugal horn (Currie, 2003b); the absence of an oval fossa on the quadrate medial surface (Loewen et al., 2013), the texture of the ectopterygoid pneumatopore posterior surface (Loewen et al, 2013); the cross section of the maxillary teeth (Larson, 2013); the presence of an anterior squamosal pneumatic foramen (Larson, 2013); the width of the distal blade of the scapula (Holtz Jr., 2001); the absence of a lateral component of the glenoid in the scapula/coracoid (Larson, 2013). The presence of a central foramen on the ventral surface of the axis, may represent a juvenile characteristic or a new distinguishing characteristic between *Albertosaurus* and *Gorgosaurus*.

Several of the ontogenetically variable characters identified herein have implications for changes in social behaviour in juvenile versus adult *Gorgosaurus*. The positively allometric growth of the lacrimal horns implies a functional importance associated with maturity. Similarly exaggerated growth is seen in cranial structures of modern animals. Some of these structures are used in intraspecific sexual combat, such as the horns of big horned sheep (Geist, 1971), as physical fitness indicators for females, such as the antlers in elk (Emlen et al., 2012), and others, like the casques of cassowaries are used in mating displays (Richardson, 1991).

Greater denticle density in juvenile teeth may reflect a change in feeding technique and diet in *Gorgosaurus*, when considered alongside evidence of reduced skull strength and bite force in juvenile tyrannosaurids compared to adults (Henderson, 2000; Molnar, 2013), and the relatively labiolingually thin teeth of juveniles compared with those of adults (Farlow, 1991). It may be that thinner and more finely serrated teeth are better adapted for a slicing method of feeding rather than puncturing, as has been hypothesised for the finely serrated teeth of *Smilodon,* in contrast to the coarsely serrated teeth of *Homotherium* (Martin, 2000).

The decreasing circularity of the orbit with ontogeny may potentially be interpreted as reflecting a change in feeding technique. Henderson (2003) showed that reducing the circularity of the orbit as the skull grows, strengthens it against the extra strain associated with increased bite forces; such a function might explain this ontogenetic change in *Gorgosaurus*. Alternatively, circular orbits may allow the reception of greater levels of light, if the postorbital flange infringes on the orbit (Chure, 1998). Juvenile *Gorgosaurus* may therefore have been better suited to a crepuscular lifestyle, as has been suggested for *Troodon* (Russell and Seguin, 1982), which displays almost perfectly circular and relatively large orbits. Crepuscular animals often have large eyes

relative to their skull size (Stevens, 2006), but this interpretation is not supported by measurements of *Gorgosaurus* in comparison to other tyrannosaurids like *Daspletosaurus*.

Growth rates change with ontogeny as well as with taxon. The growth rate of juvenile *Gorgosaurus* was lower than that of the adult, and the maximum *Gorgosaurus* growth rate was also slower that of previously published tyrannosaurids, such as *Daspletosaurus, Tarbosaurus* and *Tyrannosaurus*, (Erickson et al., 2004). The lower maximum growth rate of *Gorgosaurus* compared to *Albertosaurus*, an animal for which gregariousness is well supported, may suggest a similar, socially oriented survival strategy, or potentially nutritional stresses. Smaller carnivores in modern African ecosystems, such as spotted hyenas, form large social groups in order protect themselves and their territories from larger apex predators (Gittlleman, 1989; Packer, Sheek and Pusey, 1990). As *Gorgosaurus* displayed lower maximum growth rates than other tyrannosaurids, juveniles may have sought out similar group environments when growth was at its slowest, in order to survive with faster growing and ultimately larger apex predators, such as *Daspletosaurus*. Slow early growth rates may also reflect times of nutritional stress of young animals with limited food sources; solitary Siberian tiger are known to develop nutritional problems when young (Won et al., 2004).

The study of tooth macrowear provides evidence of feeding behaviour. Here, two specimens of *Gorgosaurus libratus,* one juvenile and one adult, were examined to contrast feeding strategies. Both specimens exhibited examples of enamel spalling, representative of traumatic feeding events or reduced enamel integrity due to continued use after damage. However, the adult teeth were dominated by tip wear, in contrast to the juvenile teeth, which presented numerous examples of longitudinal wear facets. This was hypothesised to reflect a change in feeding behaviour throughout ontogeny in tyrannosaurids, from shearing and slicing of meat with high levels of tooth on tooth contact in juveniles, to a puncture and pull method in adults well known from coprolites, stomach contents and bite marks in bone (Chin et al., 1998a; Chin et al., 1998b; Varrichio, 2001; Fowler et al., 2012; Murphy et al., 2013). These results were also substantiated by the greater denticle density recorded in juvenile specimens compared to adults. This correlates with the increase in bite force as the jaw grows throughout life, and may reflect a change in diet, and/or ecological niches between juvenile and adult *Gorgosaurus*.

Can we make justified inferences about social behaviour in dinosaurs using isolated specimens? Herein, I test several methods for doing so: observation of cranial palaeopathologies, measurement of denticle density, allometric growth in lacrimal horns, comparison of orbit shape, comparison of tooth wear, and growth rate estimation using body mass estimates and histology. Although a small number of these methods presented problems, such as the attempted extrapolation of von Ebner lines to calculate tooth replacement rates, others such as tooth wear, body growth rates, allometry of the lacrimal horns and the changing shape of the orbits throughout ontogeny, were all successfully utilised to contribute to our knowledge of social behaviour in *Gorgosaurus,* and in this regard, the objective of the thesis was achieved.

The ontogenetic changes observable in denticle density, lacrimal height, orbital shape, body growth rates and tooth wear can be used to infer behaviour and ecological niche in *Gorgosaurus*. Two hypotheses describe the likely social dependency of a juvenile *Gorgosaurus*:

1. The smaller body size, more circular orbit, greater denticle density and dominant occlusal form of tooth wear suggest that juvenile *Gorgosaurus* may have had substantially different feeding capabilities and, hence, diet than adults. The relative lack of apical tooth wear compared to adults, the reduced orbital strength (Henderson, 2003), coupled with lower bite forces (Molnar, 2013) and finer teeth, suggested that it may not have had the ability to process carcasses in the puncture and pull manner of adults (Rayfield, 2005), and instead may have hunted for smaller prey until it was large enough to tackle larger game such as hadrosaurines. Juveniles and adults with great disparities in body sizes, prolonged due to slow juvenile growth rates, have been known to occupy separate ontogenetic niches in modern ecosystems (Polis, 1983), and a similar theory has been proposed for juvenile and adult *Tyrannosaurus* (Horner et al., 2011). The slow juvenile growth rates of *Gorgosaurus* may also be indicative of nutritional stresses encountered when young due to this solitary lifestyle, as witnessed in modern Siberian tigers (Won et al., 2004) and the absence of intraspecific cranial bite marks would support the idea of minimal contact with conspecifics.

2. The orbit shape, denticle density and dominant forms of tooth wear suggest that juvenile *Gorgosaurus* would have made use of its more narrow snout and greater denticle density to slice off portions of meat from a kill from adults as has been postulated for *Allosaurus (*Bakker and Bir, 2004), and is witnessed in modern day lions (Pusey and Packer, 1994). The positively allometric growth of the lacrimal horn might be indicative of a sexual display structure in adults, similar to those known from modern animals e.g. antlers in Elk (Emlen et al., 2012). The slow growth rates are indicative of K strategists and may imply high levels of parental care, or at least crèche behaviour such as that witnessed in modern Crocodylia (Lang et al., 2013) to gain protection from larger concurrent predators; the lack of a high degree of cranial pathologies relative to other tyrannosaurids from intraspecific fighting may simply be a function of low sample size in the fossil record.

One potentially significant future study could examine the stable carbon and nitrogen isotope ratios of *Gorgosaurus* specimens in order to elucidate any dietary differences in juveniles versus adults. Stable C and N isotope ratios have been used to extract dietary information on extinct and recent mammals (Coltrain et al., 2004, Feranec, 2005, Codron et al., 2007), and may theoretically be applied to different aged individuals of *Gorgosaurus* to determine any differences in the trophic level at which they feed.

Another useful study might examine a number of isolated tyrannosaurid teeth for signs of enamel hypoplasia, a common pathology in modern mammals and reptiles that has been linked to malnutrition (Rothschild, 2006; Al-Shorman et al., 2014). Techniques are being refined to identify the taxon and ontogentic age of isolated theropod teeth (Torices et al., 2013), and the

presence of this tooth pathology might support theories of slow growth rates caused by nutritional stress in juvenile *Gorgosaurus*. *Gorgosaurus* is also one of the few well represented tyrannosaurids that has not yet had been subjected to the study of tooth replacement rates (Erickson 1996). With substantial evidence of regular spacing and width of incremental lines of von Ebner in isolated juvenile tyrannosaurid teeth, the extrapolation method devised in Chapter three may still prove successful in estimating growth rates of teeth of *Gorgosaurus libratus*.

This thesis has shown that the problems of poor sample size and subjectivity may be reduced in the study of social behaviour in juvenile dinosaurs. A multidisciplinary approach is henceforth recommended in instances where only isolated specimens are available for study. Furthermore, ontogenetic trends are good sources of evidence for reconstructing social behaviour in dinosaurs.

Bibliography

Abler, W. L. 1999. The teeth of the *Tyrannosaurus*. Scientific American, 281, 40–41.

Abler, W. L. 2001. A kerf-and-drill model of tyrannosaur tooth serrations. In: Tanke, D. & Carpenter, K. (eds.) Mesozoic Vertebrate Life. Indiana University Press, Bloomington, Indiana, 84-89.

Abler, W. L. 2013. lnternal Structure of Tooth Serrations. In: Parish, M. Molnar, R. E., Currie P. J., Koppelhus, E. B. editors. Tyrannosaurid Palaeobiology. Indiana University Press, Bloomington, Indiana. 81-86.

Al-Shorman, A., Alrousan, M. & Khwaileh, A. 2014. Rate of enamel formation and hypoplasia timing. Bulletin of the International Association for Paleodontology, 8, 203-208.

Anderson J.F., Hall-Martin, A. & Russell, D.A. 1985. Long-bone circumference and weight in mammals, birds and dinosaurs. J Zool Soc Lond A, 207, 53-61

Arbour, V. M., & Currie, P. J. 2012. Analyzing taphonomic deformation of ankylosaur skulls using retrodeformation and finite element analysis. PloS One, 7, e39323.

Aubret, F., & Shine, R. 2009. Causes and consequences of aggregation by neonatal tiger snakes (*Notechis scutatus*, Elapidae). Austral Ecology, 34, 210-217.

Bakker, R. T. 1988. The Dinosaur Heresies. London: Penguin.

Barco, J. L., Canudo, J. I., & Ruiz-Omeñaca, J. I. 2006. New data on *Therangospodus oncalensis* from the Berriasian Fuentesalvo tracksite (Villar del Río, Soria, Spain): an example of gregarious behaviour in theropod dinosaurs. Ichnos, 13, 237-248.

Barnes, F. A., & Lockley, M. G. 1994. Trackway evidence for social sauropods from the Morrison Formation, Eastern Utah (USA). Gaia, 10, 37-42.

Barsbold, R., Osmólska, H., Watabe, M., Currie, P. J., & Tsogtbaatar, K. 2000. A new oviraptorosaur (Dinosauria, Theropoda) from Mongolia: the first dinosaur with a pygostyle. Acta Palaeontologica Polonica, 45, 97-106.

Bates, K. T., & Falkingham, P. L. 2012. Estimating maximum bite performance in *Tyrannosaurus rex* using multi-body dynamics. Biology Letters, rsbl20120056.

Bates, K. T., Manning, P. L., Hodgetts, D., & Sellers, W. I. 2009. Estimating mass properties of dinosaurs using laser imaging and 3D computer modelling.PLoS One, 4, e4532.

Bekoff, M. 1995. Play signals as punctuation: The structure of social play in canids. Behaviour, 132, 419-429.

Bell, P. R. 2010. Palaeopathological changes in a population of *Albertosaurus sarcophagus* from the Upper Cretaceous Horseshoe Canyon Formation of Alberta, Canada. Canadian Journal of Earth Sciences, 47, 1263-1268.

Bell, P. R., & Currie, P. J. 2010. A tyrannosaur jaw bitten by a confamilial: scavenging or fatal agonism? Lethaia, 43, 278-281.

Bell, P. R., Currie, P. J., & Lee, Y. N. 2012. Tyrannosaur feeding traces on *Deinocheirus* (Theropoda: Ornithomimosauria) remains from the Nemegt Formation (Late Cretaceous), Mongolia. Cretaceous Research, 37, 186-190.

Bell, P. R., Fanti, F., Currie, P. J., & Arbour, V. M. 2014. A mummified duck-billed dinosaur with a soft-tissue cock's comb. Current Biology, 24, 70-75.

Benjamini, Y., Hochberg, Y., 1995. Controlling the false discovery rate: a practical and powerful approach to multiple testing. Journal of the Royal Statistical Society. Series B (Methodological) 57, 289-300.

Benson, R. B.J., Carrano, M.T. & Brusatte, S.L. 2009. A new clade of archaic large-bodied predatory dinosaurs (Theropoda: Allosauroidea) that survived to the latest Mesozoic. Naturwissenschaften, 97, 71-78.

Benson, R. B., Campione, N. E., Carrano, M. T., Mannion, P. D., Sullivan, C., Upchurch, P., & Evans, D. C. 2014. Rates of dinosaur body mass evolution indicate 170 million years of sustained ecological innovation on the avian stem lineage. PLoS Biology, 12, e1001853.

Benton, M. J., Forth, J., & Langer, M. C. 2014. Models for the Rise of the Dinosaurs. Current Biology, 24, 87-95.

Bertin, A., Hausberger, M., Henry, L. & Richard-Yris, M.A. 2007. Adult and peer influences on starling song development. Developmental Psychobiology, 49, 362-374.

Bertram, B. C. 2014. The ostrich communal nesting system. Princeton University Press.

Bhullar, B. A. S., Marugán-Lobón, J., Racimo, F., Bever, G. S., Rowe, T. B., Norell, M. A., & Abzhanov, A. 2012. Birds have paedomorphic dinosaur skulls. Nature, 487, 223-226.

Biknevicius, A. R. 1996. Functional discrimination in the masticatory apparatus of juvenile and adult cougars (*Puma concolor*) and spotted hyenas (*Crocuta crocuta*). Canadian Journal of Zoology, 74, 1934-1942.

Binder, W. J., & Valkenburgh, B. 2000. Development of bite strength and feeding behaviour in juvenile spotted hyenas (*Crocuta crocuta*). Journal of Zoology, 252, 273-283.

Binder, W. J., & van Valkenburgh, B. 2010. A comparison of tooth wear and breakage in Rancho La Brea sabertooth cats and dire wolves across time. Journal of Vertebrate Paleontology, 30, 255-261.

Bird, R. T. 1939. Thunder in his footsteps. Natural History, 43, 254-261.

Blumstein, D. T., & Armitage, K. B. 1999. Cooperative breeding in marmots. Oikos, 369-382.

Bowman, R. 2003. Apparent cooperative hunting in Florida scrub-jays. The Wilson Bulletin, 115, 197-199.

Brand, R. 2007. Evolutionary ecology of giraffes (*Giraffa camelopardalis*) in Etosha National Park, Namibia.

Brassey, C. A., Maidment, S. C., & Barrett, P. M. 2015. Body mass estimates of an exceptionally complete *Stegosaurus* (Ornithischia: Thyreophora): comparing volumetric and linear bivariate mass estimation methods. Biology letters, 11, 20140984.

Brien, M. L., Webb, G. J., Lang, J. W., McGuinness, K. A., & Christian, K. A. 2013. Born to be bad: agonistic behaviour in hatchling saltwater crocodiles (*Crocodylus porosus*). Behaviour, 150, 737-762.

Brien, Matthew L., Webb, Grahame J., Lang, Jeffrey W., and Christian, Keith A. 2013b. Intra- and interspecific agonistic behaviour in hatchling Australian freshwater crocodiles (*Crocodylus johnstoni*) and saltwater crocodiles (*Crocodylus porosus*). Australian Journal of Zoology 61, 196–205.

Brien, M. L., Lang, J. W., Webb, G. J., Stevenson, C., & Christian, K. A. 2013c. The good, the bad, and the ugly: agonistic behaviour in juvenile crocodilians.PloS one, 8, e80872.

Brochu, C. A. 2003. Osteology of *Tyrannosaurus rex*: insights from a nearly complete skeleton and high-resolution computed tomographic analysis of the skull. Journal of Vertebrate Paleontology, 22, 1-138.

Brown, C.M., Arbour, J.H., Jackson, D.A., 2012. Testing of the Effect of Missing Data Estimation and Distribution in Morphometric Multivariate Data Analyses. Systematic Biology 61, 941-954.

Brown, J. L. 2014. Helping Communal Breeding in Birds: Ecology and Evolution. Princeton University Press.

Bugnyar, T., Stoewe, M., & Heinrich, B. 2007. The ontogeny of caching in ravens, *Corvus corax*. Animal Behaviour, 74, 757-767.

Burghardt, G. M. 2015. Play in fishes, frogs and reptiles. Current Biology, 25, R9-R10. Cambridge, UK: Cambridge University Press.

Burghardt, G. M. 1977. Of iguanas and dinosaurs: Social behavior and communication in neonate reptiles. American Zoologist, 17, 177-190.

Burns, M. E., Currie, P. J., Sissons, R. L., & Arbour, V. M. 2011. Juvenile specimens of *Pinacosaurus grangeri* Gilmore, 1933 (Ornithischia: Ankylosauria) from the Late Cretaceous of China, with comments on the specific taxonomy of *Pinacosaurus*. Cretaceous Research, 32, 174-186.

Bybee, P. J., Lee, A. H., & Lamm, E. T. 2006. Sizing the Jurassic theropod dinosaur *Allosaurus*: assessing growth strategy and evolution of ontogenetic scaling of limbs. Journal of Morphology, 267, 347-359.

Campione, N. E., & Evans, D. C. 2011. Cranial growth and variation in *Edmontosaurus* (Dinosauria: Hadrosauridae): implications for latest Cretaceous megaherbivore diversity in North America. PLoS One, 6, e25186.

Campione, N. E., & Evans, D. C. 2012. A universal scaling relationship between body mass and proximal limb bone dimensions in quadrupedal terrestrial tetrapods. Bmc Biology, 10, 60.

Campione, N.E. 2013. MASSTIMATE: Body Mass Estimation Equations for Vertebrates. R Project for Statistical Computing, Comprehensive R Archive Network (CRAN).

Campione, N.E., Evans, D.C., Brown, C.M. & Carrano, M.T. 2014. A mathematically derived equation for estimating body mass in terrestrial bipedal tetrapods. Methods in Ecology and Evolution, 5, 913-923.

Carr, T. D. 1999. Craniofacial ontogeny in tyrannosauridae (Dinosauria, Coelurosauria). Journal of Vertebrate Paleontology, 19, 497-520.

Carr, T. D., & Williamson, T. E. 2004. Diversity of late Maastrichtian Tyrannosauridae (Dinosauria: Theropoda) from western North America. Zoological Journal of the Linnean Society, 142, 479-523.

Carrano, M. T. 2001. Implications of limb bone scaling, curvature and eccentricity in mammals and non-avian dinosaurs. Journal of Zoology, 254, 41-55.

Castanet, J. 1994. Age estimation and longevity in reptiles. Gerontology, 40, 174-192.

Catchpole, C.K., & Slater, P.J.B. 2008. Bird song biological themes and variations, 2nd edn. Cambridge University Press, Cambridge

Cawley, G. C., & Janacek, G. J. 2010. On allometric equations for predicting body mass of dinosaurs. Journal of Zoology, 280, 355-361.

Chapman, R. E. 1990. Shape analysis in the study of dinosaur morphology. Dinosaur systematics: approaches and perspectives, 21-42.

Charruau, P., & Hénaut, Y. 2012. Nest attendance and hatchling care in wild American crocodiles (*Crocodylus acutus*) in Quintana Roo, Mexico. Animal Biology, 62, 29-51.

Chatterjee, S., & Templin, R. J. 2004. Feathered coelurosaurs from China: new night on the arboreal origin of avian flight. In: Currie, P.J. Koppelhus, E.B., Shugar, M.A. & Wright, J.L. (eds.) Feathered Dragons: Studies on the Transition from Dinosaurs to Birds, 251-281.

Chin, K., Eberth, D.A., and Sloboda, W.J. 1998. Exceptional soft-tissue preservation in a theropod coprolite from the Upper Cretaceous Dinosaur Park Formation of Alberta. Journal of Vertebrate Paleontology, 19: 37-38.

Chin, K., Tokaryk, T. T., Erickson, G. M., & Calk, L. C. 1998. A king-sized theropod coprolite. Nature, 393, 680-682.

Chinsamy, A. 1993. Bone histology and growth trajectory of the prosauropod dinosaur *Massospondylus carinatus* Owen. Modern Geology, 18,19-329.

Chinsamy-Turan, A. 2005. The microstructure of dinosaur bone: deciphering biology with fine-scale techniques. John Wiley & Sons.

Christiansen P & Fariña, R.A. 2004. Mass prediction in theropod dinosaurs. Hist Biol, 16, 85-92.

Christiansen, P., 1998. Strength indicator values of theropod long bones, with comments on limb proportions and cursorial potential. Gaia, 15, 241-255.

Christiansen, P., 1999. Long bone scaling and limb posture on non-avian theropods: evidence for differential allometry. Journal of Vertebrate Paleontology 19, 666-680.

Chure, D. J. 1998. On the orbit of theropod dinosaurs. In: Perez-Moreno, B. P., Holtz Jr. T., Sanz, J. L. and Moratalla, J. (eds.) Aspects of Theropod Paleobiology, 233-240.

Clark, J. M., Norell, M., Chiappe, L. M., & Akademi, M. S. U. 1999. An oviraptorid skeleton from the late Cretaceous of Ukhaa Tolgod, Mongolia, preserved in an avianlike brooding position over an oviraptorid nest. American Museum novitates; no. 3265.

Clutton-Brock, T. H. 1991. The evolution of parental care. Princeton University Press.

Codron, D., Lee-Thorp, J.A., Sponheimer, M., & Codron, J. 2007. Stable carbon isotope reconstruction of ungulate diet changes through the seasonal cycle. South African Journal of Wildlife Research 37, 117-125.

Colbert, E. H. 1989. The Triassic dinosaur *Coelophysis*. Museum of Northern Arizona Bulletin, 5: 1–160.

Coltrain, J.B. J.M. Harris, T.E. Cerling, J.R. Ehleringer, M-D. Dearing, J. Ward, & J. Allen. 2004. Rancho La Brea stable isotope biogeochemistry and its implications for the palaeoecology of late Pleistocene, coastal southern California. Palaeogeography, Palaeoclimatology, Palaeoecology 205,199-219.

Cook, S. D., Skinne, H. B., & Haddad Jr., R. J. 1983. A quantitative histologic study of osteoporosis produced by nutritional secondary hyperparathyroidism in dogs. Clinical orthopaedics and related research, 175, 105-119.

Cooper, L. N., Lee, A. H., Taper, M. L., & Horner, J. R. 2008. Relative growth rates of predator and prey dinosaurs reflect effects of predation. Proceedings of the Royal Society B: Biological Sciences, 275, 2609-2615.

Currie, P. J. 1983. Hadrosaur trackways from the Lower Cretaceous of Canada. Acta Palaeontologica Polonica, 28, 63-73.

Currie, P. J. 1998. Possible evidence of gregarious behaviour in tyrannosaurids. Gaia, 15, 271-277.

Currie, P. J. 2003a. Allometric growth in tyrannosaurids (Dinosauria: Theropoda) from the Upper Cretaceous of North America and Asia. Canadian Journal of Earth Sciences, 40, 651-665.

Currie, P.J. 2003b. Cranial anatomy of tyrannosaurid dinosaurs from the Late Cretaceous of Alberta, Canada. Acta Palaeontologica Polonica, 48: 191–226.

Currie, P. J. 2005. Theropods, Including Birds. In: Currie, P.J and Koppelhus, E.B. Dinosaur Provincial Park: A spectacular ancient ecosystem revealed, 1, 367.

Currie, P. J., Hurum, J. H., & Sabath, K. 2003. Skull structure and evolution in tyrannosaurid dinosaurs. Acta Palaeontologica Polonica, 48, 227-234.

Currie, P. J., & Eberth, D. A. 2010. On gregarious behaviour in *Albertosaurus*. Canadian Journal of Earth Sciences, 47, 1277-1289.

Currie, P.J. & Carpenter, K. 2000. A new specimen of *Acrocanthosaurus atokensis* (Theropoda, Dinosauria) from the lower cretaceous antlers formation (lower cretaceous, aptian) of Oklahoma, USA. Geodiversitas, 22, 207-246.

Curry, K. A. 1999. Ontogenetic histology of *Apatosaurus* (Dinosauria : Sauropoda): new insights on growth rates and longevity. Journal of Vertebrate Paleontology, 19, 654-665

Dash, M. C. 2001. Fundamentals of ecology. Tata McGraw-Hill Education: New Dehli, India.

Davies, S.J.J.F. 2002. Ratites and Tinamous. Oxford: Oxford University Press.

De Jong, T. R., Korosi, A., Harris, B. N., Perea-Rodriguez, J. P., & Saltzman, W. 2012. Individual Variation in Paternal Responses of Virgin Male California Mice (*Peromyscus californicus*): Behavioral and Physiological Correlates. Physiological and Biochemical Zoology, 85, 740-751.

Derix, R., Van Hooff, J., De Vries, H., & Wensing, J. 1993. Male and female mating competition in wolves: female suppression vs. male intervention. Behaviour, 127, 141-174.

Díez Díaz, V., Pereda Suberbiola, X., & Sanz, J. L. 2012. Juvenile and adult teeth of the titanosaurian dinosaur Lirainosaurus (Sauropoda) from the Late Cretaceous of Iberia. Geobios, 45, 265-274.

Dilkes, D. W. 2001. An ontogenetic perspective on locomotion in the Late Cretaceous dinosaur Maiasaura peeblesorum (Ornithischia: Hadrosauridae).Canadian Journal of Earth Sciences, 38, 1205-1227.

Dodson, P. 1975. Taxonomic implications of relative growth in lambeosaurine hadrosaurs. Systematic Biology, 24, 37-54.

Donaldson, T. M., Newberry, R. C., Špinka, M., & Cloutier, S. 2002. Effects of early play experience on play behaviour of piglets after weaning. Applied Animal Behaviour Science, 79, 221-231.

Dong Z.M. & Currie P.J. 1995. On the discovery of an oviraptorid skeleton on a nest of eggs at Bayan Mandahu, Inner Mongolia, People's Republic of China. Canadian Journal of Earth Sciences, 33, 631–636.

Doody, J. S., Burghardt, G. M., & Dinets, V. 2013. Breaking the Social–Non-social Dichotomy: A Role for Reptiles in Vertebrate Social Behaviour Research? Ethology, 119, 95-103.

Doody, J. S., Sims, R. A., & Georges, A. 2003. Gregarious behavior of nesting turtles (Carettochelys insculpta) does not reduce nest predation risk. Journal Information, 2003.

Doody, J. S., Stewart, B., Camacho, C., & Christian, K. 2012. Good vibrations? Sibling embryos expedite hatching in a turtle. Animal Behaviour, 83, 645-651.

Doody, J. S., Freedberg, S., & Keogh, J. S. 2009a. Communal egg-laying in reptiles and amphibians: evolutionary patterns and hypotheses. The Quarterly review of biology, 84, 229-252.

Drea, C. M., & Carter, A. N. 2009b. Cooperative problem solving in a social carnivore. Animal Behaviour, 78, 967-977.

Drea, C. M., Hawk, J. E., & Glickman, S. E. 1996. Aggression decreases as play emerges in infant spotted hyaenas: preparation for joining the clan. Animal Behaviour, 51, 1323-1336.

Drummond, H. 2006. Dominance in vertebrate broods and litters. The Quarterly Review of Biology, 81, 3-32.

DuVal, E. H. 2013. Female mate fidelity in a lek mating system and its implications for the evolution of cooperative lekking behavior. The American Naturalist, 181, 213-22.

Eberth, D. A. 2005. The geology. In: Currie, P.J. & Koppelhus, E.B. (eds.) Dinosaur Provincial Park: A spectacular ancient ecosystem revealed, 54-82.

Eberth, D. A., & Currie, P. J. 2010. Stratigraphy, sedimentology, and taphonomy of the *Albertosaurus* bonebed (upper Horseshoe Canyon Formation; Maastrichtian), southern Alberta, Canada. This article is one of a series of papers published in this Special Issue on the theme *Albertosaurus*. Canadian Journal of Earth Sciences, 47, 1119-1143.

Emlen, D. J., Warren, I. A., Johns, A., Dworkin, I., & Lavine, L. C. 2012. A mechanism of extreme growth and reliable signaling in sexually selected ornaments and weapons. Science, 337, 860-864.

Erickson, G. M. 1996. Incremental lines of von Ebner in dinosaurs and the assessment of tooth replacement rates using growth line counts. Proceedings of the National Academy of Sciences, 93, 14623-14627.

Erickson, G. M., Van Kirk, S. D., Su, J., Levenston, M. E., Caler, W. E., & Carter, D. R. 1996. Bite-force estimation for Tyrannosaurus rex from tooth-marked bones. Nature, 382, 706-708.

Erickson, G. M. & Tumanova, T. A. 2000. Growth curve of *Psittacosaurus mongoliensis* Osborn (Ceratopsia: Psittacosauridae) inferred from long bone histology. Zoological Journal of the Linnaean Society, 130, 551-566.

Erickson, G. M., Rogers, K. C., & Yerby, S. A. 2001. Dinosaurian growth patterns and rapid avian growth rates. Nature, 412, 429-433.

Erickson, G. M., Makovicky, P. J., Currie, P. J., Norell, M. A., Yerby, S. A., & Brochu, C. A. 2004. Gigantism and comparative life-history parameters of tyrannosaurid dinosaurs. Nature, 430, 772-775.

Erickson, G. M., Currie, P. J., Inouye, B. D., & Winn, A. A. 2010. A revised life table and survivorship curve for *Albertosaurus sarcophagus* based on the Dry Island mass death assemblage. Canadian Journal of Earth Sciences, 47, 1269-1275.

Espinoza, R. E., & Quinteros, S. 2008. A hot knot of toads: Aggregation provides thermal benefits to metamorphic Andean toads. Journal of Thermal Biology, 33, 67-75.

Estes, R. 1991. The behavior guide to African mammals (Vol. 64). Berkeley: University of California Press.

Fagan, R. 1981. Animal play behavior. New York: Oxford University Press

Fanti, F., Currie, P. J., & Badamgarav, D. 2012. New specimens of *Nemegtomaia* from the Baruungoyot and Nemegt formations (Late Cretaceous) of Mongolia. PloS one, 7, e31330.

Farlow, J. O., Brinkman, D. L., Abler, W. L., & Currie, P. J. (1991). Size, shape, and serration density of theropod dinosaur lateral teeth. Modern Geology, 16, 161-198.

Farlow, J. O., & Brinkman, D. L. 1994. Wear surfaces on the teeth of tyrannosaurs. In: Dino Fest; Proceedings of a Conference for the General Public. Palaeontological Society Special Publications, 7, 165-175.

Farlow, J.O., Smith, M.B. & Robinson, J.M. 1995. Body mass, bone “strength indicator,” and cursorial potential of Tyrannosaurus rex. Journal of Vertebrate Palaeontology, 15, 713-725.

Farlow, J. O., & Planka, E. R. 2002. Body size overlap, habitat partitioning and living space requirements of terrestrial vertebrate predators: implications for the paleoecology of large theropod dinosaurs. Historical Biology, 16, 21-40.

Fernández-Juricic, E., Jokimäki, J., McDonald, J. C., Melado, F., Toledano, A., Mayo, C., ... & Martín, V. 2004. Effects of opportunistic predation on anti-predator behavioural responses in a guild of ground foragers. Oecologia, 140, 183-190.

Fiorillo, A. R. 1997. Microwear on the teeth of theropod dinosaurs (Judith River Formation) of south-central Montana: Inferences on diet. Journal of Vertebrate Paleontology, 18.

Fiorillo, A. R. 1998. Dental micro wear patterns of the sauropod dinosaurs Camarasaurus and Diplodocus: evidence for resource partitioning in the late Jurassic of North America. Historical Biology, 13, 1-16.

Fiorillo, A. R. 2008. On the occurrence of exceptionally large teeth of *Troodon* (Dinosauria: Saurischia) from the Late Cretaceous of northern Alaska. Palaios, 23, 322-328.

Fiorillo, A. R. 2011. Microwear patterns on the teeth of northern high latitude hadrosaurs with comments on microwear patterns in hadrosaurs as a function of latitude and seasonal ecological constraints. Palaeontologia Electronica, 14.

Fiorillo, A. R., & Tykoski, R. S. 2014. A diminutive new tyrannosaur from the top of the world. PloS one, 9, e91287.

Fowler, D. W., & Sullivan, R. M. 2006. A ceratopsid pelvis with toothmarks from the Upper Cretaceous Kirtland Formation, New Mexico: Evidence of Late Campanian tyrannosaurid feeding behaviour. New Mexico Museum of Natural History and Science Bulletin, 35, 127-130.

Fowler, D. W., Scannella, J. B., Goodwin, M. B., & Horner, J. R. 2012. How to eat a *Triceratops*: large sample of toothmarks provides new insight into the feeding behaviour of Tyrannosaurus. Journal of Vertebrate Paleontology, 32, 96.

Funston, G. F., Persons, W. S., Bradley, G. J., & Currie, P. J. 2015. New material of the large-bodied caenagnathid *Caenagnathus collinsi* from the Dinosaur Park Formation of Alberta, Canada. Cretaceous Research, 54, 179-187.

Geist, V. 1971. Mountain sheep-a study in behavior and evolution. Oryx, 12, 129-130.

Gentner, T. Q., & Hulse, S. H. 2000. Female European starling preference and choice for variation in conspecific male song. Animal Behaviour, 59, 443-458.

Gilbert, C., McCafferty, D., Le Maho, Y., Martrette, J. M., Giroud, S., Blanc, S., & Ancel, A. 2010. One for all and all for one: the energetic benefits of huddling in endotherms. Biological Reviews, 85, 545-569.

Gillooly, J. F., Allen, A. P., & Charnov, E. L. 2006. Dinosaur fossils predict body temperatures. PLoS biology, 4, e248.

Gillooly, J.F., Brown, J.H., West, G.B., Savage, V.M., & Charnov, E.L. 2001. Effects of size and temperature on metabolic rate. Science, 293, 2248-2251.

Gittleman, J. L. 1989. Carnivore group living: comparative trends. In: Gittleman (ed.) Carnivore behavior, ecology, and evolution, 183-207. Springer: USA.

Godfrey, D., Lythgoe, J. N., & Rumball, D. A. 1987. Zebra stripes and tiger stripes: the spatial frequency distribution of the pattern compared to that of the background is significant in display and crypsis. Biological Journal of the Linnean Society, 32, 427-433.

Goodwin, M. B., & Horner, J. R. 2004. Cranial histology of pachycephalosaurs (Ornithischia: Marginocephalia) reveals transitory structures inconsistent with head-butting behavior. Journal Information, 30.

Goswami, A., Flynn, J. J., Ranivoharimanana, L., & Wyss, A. R. 2005. Dental microwear in Triassic amniotes: implications for paleoecology and masticatory mechanics. Journal of Vertebrate Paleontology, 25, 320-329.

Graham, K.L., and Burghardt, G.M. 2010. Current perspectives on the biological study of play: Signs of progress. Quarterly Review of Biology, 85, 393–418.

Gray, H. 2009. Gray's Anatomy: With original illustrations by Henry Carter. Arcturus Publishing.

Greaves, W. S. 1983. A functional analysis of carnassial biting. Biological Journal of the Linnean Society, 20, 353-363.

Grellet-Tinner, G., & Makovicky, P. 2006. A possible egg of the dromaeosaur *Deinonychus antirrhopus*: phylogenetic and biological implications. Canadian Journal of Earth Sciences, 43, 705-719.

Grillo, O. N., & Azevedo, S. A. 2011. Recovering missing data: estimating position and size of caudal vertebrae in *Staurikosaurus pricei* Colbert, 1970.Anais da Academia Brasileira de Ciências, 83, 61-72.

Guinet, C. 1991. Intentional stranding apprenticeship and social play in killer whales (*Orcinus orca*). Canadian Journal of Zoology, 69, 2712-2716.

Guttridge, T. L., van Dijk, S., Stamhuis, E. J., Krause, J., Gruber, S. H., & Brown, C. 2013. Social learning in juvenile lemon sharks, *Negaprion brevirostris*. Animal cognition, 16, 55-64.

Hayes, L. D. 2000. To nest communally or not to nest communally: a review of rodent communal nesting and nursing. Animal Behaviour, 59, 677-688.

Hayward, M. W., & Kerley, G. I. 2008. Prey preferences and dietary overlap amongst Africa's large predators. South African Journal of Wildlife Research, 38, 93-108.

Heckert, A.B. 2009. The paleobiology of *Coelophysis bauri* (Cope) from the Upper Triassic (Apachean) Whitaker quarry, New Mexico, with detailed analysis of a single quarry block. New Mexico Bulletin: Museum of Natural History and Science.

Hedrick, B. P., & Dodson, P. 2013. Lujiatun Psittacosaurids: Understanding Individual and Taphonomic Variation Using 3D Geometric Morphometrics. PloS one, 8, e69265.

Heinrich, R. E., Ruff, C. B., & Weishampel, D. B. 1993. Femoral ontogeny and locomotor biomechanics of *Dryosaurus lettowvorbecki* (Dinosauria, Iguanodontia). Zoological Journal of the Linnean Society, 108, 179-196.

Hejnol, A. 2014. Evolutionary biology: Excitation over jelly nerves. Nature, 510, 38-39.

Henderson, D. M. 2003. The eyes have it: the sizes, shapes, and orientations of theropod orbits as indicators of skull strength and bite force. Journal of Vertebrate Palaeontology, 22, 766-778.

Holtz, T. R. 1996. Phylogenetic taxonomy of the *Coelurosauria* (Dinosauria: Theropoda). Journal of Paleontology, 536-538.

Holtz TR Jr. 2001. The phylogeny and taxonomy of the Tyrannosauridae. In: Tanke DH, Carpenter K, eds. Mesozoic vertebrate life. Bloomington and Indianapolis: Indiana University Press, 64–83.

Holtz Jr., T. R. 2004. Tyrannosauroidea. In: Weishampel, D. B., Dodson, P., & Osmólska, H. (eds.). The Dinosauria. California: University of California Press, 111-136.

Holtz Jr. 2008. A critical reappraisal of the obligate scavenging hypothesis for *Tyrannosaurus rex* and other tyrant dinosaurs. In: Larson P, Carpenter K, editors. *Tyrannosaurus rex*. Bloomington: Indiana University Press. 371–396.

Hone, D. W., Farke, A. A., Watabe, M., Shigeru, S., & Tsogtbaatar, K. 2014. A New Mass Mortality of Juvenile *Protoceratops* and Size-Segregated Aggregation Behaviour in Juvenile Non-Avian Dinosaurs. PloS one, 9, e113306.

Horner, J. R., De Ricqlès, A., & Padian, K. 2000. Long bone histology of the hadrosaurid dinosaur *Maiasaura peeblesorum*: growth dynamics and physiology based on an ontogenetic series of skeletal elements. Journal of Vertebrate Palaeontology, 20, 115-129.

Horner, J. R., & Goodwin, M. B. 2009. Extreme cranial ontogeny in the Upper Cretaceous dinosaur *Pachycephalosaurus*. PLoS One, 4, e7626.

Horner, J. R., Goodwin, M. B., & Myhrvold, N. 2011. Dinosaur census reveals abundant *Tyrannosaurus* and rare ontogenetic stages in the Upper Cretaceous Hell Creek Formation (Maastrichtian), Montana, USA. PLoS One, 6, e16574.

Huang, W. S. 2006. Parental care in the long-tailed skink, *Mabuya longicaudata*, on a tropical Asian island. Animal Behaviour, 72, 791-795.

Hunt, A.P., Lucas, S.G., Krainer, K., and Spielman, J. 2006. The taphonomy of the Cleveland-Lloyd Dinosaur Quarry, Upper Jurassic Morrison Formation, Utah: a reevaluation. New Mexico Museum of Natural History and Science Bulletin,36, 57–65.

Hurd, C. R. 1996. Interspecific attraction to the mobbing calls of black-capped chickadees (*Parus atricapillus*). Behavioral Ecology and Sociobiology, 38, 287-292.

Hutchinson, J. R., Ng-Thow-Hing, V., & Anderson, F. C. 2007. A 3D interactive method for estimating body segmental parameters in animals: application to the turning and running performance of *Tyrannosaurus re* .Journal of Theoretical Biology, 246, 660-680.

Hutton, J. M. 1987. Growth and feeding ecology of the Nile crocodile *Crocodylus niloticus* at Ngezi, Zimbabwe. The Journal of Animal Ecology, 25-38.

Ibiricu, L. M., Martínez, R. D., Casal, G. A., & Cerda, I. A. 2013. The behavioral implications of a multi-individual bonebed of a small Theropod Dinosaur. PloS one, 8, e64253.

Ingram, T. R., Tannehill, J. E., & Young, S. P. 2013. Post-Release Survival and Behaviour of Adult Shoal Bass in the Flint River, Georgia. North American Journal of Fisheries Management, 33, 717-722.

Jacobsen, A. R. 1998. Feeding behaviour of carnivorous dinosaurs as determined by tooth marks on dinosaur bones. Historical Biology, 13, 17-26.

Jepsen, G. L. 1964. Riddles of the terrible lizards. American Scientist, 52, 227-246.

Johnson, K. 2007. Natural history as stamp collecting: a brief history. Archives of natural history, 34, 244-258.

Johnson, M. & Walters, J.R. 2011. Proximate and ultimate factors that promote aggregated breeding in the Western Sandpiper. Zoological Research, 32, 128–140.

Johnston, P. A. 1979. Growth rings in dinosaur teeth. Nature, 278, 635–636.

Jungwirth, A., Josi, D., Walker, J., & Taborsky, M. 2015. Benefits of coloniality: communal defence saves anti-predator effort in cooperative breeders. Functional Ecology.

Katselidis, K. A., Schofield, G., Stamou, G., Dimopoulos, P., & Pantis, J. D. 2012. Females first? Past, present and future variability in offspring sex ratio at a temperate sea turtle breeding area. Animal Conservation, 15, 508-518.

Kearney, M., & Clark, J. M. 2003. Problems due to missing data in phylogenetic analyses including fossils: a critical review. Journal of Vertebrate Paleontology, 23, 263-274.

Kilbourne, B. M., & Makovicky, P. J. 2010. Limb bone allometry during postnatal ontogeny in non-avian dinosaurs. Journal of Anatomy, 217, 135-152.

Koprowski, J. L. 1996. Natal philopatry, communal nesting, and kinship in fox squirrels and gray squirrels. Journal of Mammalogy, 77, 1006-1016.

Lambe, L.M. 1914. On a new genus and species of carnivorous dinosaur from the Belly River Formation of Alberta, with a description of the skull of *Stephanosaurus marginatus* from the same horizon. Ottawa Naturalist 28, 13–20.

Lambe, L.M. 1917. The Cretaceous theropodous dinosaur *Gorgosaurus*. Geological Survey of Canada, Memoir 100, 1–84.

Lang, J. W., Kumar, P., Bank, M. C., & Alliance, G. C. 2013, May. Behavioral ecology of gharial on the Chambal River, India. In Crocodiles: Proceedings of the 22nd working meeting of the crocodile specialist group, 42-52.

Larson, P. L. 2013. The case for *Nanotyrannus* in J. M. Parrish, R. A. Molnar, P. J. Currie., & E. B. Koppelhus (eds.) Tyrannosaurid Paleobiology, University of Indiana Press, Bloomington and Indianapolis, 15-53.

Lee, Y. N., Barsbold, R., Currie, P. J., Kobayashi, Y., Lee, H. J., Godefroit, P. & Chinzorig, T. 2014. Resolving the long-standing enigmas of a giant ornithomimosaur *Deinocheirus mirificus*. Nature, 13874.

Lehman, T. M., & Woodward, H. N. 2009. Modelling growth rates for sauropod dinosaurs. Palaeobiology, 34, 264-281.

Leidy, J. 1856. Notice of remains of extinct reptiles and fishes, discovered by Dr. FV Hayden in the Bad Lands of the Judith River, Nebraska Territory. Proceedings of the Academy of Natural Sciences of Philadelphia, 8.

Lemmon, A. R., Brown, J. M., Stanger-Hall, K., & Lemmon, E. M. 2009. The effect of ambiguous data on phylogenetic estimates obtained by maximum likelihood and Bayesian inference. Systematic Biology, 58, 130-145.

Leuthold, W. 1977. African ungulates. Zoophysiology and ecology, 8, 1-307.

Li, Q., Gao, K., Meng, Q., Clarke, J.A., Shawkey, M.D., D'Alba, L., Pei, R., Ellison, M., Norell, M.A., and Vinther, J. 2012. A new reconstruction of *Microraptor* and the evolution of iridescent plumage. Science, 335, 1215–1219.

Lipps, J. H. 2009. The protection and conservation of paleontologic field sites worldwide. In: Portland GSA Annual Meeting.

Lockley, M.G. 1996. Dinosaur ontogeny and population structure: interpretations and speculations based on footprints. In: Carpenter, K., Hirsch, K. F., & Horner, J. R. (eds.) *Dinosaur eggs and babies*. Cambridge University Press.

Lockley, M. G., & Hunt, A. P. 1995. Ceratopsid tracks and associated ichnofauna from the Laramie Formation (Upper Cretaceous: Maastrichtian) of Colorado. Journal of Vertebrate Paleontology, 15, 592-614.

Lockley, M. G., & Matsukawa, M. 1999. Some observations on trackway evidence for gregarious behaviour among small bipedal dinosaurs. Palaeogeography, Palaeoclimatology, Palaeoecology, 150, 25-31.

Lockley, M., Schulp, A. S., Meyer, C. A., Leonardi, G., & Mamani, D. K. 2002. Titanosaurid trackways from the Upper Cretaceous of Bolivia: evidence for large manus, wide-gauge locomotion and gregarious behaviour. Cretaceous Research, 23, 383-400.

Lockley, M. G., Holbrook, J., Kukihara, R., & Matsukawa, M. 2006. An ankylosaur-dominated dinosaur tracksite in the Cretaceous Dakota Group of Colorado: paleoenvironmental and sequence stratigraphic context. Late Cretaceous Vertebrates from the Western Interior. New Mexico Museum of Natural History and Science Bulletin, 35, 95-104.

Lockley, M. G., Huh, M., Gwak, S. G., Hwang, K. G., & Paik, I. S. 2012. Multiple tracksites with parallel trackways from the Cretaceous of the Yeosu City area Korea: Implications for gregarious behaviour in ornithopod and sauropod dinosaurs. Ichnos, 19, 105-114.

Lockley, M. G., & Meyer, C. 2013. Dinosaur tracks and other fossil footprints of Europe. Columbia University Press: New York.

Loewen, M. A., Irmis, R. B., Sertich, J. J., Currie, P. J., & Sampson, S. D. 2013. Tyrant dinosaur evolution tracks the rise and fall of Late Cretaceous oceans. PloS one, 8, e79420.

Longrich, N. 2006. Structure and function of hindlimb feathers in *Archaeopteryx lithographica*. Journal Information, 32.

Longrich, N. R., & Field, D. J. 2012. *Torosaurus* is not *Triceratops*: Ontogeny in chasmosaurine ceratopsids as a case study in dinosaur taxonomy. PloS one, 7, e32623.

Loyau, A., Jalme, M. S., & Sorci, G. 2005. Intra-and Intersexual Selection for Multiple Traits in the Peacock (*Pavo cristatus*). Ethology, 111, 810-820.

Mallon, J. C., & Anderson, J. S. 2014. The functional and palaeoecological implications of tooth morphology and wear for the megaherbivorous dinosaurs from the Dinosaur Park Formation (upper Campanian) of Alberta, Canada. PloS one, 9, e98605.

Martin, L. D., Babiarz, J. P., Naples, V. L., & Hearst, J. 2000. Three ways to be a saber-toothed cat. Naturwissenschaften, 87, 41-44.

Martin, P., & Caro, T. M. 1985. On the functions of play and its role in behavioral development. Advances in the Study of Behaviour, 15, 59-103.

Maryanska, T., Chapman, R. E., & Weishampel, D. B. 2004. Pachycephalosauria. The dinosauria, 2, 464-477.

Matsukawa, M., Hamuro, T., Mizukami, T., & Fujii, S. 1997. First trackway evidence of gregarious dinosaurs from the Lower Cretaceous Tetori Group of eastern Toyama Prefecture, central Japan. Cretaceous Research, 18, 603-619.

Maxwell, W. D., & Ostrom, J. H. 1995. Taphonomy and paleobiological implications of *Tenontosaurus-Deinonychus* associations. Journal of Vertebrate Paleontology, 15, 707-712.

McAlpin, S., Duckett, P., & Stow, A. 2011. Lizards cooperatively tunnel to construct a long-term home for family members. PLoS One, 6, e19041.

McArthur, R. H., & Wilson, E. 0. 1967. The theory of island biogeography. Monographs in population biology, 1.

McDonald, J.H. 2014. Handbook of Biological Statistics, 3rd ed. Baltimore: Sparky House Publishing.

McCrea, R. T., Buckley, L. G., Farlow, J. O., Lockley, M. G., Currie, P. J., Matthews, N. A., & Pemberton, S. G. 2014. A 'terror of tyrannosaurs': the first trackways of tyrannosaurids and evidence of gregariousness and pathology in Tyrannosauridae. PloS One, 10, e0117606.

Meers, M. B. 2002. Maximum bite force and prey size of *Tyrannosaurus rex* and their relationships to the inference of feeding behaviour. Historical Biology, 16, 1-12.

Mehlum, F. 1998. Areas in Svalbard important for geese during the pre-breeding, breeding and post-breeding periods. Skrifter-Norsk Polarinstitutt, 200, 41-55.

Meng, Q., Liu, J., Varricchio, D. J., Huang, T., & Gao, C. 2004. Palaeontology: Parental care in an ornithischian dinosaur. Nature, 431, 145-146.

Michael, D. D., Whitlock, J. A., Smith, K. M., Fisher, D. C., & Wilson, J. A. 2013. Evolution of high tooth replacement rates in sauropod dinosaurs. PloS one, 8, e69235.

Mitchell, G., Van Sittert, S. J., & Skinner, J. D. 2009. Sexual selection is not the origin of long necks in giraffes. Journal of Zoology, 278, 281-286.

Miyashita, T., Tanke, D. H., & Currie, P. J. 2010. Variation in premaxillary tooth count and a developmental abnormality in a tyrannosaurid dinosaur. Acta Palaeontologica Polonica, 55, 635-643.

Miyashita, T., Arbour, V. M., Witmer, L. M., & Currie, P. J. 2011. The internal cranial morphology of an armoured dinosaur *Euoplocephalus* corroborated by X-ray computed tomographic reconstruction. Journal of anatomy, 219, 661-675.

Molnar, R.E. 1991.The cranial morphology of *Tyrannosaurus rex*. Paleontographica, 217, 137–176.

Molnar, R. 2005. Sexual selection and sexual dimorphism in theropods. In: Carpenter, K. (ed.) The carnivorous dinosaurs. Indiana University Press, Bloomington, Indiana, 284–312.

Mott, C. L., & Maret, T. J. 2011. Species-specific patterns of agonistic behavior among larvae of three syntopic species of ambystomatid salamanders. Copeia, 2011, 9-17.

Murphy, N. L., Carpenter, K., & Trexler, D. 2013. New Evidence for Predation by a Large Tyrannosaurid. In: Parish, M. Molnar, R. E., Currie P. J., Koppelhus, E. B. editors. Tyrannosaurid Palaeobiology. Indiana University Press, Bloomington, Indiana, 279-827.

Myers, T. S., & Fiorillo, A. R. 2009. Evidence for gregarious behavior and age segregation in sauropod dinosaurs. Palaeogeography, Palaeoclimatology, Palaeoecology, 274, 96-104.

Naroll, R. S., & Von Bertalanffy, L. 1956. The principle of allometry in biology and the social sciences. General Systems Yearbook, 1 (Part II), 76-89.

Ncube, S., & Ndagurwa, H. G. T. 2010. Influence of social upbringing on the activity pattern of captive lion *Panthera leo* cubs: Benefits of behavior enrichment. Current Zoology, 56, 389-394.

Neilson, J. D., & Geen, G. H. 1981. Enumeration of spawning salmon from spawner residence time and aerial counts. Transactions of the American Fisheries Society, 110, 554-556.

Norell, M. A., & Wheeler, W. C. 2003. Missing entry replacement data analysis: a replacement approach to dealing with missing data in paleontological and total evidence data sets. Journal of Vertebrate Paleontology, 23, 275-283.

Norell, M. A., Clark, J. M., Chiappe, L. M., & Dashzeveg, D. 1995. A nesting dinosaur. Nature, 378, 774-776.

Nunes, S., Muecke, E. M., Lancaster, L. T., Miller, N. A., Mueller, M. A., Muelhaus, J., & Castro, L. 2004. Functions and consequences of play behaviour in juvenile Belding's ground squirrels. Animal Behaviour, 68, 27-37.

O'Connor, J.A. & Lanyon, L.E. 1982 Influence of strain rate on adaptive bone remodelling. Journal of Biomechanics, 15, 767–781.

O'Gorman, E. J., & Hone, D. W. 2012. Body size distribution of the dinosaurs. PloS one, 7, e51925.

Oba, S., Sato, M. A., Takemasa, I., Monden, M., Matsubara, K. I., & Ishii, S. 2003. A Bayesian missing value estimation method for gene expression profile data. Bioinformatics, 19, 2088-2096.

Osborn, H.F. 1905. *Tyrannosaurus* and other Cretaceous carnivorous dinosaurs. Bulletin of the American Museum of Natural History, 21, 259–265.

Ősi, A., ApesteguÍa, S.M., & Kowalewski, M. 2010. Non-avian theropod dinosaurs from the early Late Cretaceous of Central Europe. Cretaceous Research, 31, 304-320.

Ostrom, J. H. 1969. Osteology of *Deinonychus antirrhopus*, an unusual theropod from the Lower Cretaceous of Montana (Vol. 30). Peabody Museum of Natural History, Yale University.

Ostrom, J. H. 1972. Were some dinosaurs gregarious? Palaeogeography, Palaeoclimatology, Palaeoecology, 11, 287-301.

Packer, C., & Pusey, A. E. 1982. Cooperation and competition within coalitions of male lions: kin selection or game theory? Nature, 296, 740-742.

Padian, K., & Lamm, E. T. 2013. Bone histology of fossil tetrapods: advancing methods, analysis, and interpretation. California: University of California Press.

Palagi, E. 2008. Sharing the motivation to play: the use of signals in adult bonobos. Animal Behaviour, 75, 887-896.

Paukner, A., & Suomi, S. J. 2008. Sex differences in play behaviour in juvenile tufted capuchin monkeys (*Cebus apella*). Primates, 49, 288-291.

Paul, G.S. 1988. Predatory dinosaurs of the world: a complete illustrated guide. New York: Simon and Schuster.

Payne, R. B. 1977. The ecology of brood parasitism in birds. Annual Review of Ecology and Systematics, 1-28.

Persons, W. S., & Currie, P. J. 2011a. The Tail of *Tyrannosaurus*: Reassessing the Size and Locomotive Importance of the M. caudofemoralis in Non-Avian Theropods. The Anatomical Record, 294, 119-131.

Persons, W. S., & Currie, P. J. 2011b. Dinosaur speed demon: the caudal musculature of *Carnotaurus sastrei* and implications for the evolution of South American abelisaurids. PloS one, 6, e25763.

Peterson, J. E., Henderson, M. D., Scherer, R. P., & Vittore, C. P. 2009. Face biting on a juvenile tyrannosaurid and behavioral implications. Palaios, 24, 780-784.

Peterson, J. E., & Vittore, C. P. 2012. Cranial pathologies in a specimen of *Pachycephalosaurus*. PloS one, 7, e36227.

Petti, F. M., Porchetti, S. D. O., Sacchi, E., & Nicosia, U. 2010. A new purported ankylosaur trackway in the Lower Cretaceous (lower Aptian) shallow-marine carbonate deposits of Puglia, southern Italy. Cretaceous Research, 31, 546-552.

Pitman, R. L., & Durban, J. W. 2012. Cooperative hunting behavior, prey selectivity and prey handling by pack ice killer whales (*Orcinus orca*), type B, in Antarctic Peninsula waters. Marine Mammal Science, 28, 16-36.

Polis, G. A. 1984. Age structure component of niche width and intraspecific resource partitioning: can age groups function as ecological species? American Naturalist, 541-564.

R Development Core Team, 2014. R: a language and environment for statistical computing, 3.1.2 ed. R Foundation for Statistical Computing, Vienna, Austria.

Ralrick, P.E., and Tanke, D.H. 2008. Comments on the quarry map and preliminary taphonomic observations of the *Pachyrhinosaurus* (Dinosauria: Ceratopsidae) bonebed at Pipestone Creek. In: A new Horned Dinosaur from an Upper Cretaceous Bone Bed in Alberta. In: Currie, P.J., Langston Jr., W., & Tanke, D.H. NRC Research Press, Ottawa, Ontario, 109–116.

Ramanujan, S. 1914. Modular equations and approximations to π. Quarterly Journal Math, 45, 350–372

Rayfield, E. J. 2004. Cranial mechanics and feeding in *Tyrannosaurus rex*. Proceedings of the Royal Society of London B: Biological Sciences, 271, 1451-1459.

Rayfield, E. J. 2005. Aspects of comparative cranial mechanics in the theropod dinosaurs *Coelophysis*, *Allosaurus* and *Tyrannosaurus*. Zoological Journal of the Linnean Society, 144, 309-316.

Reid, R.E.H .2012. How dinosaurs grew. In Brett-Surman, M. K., Holtz, T. R., & Farlow, J. O. (Eds.). The complete dinosaur. Indiana University Press: Bloomington, Indiana.

Reiserer, R. S., Schuett, G. W., & Earley, R. L. 2008. Dynamic aggregations of newborn sibling rattlesnakes exhibit stable thermoregulatory properties.Journal of Zoology, 274, 277-283.

Rinehart, L. F., Lucas, S. G., Heckert, A. B., Spielmann, J. A., & Celeskey, M. D. 2009. The Paleobiology of *Coelophysis bauri* (Cope) from the Upper Triassic (Apachean) Whitaker quarry, New Mexico, with detailed analysis of a single quarry block: Bulletin 45 (Vol. 45). New Mexico Museum of Natural History and Science.

Richardson, K. C. 1991. The bony casque of the Southern Cassowary Casuarius casuarius. Emu, 91, 56-58.

Richter, U., Mudroch, A., & Buckley, L. G. 2013. Isolated theropod teeth from the Kem Kem beds (early Cenomanian) near Taouz, Morocco. Paläontologische Zeitschrift, 87, 291-309.

Roach, B. T., & Brinkman, D. L. 2007. A reevaluation of cooperative pack hunting and gregariousness in Deinonychus antirrhopus and other nonavian theropod dinosaurs. Bulletin of the Peabody Museum of Natural History, 48, 103-138.

Roberts, E.M., Sampson, S.D., Deino, A.L., Bowring, S. 2013. The Kaiparowits Formation: a remarkable record of Late Cretaceous terrestrial environments, ecosystems and evolution in Western North America. In: Titus AL, Loewen MA (eds). At the Top of the Grand Staircase: The Late Cretaceous of Southern Utah Bloomington: Indiana University Press, 85–106.

Roberts, W. E. 1994. Explosive breeding aggregations and parachuting in a Neotropical frog, *Agalychnis saltator* (Hylidae). Journal of Herpetology, 193-199.

Rodríguez-de la Rosa, R. A. 2007. Hadrosaurian footprints from the late cretaceous Cerro Del Pueblo formation of Coahuila, Mexico. In 4th European Meeting on the Palaeontology and Stratigraphy of Latin America: Cuaderno del Museo Geominero (Vol. 8, 339-349).

Rothschild, B. M. 2013 Clawing their way to the top: Tyrannosaurid pathology and lifestyle. In: Parish, M. Molnar, R. E., Currie P. J., Koppelhus, E. B. editors. Tyrannosaurid Palaeobiology. Indiana University Press, Bloomington, Indiana, 210–221.

Rothschild, B. M. 2014. Unexpected behaviour in the Cretaceous: tooth-marked bones attributable to tyrannosaur play. Ethology Ecology & Evolution, Ahead of Print, 1-10.

Rothschild, B.M. & L.D. Martin. 2006. Skeletal impact of Disease. New Mexico Museum of Natural History, Albuquerque.

Russell, D. 1970. Tyrannosaurs from the Late Cretaceous of western Canada. National Museum Natural Sciences Publications in Palaeontology, 1, 1–34

Russell, D. A. 1972. Ostrich dinosaurs from the Late Cretaceous of western Canada. Canadian Journal of Earth Sciences, 9, 375-402.

Russell, D.A. & Seguin, R. 1982. Reconstruction of the small Cretaceous theropod *Stenonychosaurus inequalis* and a hypothetical dinosauroid. Syllogeus, 37, 1-43

Samman, T. 2013. Tyrannosaurid Craniocervical Mobility: A Preliminary Qualitative Assessment. In: Parish, M. Molnar, R. E., Currie P. J., Koppelhus, E. B. editors. Tyrannosaurid Palaeobiology. Indiana University Press, Bloomington, Indiana. 195-210.

Samman, T., Powell, G. L., Currie, P. J., & Hills, L. V. 2005. Morphometry of the teeth of western North American tyrannosaurids and its applicability to quantitative classification. *Acta Palaeontologica Polonica*, 50, 757-776.

Scannella, J. B., & Horner, J. R. 2010. *Torosaurus* Marsh, 1891, is *Triceratops* Marsh, 1889 (Ceratopsidae: Chasmosaurinae): synonymy through ontogeny. Journal of Vertebrate Paleontology, 30, 1157-1168.

Scannella, J. B., & Horner, J. R. 2011. 'Nedoceratops': An Example of a Transitional Morphology. PloS one, 6, e28705.

Schubert, B. W., & Ungar, P. S. 2005. Wear facets and enamel spalling in tyrannosaurid dinosaurs. Acta Palaeontologica Polonica, 50, 93-99.

Seber, G. A., & Lee, A. J. 2003. Linear regression analysis, 2nd Edition. Hoboken: John Wiley & Sons.

Seymour, R. S., Smith, S. L., White, C. R., Henderson, D. M., & Schwarz-Wings, D. 2011. Blood flow to long bones indicates activity metabolism in mammals, reptiles and dinosaurs. Proceedings of the Royal Society B: Biological Sciences, rspb20110968.

Shimada, M. 2006. Social object play among young Japanese macaques (*Macaca fuscata*) in Arashiyama, Japan. Primates, 47, 342-349.

Shine, R. 1990. Function and evolution of the frill of the frillneck lizard, *Chlamydosaurus kingii* (Sauria: Agamidae). Biological Journal of the Linnean Society, 40, 11-20.

Smith, N. D., Makovicky, P. J., Hammer, W. R., & Currie, P. J. 2007. Osteology of *Cryolophosaurus ellioti* (Dinosauria: Theropoda) from the Early Jurassic of Antarctica and implications for early theropod evolution. Zoological Journal of the Linnean Society, 151, 377-421.

Soares, D. 2002. Neurology: an ancient sensory organ in crocodilians. Nature, 417, 241-242.

Sockman, K. W., Salvante, K. G., Racke, D. M., Campbell, C. R., & Whitman, B. A. 2009. Song competition changes the brain and behaviour of a male songbird. The Journal of experimental biology, 212, 2411-2418.

Spottiswoode, C. N., Kilner, R. M., & Davies, N. B. 2012. In: Royle, N. J., Smiseth, P. T. & Kölliker, M. (eds.) Brood parasitism, Oxford University Press, Oxford, 226-356.

Starck, J. M., & Ricklefs, R. E. 1998. Patterns of development: the altricial-precocial spectrum. Oxford Ornithology Series, 8, 3-30.

Stevens, K. A. 2006. Binocular vision in theropod dinosaurs. Journal of Vertebrate Paleontology, 26, 321-330.

Stier, A. C., Geange, S. W., & Bolker, B. M. 2013. Predator density and competition modify the benefits of group formation in a shoaling reef fish. Oikos, 122, 171-178.

Strauss, R. E., Atanassov, M. N., & De Oliveira, J. A. 2003. Evaluation of the principal-component and expectation-maximization methods for estimating missing data in morphometric studies. Journal of Vertebrate Paleontology, 23, 284-296.

Sues, H.D. 1978. Functional morphology of the dome in pachycephalosaurid dinosaurs. Neues Jahrbuch für Geologie und Paläontologie, 1978, 459–472.

Tanke, D. H., & Currie, P. J. 1998. Head-biting behavior in theropod dinosaurs: paleopathological evidence. Gaia, 15, 167-184.

Thomson, K. S. 1985. Marginalia: Is paleontology going extinct? American Scientist, 570-572.

Thompson, K. V. 1998. Self assessment in juvenile play. Animal play: Evolutionary, comparative, and ecological perspective, 183-204.

Thurston, L. M. 2002. Homesite attendance as a measure of alloparental and parental care by gray wolves (*Canis lupus*) in northern Yellowstone National Park (Doctoral dissertation, Texas A & M University).

Torices, A., Bradley, G. & Currie, P. 2013. Ontogenetic variability in Upper Cretaceous theropod teeth, Journal of Vertebrate Palaeontology, Programs and Abstracts, 57.

Tschopp, E., Russo, J., & Dzemski, G. 2013. Retrodeformation as a test for the validity of phylogenetic characters: an example from diplodocid sauropod vertebrae. Palaeontologica Electronica, 16, 1-23.

Tütken, T., Pfretzschner, H. U., Vennemann, T. W., Sun, G., & Wang, Y. D. 2004. Paleobiology and skeletochronology of Jurassic dinosaurs: implications from the histology and oxygen isotope compositions of bones. Palaeogeography, Palaeoclimatology, Palaeoecology, 206, 217-238.

Ungar, P. S., & Grine, F. E. 1991. Incisor size and wear in Australopithecus africanus and Paranthropus robustus. Journal of Human Evolution, 20, 313-340.

Ungar, P. S., Krueger, K. L., Blumenschine, R. J., Njau, J., & Scott, R. S. 2012. Dental microwear texture analysis of hominins recovered by the Olduvai Landscape Paleoanthropology Project, 1995–2007. Journal of human evolution, 63, 429-437.

Van Valkenburgh, B. 1988. Incidence of tooth breakage among large, predatory mammals. American Naturalist, 291-302.

van Valkenburgh, B. 1996. Feeding behavior in free-ranging, large African carnivores. Journal of Mammalogy, 240-254.

van Valkenburgh, B. 2009. Costs of carnivory: tooth fracture in Pleistocene and Recent carnivorans. Biological Journal of the Linnean Society, 96, 68-81.

Varma, M., & Singh, G. 2008. Occlusion in Orthodontics. In: Singh, S. editor. Textbook of Orthodontics, 53-64. Jaypee Brothers Medical Publishers: New Dehli.

Varricchio, D. 2001. Gut Contents from a Cretaceous Tyrannosaurid: Implications for Theropod Dinosaur Digestive Tracts. Journal of Paleontology., 75, 401–406.

Varricchio, D. J., Horner, J. R., and Jackson, F. 2002. Embryos and eggs for the Cretaceous theropod dinosaur Troodon formosus. Journal of Vertebrate Paleontology 22,564-576.

Varricchio, D. J., Jackson, F., & Trueman, C. N. 1999. A nesting trace with eggs for the Cretaceous theropod dinosaur Troodon formosus. Journal of Vertebrate Paleontology, 19, 91-100.

Varricchio, D. J., Moore, J. R., Erickson, G. M., Norell, M. A., Jackson, F. D., & Borkowski, J. J. 2008a. Avian paternal care had dinosaur origin. Science, 322, 1826-1828.

Varricchio, D. J., Sereno, P. C., Xijin, Z., Lin, T., Wilson, J. A., & Lyon, G. H. 2008b. Mud-trapped herd captures evidence of distinctive dinosaur sociality. Acta Palaeontologica Polonica, 53, 567-578.

Visalberghi, E. 1988. Responsiveness to objects in two social groups of tufted capuchin monkeys (Cebus apella). American Journal of Primatology, 15, 349-360.

Weishampel, D. B. 1981. Acoustic analyses of potential vocalization in lambeosaurine dinosaurs (Reptilia: Ornithischia). Paleobiology, 252-261.

Weishampel, D. B. 1999. Dinosaurian cacophony. Bioscience, 150-159.

Weishampel, D.B., Fastovsky, D.E., Watabe, M., Barsbold, R., and Tsogtbaatar, K. 2000. New embryonic and hatchling dinosaur remains from the Late Cretaceous of Mongolia. Journal of Vertebrate Paleontology 20: 78A.

Werner, E. E., & Gilliam, J. F. 1984. The ontogenetic niche and species interactions in size-structured populations. Annual review of ecology and systematics, 393-425.

Werth, A. J. 2007. Adaptations of the cetacean hyolingual apparatus for aquatic feeding and thermoregulation. The Anatomical Record, 290, 546-568.

Whitlock, J. A. 2011. Inferences of diplodocoid (Sauropoda: Dinosauria) feeding behavior from snout shape and microwear analyses. PLoS One, 6, e18304.

Wiens, J. J. 2003a. Incomplete taxa, incomplete characters, and phylogenetic accuracy: is there a missing data problem? Journal of Vertebrate Paleontology, 23, 297-310.

Wiens, J. J. 2006. Missing data and the design of phylogenetic analyses. Journal of biomedical informatics, 39, 34-42.

Wiens,J.J., & Morrill, M. C. 2011. Missing data in phylogenetic analysis: reconciling results from simulations and empirical data. Systematic Biology, 60, syr025.

Wilkinson, D. M., & Ruxton, G. D. 2013. High C/N ratio (not low-energy content) of vegetation may have driven gigantism in sauropod dinosaurs and perhaps omnivory and/or endothermy in their juveniles. Functional Ecology, 27, 131-135.

Wilkinson, M. 2003. Missing entries and multiple trees: instability, relationships, and support in parsimony analysis. Journal of Vertebrate Paleontology, 23, 311-323.

Williams, V. S., Barrett, P. M., & Purnell, M. A. 2009. Quantitative analysis of dental microwear in hadrosaurid dinosaurs, and the implications for hypotheses of jaw mechanics and feeding. Proceedings of the National Academy of Sciences, 106, 11194-11199.

Wilson, E. O. 1980. Sociobiology: The abridged edition. Cambridge: Belknap Press.

Won, D. S., Park, C., IN, Y. J., & Park, H. M. 2004. A case of nutritional secondary hyperparathyroidism in a Siberian tiger cub. Journal of veterinary medical science, 66, 551-553.

Woodward, H. N., Rich, T. H., Chinsamy, A., & Vickers-Rich, P. 2011. Growth dynamics of Australia's polar dinosaurs. PloS one, 6, e23339.

Xu, X., Z. Zhou, X. Wang, X. Kuang, F. Zhang, and X. Du. 2003. Four winged dinosaurs from China. Nature 421, 335–340

Xu, X., Tan, Q., Wang, J., Zhao, X., & Tan, L. 2007. A gigantic bird-like dinosaur from the Late Cretaceous of China. Nature, 447, 844-847.

Young, M. T., Brusatte, S. L., Beatty, B. L., De Andrade, M. B., & Desojo, J. B. 2012. Tooth-On-Tooth Interlocking Occlusion Suggests Macrophagy in the Mesozoic Marine Crocodylomorph *Dakosaurus*. The Anatomical Record, 295, 1147-1158.

Zhao, Q., Benton, M. J., Xu, X., & Sander, P. M. 2013. Juvenile-only clusters and behaviour of the Early Cretaceous dinosaur *Psittacosaurus*. Acta Palaeontologica.

Appendix 1. Raw femoral circumference prediction Data Set

NP – Not Present for measurement

Gorgosaurus	Anteroposterior Diameter (mm)	Mediolateral Diameter (mm)	True Femoral Circumference (mm)
ROM 1247	95	NP	266
TMP 86.144.1	50.2	51.3	162
TMP 91.36.500	63.5	55	191
AMNH 5423	51	64	194
FMNH PR 2211	46	NP	136
Children's Museum 2001.89.1	90	98	296
NMC 350	92	132	385
TMP 94.12.602	110	NP	330

Albertosaurus	Anteroposterior Diameter (mm)	Mediolateral Diameter (mm)	True Femoral Circumference (mm)
MOR 553	103.7	107	339
AMNH 5255	50	NP	228
NMC 11315	66	112	314
TMP 1981.10.1	69	NP	305
TMP 1982.13.30	80	123.6	380
TMP 1986.64.1	63.5	81	241
TMP 1999.50.19	67	63	200
TMP 1999.50.52	NP	75	280
AMNH 5218ar	NP	102	303
AMNH 5218as	NP	97	318
UALVP (E.7, 2.1)	70	NP	170

Daspletosaurus	Anteroposterior Diameter (mm)	Mediolateral Diameter (mm)	True Femoral Circumference (mm)
NMMNH P-25049	57.5	NP	189
AMNH 5434	122	120	370
MOR 590	99	NP	335
TMP 2001.36.1	115	NP	382
UALVP 52981	98	90	320

Tarbosaurus	Anteroposterior Diameter (mm)	Mediolateral Diameter (mm)	True Femoral Circumference (mm)
CMMD1	85	87.5	273
MPC Japanese-Mongolian	55	67	203
MPC-D100/61	84	88	290
MPC-D100/63	95	140	410
MPC-D107/02	125	165	480
MPC-D107/05	57	69	209
MPC-D KID 584	97	82	330
PIN 551-2	110	NP	390
MPC-D PJC2012.48	NP	155	417
*Pohl specimen	64	63	215
ZPAL MgD-I/109	89	93	300

**Privately owned specimen measured with permission by the owner*

Tyrannosaurus	Anteroposterior Diameter (mm)	Mediolateral Diameter (mm)	True Femoral Circumference (mm)
BHI 3033 (Stan)	168	200	505
BHI 6230 "Wy-rex"	145	148	494
BMNH (Petey)	72	79.3	250
BM R8040 (AMNH 5881)	130	157	480
CM 9380 (AMNH 973) Type	180	156	534
DMNH 2827	135	160	510
FMNH PR2081 (Sue)	120	197	580
MOR 0009 "Hager"	112	150	469
MOR 0555 "Wankel"	146	165	520
MOR 1125 "B-rex"	NP	160	515
MOR 1128 "G-rex"	NP	186	580
RSM P2523.8 (Scotty)	123	199	570
TMP 81.6.1 (Black Beauty)	114	150	460
TMP 81.12.1, NMC 9950	150	180	495
USNM 6183	120	149	426
BM NH 2002.004.001	61.7	67	245

Gorgosaurus	CAP Predicted Circumferences (mm)	CML Predicted Circumferences (mm)	ELL Predicted Circumferences (mm)
ROM 1247	299.5	NP	NP
TMP 86.144.1	157.7	161.2	159.4
TMP 91.36.500	199.5	172.8	186.4
AMNH 5423	160	201	181
FMNH PR 2211	145	NP	NP
Children's Museum 2001.89.1	283	308	295
NMC 350	289	415	355
TMP 94.12.602	346	NP	NP

Albertosaurus	CAP Predicted Circumferences (mm)	CML Predicted Circumferences (mm)	ELL Predicted Circumferences (mm)
MOR 553	325.8	336.2	331.0
AMNH 5255	157	NP	NP
NMC 11315	207	352	284
TMP 1981.10.1	217	NP	NP
TMP 1982.13.30	251	388	324
TMP 1986.64.1	199.5	254.5	227.8
TMP 1999.50.19	210	198	204
TMP 1999.50.52	NP	236	NP
AMNH 5218ar	NP	320	NP
AMNH 5218as	NP	305	NP
UALVP (E.7, 2.1)	220	NP	NP

Daspletosaurus	CAP Predicted Circumferences (mm)	CML Predicted Circumferences (mm)	ELL Predicted Circumferences (mm)
NMMNH P-25049	180.6	NP	NP
AMNH 5434	383	377	380
MOR 590	311	NP	NP
TMP 2001.36.1	361	NP	NP
UALVP 52981	308	283	295

Tarbosaurus	CAP Predicted Circumferences (mm)	CML Predicted Circumferences (mm)	ELL Predicted Circumferences (mm)
CMMD1	267	275	271
MPC Japanese-Mongolian	173	211	192
MPC-D100/61	264	277	270
MPC-D100/63	299	440	373
MPC-D107/02	393	518	458
MPC-D107/05	179	217	198
MPC-D KID 584	305	258	282
PIN 551-2	346	NP	NP
MPC-D PJC2012.48	NP	487	NP
*Pohl specimen	201	198	200
ZPAL MgD-I/109	280	292	286

Tyrannosaurus	CAP Predicted Circumferences (mm)	CML Predicted Circumferences (mm)	ELL Predicted Circumferences (mm)
BHI 3033 (Stan)	528	628	579
BHI 6230 "Wy-rex"	456	465	460
BMNH (Petey)	226	249	238
BM R8040 (AMNH 5881)	408	493	452
CM 9380 (AMNH 973) Type	566	490	529
DMNH 2827	424	503	464
FMNH PR2081 (Sue)	377	619	505
MOR 0009 "Hager"	352	471	414
MOR 0555 "Wankel"	459	518	489
MOR 1125 "B-rex"	NP	503	NP
MOR 1128 "G-rex"	NP	584	NP
RSM P2523.8 (Scotty)	386	625	513
TMP 81.6.1 (Black Beauty)	358	471	417
TMP 81.12.1, NMC 9950	471	566	519
USNM 6183	377	468	424
BM NH 2002.004.001	193.8	210.5	202.3

Gorgosaurus	APR Predicted Circumferences (mm)	MLR Predicted Circumferences (mm)	ELLR Predictions (mm)
ROM 1247	329	NP	NP
TMP 86.144.1	186.6	160.9	167.5
TMP 91.36.500	230.0	171.9	188.8
AMNH 5423	189	199	195
FMNH PR 2211	173	NP	NP
Children's Museum 2001.89.1	314	299	309
NMC 350	320	398	379
TMP 94.12.602	375	NP	NP

Albertosaurus	APR Predicted Circumferences (mm)	MLR Predicted Circumferences (mm)	ELLR Predictions (mm)
MOR 553	355.6	331.7	342.0
AMNH 5255	186	NP	NP
NMC 11315	238	347	306
TMP 1981.10.1	248	NP	NP
TMP 1982.13.30	282	381	347
TMP 1986.64.1	230.0	254.1	244.0
TMP 1999.50.19	241	200	210
TMP 1999.50.52	NP	236	NP
AMNH 5218ar	NP	317	NP
AMNH 5218as	NP	302	NP
UALVP (E.7, 2.1)	251	NP	NP

Daspletosaurus	APR Predicted Circumferences (mm)	MLR Predicted Circumferences (mm)	ELLR Predictions (mm)
NMMNH P-25049	199.8	NP	NP
AMNH 5434	390	349	380
MOR 590	324	NP	NP
TMP 2001.36.1	370	NP	NP
UALVP 52981	321	265	293

Tarbosaurus	APR Predicted Circumferences (mm)	MLR Predicted Circumferences (mm)	ELLR Predictions (mm)
CMMD1	306	276.3	285.4
MPC Japanese-Mongolian	208	214	209
MPC-D100/61	302	278	286
MPC-D100/63	337	433	404
MPC-D107/02	430	507	490
MPC-D107/05	214	220	215
MPC-D KID 584	344	260	285
PIN 551-2	384	NP	NP
MPC-D PJC2012.48	NP	478	NP
*Pohl specimen	237	202	210
ZPAL MgD-I/109	318	293	302

Tyrannosaurus	APR Predicted Circumferences (mm)	MLR Predicted Circumferences (mm)	ELLR Predictions (mm)
BHI 3033 (Stan)	581	622	617
BHI 6230 "Wy-rex"	510	466	483
BMNH (Petey)	274	256.6	256.6
BM R8040 (AMNH 5881)	463	493	485
CM 9380 (AMNH 973) Type	618	490	535
DMNH 2827	479	502	497
FMNH PR2081 (Sue)	431	613	550
MOR 0009 "Hager"	406	472	450
MOR 0555 "Wankel"	513	517	520
MOR 1125 "B-rex"	NP	502	NP
MOR 1128 "G-rex"	NP	580	NP
RSM P2523.8 (Scotty)	722	619	558
TMP 81.6.1 (Black Beauty)	587	472	452
TMP 81.12.1, NMC 9950	732	562	556
USNM 6183	597	470	457
BM NH 2002.004.001	285	218	218.7

Gorgosaurus	CAP PPE (%)	CML PPE (%)	ELL PPE (%)
ROM 1247	10.9	NP	NP
TMP 86.144.1	2.7	0.5	1.6
TMP 91.36.500	4.3	10.5	2.5
AMNH 5423	21.1	3.5	7.1
FMNH PR 2211	5.9	NP	NP
Children's Museum 2001.89.1	4.7	3.9	0.2
NMC 350	33.2	7.2	8.6
TMP 94.12.602	4.5	NP	NP

Albertosaurus	CAP PPE (%)	CML PPE (%)	ELL PPE (%)
MOR 553	4.1	0.9	2.4
AMNH 5255	45.2	NP	NP
NMC 11315	51.4	10.8	10.5
TMP 1981.10.1	40.7	NP	NP
TMP 1982.13.30	51.2	2.1	17.5
TMP 1986.64.1	20.8	5.3	5.8
TMP 1999.50.19	5.0	1.1	2.1
TMP 1999.50.52	NP	18.8	NP
AMNH 5218ar	NP	5.4	NP
AMNH 5218as	NP	4.4	NP
UALVP (E.7, 2.1)	22.7	NP	NP

Daspletosaurus	CAP PPE (%)	CML PPE (%)	ELL PPE (%)
NMMNH P-25049	4.6	NP	NP
AMNH 5434	3.5	1.9	2.7
MOR 590	7.7	NP	NP
TMP 2001.36.1	5.7	NP	NP
UALVP 52981	3.9	13.2	8.3

Tarbosaurus	CAP PPE (%)	CML PPE (%)	ELL PPE (%)
CMMD1	2.2	0.7	0.8
MPC Japanese-Mongolian	17.5	3.6	5.7
MPC-D100/61	9.9	4.9	7.3
MPC-D100/63	37.4	6.8	10.1
MPC-D107/02	22.2	7.4	4.9
MPC-D107/05	16.7	3.6	5.4
MPC-D KID 584	8.3	28.1	17.2
PIN 551-2	12.9	NP	NP
MPC-D PJC2012.48	NP	14.4	NP
*Pohl specimen	6.9	8.6	7.8
ZPAL MgD-I/109	7.3	2.7	4.9

Tyrannosaurus	CAP PPE (%)	CML PPE (%)	ELL PPE (%)
BHI 3033 (Stan)	4.3	19.6	12.8
BHI 6230 "Wy-rex"	8.5	6.3	7.3
BMNH (Petey)	10.5	0.4	5.1
BM R8040 (AMNH 5881)	17.5	2.7	6.2
CM 9380 (AMNH 973) Type	5.6	9.0	1.1
DMNH 2827	20.3	1.5	9.9
FMNH PR2081 (Sue)	53.9	6.3	14.8
MOR 0009 "Hager"	33.3	0.5	13.4
MOR 0555 "Wankel"	13.4	0.3	6.4
MOR 1125 "B-rex"	NP	2.5	NP
MOR 1128 "G-rex"	NP	0.7	NP
RSM P2523.8 (Scotty)	47.5	8.8	11.1
TMP 81.6.1 (Black Beauty)	28.4	2.4	10.4
TMP 81.12.1, NMC 9950	5.0	12.5	4.7
USNM 6183	13	9	0.5
BM NH 2002.004.001	26.4	16.4	21.1

Gorgosaurus	MLR PPE (%)	APR PPE (%)	ELLR PPE (%)
ROM 1247	NP	19.1	NP
TMP 86.144.1	0.7	13.2	3.3
TMP 91.36.500	11.1	16.9	1.2
AMNH 5423	2.4	2.5	0.4
FMNH PR 2211	NP	21.2	NP
Children's Museum 2001.89.1	1.0	5.6	4.1
NMC 350	3.1	20.4	1.7
TMP 94.12.602	NP	11.9	NP

Albertosaurus	MLR PPE (%)	APR PPE (%)	ELLR PPE (%)
MOR 553	2.2	4.7	0.9
AMNH 5255	NP	22.6	NP
NMC 11315	9.4	31.9	2.6
TMP 1981.10.1	NP	23.2	NP
TMP 1982.13.30	0.2	34.6	9.5
TMP 1986.64.1	5.2	4.8	1.2
TMP 1999.50.19	0.1	17.1	4.8
TMP 1999.50.52	18.6	NP	NP
AMNH 5218ar	4.4	NP	NP
AMNH 5218as	5.3	NP	NP
UALVP (E.7, 2.1)	NP	32.2	NP

Daspletosaurus	MLR PPE (%)	APR PPE (%)	ELLR PPE (%)
NMMNH P-25049	NP	5.4	NP
AMNH 5434	6.1	5.1	2.5
MOR 590	NP	3.5	NP
TMP 2001.36.1	NP	3.3	NP
UALVP 52981	20.8	0.3	9.2

Tarbosaurus	MLR PPE (%)	APR PPE(%)	ELLR PPE (%)
CMMD1	1.2	10.6	4.4
MPC Japanese-Mongolian	5.1	2.2	2.7
MPC-D100/61	4.4	4.1	1.6
MPC-D100/63	5.3	21.6	1.6
MPC-D107/02	5.3	11.5	2.1
MPC-D107/05	5.0	2.4	2.9
MPC-D KID 584	27.1	3.9	15.8
PIN 551-2	NP	1.5	NP
MPC-D PJC2012.48	12.7	NP	NP
*Pohl specimen	6.6	9.4	2.3
ZPAL MgD-I/109	2.4	5.7	0.5

Tyrannosaurus	MLR PPE (%)	APR PPE (%)	ELLR PPE (%)
BHI 3033 (Stan)	18.8	13.1	18.2
BHI 6230 "Wy-rex"	6.0	3.2	2.3
BMNH (Petey)	2.6	8.7	2.6
BM R8040 (AMNH 5881)	2.7	3.7	1.1
CM 9380 (AMNH 973) Type	8.9	13.6	0.2
DMNH 2827	1.5	6.5	2.6
FMNH PR2081 (Sue)	5.4	34.5	5.4
MOR 0009 "Hager"	0.7	15.7	4.3
MOR 0555 "Wankel"	0.5	1.3	0.03
MOR 1125 "B-rex"	2.5	NP	NP
MOR 1128 "G-rex"	0.02	NP	NP
RSM P2523.8 (Scotty)	7.9	29.3	2.1
TMP 81.6.1 (Black Beauty)	2.6	11.7	1.8
TMP 81.12.1, NMC 9950	12.0	5.8	10.9
USNM 6183	9.2	1.2	6.8
BM NH 2002.004.001	12.2	2.6	12.0

Taxon	SEE of Anterior Posterior Circle Model Predictions (%)
Gorgosaurus	38.7
Albertosaurus	75.2
Daspletosaurus	16.7
Tarbosaurus	50.8
Tyrannosaurus	94.27

Standard Error Estimation for all CAP data: 68.1

Taxon	SEE of Mediolateral Circle Model Predictions (%)
Gorgosaurus	16.8
Albertosaurus	22.8
Daspletosaurus	26.8
Tarbosaurus	36.3
Tyrannosaurus	44.0

Standard Error Estimation for all CML data: 35.3

Taxon	SEE of Ellipse Model Predictions (%)
Gorgosaurus	14.9
Albertosaurus	29.4
Daspletosaurus	18.8
Tarbosaurus	24.3
Tyrannosaurus	43.8

Standard Error Estimation for all Ell Data: 33.1

Taxon	SEE of MLR Model Predictions (%)
Gorgosaurus	10.5
Albertosaurus	21.4
Daspletosaurus	41.8
Tarbosaurus	32.4
Tyrannosaurus	41.5

Standard Error Estimation for all MLR Data: 33.4

Taxon	SEE of APR Model Predictions (%)
Gorgosaurus	41.9
Albertosaurus	60.2
Daspletosaurus	12.5
Tarbosaurus	31.7
Tyrannosaurus	66.2

Standard Error Estimation for All APR Data: 50.6

Taxon	SEE of ELLR Model Predictions (%)
Gorgosaurus	6.9
Albertosaurus	16.0
Daspletosaurus	20.3
Tarbosaurus	16.5
Tyrannosaurus	37.6

Standard Error Estimation for All ELLR Data: 26.5

Appendix 2. Regression Data for APR, MLR and ELLR Models

Albertosaurus	True Ap Diameter (mm)	Weighted AP Diameter (mm)	Log Transormed Weighted Ap Diameter (mm)	True Circum-ference (mm)	Weighted True Circum-ference (mm)	Log 10 Weighted True AP Circumference (mm)	Predicted Log Weighted Circumferences APRWL (mm)	Backtransformed predicted APR weighted circumferences (mm)	Re-weighted, backtransformed APR predicted circumferences (mm)
MOR 553	103.7	13.0	1.1	339	42.4	1.6	1.6	44.4	355.6
AMNH 5255	50	6.3	0.8	228	28.5	1.5	1.4	23.2	186
NMC 11315	66	8.3	0.9	314	39.3	1.6	1.5	29.7	238
TMP 1981.10.1	69	8.6	0.9	305	38.1	1.6	1.5	30.9	247
TMP 1982.13.30	80	10	1	380	47.5	1.7	1.5	35.3	282
TMP 1986.64.1	63.5	7.9	0.9	241	30.1	1.5	1.5	28.7	230.0
TMP 1999.50.19	67	8.4	0.9	200	25	1.4	1.5	30.1	241
UALVP (E.7, 2.1)	70	8.8	0.9	170	21.3	1.3	1.5	31.3	250

Daspletosaurus	True AP Diameter (mm)	Weighted AP Diameter (mm)	Log Transormed Weighted Ap Diameter (mm)	True Circum-ference (mm)	Weighted True Circum-ference (mm)	Log 10 Weighted True AP Circumference (mm)	Predicted Log Weighted Circumferences APRWL (mm)	Backtransformed predicted APR weighted circumferences (mm)	Re-weighted, backtransformed APR predicted circumferences (mm)
NMMNH P-25049	57.5	11.5	1.1	189	37.8	1.6	1.6	40.0	199.8
AMNH 5434	122	24.4	1.4	370	74	1.9	1.9	78.0	389
MOR 590	99	19.8	1.3	335	67	1.8	1.8	64.8	323
TMP 2001.36.1	115	23	1.4	382	76.4	1.9	1.9	74.0	369
UALVP 52981	98	19.6	1.3	320	64	1.8	1.8	64.2	320

Tarbosaurus	True Ap Diameter (mm)	Weighted AP Diameter (mm)	Log Transormed Weighted Ap Diameter (mm)	True Circum-ference (mm)	Weighted True Circum-ference (mm)	Log 10 Weighted True AP Circumference (mm)	Predicted Log Weighted Circumferences APRWL (mm)	Backtransformed predicted APR weighted circumferences (mm)	Re-weighted, backtransformed APR predicted circumferences (mm)
CMMD1	85	8.5	0.9	273	27.3	1.4	1.5	30.5	305
MPC Japanese-Mongolian	55	5.5	0.7	203	20.3	1.3	1.3	20.7	207
MPC-D100/61	84	8.4	0.9	290	29	1.5	1.5	30.2	302
MPC-D100/63	95	9.5	1.0	410	41	1.6	1.5	33.7	337
MPC-D107/02	125	12.5	1.1	480	48	1.7	1.6	43.0	430
MPC-D107/05	57	5.7	0.8	209	20.9	1.3	1.3	21.4	214
MPC-D KID 584	97	9.7	1.0	330	33	1.5	1.5	34.4	343
PIN 551-2	110	11	1.0	390	39	1.6	1.6	38.4	384
*Pohl specimen	64	6.4	0.8	215	21.5	1.3	1.4	23.7	237
ZPAL MgD-I/109	89	8.9	0.9	300	30	1.5	1.5	31.8	318

*Privately owned specimen measured with permission by the owner

Tyrannosaurus	True Ap Diameter (mm)	Weighted AP Diameter (mm)	Log Transormed Weighted APDiameter (mm)	True Circum-ference (mm)	Weighted True Circum-ference (mm)	Log 10 Weighted True AP Circumference (mm)	Predicted Log Weighted Circumferences APRWL (mm)	Backtransformed predicted APR weighted circumferences (mm)	Re-weighted, backtransformed APR predicted circumferences (mm)
BHI 3033 (Stan)	168	11.9	1.1	505	35.9	1.6	1.6	41.3	581
BHI 6230 "Wy-rex"	145	10.3	1.0	494	35.1	1.5	1.6	36.2	510
BMNH (Petey)	72	5.1	0.7	250	17.8	1.2	1.3	19.4	273
BM R8040 (AMNH 5881)	130	9.2	1.0	480	34.1	1.5	1.5	32.9	462
CM 9380 (AMNH 973) Type	180	12.8	1.1	534	37.9	1.6	1.6	43.9	618
DMNH 2827	135	9.6	1.0	510	36.2	1.6	1.5	34.0	478
FMNH PR2081 (Sue)	120	8.5	0.9	580	41.2	1.6	1.5	30.6	431
MOR 0009 "Hager"	112	8.0	0.9	469	33.3	1.5	1.5	28.8	405
MOR 0555 "Wankel"	146	10.4	1.1	520	36.9	1.6	1.6	36.4	513
RSM P2523.8 (Scotty)	123	8.7	0.9	570	40.5	1.6	1.5	31.3	440
TMP 81.6.1 (Black Beauty)	114	8.1	0.9	460	32.7	1.5	1.5	29.2	411

TMP 81.12.1, NMC 9950	150	10.7	1.0	495	35.1	1.5	1.6	37.3	525
USNM 6183	120	8.5	0.9	426	30.2	1.5	1.5	30.6	431
BM NH 2002.004.001	61.7	4.4	0.6	245	17.4	1.2	1.2	16.9	238

Gorgosaurus	True ML Diameter (mm)	Weighted ML Diameter (mm)	Log Transormed Weighted ML Diameter (mm)	True Circum-ference (mm)	Weighted Circum-ference (mm)	Log 10 Weighted True ML Circumference (mm)	Predicted Log 10 Weighted Circumference MLRW (mm)	Backtransformed MLR Predicted Weighted Circumferences (mm)	Re-weighted backtransformed MLR predicted Circumferences (mm)
TMP 86.144.1	51.3	10.3	1.0	162	32.4	1.5	1.5	32.2	160.9
TMP 91.36.500	55	11	1.0	191	38.2	1.6	1.5	34.4	171
AMNH 5423	64	12.8	1.1	194	38.8	1.6	1.6	39.8	198
Children's Museum 2001.89.1	98	19.6	1.3	296	59.2	1.8	1.8	59.8	298
NMC 350	132	26.4	1.4	385	77	1.9	1.9	79.5	397

Albertosaurus	True ML Diameter (mm)	Weighted ML Diameter (mm)	Log Transormed Weighted ML Diameter (mm)	True Circum-ference (mm)	Weighted Circum-ference (mm)	Log 10 Weighted True ML Circumferenc e (mm)	Predicted Log 10 Weighted Circumferenc e MLRW (mm)	Backtransformed MLR Predicted Weighted Circumferences (mm)	Re-weighted backtransformed MLR predicted Circumferences (mm)
MOR 553	107	13.4	1.1	339	42.4	1.6	1.6	41.5	331
NMC 11315	112	14	1.1	314	39.3	1.6	1.6	43.3	346
TMP 1982.13.30	123.6	15.5	1.2	380	47.5	1.7	1.7	47.6	380.8
TMP 1986.64.1	81	10.1	1.0	241	30.1	1.5	1.5	31.8	254
TMP 1999.50.19	63	7.9	0.9	200	25	1.4	1.4	25.0	199
TMP 1999.50.52	75	9.4	1.0	280	35	1.5	1.5	29.5	236
AMNH 5218ar	102	12.8	1.1	303	37.9	1.6	1.6	39.6	316
AMNH 5218as	97	12.1	1.1	318	39.8	1.6	1.6	37.7	302

Daspletosaurus	True ML Diameter (mm)	Weighted ML Diameter (mm)	Log Transormed Weighted ML Diameter (mm)	True Circum-ference (mm)	Weighted Circum-ference (mm)	Log 10 Weighted True ML Circumferenc e (mm)	Predicted Log 10 Weighted Circumferenc e MLRW (mm)	Backtransformed MLR Predicted Weighted Circumferences (mm)	Re-weighted backtransforme d MLR predicted Circumferences (mm)
AMNH 5434	120	60	1.8	370	185	2.3	2.2	174.4	349
UALVP 52981	90	45	1.7	320	160	2.2	2.1	132.4	265

Tarbosaurus	True ML Diameter (mm)	Weighted ML Diameter (mm)	Log Transormed Weighted ML Diameter (mm)	True Circum-ference (mm)	Weighted Circum-ference (mm)	Log 10 Weighted True ML Circumferenc e (mm)	Predicted Log 10 Weighted Circumferenc e MLRW (mm)	Backtransformed MLR Predicted Weighted Circumferences (mm)	Re-weighted backtransformed MLR predicted Circumferences (mm)
CMMD1	87.5	8.8	0.9	273	27.3	1.4	1.4	27.6	276.3
MPC Japanese-Mongolian	67	6.7	0.8	203	20.3	1.3	1.3	21.4	214
MPC-D100/61	88	8.8	0.9	290	29	1.5	1.4	27.8	278
MPC-D100/63	140	14	1.1	410	41	1.6	1.6	43.3	433
MPC-D107/02	165	16.5	1.2	480	48	1.7	1.7	50.7	507
MPC-D107/05	69	6.9	0.8	209	20.9	1.3	1.3	22.0	220
MPC-D KID 584	82	8.2	0.9	330	33	1.5	1.4	26.0	260

MPC-D PJC2012.48	155	15.5	1.2	417	41.7	1.6	1.7	47.7	478
*Pohl specimen	63	6.3	0.8	215	21.5	1.3	1.3	20.2	202
ZPAL MgD-I/109	93	9.3	1.0	300	30	1.5	1.5	29.3	293

*Privately owned specimen measured with permission by the owner

Tyrannosaurus	True ML Diameter (mm)	Weighted ML Diameter (mm)	Log Transormed Weighted ML Diameter (mm)	True Circum-ference (mm)	Weighted Circum-ference (mm)	Log 10 Weighted True ML Circumference (mm)	Predicted Log 10 Weighted Circumference MLRW (mm)	Backtransformed MLR Predicted Weighted Circumferences (mm)	Re-weighted backtransformed MLR predicted Circumferences (mm)
BHI 3033 (Stan)	200	12.5	1.1	505	31.6	1.5	1.6	38.9	622
BHI 6230 "Wy-rex"	148	9.3	1.0	494	30.9	1.5	1.5	29.1	466
BMNH (Petey)	79.3	5.0	0.7	250	15.6	1.2	1.2	16.0	257
BM R8040 (AMNH 5881)	157	9.8	1.0	480	30	1.5	1.5	30.8	493
CM 9380 (AMNH 973) Type	156	9.8	1.0	534	33.4	1.5	1.5	30.6	490
DMNH 2827	160	10	1	510	31.9	1.5	1.5	31.4	502

FMNH PR2081 (Sue)	197	12.3	1.1	580	36.3	1.6	1.6	38.3	613
MOR 0009 "Hager"	150	9.4	1.0	469	29.3	1.5	1.5	29.5	472
MOR 0555 "Wankel"	165	10.3	1.0	520	32.5	1.5	1.5	32.3	517
MOR 1125 "B-rex"	160	10	1	515	32.2	1.5	1.5	31.4	502
MOR 1128 "G-rex"	186	11.6	1.1	580	36.3	1.6	1.6	36.3	580
RSM P2523.8 (Scotty)	199	12.4	1.1	570	35.6	1.6	1.6	38.7	619
TMP 81.6.1 (Black Beauty)	150	9.4	1.0	460	28.8	1.5	1.5	29.5	472
TMP 81.12.1, NMC 9950	180	11.3	1.1	495	30.9	1.5	1.5	35.1	562
USNM 6183	149	9.3	1.0	426	26.6	1.4	1.5	29.3	469
BM NH 2002.004.001	67	4.2	0.6	245	15.3	1.2	1.1	13.6	218

Gorgosaurus	TMP 86.144.1	TMP 91.36.500	AMNH 5423	Children's Museum 2001.89.1	NMC 350
AP for ELLRWL (mm)	50.2	63.5	51	90	92
Weighted AP (mm)	10.0	12.7	10.2	18	18.4
Log weighted AP (mm)	1.0	1.1	1.0	1.3	1.3
ML for ELLRWL (mm)	51.3	55	64	98	132
Weighted ML (mm)	10.3	11	12.8	19.6	26.4
Log Weighted ML (mm)	1.0	1.0	1.1	1.3	1.4
True Circ. (mm)	162	191	194	296	385
Weighted True Circumferences (mm)	32.4	38.2	38.8	59.2	77
Log Weighted True Circumference (mm)	1.5	1.6	1.6	1.8	1.9
Predicted Log Weighted True Circumference (mm)	1.5	1.6	1.6	1.8	1.9
Backtransformed weighted prediction (mm)	33.5	37.8	39.0	61.7	75.7
Backtransformed, re-weighted predictions (mm)	167.5	188.8	195	309	379

Albertosaurus	MOR 553	NMC 11315	TMP 1982.13.30	TMP 1986.64.1	TMP 1999.50.19
AP for ELLRWL (mm)	103.7	66	80	63.5	67
Weighted AP (mm)	20.7	13.2	16	12.7	13.4
Log weighted AP (mm)	1.3	1.1	1.2	1.1	1.1
ML for ELLRWL (mm)	107	112	123.6	81	63
Weighted ML (mm)	21.4	22.4	24.7	16.2	12.6
Log Weighted ML (mm)	1.3	1.4	1.4	1.2	1.1
True Circ (mm)	339	314	380	241	200
Weighted True Circumferences (mm)	67.8	62.8	76	48.2	40
Log Weighted True Circumference (mm)	1.8	1.8	1.9	1.7	1.6
Predicted Log Weighted True Circumference (mm)	1.8	1.8	1.8	1.7	1.6
Backtransformed weighted prediction (mm)	68.4	61.2	69.4	48.8	42.0
Backtransformed, re-weighted predictions (mm)	342.0	306	347	244.0	210

Daspletosaurus	AMNH 5434	UALVP 52981
AP for ELLRWL (mm)	122	98
Weighted AP (mm)	61	49
Log weighted AP (mm)	1.8	1.7
ML for ELLRWL (mm)	120	90
Weighted ML (mm)	60	45
Log Weighted ML (mm)	1.8	1.7
True Circ (mm)	370	320
Weighted True Circumferences (mm)	185	160
Log Weighted True Circumference (mm)	2.3	2.2
Predicted Log Weighted True Circumference (mm)	2.3	2.2
Backtransformed weighted prediction (mm)	189.8	146.5
Backtransformed, re-weighted predictions (mm)	380	293

Tarbosaurus	CMMD1	MPC Japanese-Mongolian	MPC-D100/61	MPC-D100/63	MPC-D107/02	MPC-D107/05	MPC-D KID 584	*Pohl specimen	ZPAL MgD-I/109
AP for ELLRWL (mm)	85	55	84	95	125	57	97	64	89
Weighted AP (mm)	9.4	6.1	9.2	10.5	13.8	6.3	10.7	7.0	9.8
Log weighted AP (mm)	1.0	0.8	1.0	1.0	1.1	0.8	1.0	0.8	1.0
ML for ELLRWL (mm)	87.5	67	88	140	165	69	82	63	93
Weighted ML (mm)	9.6	7.4	9.7	15.4	18.2	7.6	9.0	6.9	10.2
Log Weighted ML (mm)	1.0	0.9	1.0	1.2	1.3	0.9	1.0	0.8	1.0
True Circ (mm)	273	203	290	410	480	209	330	215	300
Weighted True Circumferences (mm)	30.0	22.3	31.9	45.1	52.8	23.0	36.3	23.7	33
Log Weighted True Circumference	1.5	1.3	1.5	1.7	1.7	1.4	1.6	1.4	1.5

(mm)									
Predicted Log Weighted True Circumference (mm)	1.5	1.4	1.5	1.6	1.7	1.4	1.5	1.4	1.5
Backtransformed weighted prediction (mm)	31.4	23.0	31.4	44.4	53.9	23.7	31.3	23.1	33.2
Backtransformed, re-weighted predictions (mm)	286	209	286	404	490	215	285	210	301.5

Tyrannosaurus	BHI 3033 (Stan)	BHI 6230 "Wy-rex"	BMNH (Petey)	BM R8040 (AMNH 5881)	CM 9380 (AMNH 973) Type	DMNH 2827	FMNH PR2081 (Sue)
AP for ELLRWL (mm)	168	145	72	130	180	135	120
Weighted AP (mm)	12.0	10.4	5.1	9.3	12.9	9.6	8.6
Log weighted AP (mm)	1.1	1.0	0.7	1.0	1.1	1.0	0.9
ML for ELLRWL (mm)	200	148	79.3	157	156	160	197
Weighted ML (mm)	14.3	10.6	5.7	11.2	11.1	11.4	14.1
Log wieghted ML (mm)	1.2	1.0	0.8	1.0	1.0	1.1	1.1
True Circ (mm)	505	494	250	480	534	510	580
Weighted True Circumferences (mm)	36.1	35.3	17.9	34.3	38.1	36.4	41.4
Log Weighted True Circumference (mm)	1.6	1.5	1.3	1.5	1.6	1.6	1.6
Predicted Log Weighted True Circumference (mm)	1.6	1.5	1.3	1.5	1.6	1.6	1.6
Backtransformed weighted prediction (mm)	44.1	34.5	18.3	34.7	38.2	35.5	39.3
Backtransformed, re-weighted predictions (mm)	617	483	257	485	535	497	550

Tyrannosaurus (contd.)	MOR 0009 "Hager"	MOR 0555 "Wankel"	RSM P2523.8 (Scotty)	TMP 81.6.1 (Black Beauty)	TMP 81.12.1, NMC 9950	USNM 6183	BM NH 2002.004.001
AP for ELLRWL (mm)	112	146	123	114	150	120	61.7
Weighted AP (mm)	8.0	10.4	8.8	8.1	10.7	8.6	4.4
Log weighted AP (mm)	0.9	1.0	0.9	0.9	1.0	0.9	0.6
ML for ELLRWL (mm)	150	165	199	150	180	149	67
Weighted ML (mm)	10.7	11.8	14.2	10.7	12.9	10.6	4.8
Log wieghted ML (mm)	1.0	1.1	1.2	1.0	1.1	1.0	0.7
True Circ (mm)	469	520	570	460	495	426	245
Weighted True Circumferences (mm)	33.5	37.1	40.7	32.8	35.3	30.4	17.5
Log Weighted True Circumference (mm)	1.5	1.6	1.6	1.5	1.5	1.5	1.2
Predicted Log Weighted True Circumference (mm)	1.5	1.6	1.6	1.5	1.6	1.5	1.2
Backtransformed weighted prediction (mm)	32.1	37.1	39.9	32.3	39.7	32.6	15.6
Backtransformed, re-weighted predictions (mm)	450	520	558	452	556	457	218.7

Appendix 3 PPE and SEE t tests

Models tested	p-value	t-stat	q-value (α=0.05) (Benjamini & Hochberg, 1995)	Significant Difference?
CAP vs. CML	0.0001	4.2358	0.0004	Yes
CML vs. ELL	0.54	0.6137	0.58	No
CAP vs. ELL	0.0004	3.7180	0.0012	Yes
APR vs. MLR	0.0042	2.9407	0.011	Yes
APR vs. CML	0.0062	2.8090	0.013	Yes
APR vs. ELL	0.024	2.3060	0.04	*No
MLR vs. CAP	0.0001	4.3287	0.0004	Yes
MLR vs. ELL	0.4314	0.07911	0.50	No
MLR vs. CML	0.8650	0.1705	0.8651	No
APR vs. CAP	0.0370	2.1185	0.0555	*No
APR vs. ELLR	0.0001	4.1336	0.0004	Yes
MLR vs. ELLR	0.0886	1.7253	0.1106	No
ELLR vs. CAP	0.0001	4.9607	0.0004	Yes

ELLR vs. CML	0.0604	1.90670	0.0824	No
ELLR vs. ELL	0.0068	2.7918	0.0126	Yes

Table A2. Summary statistics for two tailed student t-tests between SEEE values of six predictive models

Models tested	p-value	t-stat	q-value (α=0.05) (Benjamini & Hochberg, 1995)	Significant Difference?
CAP vs. CML	0.1116	1.7879	0.3702	No
CML vs. ELL	0.6715	0.4401	0.7380	No
CAP vs. ELL	0.0814	1.9926	0.3702	No
APR vs. MLR	0.2895	1.1342	0.4343	No
APR vs. CML	0.2599	1.2125	0.4332	No
APR vs. ELL	0.1759	1.4847	0.4211	No
MLR vs. CAP	0.1234	1.7219	0.3702	No
MLR vs. ELL	0.6888	0.4154	0.7380	No
MLR vs. CML	0.9811	0.0245	0.9811	No
APR vs. CAP	0.4710	0.7565	0.5895	No
ELLR vs. CAP	0.0393	2.4601	0.3702	Yes
ELLR vs. CML	0.1965	1.4091	0.4211	No
ELLR vs. ELL	0.3688	0.9525	0.5029	No
ELLR vs. APR	0.0685	2.1039	0.3702	No
ELLR vs. MLR	0.2374	1.2770	0.4332	No

Appendix 4: Previously published distinguishing characteristics between *Albertosaurus* and *Gorgosaurus*

Gorgosaurus libratus (After Holtz Jr. 2001)	*Albertosaurus sarcophagus* (After Holtz Jr. 2001)
Nasal caudal suture: lateral projections extend further caudally than medial projections (48)	Nasal caudal suture: medial projections extend as far or further caudally than lateral projections (48)
Lacrimal horn with rostrodorsal orientation (52)	Lacrimal horn with dorsal orientation (52)
Suborbital prong of postorbital absent (57)	Suborbital prong of postorbital prominent (57)
Caudal orientation of the occipital region (65)	Caudoventral orientation of the occipital region (65)
Large basitubera compared to ventral ends of basipterygoid processes (67)	Reduced basitubera compared to ventral ends of basipterygoid processes (67)
One foramina on ventral surface of palatine (71)	2 or more foramina on ventral surface of palatine (71)
First maxillary tooth incisiform in shape (rostral end of maxilla) (78)	No incisiform maxillary teeth (78)
Distal end of scapula not expanded (82)	Distal end of the scapula greatly expanded cranially and caudally to twice the midshaft width (82)
Phalanx I of manual digit I subequal to metacarpal II (85)	Phalanx I of manual digit longer than metacarpal II (85)
* Premaxillary fenestra is rostrodorsal to maxillary fenestra in adults (93)	Premaxillary fenestra is rostral to maxillary fenestra or absent (93)
*Postorbital & lacrimal contact below the orbit in adults; the orbit is more circular (dorsoventral axis not twice or more than rostrocaudal axis) than in other large theropods (94) (Discounted as individual variation in Currie et al., 2003)	Postorbital and lacrimal do not contact below the orbit in adults (94)
Rostral margin of postorbital suborbital prong is smooth or prong is absent (95)	Rostral margin of postorbital suborbital prong is jagged (95)
Basisphenoid foramina in sphenoidal sinus lies within same surface (96)	Each basisphenoid foramina in sphenoidal sinus lies within a distinct fossa (96)

Table 1. Distinguishing characteristics between *Albertosaurus sarcophagus* and *Gorgosaurus libratus* after Holtz Jr. (2001) *Autapomorphies in adults

Gorgosaurus libratus (After Currie et al. 2003)	*Albertosaurus sarcophagus* (After Currie et al., 2003)
Basisphenoid foramina in sphenoidal sinus	Each basisphenoid foramina in sphenoidal sinus

(basisphenoidal recess) lies within same surface (6)	(basisphenoidal recess) lies within a distinct fossa (6)
Basisphenoid, recess oriented ventrally (7)	Basisphenoid, recess oriented posteroventrally (7)
Braincase, rectangle defined by positions of both basal tubera and both basipterygoid processes anteroposteriorly longer than wide (8)	Braincase, rectangle defined by positions of both basal tubera and both basipterygoid processes anteroposteriorly longer than wide mediolaterally wider than long (8)
Nasal, posterior suture shape- lateral projections extend further posteriorly than medial projections (40)	Nasal, posterior suture shape- medial projection extends as far or further posteriorly than lateral projections (40)
Skull, occipital region faces posteriorly (63)	Skull, occipital region faces posteroventrally (63)

Table 2. Distinguishing characteristics between *Albertosaurus sarcophagus* and *Gorgosaurus libratus* after Currie et al., (2003)

Gorgosaurus libratus (After Currie 2003b)	*Albertosaurus sarcophagus* (After Currie 2003b)
Dinosaur Park Formation, Late Campanian	Horseshoe Canyon Formation, Maastrichtian
Adults Less Robust	Adults, more robust
Less numerous, deeper pits in the ventral surface of the maxillary palatal shelves to accommodate the tips of the dentary teeth (Along with all other tyrannosaurids).	More numerous, deeper pits in the ventral surface of the maxillary palatal shelves to accommodate the tips of the dentary teeth.
Occipital condyle oriented less ventrally than Albertosaurus.	Occipital condyle oriented more ventrally than in Gorgosaurus, though not as much as in other tyrannosaurids
The braincase box is mediolaterally longer than anteroposteriorly wide.	The braincase box is mediolaterally wider than anteroposteriorly long.
Nasal frontal suture less complex, paired midline processes of nasals taper, and do not extend further backwards than postorbital process of nasal.	Nasal frontal suture is more complex than Gorgosaurus and the paired midline processes of the nasals expand posteriorly (rather than taper) and extend farther backwards than the postorbital process of the nasal
The prefrontal and lacrimal have more vertical contacts with the frontal , the lacrimal plugs into a socket in the anterior face of the frontal as in *Daspletosaurus*	Prefrontal has very limited dorsal exposure and lacrimal does not plug into a socket in the frontal.
Does not have angular suture between exoccipital and basioccipital in the occipital	Unlike other Tyrannosaurids, has an angular suture between exoccipital and basioccipital in

condoyle.	the occipital condoyle.

Table 3. Distinguishing characteristics between *Albertosaurus sarcophagus* and *Gorgosaurus libratus* after Currie (2003b)

Gorgosaurus libratus (After Loewen et al. 2013)	*Albertosaurus sarcophagus* (After Loewen et al. 2013) Tyrant Dinosaur Evolution Supporting Information (pg53)
Lacrimal vacuity height to length ratio- tall, greater than 1.1 (76)	Lacrimal vacuity height to length ratio- short, less than 0.9 (76)
Jugal, maxillary process dorsoventral depth is- shallow, not expanded relative to suborbital portion of the bone (135)	Jugal, maxillary process dorsoventral depth is- deep, expanded relative to suborbital portion of the bone (135)
Dorsal process of supraoccipital form of dorsal surface is flat or peaked (165)	Dorsal process of supraoccipital form of dorsal surface is forked (165)
Quadrate: Oval fossa on medial surface of pterygoid wing is- ? (160)	- Quadrate: Oval fossa on medial surface of pterygoid wing is present and shallow (160)
Basioccipital, ventral surface across basal tubera & basisphenoid oriented nearly horizontally (195)	Basioccipital , ventral surface across basal tubera & basisphenoid oriented caudoventrally (195)
Parabasisphenoid, orientation of division of basisphenoid recess is divided by a 'Y' shaped strut of bone forming three processes (200)	Parabasisphenoid, orientation of division of basisphenoid recess is divided by a single midline strut into two laterally separate chambers (200)
Palatine, position of the posterior edge of the posterior pneumatic recess compared to the posterior edge of the dorsal process- ? (217)	palatine, position of the posterior edge of the posterior pneumatic recess compared to the posterior edge of the dorsal process- ? (217)
Ectopterygoid, surface posteriorly adjacent to external opening of pneumatic recess form is flat; recess grades smoothly into the floor of the lateral temporal fenestra (=subtemporal fenestra) (227)	Ectopterygoid, surface posteriorly adjacent to external opening of pneumatic recess form is a lip; the recess is separated from the lateral temporal fenestra (=subtemporal fenestra) (227)
Supradentary & coronoid ossifications form of contact at their zone of fusion: ? (257)	Supradentary & coronoid ossifications form of contact at their zone of fusion: ? (257)
Post Cranial	
Sacral ribs, position of rib attachment for ribs on individual sacrals- ? (344)	Sacral ribs, position of rib attachment for ribs on individual sacrals- span centrum & neural arch (344)
Sacral ribs, position of ribs on sacrum: ? (343)	Sacral ribs, position of ribs on sacrum- limited to a single sacral (343)

Sacral vertebrate, fenestrae between fused neural spines: ? (342)	Sacral vertebrate, fenestrae between fused neural spines: spines fused but fenestrae absent (342)
Cervical vertebrae, neural spine anterioposterior minimum width: wide, ½ or more than the length of the centrum (323)	Cervical vertebrae, neural spine anterioposterior minimum width: narrow, less than ½ the length of the centrum (323)
Axis, pneumatic foramina & fossae on each side of the anterior ridge on the neural spine: ? (312)	Axis, pneumatic foramina & fossae on each side of the anterior ridge on the neural spine present (312)
Axis, epipophyses, posterior extent: large, rugose flange that extends posterior to postzygapophysis (315)	Axis, epipophyses, posterior extent: ? (315)
Axis, ridge on ventral surface of centrum: ? (308)	Axis, ridge on ventral surface of centrum: present (308)
Femur, fossa on the posterior surface of the femoral head, just lateral to the articular surface: ? (446)	Femur, fossa on the posterior surface of the femoral head, just lateral to the articular surface: deep, wide fossa (446)
Femur, circular scar (Madductor femoralis. 1) on posterior surface of shaft distal to fourth trochanter, mediolateral position: ? (452)	Femur, circular scar (Madductor femoralis. 1) on posterior surface of shaft distal to fourth trochanter, mediolateral position: positioned closer to the medial edge of shaft (452)
Metatarsal IV, scar for the insertion of M. gastrocnemius lateralis covering medial third of posterior surface on metatarsal IV: absent or elongate scar (495)	Metatarsal IV, scar for the insertion of M. gastrocnemius lateralis covering medial third of posterior surface on metatarsal IV: narrow oval rugosity (495)

Table 4. Distinguishing characteristics and potential distinguishing characteristics between *Albertosaurus sarcophagus* and *Gorgosaurus libratus* after Loewen et al., (2013)

Gorgosaurus libratus (After Larson, 2013)	*Albertosaurus sarcophagus* (After Larson, 2013)
Maxillary fenestra does not reach ventral margin of antorbital fossa (Carr et al. 2005)	Maxillary fenestra approaches ventral margin of antorbital fossa
Vomer expansion is dorsoventral	Vomer expansion is…?
Posterior dorsal quadratojugal notch is present	Posterior dorsal quadratojugal notch is not present
Central dorsal quadratojugal notch is present	Central dorsal quadratojugal notch is not present
Quadrate-squamosal has double articulation	Quadrate-squamosal has single articulation

Cranial nerve V-2 bounded by maxilla only	Cranial nerve V-2 bounded by…?
Anterior maxilla fossa at cranial nerve V-2-maxilla only	Anterior maxilla fossa at cranial nerve V-2…?
Tooth cross section at base of crown is ovate.	Tooth cross section at base of crown is compressed
Fourth maxillary tooth length/width at base of crown= 1.36	Fourth maxillary tooth length/width at base of crown=?
Fourth dentary tooth length/width at base of crown= 1.23	Fourth dentary tooth length/width at base of crown=?
First maxillary tooth small and incisiform	First maxillary tooth not small and incisiform
D-shaped first dentary tooth: NO	D-shaped first dentary tooth: ?
First dentary tooth reduced: NO	First dentary tooth reduced: ?
Foramen on lateral aspect (centre) of quadratojugal: small	Foramina on lateral aspect (centre) of quadratojugal: absent
Anterior squamosal pneumatic foramen: small	Anterior squamosal pneumatic foramina: absent
Medial lachrymal pneumatic foramen: small	Medial lachrymal pneumatic foramina: absent
Jugal pneumatic foramina: anterolateral facing	Jugal pneumatic foramina: ?
Post Cranial	
Anterior iliac hook: present	Anterior iliac hook: absent
Lateral component of glenoid: absent	Lateral component of glenoid: present in juvenile?

Table 5. Distinguishing characteristics and potential distinguishing characteristics between *Albertosaurus sarcophagus* and *Gorgosaurus libratus* after Larson (2013)

Appendix 5. Cranial, Tooth, Axial (Excluding Cranial) Appendicular measurements of UALVP 49500

Cranial Element Measurement	Measurement value (mm)	Cranial Element Measurement	Measurement value (mm)
Maximum maxillary height	173	Ectopterygoid; dorsoventral length at medial end of left jugal process	29.5
Maxilla anteroposterior length	407	Ectopterygoid; anteroposterior length of right jugal process	25.3
Length of left maxillary tooth row	276	Frontal anteroposterior length	>161
Length of right maxillary tooth row	288	Frontal mediolateral width	118
Maxillary fenestra dorsoventral height	38.8	Maximum height of sagittal crest	27.5
Maxillary fenestra anteroposterior length	40.4	Palatine dorsoventral height	25.7
Orbit anteroposterior length	94	Palatine maximum mediolateral width	37.2
Orbit dorsoventral height	98	Palatine; height of posterior pneumatopore on maxillary process	14.9
Postorbital dorsoventral height	79	Palatine; length of posterior pneumatopore on maxillary process	21.7
Postorbital anteroposterior length	>156	Palatine; height of anterior pneumatopore on maxillary process	11.2
Mediolateral thickness of dorsal postorbital ridge	10.9	Palatine; length of anterior pneumatopore on maxillary process	13.8
Anteroposterior length of lateral postorbital foramen	21.1	Dentary maximum anteroposterior length	485

Dorsoventral height of lateral postorbital foramen	7.7	Dentary tooth row anteroposterior length	293
Lacrimal dorsoventral height	127	Dentary minimum height	58
Lacrimal dorsal bar anteroposterior length	>131	Posterior surangular fenestra anterolateral length	19.6
Dorsoventral height of lacrimal horn	14	Posterior surangular fenestra dorsoventral height	17
Dorsoventral height of lacrimal pneumatic fossa	20	Surangular dorsal shelf maximum width	35.8
Quadratojugal height	129	Surangular dorsal shelf maximum width	23
Dorsal anteroposterior width of quadratojugal squamosal process	48.6	Surangular height	88
Quadratojugal; anteroposterior length of jugal bar	108	Surangular anteroposterior length	324
Quadratojugal; anteroposterior length of quadrate bar	55	Angular dorsoventral height	56
Quadrate anteroposterior length	159	Angular anteroposterior length	272
Quadrate dorsoventral height	136	External mandibular fenestra anteroposterior length	53.1
Quadrate pneumatopore mediolateral width	10.8	External mandibular fenestra dorsoventral height	17.4
Quadrate pneumatopore anteroposterior length	21.1	Splenial anteroposterior length	260
Epipterygoid	44	Splenial posterior	34.2

anteroposterior length		dorsoventral height	
Epipterygoid dorsoventral height	98	Splenial maximum dorsoventral height	80.5
Epipterygoid mediolateral width	7.3	McKelian Canal anteroposterior length	176
Squamosal dorsoventral height	59	Mylohyoid fenestra dorsoventral height	13.8
Squamosal quadrate process anteroposterior length	96	Mylohyoid fenestra anteroposterior length	48.2
Squamosal anterior pneumatic foramen anteroposterior length	50.7	Prearticular anteroposterior length	352
Squamosal anterior pneumatic foramen dorsoventral depth	17	Prearticular mid. Dorsoventral height	21.1
Jugal anteroposterior length	289	Retroarticular process dorsoventral height	75.4
Jugal dorsoventral height	>129	Retroarticular process anteroposterior length	76.6
Jugal pneumatic foramen length	19	Supradentary; max. dorsoventral height	20.4
Jugal pneumatic formaen width	7.5	Supradentary; min. dorsoventral height	5.61
Jugal postorbital bar width at base	42		
Ectopterygoid; dorsoventral height of left jugal contact	19		
Ectopterygoid; dorsoventral height of right jugal contact	16		
Ectopterygoid; dorsoventral height at medial end of left jugal process	15.8		
Ectopterygoid; dorsoventral height at	12.7		

medial end of right jugal process			

Table 1. Cranial measurements of UALVP 49500 (mm)

Tooth position in Maxilla/12	FABL (mm)	Crown Height (Posterior Carina) (mm)	Base Crown Width (mm)	Posterior Denticles/mm	Anterior Denticles/mm
6	21.2	47.5	13.15	3	3
8	24	45.1	13.7	3	3

Table 2. Tooth measurements for two in situ teeth of UALVP 49500 right maxilla

Alveoli Position	12	11	10	9	8	7	6	5	4	3	2	1
FABL (mm)	15.01	23.32	19.99	22.71	23.29	24.23	24.57	27.47	25.72	25.13	22.52	N/P

Table 3. Alveoli FABL of UALVP 49500 right maxilla

Alveoli Position	12	11	10	9	8	7	6	5	4	3	2	1
Basal width (mm)	14.84	16.75	18.20	15.19	15.55	14.23	15.27	19.55	16.52	18.25	NP	NP

Table 4. Alveoli mediolateral width of UALVP 49500 right maxilla

Tooth position in maxilla/12	FABL (mm)	Crown Height (Posterior Carina) (mm)	Base Crown Width (mm)	Posterior Denticles/mm	Anterior Denticles/mm
12	12.85	22.76	9.46	3	3.5/4
11	17.44	30.71	8.53	2.5/3	3
10	18.44	30.29	12.32	3	3
9	19.77	30.94	10.56	3	3

8	19.72	40.52	12.96	3	3
7	19.86	34.53	11.01	3	3
6	21.28	44.44	14.99	3	3
5	19.97	38	12.87	3	3
4	22.59	54.36	13.74	3	3

Table 5. Tooth measurements for in situ teeth of UALVP 49500 left maxilla

Alveoli Position	12	11	10	9	8	7	6	5	4	3	2	1
FABL (mm)	13.03	15.97	20.13	23.59	27.59	29.88	31.46	30.57	27.98	30.70	24.06	N/P

Table 6. Alveoli FABL of UALVP 49500 left maxilla

Alveoli Position	12	11	10	9	8	7	6	5	4	3	2	1
FABL (mm)	9.46	8.53	12.32	10.56	12.96	11.01	14.99	12.87	13.74	NP	NP	NP

Table 7. Alveoli mediolateral width of UALVP 49500 left maxilla

Interdental Plate Position	12.5	11.5	10.5	9.5	8.5	7.5	6.5	5.5	4.5	3.5	2.5	1.5
FABL (mm)	NP	NP	13.56	16.6	20.22	22.79	22.48	25.08	20.14	NP	NP	NP

Table 8. FABL of interdental plates of UALVP 49500 left maxilla

Interdental Plate Position	11.5	10.5	9.5	8.5	7.5	6.5	5.5	4.5	3.5	2.5	1.5
FABL (mm)	10.36	16.58	17.79	21.36	21.64	23.40	26.45	25.15	26.22	*19.49	*16.26

Table 9. FABL of interdental plates of UALVP 49500 right maxilla (*Taphonomically worn)

Left dentary tooth number	FABL (mm)	Base Crown Width (mm)	Crown Height (mm)	Post. Dent (mm)	Ant. Dent (mm)

15	7	5.96	13.34	3	NP
14	10.92	6.86	16.77	3	3 or 4
13	13.38	8.19	18.58	3	3 or 4
12	14.89	9.08	24.06	3/3.5	3
11	12.09	6.97	12.35	3	3
10	17.85	12.44	30.46	3	3MW
9	17.02	11.61	32.87	3	3MW
8	17.89	11.18	35.18	3	3
7	15.59	11.45	34.35	3	3MW
6	16.53	11.38	30.45	2.5	3
5	16.88	11.96	31.47	3	3
4	16.28	11.38	29.15	3	3
3	13.59	11.42	18.19	3	NP

Table 10. Tooth Measurements of Left Dentary of UALVP 49500 (#Replacement, not fully descended; *Badly worn; MW- Middle Worn, measurement taken as low as possible)

Alveoli Position	15	14	13	12	11	10	9	8	7	6	5	4	3	2	1
FABL (mm)	6	6.9	8.2	9.1	7	12.4	11.6	11.2	11.5	11.4	12	11.4	11.4	NP	NP

Table 11. Alveoli Mediolateral width of Left Dentary UALVP 49500

Alveoli Position	15	14	13	12	11	10	9	8	7	6	5	4	3	2	1

FABL (mm)	13.5	15.6	18.9	18.4	21.9	24.1	19.6	24.1	21	22.4	25.1	26.3	NP	NP	NP

Table 12. FABL of Alveoli Left Dentary UALVP 49500

Right Dentary tooth number	FABL (mm)	Base Crown Width (mm)	Crown Height (mm)	Post. Dent (mm)	Ant. Dent (mm)
15	7.84	7.29	>8.61	NP	NP
14	NP	NP	NP	NP	NP
13	12.17	8.14	13.21	3	NP
12	13.77	8.93	18.09	3	NP
11	13.7	8.96	23.99	3/3.5	3
10	15.65	10.36	27.98	3/3.5	3MW
*9	NP	NP	NP	NP	NP
8	17.14	11.3	36.04	3	3
7	17.42	11.61	36.08	3	3
6	16.45	12.09	35.15	3	3
5	18.31	12.7	38.56	3	3
4	NP	NP	NP	NP	NP
3	17.52	12.29	21.59	3	NP
2	15.17	12.26	26.09	3	3
1	NP	12.83	NP	NP	NP

Table 13. Tooth Measurements of Right Dentary of UALVP 49500 (#Replacement, not fully descended; *Badly worn; MW- Middle Worn, measurement taken as low as possible)

Alveoli Position	15	14	13	12	11	10	9	8	7	6	5	4	3	2	1

FABL (mm)	14.2	14.2	21.6	20.9	19.7	22	22.3	23.8	22.4	22.7	23.5	22.6	23.6	21.3	21

Table 14. FABL of Alveoli Right Dentary UALVP 49500

Alveoli Position	15	14	13	12	11	10	9	8	7	6	5	4	3	2	1
FABL (mm)	7.3	NP	8.1	8.9	9	10.3	NP	11.3	11.6	12.1	12.7	NP	12.3	12.3	12.8

Table 15. Alveoli Mediolateral width of Right Dentary UALVP 49500

Axial Measurement	Measurement value (mm)	Axial Measurement	Measurement value (mm)
Length of C1-C9	610	Most posterior dorsal vertebra neural spine height	110
Atlas-axis combined anteriorposterior centra length	60	Dorsal rib A length	573
Atlas intercentrum anteroposterior length	22	Dorsal rib A min. dorsoventral shaft width	17
Atlas intercentrum dorsoventral height	23	Dorsal rib A proximal head dorsoventral height	133
Odontoid dorsoventral height	31	Dorsal rib A proximal head mediolateral width	39
Axis intercentrum anteroposterior length	32	Dorsal rib B length	>235
Axis intercentrum	62	Dorsal rib B min.	21.5

dorsoventral height		dorsoventral shaft width	
Axis neural spine dordoventral height	97	Dorsal rib B proximal head dorsoventral height	>27.7
Axis neural spine anteroposterior width	41.66	Dorsal rib B proximal head mediolateral width	16.9
Axis neural spine lateral width	52	Dorsal rib C length	>210
C3 Centrum length	49	Dorsal rib C min. dorsoventral shaft width	25.2
C3 Centrum height	NP	Dorsal rib D proximal head mediolateral width	42.2
C3 neural spine anteroposterior width	26.20	Dorsal rib D proximal head dorsoventral height	124
C4 Centrum length	60	Caudal Vertebra A centrum length	102
C4 Centrum height	NP	Caudal Vertebra A height	78
C4 neural spine anteroposterior width	27.31	Caudal Vertebra A proximal centrum width	43
C5 Centrum length	69	Caudal Vertebra A distal centrum width	40
C5 Centrum height	NP	Caudal Vertebra B centrum length	>86
C5 neural spine anteroposterior width	19.83	Caudal Vertebra B height	67
C6 Centrum length	74	Caudal Vertebra B proximal centrum width	>32
C6 Centrum height	41	Caudal Vertebra B distal centrum width	NP
C6 neural spine	28.42	Caudal Vertebra C	98

anteroposterior width		centrum length	
C7 Centrum length	71	Caudal Vertebra C height	64
C7 Centrum height	42	Caudal Vertebra C proximal centrum width	38
C7 neural spine anteroposterior width	23.69	Caudal Vertebra C distal centrum width	36
C8 Centrum length	69	Caudal Vertebra D centrum length	87
C8 Centrum height	46	Caudal Vertebra D height	44
C8 neural spine anteroposterior width	NP	Caudal Vertebra D proximal centrum width	37
C9 Centrum length	80	Caudal Vertebra D distal centrum width	34
C9 Centrum height	58	Caudal Vertebra E centrum length	96
C9 neural spine anteroposterior width	NP	Caudal Vertebra E height	44
Most anterior dorsal vertebra centrum length	34	Caudal Vertebra E proximal centrum width	36
Most anterior dorsal vertebra centrum height	>58	Caudal Vertebra E distal centrum width	33
Most anterior dorsal vertebra neural spine height	81	Caudal Vertebra F centrum length	74
Second most anterior dorsal vertebra centrum length	50	Caudal Vertebra F height	30
Second most anterior dorsal vertebra centrum height	78	Caudal Vertebra F proximal centrum width	32
Second most anterior dorsal vertebra neural	88	Caudal Vertebra F distal centrum width	29

spine height			
Most posterior dorsal vertebra centrum length	60		
Most posterior dorsal vertebra centrum height	90		

Table 16. Axial skeleton (excluding cranial) measurements of UALVP 49500

Appendicular Element Measurement	Measurement value (mm)	Appendicular Element Measurement	Measurement value (mm)
Caudal scapula blade width	>73	Pubic boot length	220
Minimum scapula shaft width	27.5	Pubis length	315
Minimum scapula shaft circumference	87	Pubis minimum shaft width	36.3
Scapula length	425	Right Femur length (Unprepared; from field notes)	730
Scapula-coracoid length	520	Right Femur mediolateral diameter	65
Coracoid length	95	Right fibula length	710
Coracoid width	>186	Right fibula minimum shaft width	21.6
Humerus	20.9		

minimum dorsoventral height			
Humerus minimum mediolateral width	23.2	Right fibula Proximal width	140
Humerus length	260	Right fibula Distal width	27
Extension of deltapectoral crest	10	Metatarsal I proximal width	25.5
Manus I- Phalanx 1; length	81.53	Metatarsal I distal width	11.3
Manus I- Phalanx 1; proximal width	29.66	Metatarsal I length	81.7
Manus I- Phalanx 1; distal width	23.61	Metatarsal II proximal width	68
Manus I- Phalanx 1; minimum midshaft width	24.35	Metatarsal II distal width	68.8
Manus II- Phalanx 2; length	13.02	Metatarsal II length	512
Manus II- Phalanx 2; proximal width	19.47	Metatarsal III proximal width	<14.2
Manus II- Phalanx 2; distal width	17.02	Metatarsal III distal width	39
Manus II- Phalanx 2; minimum midshaft width	12.96	Metatarsal III length	>212
Right Ischium dorsoventral height	18.62	Metatarsal IV available shaft width (3/4 proximal)	44.3
Right Ischium mediolateral width	15.38	Metatarsal IV available length	>360
Left Ischium	17.25	Metatarsal V	20.2

dorsoventral height		proximal width	
Left Ischium mediolateral width	15.18	Metatarsal V distal width	<8.3
Ischia length	>291	Metatarsal V length	239
Pubic boot height	101		

Table 17. Appendicular skeleton (excluding pedal phalanges) measurements of UALVP 49500

Pedal Phalanges	Proximal Width (mm)	Distal Width (mm)	Midshaft width (mm)	Length (mm)
Right Digit II				
Phalanx 1	51.45	42.28	28.48	143
Right digit III				
Phalanx 1	62.14	54.14	32.34	145
Phalanx 2	50.47	43.54	28.01	95
Phalanx 3	43.92	36.14	26.56	77
Right Digit IV				
Phalanx 1	NP	33.7	30	91
Phalanx 2	45	28	21	73
Left Digit II				
Phalanx 1	51.93	45.08	29.13	137
Phalanx 2	43.80	35.54	28.38	96
Left Digit IV				
Phalanx 1	61.92	55.12	39.19	73
Phalanx 2	53.36	46.16	40.01	51
Phalanx 3	42.35	36.71	33.35	42
Phalanx 4	34.01	30.12	27.17	30
Phalanx 5 (Ungual)	19.72	3.45	18.68	77
Isolated unguals				
Ungual A	23.45	<5.97	21.69	64
Ungual B	23.16	2.76	18.62	79
Ungual C	27.09	<5.22	22.99	77
Ungual D	32.68	<19.22	27.29	>62

Table 18. Pedal phalanges measurements of UALVP 49500